Peralkyl Guanidines

in

Copper Catalyzed Oxidative Transformations

and

Novel Proton Sponges

Dissertation

zur

Erlangung des Doktorgrades

der Naturwissenschaften

(Dr. rer. nat.)

dem

Fachbereich Chemie

der Philipps-Universität Marburg

vorgelegt von

Volker Raab

aus

Gießen

Marburg / Lahn 2001

Die vorliegende Dissertation entstand in der Zeit von April 1998 bis April 2001 unter Leitung von Herrn Prof. Dr. J. Sundermeyer am Fachbereich Chemie der Philipps-Universität Marburg.

Vom Fachbereich Chemie der Philipps-Universität Marburg als Dissertation angenommen am 23.04.2001

Erstgutachter: Herr Prof. Dr. J. Sundermeyer
Zweitgutachter: Herr Prof. Dr. W. Petz

Tag der mündlichen Prüfung: 2. Mai 2001

„Predictions are difficult, especially if they concern the future.“

Mark Twain

To my families

PREFACE

This dissertation is written in a manuscript style, each chapter can be read independently, yet they are interacting.

Each chapter contains a separate introduction, results and discussion part, conclusion, experimental section and literature references. It is noted that repetition of certain facts, experimental descriptions and citation of literature from chapter to chapter is useful under these circumstances and cannot be avoided for the sake of independence and clarity within each individual chapter.

In the „General Introduction" an overview of „Copper Catalyzed Oxidative Transformations" is given, whereas more details about specific topics are discussed in the introduction of the relevant chapter.

Whenever separate results of further investigations are reported which are not part of the publication, an appendix organized in an analogous manner as the manuscript is supplied.

Finally, an overall summary which sets the separate chapters and its results in context to each other is provided (in English and German language).

PARTS OF THIS DISSERTATION HAVE BEEN PUBLISHED

Publications

H. Wittmann, V. Raab, A. Schorm, J. Plackmeyer, J. Sundermeyer*, „Complexes of Manganese, Iron, Zinc, and Molybdenum with a Superbasic Tris(guanidine) Derivative of Tris(2-aminoethyl)amine (Tren) as Tripod Ligand" *Eur. J. Inorg. Chem.* **2001**, 1937-1948.

V. Raab, M. Merz, J. Sundermeyer*, „Ligand Effects in the Copper Catalyzed Aerobic Oxidative Carbonylation of Methanol to Dimethyl Carbonate (DMC)" *J. Mol. Catal. A: Chem.* **2001**, *175*, 51-63.

V. Raab, J. Kipke, O. Burghaus, J. Sundermeyer*, „Copper Complexes of Novel Superbasic Peralkylguanidine Derivatives of Tris(2-aminoethyl)amine (Tren) as Constraint Geometry Ligands" *Inorg. Chem.* **2001**, *40*, 6964-6971.

V. Raab, J. Kipke, R. M. Gschwind, J. Sundermeyer*, „1,8-Bis(tetramethylguanidino) naphthalene (TMGN): A New, Superbasic and Kinetically Active „Proton Sponge"" *Chem. Eur. J.* **2002**, *8*, in press.

V. Raab, J. Kipke, A. Schorm, J. Sundermeyer*, „Preparation of New Chiral, C_2 symmetric Peralkyguanidine Ligands, Copper Complexation, and Evaluation in the Aziridination of Styrene" *J. Chem. Soc. Dalton Trans.* **2002**, submitted.

Patents

„1,8-Bisimidonaphthalin-Protonenschwämme und Verfahren zu deren Darstellung", Erfinder: V. Raab, J. Sundermeyer, Anmelder: BASF AG, Anmeldungsnummer: OZ 0050/52862, DPMA **2001**.

Presentations

„Kupfer-Katalysierte Oxidative Transformationen - Katalyse und Modellchemie" Doktorandensymposium des SFB 260, Philipps Universität Marburg, 29. Juni - 01. Juli **2000**.

„Novel Chelating Ligands based on Peralkylated Oligoguanidines and Oligoiminophosphoranes" VIth Regional Seminar on Organometallic and Organophosphorous Chemistry, Karpacz, Poland, 09.-13. April **2000**.

„Kupfer-Katalysierte Oxidative Carbonylierung von MeOH mit CO/O_2 zu Dimethylcarbonat (DMC)" Vortrag zu aktuellen Ergebnissen, Bayer AG, Leverkusen, 27. März **2000**.

Poster

„Ligand Effects in the Copper Catalyzed Aerobic Oxidative Carbonylation of Methanol to Dimethyl Carbonate (DMC)", Heidelberg Forum of Molecular Catalysis, Heidelberg, 7. Dezember **2001**.

Online

„Peralkyl Guanidines in Copper Catalyzed Oxidative Transformations and Novel Proton Sponges", V. Raab, Dissertation, Marburg **2001**: http://www.ub.uni-marburg.de/digibib/ediss.

Verlag

„Peralkyl Guanidines in Copper Catalyzed Oxidative Transformations and Novel Proton Sponges", V. Raab, Dissertation, Marburg **2001**: Klaus Bielefeld Verlag, Friedland, Germany, ISBN 3-89833-053-2.

INTRODUCTORY EXPLANATIONS

Abbreviations

APCI	Atmospheric Pressure Chemical Ionization
*t*Bu	*tert*-Butyl
DMPG	Dimethylpropyleneguanidine
DMSO	Dimethylsulfoxide
EI	Electron Ionization
Et	Ethyl
Ether	Diethyl ether (Et_2O)
ESI	Electrospray Ionization
FD	Field Desorption
HMPT	Hexamethylphosphoric acid triamide
L	Ligand
M	Metal
Me	Methyl
NMR	Nuclear Magnetic Resonance
Ph	Phenyl
R	Alkyl
RT	Room temperature
OTf	Triflate, Trifuormethanesulfonate ($CF_3SO_3^-$)
THF	Tetrahydrofurane
TMG	Tetramethylguanidine
Ts	*p*-Toluenesulfonyl
X	Monoanionic ligand

Numbers

Complexes, ligands and compounds are labeled with full-size, bold numbers, e.g. **1**.

Elevated numbers in plain text format indicate a reference (e.g. article[12]).

TABLE OF CONTENTS

Chapter 1

Preparation of New, Chiral, C_2 Symmetric Peralkyguanidine Ligands, Copper Complexation, and Evaluation in the Aziridination of Styrene

Chapter 2

Ligand Effects in the Copper Catalyzed Aerobic Oxidative Carbonylation of Methanol to Dimethyl Carbonate (DMC)

Chapter 3.1

Copper Complexes of Novel Superbasic Peralkylguanidine Derivatives of Tris(2-aminoethyl)amine (Tren) as Constraint Geometry Ligands

Chapter 3.2

The Reactivity of TMG₃tren Copper Complexes

Chapter 3.3

Copper Complexes with HMPI₃tren as Ligand

Chapter 4

Complexes of Manganese, Iron, Zinc, and Molybdenum with a Superbasic Tris(guanidine) Derivative of Tris(2-aminoethyl)amine (Tren) as Tripod Ligand

Chapter 5.1

1,8-Bis(tetramethylguanidino)naphthalene (TMGN): A New, Superbasic and Kinetically Active „Proton Sponge"

Chapter 5.2

1,8-Bis(hexamethylphosphoraneimino)naphthalene (HMPIN): The Next Generation of Superbasic „Proton Sponges"

ZUSAMMENFASSUNG

Die vorliegende Arbeit offenbart neue Perspektiven in der Chemie von Peralkylguanidinen. Einige mehrzähnige chirale oder tripodale Oligoguanidine wurden synthetisiert, deren Kupfer(I/II)-Komplexe dargestellt und ihr Potenzial in oxidativen Nitren- bzw. OR-Radikal-Übertragungsreaktionen untersucht.

Kapitel 1. In der asymmetrischen Aziridinierung von Styrol wurden gute Ausbeuten von bis zu 98% erreicht, wohingegen der Enantiomerenüberschuss leider auf einem unbefriedigenden Niveau von ≤ 8% ee im Falle des besten Katalysatorsystems [TMG$_2$BN × Cu(I)ClO$_4$] verblieb (Abbildung 1).
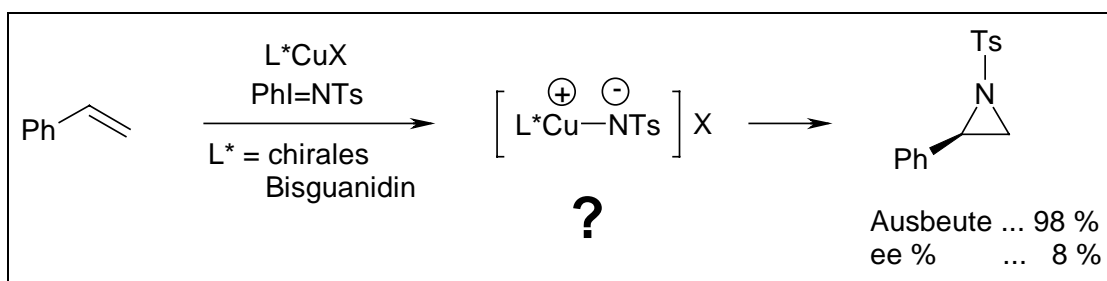
Abbildung 1. Kupfer-katalysierte, asymmetrische Aziridinierung von Styrol.

Die hohe Aktivität, begleitet von geringer Enantioselektivität, wird der Tatsache zugeschrieben, dass Cu(I) eine lineare und nicht tetraedrische Koordinationschemie bevorzugt, so dass unsere C_2-symmetrischen, chiralen Guanidine keine Chelatkomplexe mit Kupfer (I) ausbilden (Abbildung 2). Gemäß einer Kristallstrukturbestimmung trifft dies jedoch für Kupfer(II) zu (Abbildung 3).
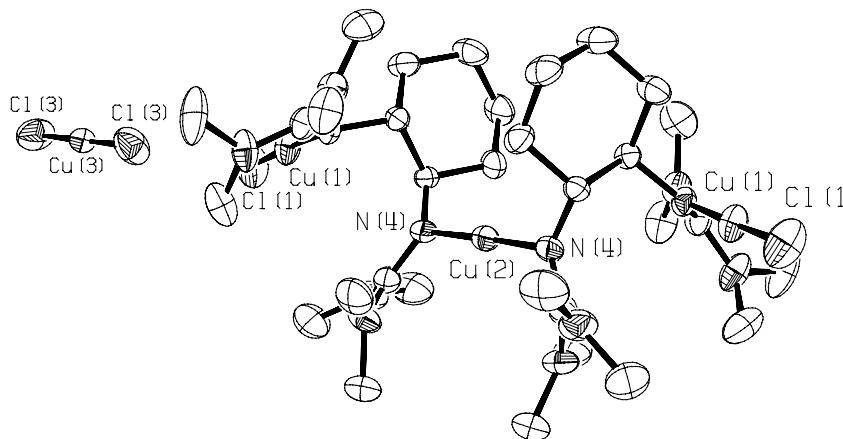
Abbildung 2. Molekülstruktur von [Cu^I{(μ^2-L)Cu^{I}Cl}$_2$][Cu^{I}Cl$_2$].
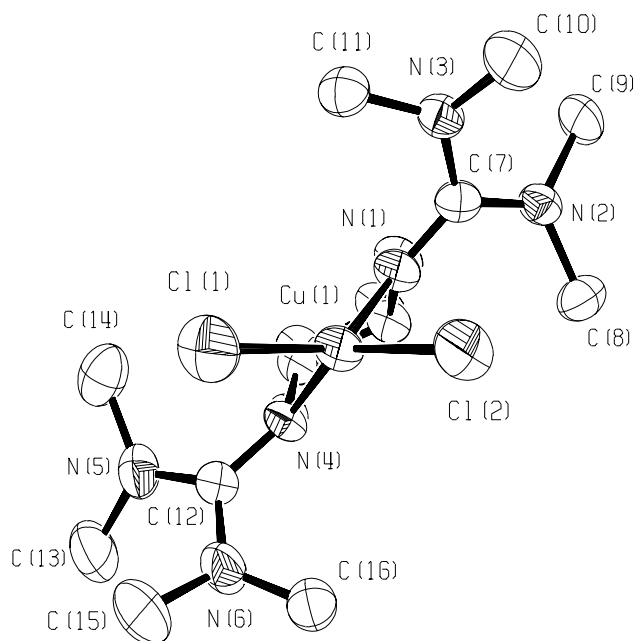
Abbildung 3. Molekülstruktur von [(L)Cu^{II}Cl$_2$].

Kapitel 2. Peralkylguanidin-Kupferkomplexe zeigen darüber hinaus ihre Fähigkeit zur Aktivierung von molekularem Sauerstoff in der katalytischen, oxidativen Carbonylierung von Methanol zu Dimethylcarbonat (DMC) (Abbildung 4). Im Vergleich zu unkoordiniertem Kupfer(II)-chlorid, ein häufig in Patenten angewendeter Katalysator, ergab die Katalyse mit dem tripodalen Guanidinkomplex [(TMG$_3$tren)CuCl]Cl eine Verdopplung des Umsatzes von 15 auf 29% bei ebenfalls erhöhter Selektivität (46 vs. 55%). Die höchste Aktivität (55% Umsatz) und Selektivität (95%) wurde jedoch mit einem L$_4$CuCl$_2$ Komplex erreicht, der *N*-methylimidazol als Liganden enthält. Dieses Ergebnis konnte durch den Einsatz von 3Å Molsieb als wasserentziehendes Mittel nochmals auf 87% Umsatz, allerdings bei geringerer Selektivität von 75%, gesteigert werden. Die Optimierung mehrerer Parameter innerhalb dieser homogenen Oxidationskatalyse führte zur höchsten Aktivität und Selektivität, die je für die DMC-Synthese berichtet wurde.
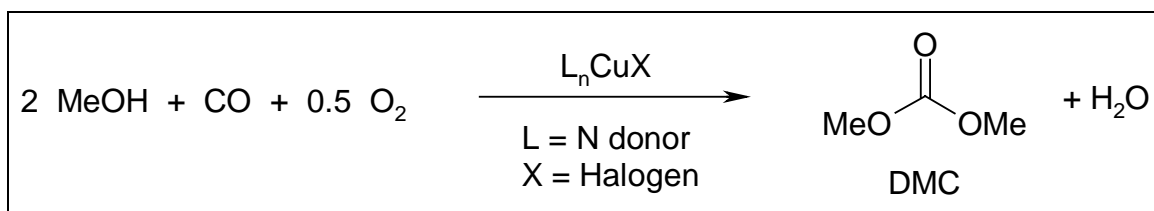
Abbildung 4. Kupfer-katalysierte, oxidative Carbonylierung von MeOH zu DMC.

Kapitel 3 und 4. Unser Interesse eine Koordinationschemie mit biomimetischen 3d-Übergangsmetallen wie Kupfer, Mangan, Eisen und Zink zu entwickeln, welche als Precursor in der Aktivierung, z.B. von molekularem Sauerstoff, dienen könnten, führte uns zur Synthese und strukturellen Charakterisierung einer Reihe von Komplexen mit dem Liganden TMG_3tren (Abbildung 5, Abbildung 6). Insbesondere die trigonal-monopyramidalen Cu(I)-Komplexe sind in dieser Hinsicht viel versprechend, da sie ein bemerkenswertes Strukturmerkmal aufweisen - eine freie Koordinationsstelle am Kupferzentrum innerhalb der TMG_3tren Ligand-„Tasche".
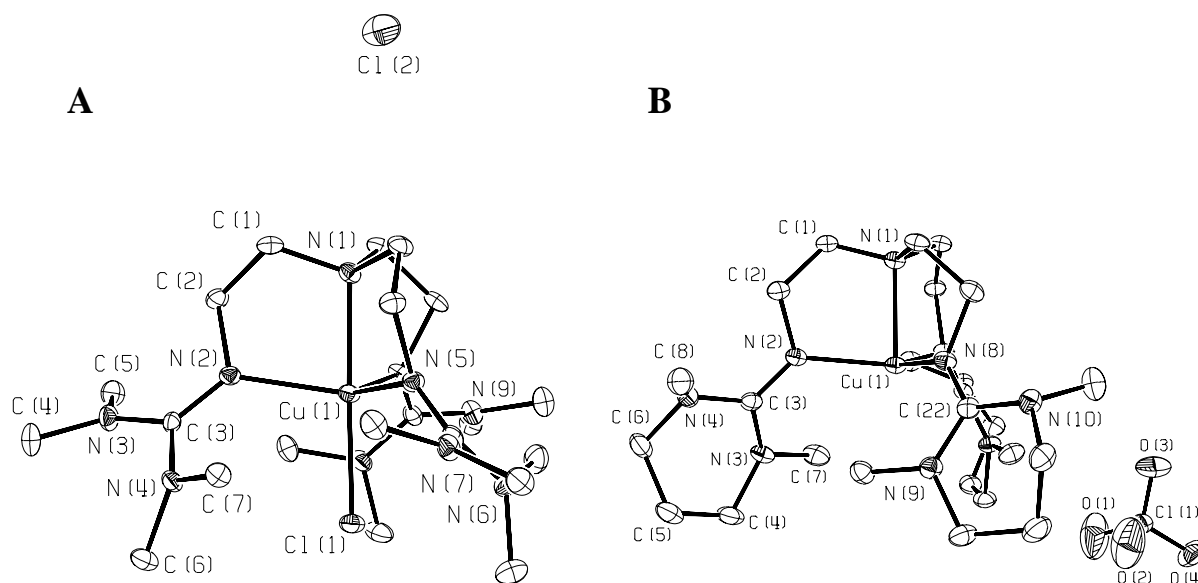
Abbildung 5. Molekülstrukturen von $[(TMG_3tren)Cu^{II}Cl]Cl$ (**A**) und $[(DMPG_3tren)Cu^{I}]ClO_4$ (**B**).
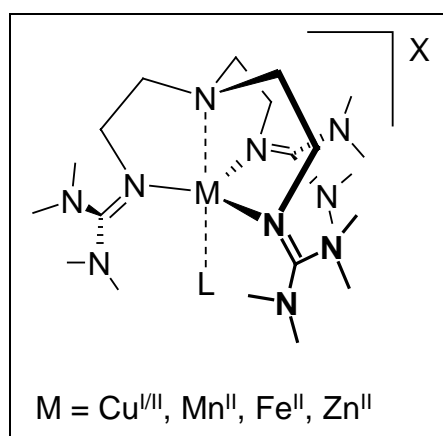
Abbildung 6. Übergangsmetallkomplexe mit dem Trisguanidin TMG_3tren.

Erste Ergebnisse in der Sauerstoffaktivierung wurden bereits durch UV/Vis und Resonance-Raman Spektroskopie erhalten, welche die reversible Ausbildung eines monomeren, end-on gebundenen Superoxo-Komplexes enthüllte (Abbildung 7). Weitere Untersuchungen und Bestrebungen Einkristalle für eine Röntgenstrukturanalyse zu erhalten sind im Gange.
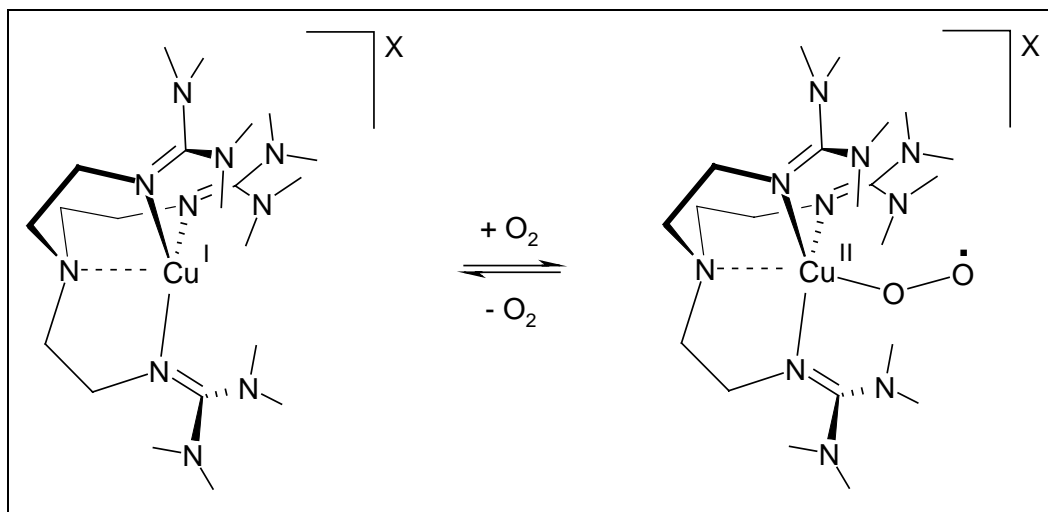
Abbildung 7. Reversible Reaktion von [(TMG₃tren)Cu]X mit Sauerstoff zu einem mononuklearen, end-on gebundenen Superoxo-Komplex.

Kapitel 5.1. Schließlich wurde das generelle Konzept, der Entwicklung multifunktionaler Metallkation- und Protonen-Rezeptoren, durch die Synthese eines neuen „Protonen-schwamms" mit chelatisierenden, superbasischen Tetramethylguanidinfunktionen erweitert. Der „Protonenschwamm" TMGN basiert auf dem Gerüst des 1,8-Diaminonaphthalins (Abbildung 8). TMGN besitzt nicht nur einen extrem hohen pK_{BH+}-Wert von 25.1 (MeCN), sondern zeigt zusätzlich zu seiner hohen thermodynamischen Basizität auch noch eine ungewöhnlich hohe kinetische Basizität, was diese Superbase außerordentlich attraktiv für basenkatalysierte Anwendungen erscheinen läßt. Die protonierten Formen zeigen faszinierende Koaleszenzphänomene in deren Tieftemperatur ¹H NMR Spektren, welche Einsicht in die Bindungssituation des Guanidinsystems, sowie der Kinetik des Protonen-Selbstaustausches gewähren (Abbildung 9).
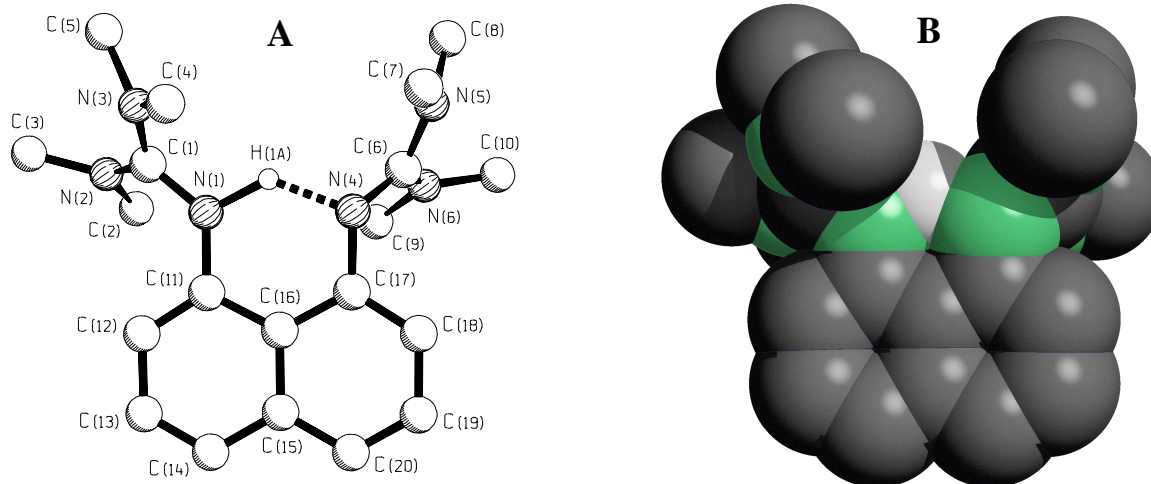
Abbildung 8. Molekülstruktur (**A**) und Kalottenmodell (**B**) von [TMGNH]$^{+}$.
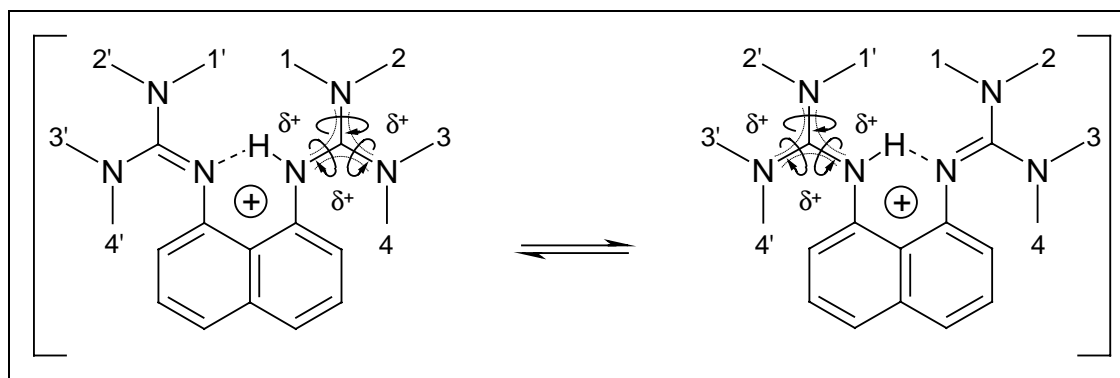
Abbildung 9. Dynamisches Verhalten von monoprotoniertem TMGN.

Im Zuge der Untersuchungen an Peralkyl-guanidinen konnte ein struktureller Parameter $\rho = 2a / (b + c)$ (Quotient der mittleren C=N vs. C-NR$_2$ Bindungslänge) abgeleitet werden, der die Abschätzung der Ladungs-delokalisation in Abhängigkeit vom Elektrophil (E) innerhalb der Guanidin-funktion erlaubt (Abbildung 10).
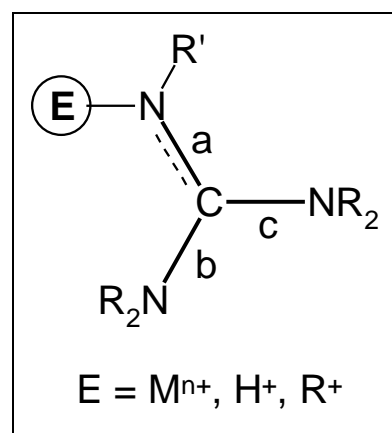
Abbildung 10. C-N Bindungen a, b und c zur Bestimmung des Quotienten ρ.

Kapitel 5.2. Letztlich konnte noch ein weiterer superbasischer Phosphazen-„Protonenschwamm" synthetisiert werden, der zwei Iminophosphoran-gruppen als chelatisierende Protonen-akzeptoren trägt (Abbildung 11). Seine Eigenschaften sind noch Gegenstand weiterer Untersuchungen, es kann aber angenommen werden, dass HMPIN einen pK_{BH+}-Wert aufweisen sollte der nochmals 2-3 Größenordnungen höher liegt als der des Guanidin-Vertreters.
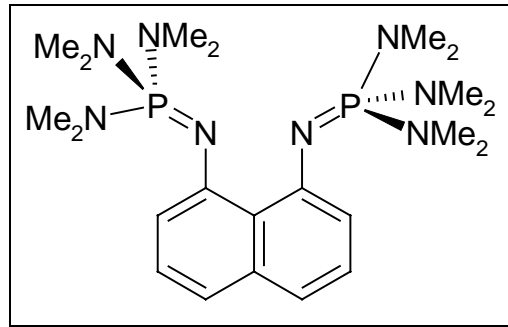
Abbildung 11. Superbasischer Imino-phosphoran „Protonenschwamm" HMPIN.

GENERAL INTRODUCTION AND OBJECTIVE

Copper is the transition metal of choice in numerous catalytic processes involving oxidative transfer of either oxygen or nitrogen (Scheme 1). Industrial applications of copper catalysts in homogeneous phase and oxygen as oxidizing agent have been reviewed by Tolman,[1] Rossi,[2] and Sheldon.[3] One example is the copper mediated oxidative decarboxylation of benzoic acid to phenol which was patented by Dow Chemical in 1955[4] and was recently reinvestigated in terms of mechanistic aspects by Reedijk et al.[5] Behind the Cumol process it is the second most important process (200,000 t/a) in industrial phenol production. Also of technical interest is the oxidation of aromatic substrates[6] such as phenols to quinones,[7,8] e.g. 2,3,6-trimethylphenol to trimethyl-*p*-benzoquinone, an important vitamin E precursor, that had been claimed by a patent of the Mitsubishi Gas Corp. in the mid 80´s.[9] Aerobic oxidation of catechols to *o*-quinones[10] and the hydroxylation of arenes[11] are just two more copper induced catalytic processes that are currently studied. The oxidative carbonylation of alcohols attracted particular attention in the past because a row of products (e.g. polyurethanes, polycarbonates) are based on the organic carbonates that are formed in that catalysis.[12] Ongoing patent activity can be observed for the production of dimethyl carbonate from MeOH, CO and O_2 with copper catalysts (Enichem, Italy: 8,000 t/a; General Electric, Japan: 12,000 t/a, Scheme 1).[13] Furthermore, the oxidation of unsaturated alcohols[14] mediated by copper catalysts, or olefins in combination with Pd salts (Wacker process),[15] is considered an important route to aldehydes and ketones. In turn, aldehydes can be oxidized to carboxylic acids of industrial use.[16]

Further perspectives in fine chemical and pharmaceutical synthesis are provided by the asymmetric aziridination of olefins with chiral copper complexes as nitrene transfer catalysts.[17,18] Other transition metals also proved to be capable of catalyzing the aziridine formation and the synthetic goal is to achieve high selectivities along with good conversion and cheap nitrene sources. So far, a method incorporating all these demands remains to be explored, whereas the analogous oxo transfer reactions in the preparation of epoxides is well-established in organic synthesis.[19] The versatility of copper catalysts is emphasized in reactions such as the benzylic and allylic amination[20] along with its oxo counterpart the allylic oxidation.[21]
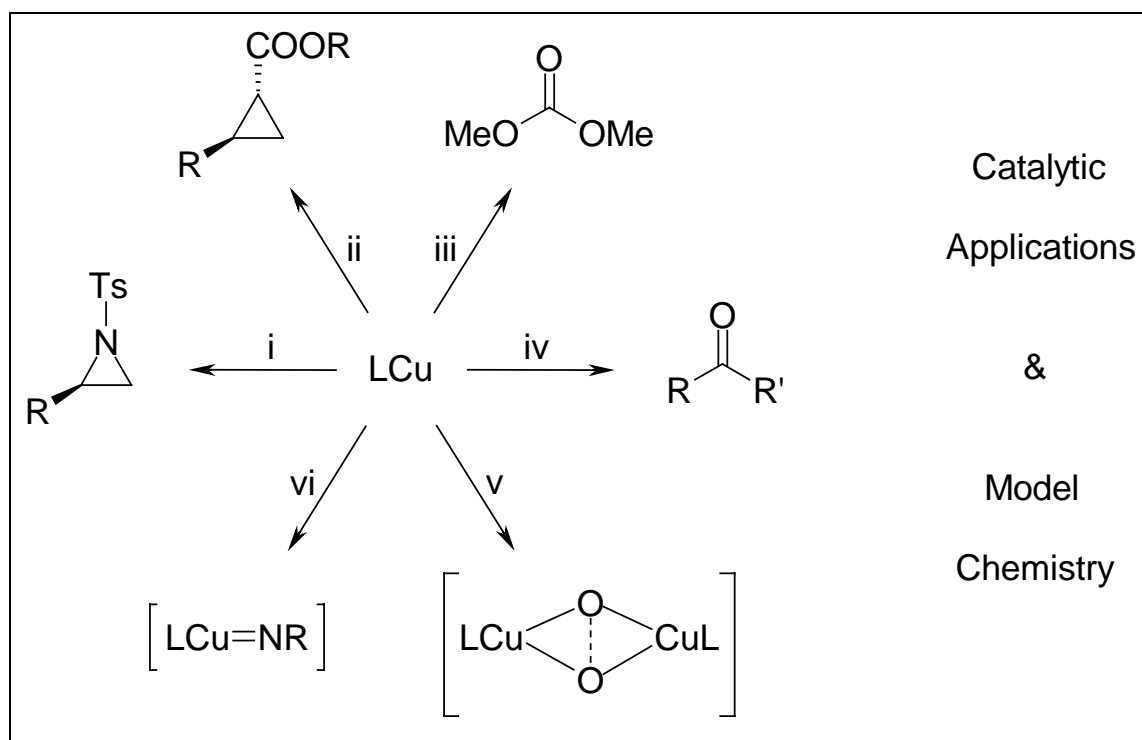
Scheme 1. Versatile applications of N donor ligated (L) copper in catalytic oxidative transfomations. i) Olefin, PhI=NTs; ii) Olefin, $N_2CHCOOR$; iii) MeOH, CO, O_2; iv) R'RCHOH, O_2; v) O_2; vi) X=NR.

Ligands used to stabilize copper in the oxidation states Cu(I/II/III) are often based on the amine functionality. If the concept of using amines and polyamines receives widespread appreciation - how about introducing peralkyl guanidines instead? Due to their high basicity guanidines practically occur only in protonated form in nature.[22] As such, they are known for their capability as anion receptors via hydrogen bonds, e.g. in peptide chemistry (arginine).[23,24] The question arises whether novel oligoguanidines might also show potential as cation receptors, e.g. in „proton sponges" and lewis acid complexes, and moreover - could complexes of that type be utilized in catalytic applications?

The objective of this Thesis was to develop the largely unexplored chemistry of multidentate peralkyl guanidine cation receptors for transition metal ions and protons.

In a first approach a set of new chiral, C_2 symmetric peralkyl *bis*guanidines are to be synthesized (Scheme 2),[25] their copper complexes prepared, and evaluated in the asymmetric aziridination of styrene (Chapter 1).
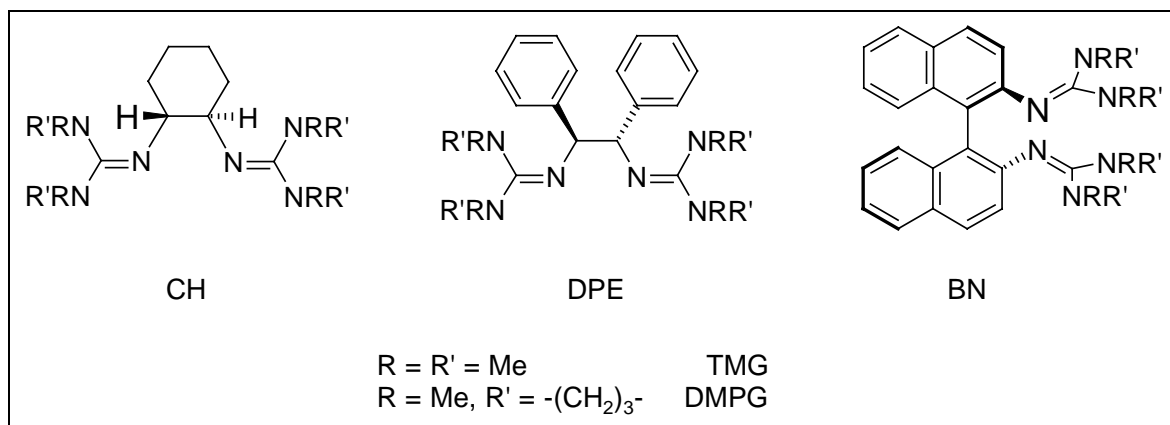
Scheme 2. Novel C_2 symmetric target ligands for the asymmetric aziridination of styrene.
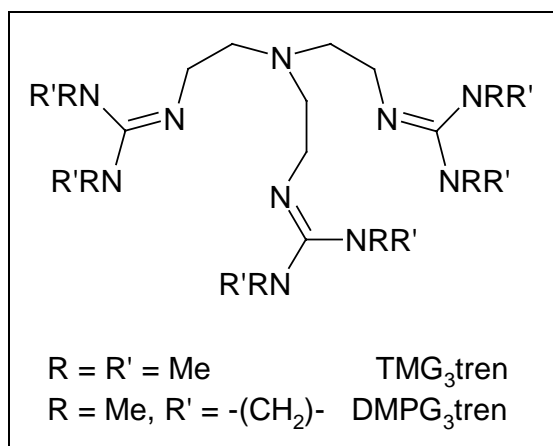
Scheme 3. Superbasic N ligand for the DMC-Catalysis.

In Chapter 2 the use of a tripodal trisguanidine based on the tren backbone (Scheme 3) is to be evaluated in the technically relevant copper catalyzed oxidative carbonylation of MeOH to dimethyl carbonate (DMC). Other superbasic ligands, such as *N*-methyl imidazole and DMAP are to be compared in their activity as promotors in this CO oxidation process.

Stimulated by the success in both, the oxidative transfer of nitrogen and oxygen (via OR radicals), we set out to synthesize and structurally characterize model complexes of copper(I/II) and other biomimetically relevant transition metals (Mn, Fe, Zn, and Mo, Scheme 4, Chapter 3.1 and 4). Emphasis is put on the modeling of the active site of copper, e.g. its reactivity towards molecular oxygen and other oxidants (Chapter 3.2).
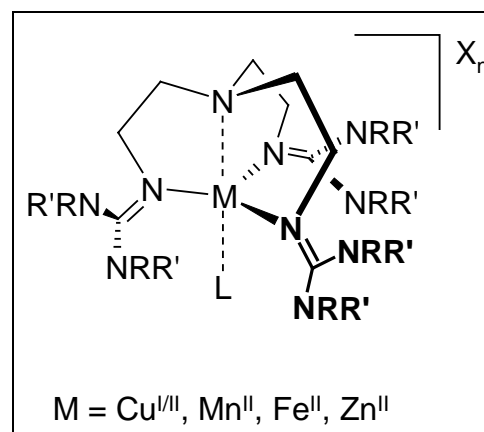
Scheme 4. Guanidine tren complexes.
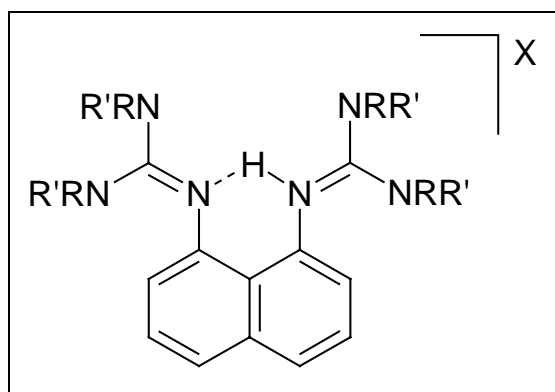
Scheme 5. Guanidine „proton sponge".

Finally, the know-how in the synthesis of multifunctional *bis*guanidines is to be used in the creation of novel „proton sponges" based on the 1,8-diaminonaphthalene spacer (Scheme 5, Chapter 5).

References

[1]   W. B. Tolman, *Acc. Chem. Res.* **1997**, *30*, 227-237.

[2]   L. Prati, N. Ravasio, M. Rossi, *Chim. Ind.* **1997**, *79*, 189-196.

[3]   R. A. Sheldon, *Catal. Oxid.* **1995**, 1-15.

[4]   US Patent 2 893 541 and 2 831 895, **1955** to Dow Chemical Co.

[5]   a) F. Agterberg, J. Reedijk, *Stud. Surf. Sci. Catal.* **1994**, *82*, 639-646; b) F. Agterberg, J. Reedijk, *Inorg. Chem.* **1997**, *36*, 4321-4328; c) F. Agterberg, J. Reedijk, *Inorg. Chim. Acta* **1998**, *267*, 183-192.

[6]   R. W. Fischer in: *Applied Homogeneous Catalysis with Organometallic Compounds*, B. Cornils, W. A. Herrmann (Eds.), VCH, Weinheim, **1996**, pp. 374-393 and refs. cited.

[7]   a) Ger. Offen. 2 221 624, **1972** to Hoffmann-La Roche AG; b) EP 475 272 A2, **1992** to BASF AG.

[8]   a) K. Takehira, M. Shimizu, Y. Watanabe, H. Orita, T. Hayakawa in: *New Developments in Selective Oxidations*, G. Centi, F. Trifiró (Eds.), Elsevier, New York, **1990**, p. 133; b) S. Ito, K. Ahihara, M. Matsumoto, *Tetrahedron Lett.* **1983**, *24*, 5249-5252; b) M. Shimizu, H. Orita, T. Hayakawa, K. Takehira, *Tetrahedron Lett.* **1989**, *30*, 471-474; c) K. Takehira, M. Shimizu, Y. Watanabe, H. Orita, T. Hayakawa, *J. Chem. Soc. Chem. Comm.* **1989**, 1705-1706; d) K. Takehira, M. Shimizu, Y. Watanabe, H. Orita, T. Hayakawa, *Tetrahedron Lett.* **1989**, *30*, 6691-6692; e) N. Ravasio, M. Gargano, M. Rossi, in: *New Developments in Selective Oxidations*, G. Centi, F. Trifiró (Eds.), Elsevier, New York, **1990**, p. 139; f) M. Shimizu, Y. Watanabe, H. Orita, T. Hayakawa, K. Takehira, *Bull. Chem. Soc. Jpn.* **1992**, *65*, 1522-1526.

[9]   EP Patent 0 127 888, **1984**, EP 0 167 153, **1985**, US Patent 4 828 762, **1986** to Mitsubishi Gas Chemical Corp.

[10]   L. M. Berreau, S. Mahapatra, J. A. Halfen, R. P. Houser, V. G. Young, Jr., W. B. Tolman, *Angew. Chem.* **1999**, *111*, 180-183; *Angew. Chem. Int. Ed. Engl.* **1999**, *38*, 207-210.

[11]   Holland, P. L.; Rodgers, K. R.; Tolman, W. B. *Angew. Chem.* **1999**, *111*, 1210-1213; *Angew. Chem. Int. Ed. Engl.* **1999**, *38*, 1139-1142.

[12]   R. Jira in: *Applied Homogeneous Catalysis with Organometallic Compounds*, B. Cornils, W. A. Herrmann (Eds.), VCH, Weinheim, **1996**, pp. 405-406.

[13]   This topic and patent literature is dealt with in more detail in Chapter 2.

[14] a) M. F. Semmelhack, C. R. Schmid, D. A. Cortés, C. S. Chou, *J. Am. Chem. Soc.* **1984**, *106*, 3374-3376; b) I. E. Markó, P. R. Giles, M. Tsukazaki, S. M. Brown, C. J. Urch, *Science* **1996**, *274*, 2044-2045; c) I. E. Markó, M. Tsukazaki, P. R. Giles, S. M. Brown, C. J. Urch, *Angew. Chem.* **1997**, *109*, 2297-2299; *Angew. Chem. Int. Ed. Engl.* **1997**, *36*, 2208-2210.

[15] a) R. Jira in: *Applied Homogeneous Catalysis with Organometallic Compounds*, B. Cornils, W. A. Herrmann (Eds.), VCH, Weinheim, **1996**, pp. 374-393 and refs. cited therein; b) E. Montflier, A. Mortreux in: *Aqueous Phase Organometallic Catalysis*, B. Cornils, W. A. Herrmann (Eds.), VCH, Weinheim, **1997**, pp. 513-518; c) G.-J. ten Brink, I. W. C. E. Arends, G. Papadogianakis, R. A. Sheldon, *Chem. Commun.* **1998**, 2359-2360.

[16] P. Lappe, E. Schulz in: *Applied Homogeneous Catalysis with Organometallic Compounds*, B. Cornils, W. A. Herrmann (Eds.), VCH, Weinheim, **1996**, pp. 424-429 and refs. cited therein.

[17] For more details and literature references see Chapter 1.

[18] a) P. Müller in: *Transition Metal Catalyzed Nitrene Transfer: Aziridination and Insertion in Asymmetric Catalysis*, *Vol. 2*, M. P. Doyle (Ed.), Greenwich, Conn., **1997**, pp. 113-151; b) H. M. I. Osborn, J. Sweeney, *Tetrahedron: Asymmetry* **1997**, *8*, 1693-1715; c) E. N. Jacobsen in: *Aziridination in Comprehensive Asymmetric Catalysis*, E. N. Jacobsen, A. Pfaltz, H. Yamamoto (Eds.), Springer, Berlin, **1999**, pp. 607-621.

[19] a) R. Irie, K. Noda, Y. Ito, N. Matsumoto, T. Katsuki, *Tetrahedron Lett.* **1990**, *31*, 7345-7348; b) W. Zhang, J. L. Loebach, R. S. Wilson, E. N. Jacobsen, *J. Am. Chem. Soc.* **1990**, *112*, 2801-2803; c) W. Zhang, E. N. Jacobsen, *J.Org. Chem.* **1991**, *56*, 2296-2298; d) R. Irie, K. Noda, Y. Ito, T. Katsuki, *Tetrahedron Lett.* **1991**, *32*, 1055-1058; e) R. Irie, Y. Ito, T. Katsuki, *Synlett* **1991**, 265-266; f) N. Hosoya, R. Irie, Y. Ito, T. Katsuki, *Synlett* **1991**, 691-692; g) D. Feichtinger, D. A. Plattner, *Angew. Chem.* **1997**, *109*, 1796-1798; *Angew. Chem. Int. Ed. Engl.* **1997**, *36*, 1718-1719; h) N. End, A. Pfaltz, *J. Chem. Soc. Chem. Comm.* **1998**, 589-590; i) M. B. Francis, E. N. Jacobsen, *Angew. Chem.* **1999**, *111*, 987-991; *Angew. Chem. Int. Ed. Engl.* **1999**, *38*, 937-941.

[20] Y. Kohmura, K.-I. Kawasaki, T. Katsuki, *Synlett* **1997**, 1456-1458.

[21] a) M. S. Kharasch, G. Sosnovsky, *J. Am Chem. Soc.* **1958**, *80*, 756; b) M. S. Kharasch, A. Fono, *J. Org. Chem.* **1958**, *23*, 324-325; c) D. J. Rawlinson, G. Sosnovsky, *Synthesis* **1972**, 1-28.

[22] H. Dugas, C. Penney in: *Bioorganic Chemistry*, Springer, New York, **1981**, p. 15.

[23] *Ullmann's Encyclopedia of Industrial Chemistry, Vol. A 12* (Hrsg.: B. Elvers, S. Hawkins, M. Ravenscroft, J. F. Rounsaville, G. Schulz), 5. Aufl., VCH, Weinheim, **1989**, p. 545-557.

[24] a) E. M. A. Ratilla, B. K. Scott, M. S. Moxness, N. M. Kostic, *Inorg. Chem.* **1990**, *29*, 918-926; b) P. D. Beer, D. K. Smith, *Prog. Inorg. Chem.* **1997**, *46*, 1-96; c) F. P. Schmidtchen, M. Berger, *Chem. Rev.* **1997**, *97*, 1609-1646; d) A. Hessler, O. Stelzer, H. Dibowski, K. Worm, F. P. Schmidtchen, *J. Org. Chem.* **1997**, *62*, 2362-2369.

[25] Based on a procedure in large part developed and documented in the dissertation of H. Wittmann, *Ph. D. Thesis* **1999**, Philipps University Marburg, Germany.

— Chapter 1 —

Preparation of New Chiral, C$_2$ Symmetric Peralkylguanidine Ligands, Copper Complexation, and Evaluation in the Aziridination of Styrene

Keywords: N ligands • Bidentate ligands • Chiral ligands • Guanidines • Coordination chemistry • Copper • Asymmetric olefin aziridination

Abstract

The preparation and full spectroscopic characterization of a set of new chiral, C$_2$ symmetric peralkyl *bis*guanidine ligands is described. (*1R,2R*)-(-)-1,2-Bis[*N*^{2}-(1,1,3,3-tetramethylguanidino)]cyclohexane (TMG$_2$CH, **1a**), (*1R,2R*)-(+)-1,2-Bis[*N*^{2}-(1,1,3,3-tetramethylguanidino)]diphenylethane (TMG$_2$DPE, **2a**), *R*(+)-2,2´-Bis[*N*^{2}-(1,1,3,3-tetramethylguanidino)]-1,1´-binaphthalene (TMG$_2$BN, **3a**), as well as their cyclic bis(dimethylpropyleneguanidino) analogues (DMPG$_2$CH (**1b**), DMPG$_2$DPE (**2b**), DMPG$_2$BN (**3b**)) were synthesized by condensation of the Vilsmeyer salts [Cl-C(NMe$_2$)$_2$]Cl and [Cl-C(NMe)$_2$(CH$_2$)$_3$]Cl, respectively, with the corresponding primary amine. The activity of the copper complexes of these novel chiral *bis*guanidines was evaluated in the asymmetric aziridination of styrene by PhI=NTs. Although good activity and yields of *N*-tosylaziridine up to 98% were achieved, enantioselectivity remained at a level of only 5-7% ee at the best results. In an attempt to explain the poor selectivity, representative coordination compounds of **1a** with Cu(I) and Cu(II) as well as their hydrolytic reactions were examined. The crystal structures of an 1:2 complex [Cu^I{(μ^2-**1a**)Cu^{I}Cl}$_2$][Cu^{I}Cl$_2$] (**5**), an 1:1 complex [(**1a**)Cu^{II}Cl$_2$] (**6**), and the protonated ligand **1b** × 2 HClO$_4$ (**1c**) are described.

Introduction

The most common neutral nitrogen chelate ligands[1] used in asymmetric synthesis[2] are typically either alkaloids[3] or derivatives of azaaromatic compounds, e.g., bipyridines,[4] or imines such as bis(oxazolines) (box),[5,6] phosphinooxazolines,[7] corrins,[8] or salen-type[9] ligands (Scheme 1). However, chiral guanidines as ligands in coordination chemistry and catalytic transformations are unknown. In previous investigations we explored the donor properties of

tridentate and tetradentate peralkylguanidine ligands based on the tame and tren backbone.[10] A set of achiral neutral superbases ($pK_{BH+} > 24$) with a constraint geometry for trigonal bipyramidal complexes was synthesized and coordination compounds with Fe, Mn, Zn, Mo and Cu structurally characterized.

bis(oxazoline)-type "box"

salen-type

CH (**1**)

DPE (**2**)

BN (**3**)

R = R' = Me   TMG (**a**)
R = Me, R' = -(CH$_2$)$_3$-   DMPG (**b**)
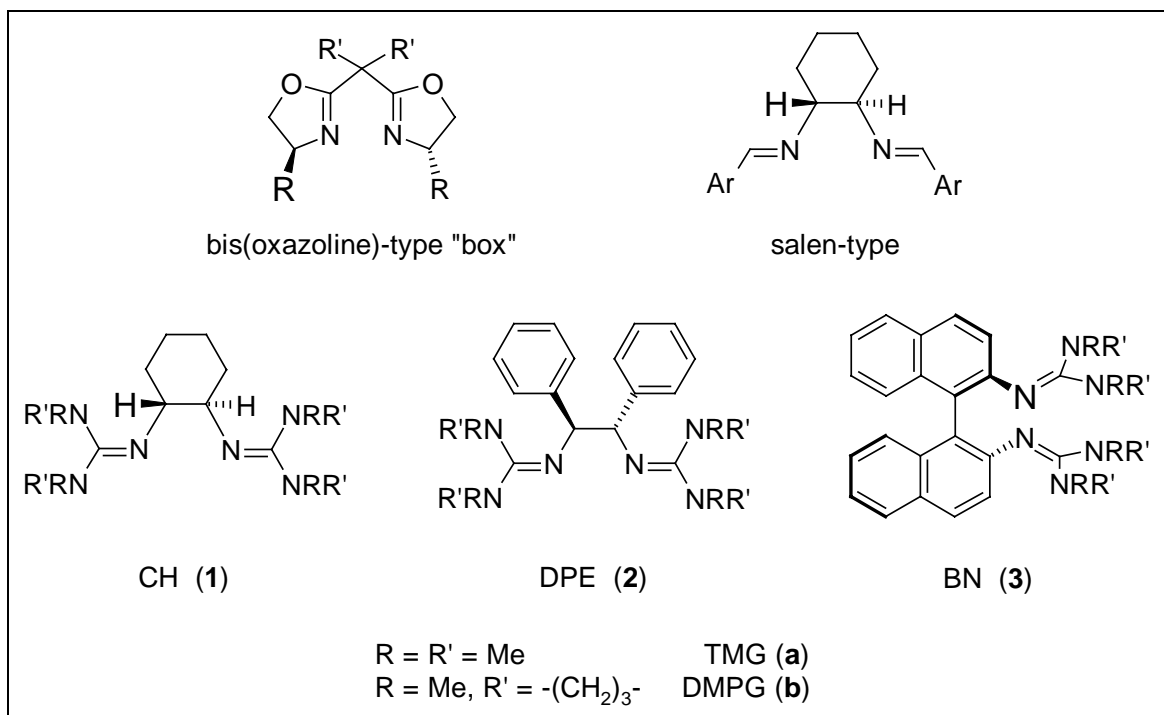
Scheme 1. C_2 symmetric ligands for the asymmetric olefin aziridination.

Chiral ligands are valuable tools in asymmetric synthesis and catalysis.[8a,11] Numerous ligands based on various skeletons and applications have evolved among which the asymmetric aziridination[12] and cyclopropanation[5a,b,6a,13,14] are most common for the evaluation of stereoselectivity of their complexes. Optically active aziridines are useful building blocks for nitrogen containing compounds.[15] Furthermore, aziridines occur in several natural products as subunits and their biological activities are influenced by the stereochemistry of the aziridine moiety.[15,16] While the development of catalysts for the alkene cyclopropanation belonged to the first examples of enantioselective metal catalysis mediated by a chiral Schiff base Cu(I) complex,[17] examples of reactions that involve catalytic enantioselective nitrogen-group transfer of either a nitrene species to an olefin or starting from imines have emerged only over the past decade.[6,9,12,18,19] Prominent ligands in asymmetric aziridinations were introduced by Evans et al.[6] and Jacobsen et al.[9] and belong to the bis(oxazoline)- (box) and salen-type. In combination with preferably Cu(I) (Rh(II),[12b,19d,e] Mn(III),[19a,b,c,f] and Fe(III)[19a] salts have also been investigated), these ligands catalyze the asymmetric aziridination of olefins by [*N*-(*p*-

2

toluenesulfonyl)imino]phenyliodinane (PhI=NTs).[20] The best results achieved in the copper-catalyzed aziridination of styrene with PhI=NTs are the landmarks set by Evans et al.[6c] (yield%/ee%: 89/57) and Jacobsen et al.[9a] (79/66) (Scheme 2). The results are very much dependent on the specific character of the ligands, as it is expressed by the deviation in terms of yield and enantiomeric excess, which in turn also depends on the substrate.
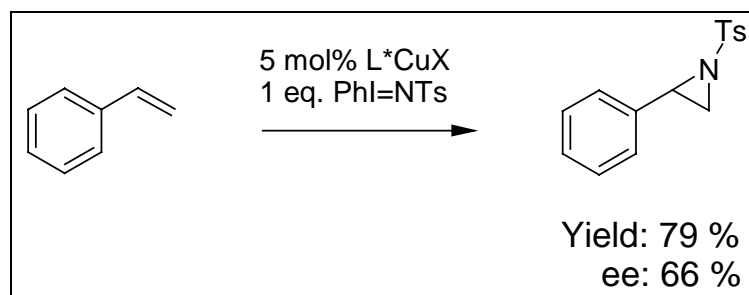
Scheme 2. Asymmetric aziridination of styrene with PhI=NTs in the presence of copper and a chiral ligand (L* = salen-type) as catalyst.[9a]

As for the mechanistic elucidation,[9b,c,21,22a,23] the involvement of a discrete Cu(III)-nitrene intermediate has been postulated by Jacobsen et al. indicating that a Cu(I)/Cu(III)-cycle participates in the catalysis.[9c] These findings suggest a remarkable similarity in the geometries of the transient species in asymmetric cyclopropanation[14,24] and aziridination.[18i,25]

PhI=NTs still seems to remain the nitrogen source of choice for the catalysis, although a number of endeavours have been undertaken in the search for alternatives. One attempt was the application of PhI=NSO$_2$Ar (Ar = PhOMe) by Andersson and coworkers,[26a] which gave higher ee´s (78%), along with good yields (86%). Other examples are e.g. PhI=NSO$_2$Ar (Ar = PhNO$_2$, PhOMe, etc.),[26] PhI=NSO$_2$R (R = 1-methylimidazolyl, 2-pyridyl, etc.),[27] PhI=NSes (TM*S-e*thane*s*ulfonyl),[28] chloramine-T,[29] bromamine-T,[30] and tert-butylsulfonamide.[31]

A recent paper describes a different approach to the stereoselective aziridination of alkenes via a chiral nitrido-manganese complex.[32] Other recent advances for commercial catalysts in a heterogenous processes involve the usage of microporous materials such as zeolite and result in respectable enantioselectivities of up to 61% ee when chiral modifiers e.g. bis(oxazolines) are employed.[33]

Peralkylated guanidines belong to the strongest organic neutral bases known.[34] They are several magnitudes superior in basicity than tertiary amines due to the excellent stabilization of the positive charge in their resonance stabilized cations.[35] This trend may be demonstrated by the pK_{BH+} (MeCN) values of the 1,2,2,6,6-pentamethyl piperidinium cation (18.62), the parent guanidinium cation (23.3), and the pentamethyl guanidinium cation (25.00).[35c] We set out to sythesize a new class of superbasic, C_2 symmetric ligands as chiral, peralkyl guanidine chelators, to test the new ligands in the asymmetric aziridination, and to structurally characterize complexes with Cu(I) and Cu(II). So far, all attempts to model this reaction, e.g. with achiral tris(pyrazolylborate) copper complexes, failed.[22] We intended to provide a ligand which due to the superbasic character of guanidines might stabilize the proposed Cu(III) nitrene species in order to gain insight in the mechanism.

Results and Discussion

Ligand preparation. The chiral ligands L* (**1a**-**3b**) were synthesized analogous to a method previously published.[10] The main problem associated with this synthesis is that polyguanidines as well as their hydrochlorides are extremely hygroscopic. Typically, they cannot be purified by destillation or sublimation without decomposition, and may not be subjected to column chromatography on polar phases (SiO_2, Al_2O_3). Therefore, high selectivity of the reaction was essential. By reaction of the corresponding primary amine with the Vilsmeyer salts [Cl-C(NMe$_2$)$_2$]Cl and [Cl-C(NMe)$_2$(CH$_2$)$_3$]Cl, respectively, in acetonitrile solution and triethylamine as auxiliary base at elevated temperatures, a nearly quantitative transformation was accomplished (Scheme 3). This method was first described by Eilingsfeld and Seefelder[36] and later improved by Kantlehner et al.[37] for *mono*guanidines. The Vilsmeyer salts are obtained by reaction of the ureas with phosgene[38] or oxalyl chloride in toluene.[39] Separation from the by-product HNEt$_3$Cl is accomplished by the addition of 1 eq. of NaOH per guanidine functionality and removal of the NEt$_3$ and NaCl by crystallization from acetonitrile / diethyl ether. Deprotonation of the guanidinium hydrochlorides with 50% KOH yield the free guanidine bases in 75 - 89%. The DMPG analogues are difficult to be liberated from water and therefore are better deprotonated with 10 eq. NaH in dry THF. The ligands are air-stable but slowly hydrolyze within days when exposed to aqueous media under the formation of the corresponding ureas.
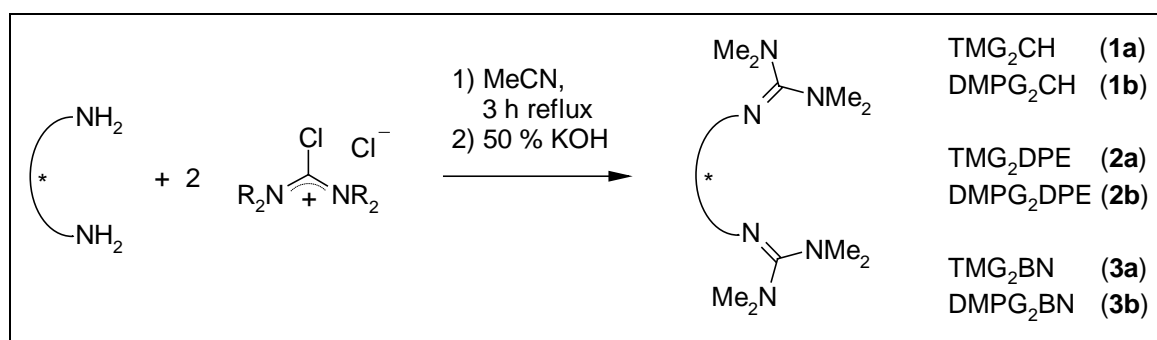
Scheme 3. Synthesis of chiral ligands L* for asymmetric copper-catalyzed aziridination.

Spectroscopic studies. EI mass spectra of the ligands display the molecular ions of **1** - **3**. Their IR spectra reveal a strong single absorption at wavenumbers of 1630-1580 cm^{-1}, which is assigned to the ν(C=N) vibration. ^{1}H NMR spectra of **1** and **2** show two singlets for the *N*-methyl groups, while for ligand **3** only one singlet is observed at room temperature. The rt 200 MHz ^{13}C NMR spectra of **1** reveal two methyl signals, **2** and **3** exhibit just one methyl resonance. The appearance of two chemically inequivalent methyl groups is due to hindered rotation about the C=N double bond of pentaalkylguanidines leading to the literature known *syn/anti*-isomerization (Scheme 4).[35b,40] This barrier to rotation is markedly lowered by protonation or by increased steric demand of the alkyl groups.
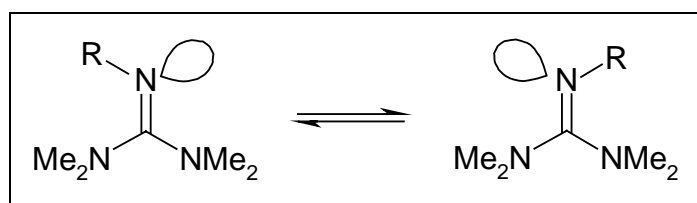
Scheme 4. The *syn/anti*-isomerization of pentasubstituted guanidines.

Aziridination studies. According to Evans´ procedure[6c] the copper complexes were formed *in situ* prior to combination with the suspension containing PhI=NTs as nitrene source and styrene in the corresponding solvent. A calibration experiment with box and CuOTf was carried out, the analytic protocol verified within an experimental error of 1-2% (entries 1, 2 compared to entries 5-7), and the results of the aziridination reactions including entries with literature known ligands summarized in Table 1. From the literature it is known that ligand-free Cu salts with noncoordinating anions (entries 0a) promote the formation of aziridines well in comparison to Cu salts with coordinating anions (entries 0b).

In C_6H_6 nearly quantitative yields and at the same time literally no enantioselectivities were obtained, regardless of the catalyst applied (entries 8-10, 12-14, 16, 18, 20, 22, 24). This may have occured because of the poor solubility of the catalyst - thus inhomogenous and containing uncoordinated copper centers - a fast, non-enantioselective reaction takes place. In MeCN good solubility was achieved at the expense of styrene conversion, yields of just up to 48-65% after workup were achieved, yet ee´s remained at a low level of <2-7% (entries 11, 15, 17, 19, 21, 23). This behavior can be interpreted in such way that contrary to the reactions performed in benzene, no free copper centers are present in acetonitrile solutions. It is assumed that in MeCN solution copper is chelated by the ligand (although this supposition has not quite been established for all complexes in the solid state and has even been disproved for complex **5**, Figure 1) and due to the steric hindrance induced by the guanidine ligands, approach of the substrate molecule styrene to the copper-nitrene species[9b,c] is limited.[21] Neither employing 2.2 eq. of ligand (entries 29-31) instead of the typically used 1.2 eq. nor solvents of medium polarity (CH_2Cl_2, Me_2CO, entries 27, 28, 30), nor working at lower temperatures (entries 25-33) did significantly improve the enantioselecitivity. Application of other nitrene sources such as *p*-toluenesulfonyl azide or BOC azide also proved to be ineffective (entries 34-37 and 38, 39). Nevertheless, we still believe that these ligands unfold a higher potential in other asymmetric catalytic reactions, such as the cyclopropanation or epoxidation of alkenes, as is known for other ligands with limited utility as aziridination catalysts.[41] In summary, it can be said that no trend of ligand inhibition rather than a certain degree of ligand acceleration was observed to approximately 5% higher yield, compared to the blind experiment without ligands.[6d]

Table 1. Aziridination of styrene with copper catalyst and chiral ligands.[a]

Entry	L*	CuX	Solvent	Time (Temp)	Yield [%][b]	ee [%][c]
0a (lit.)[6d]	-	CuClO₄	CH_2Cl_2	n.n. (RT)	90	-
0a (lit.)[6d]	-	CuOTf	CH_2Cl_2	n.n. (RT)	92	-
0a (lit.)[6d]	-	Cu(OTf)₂	MeCN	n.n. (RT)	92	-
0b (lit.)[6d]	-	CuCl	CH_2Cl_2	n.n. (RT)	61	-
0b (lit.)[6d]	-	CuBr	CH_2Cl_2	n.n. (RT)	56	-
1 (lit.)[6c]	box	CuOTf	C_6H_6	10 h (21 °C)	99	57
2 (lit.)[6c]	box	CuOTf	styrene	2.5 h (0 °C)	89	63
3 (lit.)[9c]	salen	CuPF₆	CH_2Cl_2	(10 °C)	-[d]	41[e]
4 (lit.)[9a]	salen	CuOTf	CH_2Cl_2	(-78 °C)	79	66

5 (own)	box	CuOTf	C$_6$H$_6$	12 h (RT)	98	58
6 (own)	box	Cu(OTf)$_2$	C$_6$H$_6$	18 h (RT)	97	56
7 (own)	box	CuClO$_4$	MeCN	36 h (-18 °C)	98	55
8	TMG$_2$CH	CuOTf	C$_6$H$_6$	12 h (RT)	98	2
9	TMG$_2$CH	Cu(OTf)$_2$	C$_6$H$_6$	12 h (RT)	97	3
10	TMG$_2$CH	CuPF$_6$	C$_6$H$_6$	10 h (RT)	95	<2
11	TMG$_2$CH	CuPF$_6$	MeCN	20 h (RT)	65	<2
12	DMPG$_2$CH	CuOTf	C$_6$H$_6$	12 h (RT)	97	3
13	DMPG$_2$CH	Cu(OTf)$_2$	C$_6$H$_6$	18 h (RT)	95	5
14	TMG$_2$DPE	CuOTf	C$_6$H$_6$	12 h (RT)	96	<2
15	TMG$_2$DPE	CuOTf	MeCN	12 h (RT)	53	3
16	DMPG$_2$DPE	CuOTf	C$_6$H$_6$	12 h (RT)	96	<2
17	DMPG$_2$DPE	CuOTf	MeCN	12 h (RT)	48	<2
18	TMG$_2$BN	CuOTf	C$_6$H$_6$	12 h (RT)	98	4
19	TMG$_2$BN	CuOTf	MeCN	12 h (RT)	62	5
20	TMG$_2$BN	Cu(OTf)$_2$	C$_6$H$_6$	12 h (RT)	96	<2
21	TMG$_2$BN	Cu(OTf)$_2$	MeCN	12 h (RT)	59	3
22	DMPG$_2$BN	CuOTf	C$_6$H$_6$	12 h (RT)	93	3
23	DMPG$_2$BN	CuOTf	MeCN	12 h (RT)	54	2
24	DMPG$_2$BN	Cu(OTf)$_2$	C$_6$H$_6$	12 h (RT)	95	<2
25	TMG$_2$BN	CuClO$_4$	MeCN	36 h (-18 °C)	17	3
26	TMG$_2$CH	CuClO$_4$	MeCN	36 h (-18 °C)	10	<2
27	TMG$_2$CH	CuClO$_4$	CH$_2$Cl$_2$	36 h (-18 °C)	8	<2
28	TMG$_2$CH	CuClO$_4$	Me$_2$CO	36 h (-18 °C)	9	3
29[f]	TMG$_2$BN	CuClO$_4$	MeCN	36 h (-18 °C)	11	8
30[f]	TMG$_2$BN	CuClO$_4$	CH$_2$Cl$_2$	36 h (-18 °C)	9	6
32[f]	TMG$_2$BN	CuClO$_4$	Mix[g]	36 h (-18 °C)	9	4
33[f]	TMG$_2$BN	Cu(ClO$_4$)$_2$	MeCN	36 h (-18 °C)	8	3
31[f]	TMG$_2$BN	CuClO$_4$	MeCN	36 h (RT)	51	7
34[h]	TMG$_2$CH	CuPF$_6$	MeCN	3 h (reflux)	58	<2
35[h]	TMG$_2$CH	CuPF$_6$	MeCN	15 h (RT)	<1	n.d.
36[h]	TMG$_2$CH	CuPF$_6$	C$_6$H$_6$	15 h (RT)	<2	n.d.
37[h]	TMG$_2$CH	CuPF$_6$	C$_6$H$_6$	15 h (reflux)	32	<2
38[i]	TMG$_2$CH	CuPF$_6$	MeCN	18 h (RT)	0	n.d.
				3 h (reflux)	0	n.d.
39[i]	TMG$_2$CH	CuOTf	C$_6$H$_6$	15 h (RT)	0	n.d.
		Cu(OTf)$_2$	MeCN		0	n.d.

[a] Typical experiment: styrene : PhI=NTs : CuX : L* = 5 : 2 : 0.1 : 0.12. [b] Values represent isolated yields of aziridine based on PhI=NTs as limiting reagent. [c] Enantiomeric excess was determined by ^{1}H NMR chiral shift reagents, absolute configurations not distinguished / [d] not reported / [e] chiral HPLC. [f] 2.2 eq. of L*. [g] C$_6$H$_6$ / MeCN (1:1). [h] Nitrene source: TsN$_3$. [i] Nitrene source: BOCN$_3$.

Complex formation. The poor enantioselectivity observed in the asymmetric aziridination reactions gave rise to the question of the coordination geometry of the copper complexes employed as catalysts. With the aim to isolate well defined 1:1 complexes equimolar amounts of the ligands L and dehydrated copper (I/II) chlorides, triflates or perchlorates dissolved in dry, degassed MeCN were combined. The complexes were precipitated by addition of diethyl ether to the MeCN solution. The precipitates were perfectly soluble in MeCN, however, sparingly soluble in Me_2CO. Decomposition in DMSO or in protic solvents such as D_2O or EtOH occurs. The triflate derived complexes turned out to be difficult to characterize because they did not tend to crystallize and because of intrinsic problems associated with their combustion analysis. Better reproducible results were obtained with chloro or perchlorate derived complexes. With CuCl and **1a** well defined coordination compounds of the composition (CuCl)L and (CuCl)$_2$L but no counterpart (CuCl)L$_2$ have been isolated (Scheme 5).
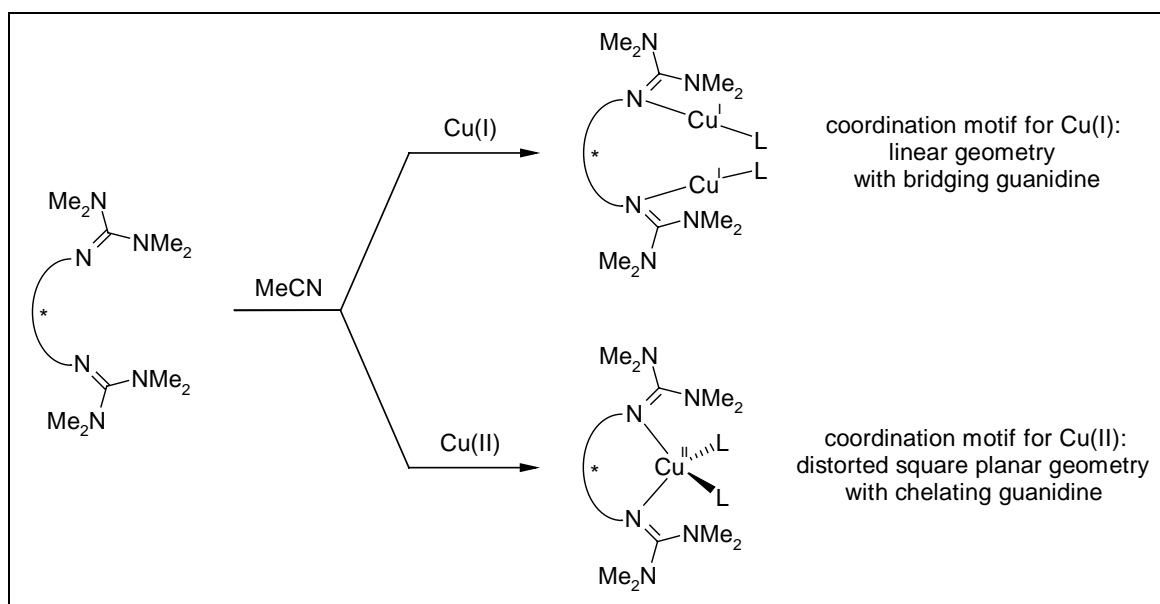
Scheme 5. Schematic synthesis of chiral copper (I/II) complexes.

The Cu(I) complexes are nearly colorless and extremely sensitive to air while the Cu(II) complexes appear in green color. In general, it was observed that metal hydroxides along with the protonated ligand were formed when the complexes were exposed to aqueous solvent mixtures. These findings are explained by the extremely high proton affinity of guanidines: Deprotonation of an aqua ligand irreversibly induces the hydrolytic cleavage of the metal-nitrogen bond, a pattern that is also typical for amido complexes (Scheme 6).
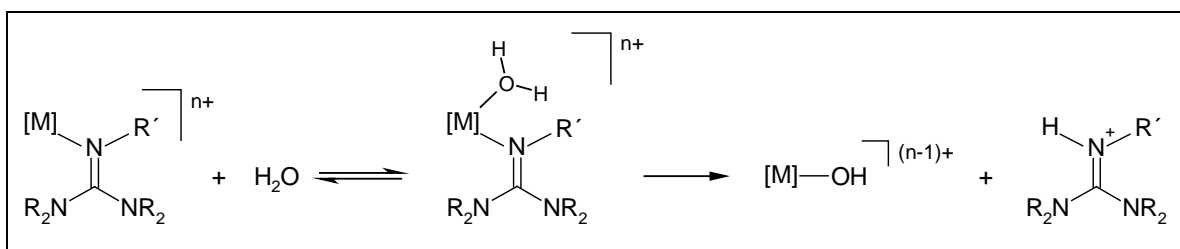
Scheme 6. Hydrolytic cleavage of the metal-nitrogen bond.

Spectroscopic studies. The copper complexes could not be detected by EI mass spectroscopy. The parent molecular ions or a ligand-Cu fragment were detected by FD mass spectroscopy. In some cases the ligand as cluster together with the anion provided by the copper salt was detected, either along with the parent molecular ion or by itself. In the case of the unusual 1:2 tetranuclear complex $[Cu^I\{(\mu^2\text{-}\mathbf{1a})Cu^ICl\}_2][Cu^ICl_2]$ (**5**), APCI proved to be a powerful method of mass spectroscopy to confirm its structure (see below).

While correct elemental analyses were received for **4**-**7**, all other attempts of complex synthesis in a copper salt to ligand ratio of 1:1 yielded reproducible results that hint formation of more complex compounds despite showing the correct fragment in the FD mass spectra.

As expected the Cu(II) complexes are paramagnetic, whereas the Cu(I) complexes are diamagnetic and colorless. Their 200 MHz room temperature ^{1}H and ^{13}C NMR spectra in CD₃CN show one broad resonance for the guanidine *N*-methyl protons in contrast to a series of tripod copper complexes[10c] which exhibit two signals for the NMe₂ protons. This behavior is explained by a rigid >C=N- bonding axis on the NMR time scale rendering one NMe₂ group *cis* and the other one *trans* with respect to the Cu substituent. Obviously, when the charge of the metal cation is distributed over three guanidine groups the individual bond characters remain more pronounced and the barrier to rotation is higher than in the noncoordinated *bis*guanidine. There is probably also an increased steric congestion in complexes. By lowering the temperature, coalescence of the proton signals is observed at 301 K for **7** (**1a** × Cu^{I}ClO₄) (500 MHz, CD₃CN). The barrier to rotation about the C=N bond could not be estimated because in the low temperature region other coalescence phenomena occurred and made its determination impossible.[42]

In their IR spectra, the copper complexes show a split of the absorption for the ν(C=N) vibration. A similar behavior is observed for the protonated ligand **1c**. This splitting is a typical feature due to lowering of the molecular symmetry in guanidinium cations. It is also found in the hexamethylguanidinium cation.[43]

Molecular structure of $[Cu^I\{(\mu^2\text{-}\mathbf{1a})Cu^ICl\}_2][Cu^ICl_2]$ (**5**) (Figure 1)**.** Selected bond lengths and angles are listed in Table 2. Light green single crystals of **5** were obtained by diffusion of dry ether into saturated acetonitrile solution.
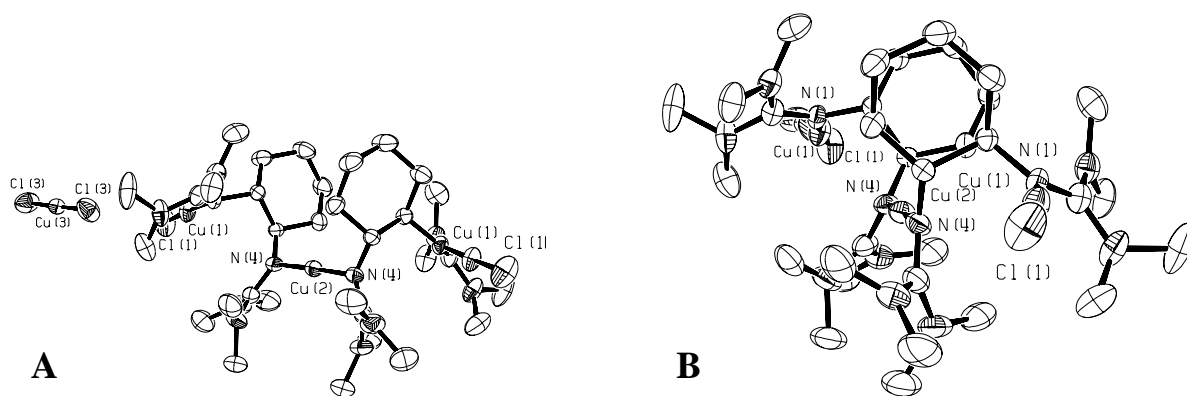
Figure 1. ORTEP Plot of $[Cu^I\{(\mu^2\text{-}\mathbf{1a})Cu^ICl\}_2][Cu^ICl_2]$ (**5**), thermal ellipsoids at 50% probability level, H atoms omitted for clarity.[62]

The structure of **5** confirms the tendency of copper(I) to form complexes with linear coordination geometry.[44,45] Four linearly coordinated copper(I) centers, three each with different counterparts, are realized. One lies in between of two bridging ligand molecules (Cu(2): 178.1°), the second guanidine function of each **1a** linearly binds another copper atom (Cu(1): 174.4°) which carries a terminal chlorine atom. Finally, the structure contains a linear $[Cu^ICl_2]^-$ anion (Cu(3): 179.6°) for electroneutrality. Interestingly, the Cu-N distances N-Cu-N and N-Cu-Cl are nearly equal despite of having different co-ligands (N(4)-Cu(2): 188.2 pm and N(1)-Cu(1): 187.9 pm). They are of typical length for biscoordinated copper(I), the Cu-Cl distances (208.5 pm) also do not show any abnormality. The configuration (R) of the ligand is preserved in the complex, while the cyclohexane rings of the two ligand molecules and guanidine groups N-Cu-N are located in an almost ecliptical positions. The remaining two guanidine units (N-Cu-Cl) are situated at maximal distance to each other, *trans* relative to the N-Cu-N axis (Figure 1B). The situation of the guanidine functionality can be summarized by reviewing the quotient ρ (see below, Figure 4, Table 5). A value of 0.97 symbolizes a rather

strong effect of positive charge from the copper atom to the guanidine, including the consequences mentioned below.

Table 2. Selected bonding distances [pm], angles, dihedral angles and sum of bond angles [°] in $[Cu^I\{(\mu^2\text{-}\mathbf{1a})Cu^ICl\}_2][Cu^ICl_2]$ (**5**); crystallographic standard deviations in parentheses.

Cu(1)-N(1)	188.2(3)	Cu(2)-N(4)	187.9(3)
Cu(1)-Cl(1)	208.5(1)	Cu(3)-Cl(3)	208.5(1)
N(1)-C(7)	132.0(5)	N(4)-C(12)	132.5(5)
N(2)-C(7)	136.7(5)	N(5)-C(12)	136.9(6)
N(3)-C(7)	135.5(5)	N(6)-C(12)	135.5(6)
N(1)-C(1)	148.5(5)	N(4)-C(2)	145.6(5)
N(2)-C(8)	145.7(5)	N(5)-C(13)	147.3(6)
N(2)-C(9)	145.6(7)	N(5)-C(14)	145.1(7)
N(3)-C(10)	144.6(7)	N(6)-C(15)	146.5(7)
N(3)-C(11)	146.2(6)	N(6)-C(16)	145.6(7)
N(1)-Cu(1)-Cl(1)	174.43(10)	Cl(3)-Cu(3)-Cl(3a)	179.59(11)
N(4)-Cu(2)-N(4a)	178.1(2)		
N(1)-C(1)-C(2)-N(4)	-62.7(4)		
N(1)-C(7)-N(2)-C(8)	-144.5(4)	N(4)-C(12)-N(5)-C(13)	-138.7(5)
N(1)-C(7)-N(2)-C(9)	46.0(6)	N(4)-C(12)-N(5)-C(14)	27.0(6)
N(1)-C(7)-N(3)-C(10)	22.6(6)	N(4)-C(12)-N(6)-C(15)	-145.9(5)
N(1)-C(7)-N(3)-C(11)	-140.0(4)	N(4)-C(12)-N(6)-C(16)	37.2(7)
Σ°C(7)	360.0	Σ°C(12)	360.0
Σ°N(1)	359.9	Σ°N(4)	359.1
Σ°N(2)	359.3	Σ°N(5)	358.6
Σ°N(3)	357.9	Σ°N(6)	359.9

A contrary example, bearing an identical backbone to ligand **1,** was found by Stack et al.[46] In this structure Cu(I) possesses an unusual trigonal planar geometry with peralkylated amine functions of a cyclohexane diamine ligand and one molecule of acetonitrile. In a complex published by Evans et al., it is hinted that the bidentate, and usually chelating bisoxazoline ligand, forms a helical structure with linear coordination of the copper(I) centers by two N

atoms of two different ligand molecules.[47] A 1:1 complex of **1a** with Cu^ICl could not be crystallized so far which is probably because of the known difficulties in crystallization of helical structures. The proposed structure of a 1:1 complex based on the molecular structure of the 1:2 complex is shown in Scheme 7.
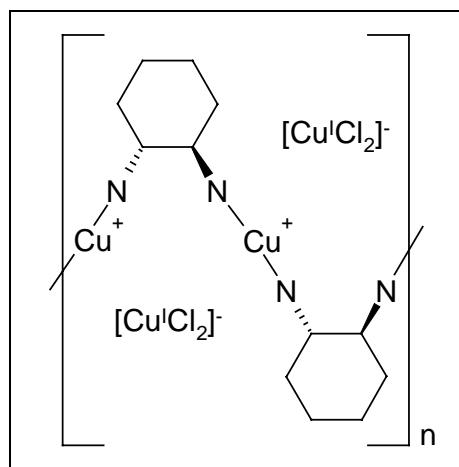
Scheme 7. Proposed helical structure of a 1:1 complex of **1a** and Cu^ICl.

Molecular structure of [(**1a**)Cu^{II}Cl₂] (**6**) (Figure 2)**.** Selected bond lengths and angles are listed in Table 2. Complex **6** was prepared as 1:1 complex of **1a** and CuCl₂, and X-ray quality crystals were obtained by slow diffusion of dry diethyl ether into saturated acetonitrile solution.
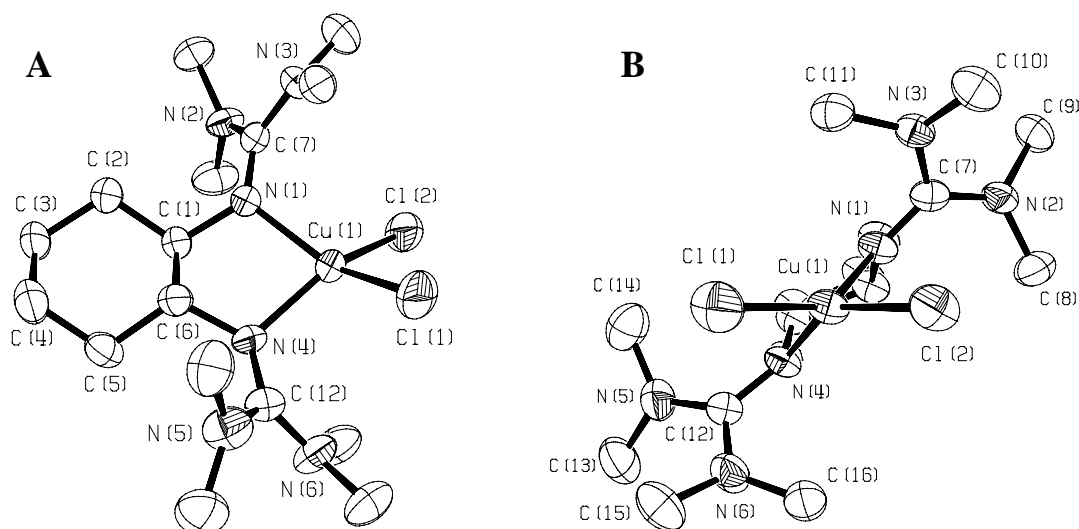
Figure 2. ORTEP Plot of [(**1a**)Cu^{II}Cl₂] (**6**), thermal ellipsoids at 50% probability level, H atoms omitted for clarity.[62]

12

Table 3. Selected bonding distances [pm], angles, dihedral angles and sum of bond angles [°] in [(**1a**)Cu^{II}Cl$_2$] (**6**); crystallographic standard deviations in parentheses.

Cu(1)-N(1)	196.7(6)	Cu(1)-Cl(1)	224.2(3)
Cu(1)-N(4)	197.9(6)	Cu(1)-Cl(2)	223.9(2)
N(1)-C(1)	145.9(9)	N(4)-C(6)	146.1(10)
C(7)-N(1)	130.6(10)	C(12)-N(4)	132.1(10)
C(7)-N(2)	138.3(10)	C(12)-N(5)	139.4(11)
C(7)-N(3)	135.5(10)	C(12)-N(6)	134.0(11)
N(1)-Cu(1)-N(4)	83.5(3)	Cl(1)-Cu(1)-Cl(2)	102.12(11)
N(1)-Cu(1)-Cl(1)	142.4(2)	N(4)-Cu(1)-Cl(2)	143.8(2)
N(1)-Cu(1)-Cl(2)	97.9(2)	N(4)-Cu(1)-Cl(1)	98.0(2)
C(1)-N(1)-Cu(1)	111.6(5)	C(6)-N(4)-Cu(1)	110.5(5)
C(1)-N(1)-C(7)	122.0(6)	C(6)-N(4)-C(12)	122.4(7)
N(1)-C(1)-C(6)-N(4)	-51.6(8)		
N(1)-C(7)-N(2)-C(8)	-32.5(12)	N(4)-C(12)-N(5)-C(13)	139.0(10)
N(1)-C(7)-N(2)-C(9)	138.5(8)	N(4)-C(12)-N(5)-C(14)	-40.3(13)
N(1)-C(7)-N(3)-C(10)	145.4(8)	N(4)-C(12)-N(6)-C(16)	145.7(9)
N(1)-C(7)-N(3)-C(11)	-14.7(11)	N(4)-C(12)-N(6)-C(16)	-13.2(14)
Σ°C(7)	360.0	Σ°C(12)	359.9
Σ°N(1)	356.5	Σ°N(4)	353.2
Σ°N(2)	359.4	Σ°N(5)	360.0
Σ°N(3)	357.2	Σ°N(6)	356.8

In contrast to the copper(I) structure, the copper(II) cation is coordinated by a chelating ligand in a *C*$_2$ symmetric distorted square planar coordination with an interplanar angle of 50.4° between the planes defined by N(1)-Cu(1)-N(4) and Cl(1)-Cu(1)-Cl(2). The average Cu-N distance in **6** (197.3 pm) is about 9 pm longer than the average Cu-N distance in **5** (188.1 pm). At the same time, the average Cu-Cl distance is almost 16 pm longer than the corresponding distance in the Cu(I) structure (224.1 vs. 208.5 pm). The ρ values of **6** are slightly lower compared to the Cu(I) complex **5** (0.96 vs. 0.97). This is due to two anionic chloro ligands that lower the effective charge at the Cu(II) atom in **6** and result in less delocalization effects in the guanidine group. The latter is consistent with the ρ quotients of

copper (I/II) complexes and the tripodal ligand TMG$_3$tren[51] (second section Table 5). In these complexes Cu(I) shows the lower value (0.94 in Cu(I) vs. 0.96 in Cu(II)) as expected for the lower effective charge at a Cu(I) center.

In another structural example, a Cu(II) core is coordinated by 2 or even 3 ligand molecules of 1,2-diaminocyclohexane.[48] This behavior could not be verified in case of our sterically demanding guanidines **1**-**3**. Even if a twofold excess of ligand **1**-**3** was employed, a maximum of 2 guanidine N atoms per Cu center is realized.

Molecular structure of protonated ligand 1b × 2 HClO₄ (1c). Selected bond lengths and angles are listed in Table 4, the H atom positions were calculated. The hydrolytic reaction of the copper complexes was studied. Proof for the above mentioned mechanism was obtained by the X-ray determination of the crystal structure of **1c**. The guanidinium hydroperchlorate was received by reaction of **1b** and Cu(I)ClO₄ in the presence of traces of water and crystallization from MeCN / Et₂O. A mixture of insoluble copper hydroxides was formed during the reaction as green precipitate and removed by filtration.
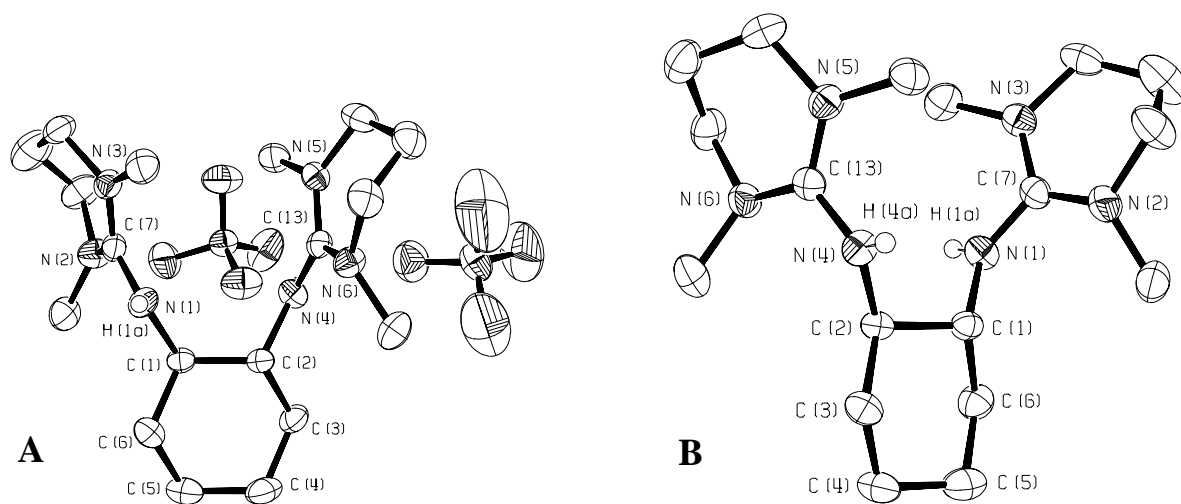
Figure 3. ORTEP Plot of **1b** × 2 HClO₄ (**1c**), thermal ellipsoids at 50% probability level, H atoms (except H1A and H4A) omitted for clarity.[62]

The structure shows the six-membered cyclohexane ring in a typical chair conformation while the two guanidine groups as well as the attached H atoms (H1A and H4A) are located *anti* to each other with a torsion angle N(1)-C(1)-C(2)-N(4) of -56.8° (Figure 3B). The ρ value (Table 5) is calculated to 1.004 which indicates perfect delocalization of positive charge

14

within the guanidine moiety and three equal C-N bonds as it has been observed in TMG$_2$en $\times$ 2 HCl[10a] and the hexamethylguanidinium cation.[49] The bond angle sums about the CN$_3$ unit are close to 360° for each carbon atom.

Table 4. Selected bonding distances [pm], angles, dihedral angles and sum of bond angles [°] in **1b** $\times$ 2 HClO$_4$ (**1c**); crystallographic standard deviations in parentheses.

N(1)-C(1)	146.3(5)	N(4)-C(2)	146.9(5)
C(7)-N(1)	134.4(5)	N(4)-C(13)	133.9(5)
C(7)-N(2)	134.1(5)	N(5)-C(13)	132.6(5)
C(7)-N(3)	133.0(5)	N(6)-C(13)	135.0(5)
N(1)-H(1A)	88.0(calc.)	N(4)-H(4A)	88.0(calc.)
C(1)-N(1)-C(7)	126.5(3)	C(2)-N(4)-C(13)	125.3(3)
N(1)-C(1)-C(2)-N(4)	-56.8(4)		
N(1)-C(7)-N(2)-C(8)	-166.3(4)	N(4)-C(13)-N(5)-C(14)	-162.4(4)
N(1)-C(7)-N(2)-C(11)	38.4(6)	N(4)-C(13)-N(5)-C(17)	10.1(5)
N(1)-C(7)-N(3)-C(10)	-161.9(4)	N(4)-C(13)-N(6)-C(16)	-167.0(4)
N(1)-C(7)-N(3)-C(12)	9.2(6)	N(4)-C(13)-N(6)-C(18)	38.3(6)
Σ°C(7)	359.9	Σ°C(13)	359.9
Σ°N(2)	355.5	Σ°N(5)	359.6
Σ°N(3)	359.4	Σ°N(6)	355.3

Structural parameter ρ. As a structural parameter that allows estimation of charge delocalization within the guanidine moiety by comparing the shortest C=N bond distance to the average of the other two C-NR$_2$ distances (a to b,c in Figure 4), the value $\rho = 2a / (b + c)$ was established.[50] In the free guanidine (one pure double bond (C=N) vs. two single bonds (C-N$_{NMe2}$), first section of Table 5), ρ assumes a value of 0.92 (when attached to an aromatic system ρ can become 0.93[51]). In transition metal complexes the C=N bond is stretched while the C-N$_{NMe2}$ bonds are getting shorter which results in ρ values of 0.94 to 0.97 depending on the effective charge of the metal cation. Finally, when a guanidine is protonated three partial double bonds are formed with equal bond lengths and perfect charge delocalization: $\rho = 1.00$ (last section in Table 5).
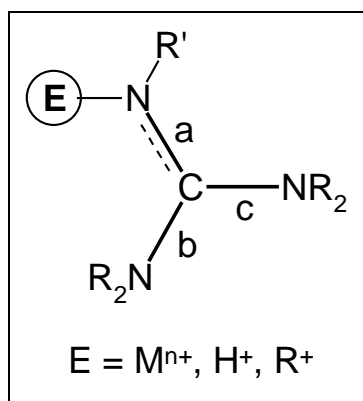
Figure 4. C-N bonds a, b and c for the determination of quotient ρ.

Table 5. Average C=N vs. C-NR$_2$ distances [pm] and quotient ρ, standard deviations (±).[a]

Complex	$\varnothing$ C=N (a)	$\varnothing$ C-NR$_2$ (b, c)	ρ
[(**A**)Mo(CO)$_3$] [b,c,10b]	127.6±0.0	138.7±0.9	0.920
[(**C**)Zn^{II}Cl$_2$] [b,e,10a]	127.9±0.0	139.5±0.4	0.917
[(**A**)Cu^{II}Cl]Cl [c,10c]	131.4±0.3	136.4±0.5	0.964
[(**A**)Cu^{II}(NCMe)](ClO$_4$)$_2$ [c,10c]	130.8±0.7	136.3±0.8	0.960
[(**A**)Cu^I]Cl [c,10c]	129.4±0.0	137.6±0.6	0.940
[(**B**)Cu^I]ClO$_4$ [d,10c]	130.3±0.5	137.8±1.6	0.945
[(**1a**)Cu^{II}Cl$_2$] (**6**)	131.4±0.8	136.8±2.2	0.960
[Cu^I{(μ^2-**1a**)Cu^{I}Cl}$_2$]$^+$ (**5**) (N-Cu-Cl)	132.0±0.0	136.1±0.6	0.970
[Cu^I{(μ^2-**1a**)Cu^{I}Cl}$_2$]$^+$ (**5**) (N-Cu-N)	132.5±0.0	136.2±0.7	0.973
[(DMPG$_2$CH)H$_2$](ClO$_4$)$_2$ (**1c**)	134.2±0.3	133.7±0.9	1.004
[(**D**)H$_2$]Cl$_2$ [f,10a]	133.6±0.0	134.0±0.2	0.997
[(**E**)][Fe(CO)$_4$C(O)NMe$_2$] [g,49]	132.9±0.0	133.7±0.7	0.994[52]

[a] Structural parameter ρ = $\varnothing$ C=N / $\varnothing$ C-NR$_2$. [b] Complex bears a free guanidine group in form of a noncoordinated „dangling" arm of a tripodal ligand. [c] Ligand (**A**) = 1,1,1-Tris{2-[N^2-(1,1,3,3-tetramethylguanidino)]ethyl}amine (TMG$_3$tren). [d] Ligand (**B**) = 1,1,1-Tris{2-[N^2-(1,3-dimethylpropyleneguanidino)]ethyl}amine (DMPG$_3$tren). [e] Ligand (**C**) = 1,1,1-Tris[N^2-(1,1,3,3-tetramethylguanidino)methyl]ethane. [f] Ligand (**D**) = 1,2-Di[N^2-(1,1,3,3-tetramethylguanidinium)]ethane dichloride tetrahydrate (TMG$_2$en × 2 HCl). [g] Ligand (**E**) = [C(NMe$_2$)$_3$]$^+$.

Conclusions

The synthesis of novel chiral bidentate ligands with extremely basic peralkyl guanidine functions and complexes thereof with Cu(I) and Cu(II) has been presented. Due to the ability of guanidines to delocalize positive charge into the guanidinium moieties, the ligands **1a**-**3b** stabilize cationic and dicationic complexes. The structural solution of two complexes formed from ligand **1a** with Cu$^\text{I}$Cl (**5**) and Cu$^\text{II}$Cl$_2$ (**6**) is described as well as the structure of protonated ligand **1b** $\times$ 2 HClO$_4$ (**1c**). Whereas the Cu(I) structure reveals a linear ligand coordination, Cu(II) shows distorted square planar geometry. Various copper ligand combinations have been evaluated in the catalytic asymmetric aziridination of styrene by PhI=NTs. High activity but poor enantioselectivity was observed. Future perspectives of our chiral guanidines may be found in the catalytic asymmetric cyclopropantion or epoxidation.

Experimental Section

Materials and methods. All experiments were carried out in hot assembled and under vacuum cooled glassware under inert atmosphere of argon 4.8 dried with P$_4$O$_{10}$ granulate. Solvents, triethylamine and styrene were purified according to literature procedures[53] and also kept under inert atmosphere. Enantiomerically pure (*1R,2R*)-1,2-diaminocyclohexane was obtained from the commercially available racemic substrate by racemate separation according to a published method.[54] (*1R,2R*)-(+)-1,2-diamino-1,2-diphenylethane[55] was synthesized by a literature method. *R*(+)-2,2´-diamino-1,1´-binaphthalene was used as purchased from Aldrich. [CuOTf] $\times$ 0.5 C$_6$H$_6$,[56] [Cu(CH$_3$CN)$_4$]PF$_6$ and [Cu(CH$_3$CN)$_4$]ClO$_4$[57] were prepared by literature methods. CuCl[58] and CuCl$_2$[59] were purified and liberated from water, respectively according to literature. Substances sensitive to moisture and air were kept in a glove-box (Braun, Type MB 150 BG-1) under an atmosphere of nitrogen. PhI=NTs[60] was prepared by a published method and recrystallized from methanol/water at 5 °C. Purification of aziridination products was carried out by flash chromatography using MERCK silica gel 60 (0.063-0.200 mm). Analytical thin layer chromatography was performed on MERCK TLC aluminium sheets silica gel 60 F$_{254}$, visualization accomplished with UV light. Chiral shift reagent tris[3-(heptafluoropropylhydroxymethylene)-(+)-camphorato]europium(III), Eu(hfc)$_3$ was used as purchased from Aldrich.

Analytical data were recorded on the following instruments: - NMR: Bruker ARX 200 and DRX 500, - IR: Bruker IFS 88 FT, - MS(EI-70 eV): Varian MAT CH-7a, MS(FD): Finnigan MAT 95 S, MS(APCI): Hewlett Packard HP 5989 B, Elemental Analysis: Heraeus CHN-Rapid, Melting points: Büchi MP B-540 (uncorrected), X-ray: ENRAF-Nonius CAD4.

Caution! Phosgene is a severe toxic agent that can cause pulmonary embolism and in case of heavy exposition may be lethal. Use only at a good ventilated fume hood. Perchlorate salts are potentially explosive and should be handled with care.

The preparation of *N,N,N´,N´*-tetramethylformamidiniumchloride (**A**)[10b] and *N,N´*-dimethylpropylene-chlorformamidiniumchloride (**B**)[10c] is described elsewhere.

General procedure for the synthesis of the guanidine ligands. To a solution of the diamine and triethylamine in acetronitrile, 2 eq. of [(Me$_2$N)$_2$C-Cl]Cl (**A**), [{(CH$_2$)$_3$(NMe)$_2$}$_2$C-Cl]Cl (**B**), respectively, dissolved in the same solvent were slowly added under cooling in an ice bath. After the exothermic reaction declined, the mixture was refluxed for 3 h. Afterwards 2 eq. of NaOH dissolved in a minimum amount of water were added under vigorous stirring in order to deprotonate the HNEt$_3$Cl. After removal of the solvent as well as excess NEt$_3$ the precipitate was washed three times with dry ether to remove unreacted amine and dried in vacuo. The free base was obtained by complete deprotonation of the bishydrochloride with excess 50% KOH and extracting the aqueous phase with MeCN (alternatively (DMPG analogues) stirred in the presence of 10 eq. NaH in THF for 3 h at 60 °C). The combined filtrates were evaporated to dryness, redissolved (for solvent see details below), dried over MgSO$_4$, stirred over activated charcoal and filtered warm through Celite.

(*1R,2R*)-(-)-1,2-Bis[*N*^{2}-(1,1,3,3-tetramethylguanidino)]cyclohexane (TMG$_2$CH = 1a):
Diamine: (*1R,2R*)-1,2-diaminocyclohexane (5.7 g, 50 mmol), triethylamine (10.1 g, 14.0 mL, 100 mmol), 17.1 g (100 mmol) of [(Me$_2$N)$_2$C-Cl]Cl (**A**); 4.0 g (100 mmol) NaOH. Solvent used for purification: hexane. Yield: 13.8 g clear, yellow oil (89 mmol, 89%).
^{1}H NMR (200.1 MHz, CD$_3$CN, 25 °C): δ = 3.07-2.88 (m, 2 H, C$_{1/2}$*H*), 2.68 (s, 12 H, C*H*$_3$), 2.46 (s, 12 H, C*H*$_3$), 1.79-1.50 (m, 4 H, C$_{3/6}$*H*$_2$), 1.44-1.13 (m, 4 H, C$_{4/5}$*H*$_2$) ppm; ^{13}C NMR (50.3 MHz, CD$_3$CN, 25 °C): δ = 158.6 (*C*N$_3$), 63.8 (*C*$_{1/2}$H), 40.1 (*C*H$_3$), 38.8 (*C*H$_3$), 34.7 (*C*$_{3/6}$H$_2$), 26.2 (*C*$_{4/5}$H$_2$) ppm; IR (KBr): $\tilde{v}$ = 2924 s, 2853 s, 2793 m, 1627 s(br), 1493 s, 1454

18

m, 1358 s, 1233 m, 1128 s, 1009 s, 997 w, 907 w, 615 w cm^{-1}; MS (70 eV, EI): m/z (%) = 310 (21) [(**1a**)]$^+$, 195 (39) [(**1a**)-TMG]$^+$, 85 (100) [CH]$^+$; elemental analysis calcd. (%) for C$_{16}$H$_{34}$N$_6$ (310.5): C 61.90, H 11.04, N 27.07; found C 61.60, H 10.80, N 26.82.

(*1R,2R*)-(-)-Bis[*N²*-(1,3-dimethylpropyleneguanidino)]cyclohexane (DMPG$_2$CH = 1b):

Diamine: (*1R,2R*)-1,2-diaminocyclohexane (1.14 g, 10 mmol), triethylamine (2.00 g, 2.8 mL, 20 mmol), 3.66 g (20 mmol) of [{(CH$_2$)$_3$(NMe$_2$)$_2$}$_2$C-Cl]Cl (**B**) ; 0.80 g (20 mmol) NaOH. Deprotonation: 2.40 g NaH (100 mmol)/ 30 mL THF. Solvent used for purification: benzene. Yield: 2.7 g beige, wax-like material (8.1 mmol, 81%).

^{1}H NMR (200.1 MHz, CD$_3$CN, 25 °C): δ = 3.36-3.02 (m, 6 H, C*H*$_2$+C*H*), 2.73 (s, 6 H, C*H*$_3$), 2.44-2.38 (m, 4 H, C*H*$_2$), 2.29 (s, 6 H, C*H*$_3$), 1.68-1.51 (m, 6 H, CH$_2$), 1.32-1.15 (m, 6 H, C*H*$_2$) ppm; ^{13}C NMR (50.3 MHz, CD$_3$CN, 25 °C): δ = 159.8 (*C*N$_3$), 55.6 (*C*H), 48.0 (*C*H$_2$), 46.0 (*C*H$_2$), 35.7 (*C*H$_3$), 33.8 (*C*H$_3$), 27.5 (*C*H$_2$), 25.5 (*C*H$_2$) ppm; IR (KBr): $\tilde{v}$ = 3301 s, 2930 vs, 1633 vs(br), 1531 vs, 1482 s, 1450 s, 1392 s, 1256 s, 1237 s, 1139 m, 1112 m, 1053 m, 1021 m, 767 m, 622 m cm^{-1}; MS (70 eV, EI): m/z (%) = 334 (33) [M]$^+$, 207 (50) [M-DMPG]$^+$, 127 (54) [DMPG]$^+$, 112 (85) [DMPG-N]$^+$; elemental analysis calcd. (%) for C$_{18}$H$_{34}$N$_6$ (334.5): C 64.63, H 10.24, N 25.12; found C 63.71, H 10.32, N 24.25.

(*1R,2R*)-(-)-Bis[*N²*-(1,3-dimethylpropyleneguanidinium)]cyclohexane Diperchlorate (DMPG$_2$CH × 2 HClO$_4$ = 1c):

General procedure for the preparation of copper complexes with [Cu(CH$_3$CN)$_4$]ClO$_4$ (654 mg, 2.00 mmol), 335 mg (1.00 mmol) **1b** and 36 mg dest. H$_2$O (2.00 mmol). The precipitated pale yellow Cu hydroxides were separated from the solution by filtration through Celite. Yield: 417 mg (0.78 mmol, 78%) colorless crystals.

^{1}H NMR (200.1 MHz, CD$_3$CN, 25 °C): δ = 5.37 (m, 2 H, N-*H*), 3.42-3.08 (m, 10 H, C*H* + C*H*$_2$), 2.91 (s, 12 H, C*H*$_3$), 1.99-1.08 (m, 12 H, C*H*$_2$) ppm; ^{13}C NMR (50.3 MHz, CD$_3$CN, 25 °C): δ = 157.8 (*C*N$_3$), 58.1 (*C*H), 48.8 (*C*H$_2$), 40.7 (*C*H$_2$), 33.2 (*C*H$_2$), 25.3 (*C*H$_3$), 22.0 (*C*H$_2$) ppm; IR (KBr): $\tilde{v}$ = 3355 m, 2944 m, 2859 w, 1621 s, 1568 s, 1447 w, 1421 w, 1377 w, 1326 w, 1107 s(br), 1068 s, 1023 w, 623 m cm^{-1}; MS (FD, MeCN): m/z (%) = 435 [(**1b**)-ClO$_4$]$^+$, 335 [(**1b**)]$^+$; elemental analysis calcd. (%) for C$_{18}$H$_{36}$N$_6$Cl$_2$O$_8$ (535.4): C 40.38, H 6.78, N 15.70; found C 39.96, H 6.57, N 15.09.

(*1R*,*2R*)-(+)-1,2-Bis[*N*^{2}-(1,1,3,3-tetramethylguanidino)]diphenylethane

(TMG$_2$DPE = 2a):

Diamine: (*1R*,*2R*)-(+)-1,2-diamino-1,2-diphenylethane (2.12 g, 10 mmol), triethylamine (2.0 g, 2.8 mL, 20 mmol), 3.42 g (20 mmol) of [(Me$_2$N)$_2$C-Cl]Cl (**A**); 0.80 g (20 mmol) NaOH. Solvent used for purification: benzene. Yield: 3.06 g white solid (7.5 mmol, 75%).

M.p.: 153 °C; ^{1}H NMR (200.1 MHz, CD$_3$CN, 25 °C): δ = 7.71 (m, 4 H, ortho-*H*), 7.29 (m, 6 H, meta- + para-*H*), 5.77 (d, ^{3}J$_{HH}$ = 9.3 Hz, 2 H, C*H*), 2.69 (s, 12 H, C*H*$_3$), 2.65 (s, 12 H, C*H*$_3$), ppm; ^{13}C NMR (50.3 MHz, CD$_3$CN, 25 °C): δ = 162.4 (*C*N$_3$), 138.7 (*C*$_1$), 128.7 (*C*$_{2,6}$), 128.1 (*C*$_4$), 127.8 (*C*$_{3,5}$), 64.4 (*C*H), 40.3 (*C*H$_3$) ppm; IR (KBr): $\tilde{\nu}$ = 3028 m, 2866 m, 2830 m, 1612 vs, 1489 s, 1451 s, 1400 m, 1360 m, 1348 m, 1263 m, 1226 m, 1191 m, 830 m, 771 m, 753 m, 701 s, 619 m, 539 m cm^{-1}; MS (70 eV, EI): *m/z* (%) = 364 (51) [(**2a**)-NMe$_2$]$^+$, 204 (100) [(**2a**)$_{1/2}$]$^+$; elemental analysis calcd. (%) for C$_{24}$H$_{36}$N$_6$ (408.6): C 70.55, H 8.88, N 20.57; found C 70.73, H 8.59, N 19.36.

(*1R*,*2R*)-(+)-Bis[*N*^{2}-(1,3-dimethylpropyleneguanidino)]diphenylethane

(DMPG$_2$DPE = 2b):

Diamine: (*1R*,*2R*)-(+)-1,2-diamino-1,2-diphenylethane (2.12 g, 10 mmol), triethylamine (2.0 g, 2.8 mL, 20 mmol), 3.66 g (20 mmol) of [{(CH$_2$)$_3$(NMe)$_2$}$_2$C-Cl]Cl (**B**) ; 0.80 g (20 mmol) NaOH. Deprotonation: 2.40 g NaH (100 mmol)/ 30 mL THF. Solvent used for purification: benzene. Yield: 3.59 g beige, wax-like material (8.3 mmol, 83%).

^{1}H NMR (200.1 MHz, CD$_3$CN, 25 °C): δ = 7.35-6.98 (m, 10 H, aromat.-*H*), 4.48 (d, ^{3}J$_{HH}$ = 11.5 Hz, 2 H, C*H*), 3.43-2.14 (m, 20 H, C*H*$_2$+C*H*$_3$), 1.88-1.54 (m, 4 H, C*H*$_2$) ppm; ^{13}C NMR (50.3 MHz, CD$_3$CN, 25 °C): δ = 162.7 (*C*N$_3$), 145.8 (*C*$_1$), 128.8 (*C*$_{2,6}$), 127.1 (*C*$_{3,5}$), 125.8 (*C*$_4$), 71.0 (*C*H), 48.4 (*C*H$_3$), 27.9 (N*C*H$_2$), 25.9 (N*C*H$_2$), 20.1 (*C*H$_2$) ppm; IR (KBr): $\tilde{\nu}$ = 3443 m, 3059 m, 3023 m, 2936 s, 2863 s, 1618 vs(br), 1490 s, 1448 s, 1394 s, 1319 s, 1295 m, 1271 m, 1219 m, 1163 m, 1110 m, 1062 m, 915 m, 851 m, 757 m, 702 m, 621 m, 541 m cm^{-1}; MS (70 eV, EI): *m/z* (%) = 407 (3) [(**2b**)-NMe]$^+$, 216 (100) [(**2b**)$_{1/2}$]$^+$, 91 (65) [C$_7$H$_7$]$^+$; elemental analysis calcd. (%) for C$_{26}$H$_{34}$N$_6$ (432.6): C 72.19, H 8.39, N 19.43; found C 71.60, H 8.24, N 18.88.

R(+)-2,2´-Bis[*N*^{2}-(1,1,3,3-tetramethylguanidino)]-1,1´-binaphthalene (TMG$_2$BN = 3a):

Diamine: *R*(+)-2,2´-diamino-1,1´-binaphthalene (2.84 g, 10 mmol), triethylamine (2.0 g, 2.8 mL, 20 mmol), 3.42 g (20 mmol) of [(Me$_2$N)$_2$C-Cl]Cl (**A**); 0.80 g (20 mmol) NaOH. Solvent used for purification: MeCN/Et$_2$O. Yield: 3.99 g white solid (8.3 mmol, 83%).

M.p.: 199 °C; ^{1}H NMR (200.1 MHz, CD$_3$CN, 25 °C): δ = 7.93-7.85 (m, 4 H, *H*$_{aromat}$), 7.34-7.20 (m, 2 H, *H*$_{aromat}$), 7.16-6.97 (m, 4 H, *H*$_{aromat}$), 6.90-6.83 (m, 2 H, *H*$_{aromat}$), 2.63 (s, 24 H, C*H*$_3$) ppm; ^{13}C NMR (50.3 MHz, CD$_3$CN, 25 °C): δ = 159.7 (*C*N$_3$), 129.3, 128.6, 126.6, 126.0, 124.3, 123.8 (*C*$_{aromat}$), 39.8 (*C*H$_3$) ppm; IR (KBr): $\tilde{\nu}$ = 3044 m, 3000 m, 2926 m, 2864 m, 2794 m, 1621 s, 1603 s, 1578 s, 1498 s, 1422 s, 1377 s, 1205 m, 1135 s, 1062 m, 1035 m, 1018 m, 975 m, 824 s, 753 m, 739 m cm^{-1}; MS (70 eV, EI): *m/z* (%) = 480 (100) [(**3a**)]$^+$, 465 (18) [(**3a**)-Me]$^+$, 436 (48) [(**3a**)-NMe$_2$]$^+$, 393 (17) [(**3a**)-2 NMe$_2$]$^+$, 366 (36) [(**3a**)-TMG]$^+$, 280 (48) [DABN]$^+$, 240 (19) [(**3a**)$_{½}$]$^+$, 100 (53) [C(NMe$_2$)$_2$]$^+$; elemental analysis calcd. (%) for C$_{30}$H$_{36}$N$_6$ (480.7): C 74.97, H 7.55, N 17.48; found C 74.58, H 6.98, N 16.75.

R(+)-2,2´-Bis[*N*^{2}-(1,3-dimethylguanidino)]-1,1´-binaphthalene (DMPG$_2$BN = 3b):

Diamine: *R*(+)-2,2´-diamino-1,1´-binaphthalene (2.84 g, 10 mmol), triethylamine (2.0 g, 2.8 mL, 20 mmol), 3.66 g (20 mmol) of [{(CH$_2$)$_3$(NMe)$_2$}$_2$C-Cl]Cl (**B**); 0.80 g (20 mmol) NaOH. Deprotonation: 2.40 g NaH (100 mmol)/ 30 mL THF. Solvent used for purification: MeCN/Et$_2$O. Yield: 4.14 g light beige wax-like solid (8.2 mmol, 82%).

^{1}H NMR (200.1 MHz, CD$_3$CN, 25 °C): δ = 7.60-7.39 (m, 4 H, *H*$_{aromat}$), 7.02-6.77 (m, 6 H, *H*$_{aromat}$), 6.69-6.65 (m, 2 H, *H*$_{aromat}$), 2.96 (t, ^{3}J$_{HH}$ = 6.0 Hz, 8 H, NC*H*$_2$), 2.60 (s, 12 H, CH$_3$), 1.67 (quint, ^{3}J$_{HH}$ = 6.1 Hz, 4 H, C*H*$_2$) ppm; ^{13}C NMR (50.3 MHz, CD$_3$CN, 25 °C): δ = 156.9 (*C*N$_3$), 144.3, 134.3, 129.5, 128.5, 126.8, 123.8, 122.1, 122.0, 118.9, 111.9 (*C*$_{aromat}$), 48.0 (N*C*H$_2$), 35.3 (*C*H$_3$), 22.5 (*C*H$_2$) ppm; IR (KBr): $\tilde{\nu}$ = 3444 m, 3305 m, 3195 m, 2931 m, 2863 m, 1615 s(br), 1524 s, 1291 s, 1246 m, 1212 m, 1145 m, 1055 m, 825 s, 754 s, 708 m cm^{-1}; MS (70 eV, EI): *m/z* (%) = 504 (66) [(**3b**)]$^+$, 378 (30) [(**3b**)-DMPG]$^+$, 252 (37) [M$_{½}$]$^+$, 127 (21) [DMPG]$^+$, 112 (100) [DMPG-N]$^+$; elemental analysis calcd. (%) for C$_{32}$H$_{36}$N$_6$ (504.7): C 76.16, H 7.19, N 16.65; found C 76.32, H 7.12, N 15.79.

General Procedure for the synthesis of the copper complexes. Equimolar amounts of dehydrated metal salt and ligand were each dissolved in 5 mL of dry MeCN under argon. The solutions were combined and stirred for 30 minutes at 40-50 °C, filtered through Celite and reduced in volume to approximately 2 mL. The complex was then precipitated by the addition of 15 mL dry ether, washed with absolute ether and dried in vacuo.

{(*1R,2R*)-(-)-1,2-Bis[*N*²-(1,1,3,3-tetramethylguanidino)]cyclohexane}copper(I) Chloride [(1a)Cu^{I}Cl] (4):

General procedure with CuCl (99 mg, 1.00 mmol), 320 mg (1.03 mmol) **1a**. Yield: 375 mg (0.92 mmol, 92%) light yellow crystals.

M. p.: 163 °C (dec.); ^{1}H NMR (200.1 MHz, CD₃CN, 25 °C): δ = 2.89 (sh, 2 H, C*H*), 2.74 (s, br, 24 H, C*H₃*), 1.82-1.52 (m, 4 H, C*H₂*), 1.46-0.93 (m, 4 H, C*H₂*) ppm; ^{13}C NMR (50.3 MHz, CD₃CN, 25 °C): δ = 164.0 (*C*N₃), 64.3 (*C*H), 39.4 (*C*H₃), 39.1 (*C*H₃), 33.4 (*C*H₂), 25.9 (*C*H₂) ppm; IR (KBr): $\tilde{\nu}$ = 3219 w(br), 2985 m, 2929 m, 2875 m, 1582 s, 1555 s(br), 1517 s, 1462 s, 1419 s, 1385 s, 1372 s, 1232 m, 1141 s, 1016 m, 953 m, 775 w, 630 w cm⁻¹; MS (APCI): *m/z* = 410 [(**1a**)CuCl]⁺, 311 [(**1a**)]⁺; elemental analysis calcd. (%) for C₁₆H₃₄N₆ClCu (409.5): C 46.93, H 8.37, N 20.52, Cl 8.66, Cu 15.52; found C 46.26, H 8.25, N 20.19, Cl 8.96, Cu 16.21.

[Cu^I{(μ²-1a)Cu^{I}Cl}₂][Cu^{I}Cl₂] (5):

General procedure with CuCl (198 mg, 2.00 mmol), 310 mg (1.00 mmol) **1a**. Yield: 390 mg (0.95 mmol, 95%) light yellow crystals. Single crystals suitable for X-ray analysis were grown by slow diffusion of ether into the acetonitrile solution.

M. p.: 245 °C (dec.); ^{1}H NMR (200.1 MHz, CD₃CN, 25 °C): δ = 3.20-2.91 (m, 2 H, C*H*), 2.77 (s, br, 24 H, C*H₃*), 1.86-0.96 (m, 8 H, C*H₂*) ppm; ^{13}C NMR (50.3 MHz, CD₃CN, 25 °C): δ = 163.8 (*C*N₃), 64.5 (*C*H), 39.5 (*C*H₃), 39.2 (*C*H₃), 33.5 (*C*H₂), 25.9 (*C*H₂) ppm; IR (KBr): $\tilde{\nu}$ = 3460 w(br), 2925 s, 2884 m, 1568 vs, 1557 vs, 1527 vs, 1471 s, 1425 s, 1390 vs, 1338 w, 1237 w, 1158 m, 1061 w, 1028 s, 932 w, 902 w, 856 w, 789 w cm⁻¹; MS (APCI): *m/z* = 882 [M-[CuCl₂]]⁺, 783 [M-CuCl, -[CuCl₂]]⁺, 410 [(**1a**)CuCl]⁺, 311 [(**1a**)]⁺; elemental analysis calcd. (%) for C₃₂H₆₈N₁₂Cl₄Cu₄ (1017.0): C 37.79, H 6.74, N 16.53; found C 38.39, H 6.65, N 15.83.

{(*1R,2R*)-(-)-1,2-Bis[*N²*-(1,1,3,3-tetramethylguanidino)]cyclohexane}copper(II) Dichloride [(1a)Cu^II^Cl₂] (6):

General procedure with CuCl₂ (134 mg, 1.00 mmol), 320 mg (1.03 mmol) **1a**. Yield: 390 mg (0.93 mmol, 93%) green crystals.

M.p.: 239 °C (dec.); IR (KBr): $\tilde{v}$ = 3453 w(br), 2930 m, 2861 m, 1532 s(br), 1464 m, 1421 s, 1389 s, 1334 m, 1241 m, 1025 m, 906 m, 793 m, 636 w cm^{-1}; MS (FD, MeCN): m/z = 410 [M-Cl$^-$]$^+$, 374 [(**1a**)Cu]$^+$, 311 [(**1a**)]$^+$; elemental analysis calcd. (%) for C₁₆H₃₄N₆Cl₂Cu (444.9): C 43.19, H 7.70, N 18.89; found C 43.41, H 7.48, N 18.36.

{(*1R,2R*)-(-)-1,2-Bis[*N²*-(1,1,3,3-tetramethylguanidino)]cyclohexane}copper(I) Perchlorate [(1a)Cu^I^]ClO₄ (7):

General procedure with [Cu(CH₃CN)₄]ClO₄ (327 mg, 1.00 mmol), 320 mg (1.03 mmol) **1a**. Yield: 430 mg (0.91 mmol, 91%) colorless powder.

^{1}H NMR (200.1 MHz, CD₃CN, 25 °C): δ = 2.74 (s, br, 26 H, C$_{1/2}$*H* + C*H₃*), 1.80-1.48 (m, 4 H, C$_{3/6}$*H₂*), 1.46-1.13 and 1.04-0.71 (m, 4 H, C$_{4/5}$*H₂*) ppm; ^{13}C NMR (50.3 MHz, CD₃CN, 25 °C): δ = 163.9 (*C*N₃), 63.7 (*C*$_{1/2}$H), 38.9 (*C*H₃), 31.5 (*C*$_{3/6}$H₂), 25.5 (*C*$_{4/5}$H₂) ppm; IR (KBr): $\tilde{v}$ = 3438 w(br), 2926 m, 1615 m, 1559 s, 1539 s, 1461 m, 1426 m, 1393 m, 1240 w, 1093 s, 1027 m, 624 m cm^{-1}; MS (FD, MeCN): m/z = 474 [(**1a**)CuClO₄]$^+$, 411 [(**1a**)ClO₄]$^+$; elemental analysis calcd. (%) for C₁₆H₃₄N₆ClCuO₄ (473.5): C 40.59, H 7.24, N 17.75; found C 40.18, H 6.82, N 16.28.

Reaction of {(*1R,2R*)-(-)-1,2-Bis[*N²*-(1,1,3,3-tetramethylguanidino)]cyclo-hexane} (1a) with copper(II) diperchlorate:

General procedure with Cu(ClO₄)₂ (262 mg, 1.00 mmol), 320 mg (1.03 mmol) **1a**. Yield: 510 mg green powder.

IR (KBr): $\tilde{v}$ = 3315 w(br), 2933 m, 2863 m, 1617 s, 1546 vs, 1475 m, 1425 m, 1396 m, 1336 w, 1237 m, 1159 m, 1094 vs, 1025 m, 623 s cm^{-1}; MS (FD, MeCN): m/z = 472 [(**1a**)CuClO₄]$^+$, 411 [(**1a**)ClO₄]$^+$; 311 [(**1a**)]$^+$; elemental analysis found (%) C 40.51, H 7.41, N 15.57; (1:1 complex) C₁₆H₃₄N₆Cl₂CuO₈ (572.9) calcd. C 33.54, H 5.98, N 14.67; ; (2:1 complex) (C₁₆H₃₄N₆)₂Cl₂CuO₈ (883.4) calcd. C 43.51, H 7.76, N 19.03; (3:2 complex) (C₁₆H₃₄N₆)₃Cl₄Cu₂O₁₆ (1456.4) calcd. C 39.59, H 7.06, N 17.31.

Reaction   of   {(*1R,2R*)-(+)-1,2-Bis[*N*^{2}-(1,1,3,3-tetramethylguanidino)]-1,2-di-phenyl ethane} (2a) with copper(I) perchlorate:

General procedure with [Cu(CH$_3$CN)$_4$]ClO$_4$ (327 mg, 1.00 mmol), 420 mg (1.03 mmol) **2a**. Yield: 430 mg colorless powder.

^{1}H NMR (200.1 MHz, CD$_3$CN, 25 °C): δ = 7.74-7.19 (m, 10 H, H_{aromat}), 5.38 (d, ^{3}J$_{HH}$ = 7.0 Hz, 2 H, C*H*), 2.62 (s, br, 24 H, C*H*$_3$) ppm; ^{13}C NMR (50.3 MHz, CD$_3$CN, 25 °C): δ = 162.4 (*C*N$_3$), 137.7 (*C*$_1$), 129.3 (*C*$_{2,6}$), 128.7 (*C*$_4$), 127.1 (*C*$_{3,5}$), 64.4 (*C*H), 40.1 (*C*H$_3$) ppm; IR (KBr): $\tilde{v}$ = 3312 m, 2944 w, 1625 s, 1587 m, 1562 s, 1499 m, 1471 m, 1450 m, 1406 m, 1309 m, 1232 w, 1170 m, 1120 s(br), 1030 s, 949 w, 927 w, 904 w, 754 m, 704 m, 623 m cm^{-1}; MS (FD, MeCN): *m/z* (%) = 509 [(**2a**)ClO$_4$]$^+$, 409 [(**2a**)]$^+$, 205 [(**2a**)$_{1/2}$]$^+$; elemental analysis found (%) C 42.38, H 5.79, N 11.41; (1:1 complex) calcd. C$_{24}$H$_{36}$N$_6$CuClO$_4$ (571.6): C 50.43, H 6.35, N 14.70; (1:2 complex) calcd. C$_{24}$H$_{36}$N$_6$(CuClO$_4$)$_2$ (734.6): C 39.24, H 4.94, N 11.44; (2:3 complex) calcd. (C$_{24}$H$_{36}$N$_6$)$_2$(CuClO$_4$)$_3$ (1306.2): C 44.14, H 5.56, N 12.87.

Reaction   of   {(*1R,2R*)-(+)-1,2-Bis[*N*^{2}-(1,1,3,3-tetramethylguanidino)]-1,2-di-phenyl ethane} (2a) with copper(II) diperchlorate:

General procedure with Cu(ClO$_4$)$_2$ (262 mg, 1.00 mmol), 420 mg (1.03 mmol) **2a**. Yield: 520 mg green powder.

IR (KBr): $\tilde{v}$ = 3313 m, 2941 w, 1682 s, 1624 m, 1533 s, 1455 m, 1399m, 1107 s(br), 769 w, 702 m, 624 m cm^{-1}; MS (FD, MeCN): *m/z* (%) = 509 [(**2a**)ClO$_4$]$^+$, 266 [(**2a**)$_{1/2}$Cu]$^+$, 204 [(**2a**)$_{1/2}$]$^+$; elemental analysis found (%) C 43.85, H 5.04, N 10.68, (1:1 complex) calcd. C$_{24}$H$_{36}$N$_6$CuCl$_2$O$_8$ (671.0): C 42.96, H 5.41, N 12.52; (1:1 complex $\times$ CH$_3$CN) calcd. C$_{24}$H$_{36}$N$_6$CuCl$_2$O$_8$ $\times$ CH$_3$CN (712.9): C 43.85, H 5.52, N 13.77.

Reaction of {*R*(+)-2,2´-Bis[*N*^{2}-(1,1,3,3-tetramethylguanidino)]-1,1´-bi-naphthalene} (3a) with copper(I) chloride:

General procedure with CuCl (99 mg, 1.00 mmol), 495 mg (1.03 mmol) **3a**. Yield: 490 mg white powder.

^{1}H NMR (200.1 MHz, CD$_3$CN, 25 °C): δ = 7.98-7.79 (m, 4 H, H_{aromat}), 7.36-7.27 (m, 2 H, H_{aromat}), 7.26-7.01 (m, 4 H, H_{aromat}), 6.93-6.75 (m, 2 H, H_{aromat}), 2.73 (s, br, 24 H, C*H*$_3$) ppm; ^{13}C NMR (50.3 MHz, CD$_3$CN, 25 °C): δ = 159.6 (*C*N$_3$), 129.5, 128.7, 127.7, 126.3, 126.2, 124.6 (*C*$_{aromat}$), 39.9 (*C*H$_3$) ppm; IR (KBr): $\tilde{v}$ = 3437 m(br), 2929 m, 1618 m, 1554 s, 1515 s, 1467 m, 1420 m, 1405 s, 1367 m, 1314 m, 1146 m, 1046 w, 813 w, 745 w cm^{-1}; MS (FD,

MeCN): *m/z* (%) = 580 [(**3a**)CuCl]$^+$, 546 [(**3a**)Cu]$^+$, 480 [(**3a**)]$^+$; elemental analysis found (%) C 53.88, H 5.56, N 11.93; (1:1 complex) calcd. C$_{30}$H$_{36}$N$_6$CuCl (579.7): C 62.16, H 6.26, N 14.50; (1:2 complex) calcd. C$_{30}$H$_{36}$N$_6$(CuCl)$_2$ (678.7): C 53.09, H 5.35, N 12.38.

Reaction of {*R*(+)-2,2´-Bis[*N*^{2}-(1,1,3,3-tetramethylguanidino)]-1,1´-bi-naphthalene} (3a) with copper(II) dichloride:

General procedure with CuCl$_2$ (134 mg, 1.00 mmol), 495 mg (1.03 mmol) **3a**. Yield: 560 mg green powder.

IR (KBr): $\tilde{v}$ = 3434 m(br), 2927 m, 1621 m, 1571 s, 1550 s, 1524 s, 1467 m, 1414 m, 1397 m, 1159 m, 1046 w, 839 w, 752 w cm^{-1}; MS (FD, MeCN): *m/z* (%) = 580 [(**3a**)CuCl]$^+$, 543 [(**3a**)Cu]$^+$, 481 [(**3a**)]$^+$; elemental analysis found (%) C 54.88, H 5.44, N 12.70; (1:1 complex) calcd. C$_{30}$H$_{36}$N$_6$CuCl$_2$ (615.1): C 58.58, H 5.90, N 13.66; (1:2 complex) calcd. C$_{30}$H$_{36}$N$_6$(CuCl$_2$)$_2$ (749.6): C 48.07, H 4.84, N 11.21; (2:3 complex) calcd. (C$_{30}$H$_{36}$N$_6$)$_2$(CuCl$_2$)$_3$ (1364.7): C 52.81, H 5.32, N 12.32.

Reaction of {*R*(+)-2,2´-Bis[*N*^{2}-(1,1,3,3-tetramethylguanidino)]-1,1´-bi-naphthalene} (3a) with copper(I) perchlorate:

General procedure with [Cu(CH$_3$CN)$_4$]ClO$_4$ (327 mg, 1.00 mmol), 495 mg (1.03 mmol) **3a**. Yield: 590 mg colorless powder.

^{1}H NMR (200.1 MHz, CD$_3$CN, 25 °C): δ = 8.01-7.76 (m, 4 H, *H*$_{aromat}$), 7.39-7.23 (m, 2 H, *H*$_{aromat}$), 7.22-6.97 (m, 4 H, *H*$_{aromat}$), 6.96-6.76 (m, 2 H, *H*$_{aromat}$), 2.70 (s, br, 24 H, C*H*$_3$) ppm; ^{13}C NMR (50.3 MHz, CD$_3$CN, 25 °C): δ = 159.5 (*C*N$_3$), 129.3, 128.6, 127.5, 126.5, 126.1, 124.5 (*C*$_{aromat}$), 39.8 (*C*H$_3$) ppm; IR (KBr): $\tilde{v}$ = 3440 w(br), 2929 m, 1619 m, 1548 s(br), 1525 s, 1470 s, 1422 s, 1394 s, 1369 m, 1339 m, 1235 w, 1147 m, 1095 s(br), 1045 m, 830 m, 749 m, 623 s cm^{-1}; MS (FD, MeCN): *m/z* (%) = 644 [(**3a**)CuClO$_4$]$^+$, 581 [(**3a**)ClO$_4$]$^+$, 543 [(**3a**)Cu]$^+$, 481 [(**3a**)]$^+$, 239 [(**3a**)$_{½}$]$^+$; elemental analysis found (%) C 53.40, H 5.61, N 12.85; (1:1 complex) calcd. C$_{30}$H$_{36}$N$_6$CuClO$_4$ (643.7): C 55.98, H 5.64, N 13.06; (1:2 complex) calcd. C$_{30}$H$_{36}$N$_6$(CuClO$_4$)$_2$ (806.7): C 44.67, H 4.50, N 10.42; (2:3 complex) calcd. (C$_{30}$H$_{36}$N$_6$)$_2$(CuClO$_4$)$_3$ (1450.3): C 49.69, H 5.00, N 11.59.

Reaction of {*R*(+)-2,2′-Bis[N^2-(1,1,3,3-tetramethylguanidino)]-1,1′-bi-naphthalene} (3a) with copper(II) diperchlorate:

General procedure with $Cu(ClO_4)_2$ (262 mg, 1.00 mmol), 495 mg (1.03 mmol) **2a**. Yield: 630 mg green powder.

IR (KBr): $\tilde{\nu}$ = 3441 w(br), 2931 m, 1618 s, 1549 s, 1472 m, 1423 m, 1390 m, 1148 m, 1092 s(br), 1045 m, 828 w, 753 w, 623 m cm^{-1}; MS (FD, MeCN): *m/z* (%) = 741 [(**3a**)Cu(ClO$_4$)$_2$]$^+$, 643 [(**3a**)CuClO$_4$]$^+$, 581 [(**3a**)ClO$_4$]$^+$, 481 [(**3a**)]$^+$, 239 [(**3a**)$_{1/2}$]$^+$; elemental analysis found (%) C 52.30, H 5.47, N 12.83; (1:1 complex) calcd. C$_{30}$H$_{36}$N$_6$CuCl$_2$O$_8$ (743.1): C 48.49, H 4.88, N 11.31; (2:1 complex) calcd. (C$_{30}$H$_{36}$N$_6$)$_2$CuCl$_2$O$_8$ (1223.8): C 58.89, H 5.93, N 13.73; (3:2 complex) calcd. (C$_{30}$H$_{36}$N$_6$)$_3$(CuCl$_2$O$_8$)$_2$ (1966.9): C 54.96, H 5.53, N 12.82.

Asymmetric aziridination reactions, general procedure. 0.1 mmol Copper salt (5 mol% relative to limiting agent: PhI=NTs) and typically 1.2 eq. of the guanidine ligand (for variation of equivalents see Table 1) were charged in a schlenk tube and stirred with 3 mL of dry solvent (see Table 1 for details) for 10 min. The solution was transferred via syringe to a septum-capped schlenk tube containing a suspension of styrene (5.0 mmol, 0.57 mL) and PhI=NTs (746 mg, 2 mmol) as limiting agent in 5 mL of the same solvent. After the reaction times and temperatures listed in Table 1 the mixture was quenched by diluting with 50% hexane-ethyl acetate (10 mL) and filtered through a short plug of silica gel. The silica gel was washed with additional portions of 50% hexane-ethyl acetate (3 × 15 mL) and the filtrate was concentrated by rotary evaporation. The aziridine product was purified by chromatography eluting with hexane:ethyl acetate (7:1) and isolated after evaporation of the solvents as white crystalline solid, m.p. 88-89 °C.[61] The enantiomeric excess of *N*-*p*-toluenesulfonyl-2-phenylaziridine was determined by ^{1}H NMR (500 MHz) employing the chiral shift reagent Eu(hfc)$_3$. To 0.5 mL of the aziridine (0.08 M) dissolved in [D$_6$]-benzene typically 0.3 mL (0.07 M) of the shift reagent in the same solvent were added for baseline separation of diagnostic resonances. Enantiomeric excess was calculated from the integrated area of the two corresponding resonances and averaged with a second set of resonances within a deviation of ± 1-2%.

Table 6. Crystal data and structure refinement for **1c**, **5** and **6**.

Complex	[(**1b**)H₂](ClO₄)₂	[Cu^{I}{(μ²-**1a**)Cu^{I}Cl}₂][Cu^{I}Cl₂]	[(**1a**)Cu^{II}Cl₂]
	(**1c**)	(**5**)	(**6**)
empirical formula	$C_{18}H_{36}N_6Cl_2O_8$	$C_{16}H_{34}N_6Cu_2Cl_2$	$C_{32}H_{68}N_{12}Cu_2Cl_4$
formula weight [g mol⁻¹]	535.4	508.5	889.9
temperature [K]	193(2)	203(2)	213(2)
crystal system	orthorhombic	monoclinic	monoclinic
space group	P2₁2₁2₁	C2	P2₁/c
a [pm]	1139.0(1)	2412.0(1)	1921.3(2)
b [pm]	1413.6(1)	1078.6(2)	1206.2(1)
c [pm]	1506.1(1)	954.0(1)	1904.6(1)
α [°]	90	90	90
β [°]	90	108.281(10)	95.874(12)
γ [°]	90	90	90
volume [Å³]	2425.0(2)	2356.7(5)	4390.6(7)
Z	4	4	4
ρ [Mgm⁻³]	1.467	1.433	1.346
μ [mm⁻¹]	0.324	2.043	3.726
F(000)	1136	1056	1880
crystal size [mm³]	0.54 × 0.45 × 0.30	0.50 × 0.30 × 0.25	0.45 × 0.30 × 0.20
diffractometer	Enraf Nonius CAD4	Siemens P4	Enraf Nonius CAD4
radiation / wavelength [pm]	MoK$_α$ / 71.073	MoK$_α$ / 71.073	CuK$_α$ / 154.178
scan technique	ω-scan	ω-scan	ω-scan
θ-range for data collection [°]	2.24...24.96	1.78...25.01	4.33...69.92
index ranges	-13 ≤ h ≤ 0,	-28 ≤ h ≤ 27,	-23 ≤ h ≤ 23,
	-16 ≤ k ≤ 0,	-12 ≤ k ≤ 12,	0 ≤ k ≤ 14,
	-17 ≤ l ≤ 0	-11 ≤ l ≤ 10	0 ≤ l ≤ 23
reflections collected	2418	4471	8578
independent refl.	2418	3803	8305
R_{int}	0.0000	0.0272	0.0976
observed reflections [F ≥ 4σ(F)]	2324	3458	6733
data / restraints / parameters	2418 / 0 / 312	3803 / 1 / 245	8305 / 0 / 468
goodness of fit on *F*²	1.065	0.991	1.080
R1 [F₀ ≥ 4σ(F)][a]	0.0446	0.0334	0.1004
wR₂ (all data) [a]	0.1244	0.0837	0.2811
largest diff. Peak and hole [eÅ⁻³]	0.603 / -0.386	0.357 / -0.329	0.964 / -1.172

[a] $R_1 = \Sigma||F_0|-|F_c||/\Sigma|F_0|$; $wR_2 = \{\Sigma[w(F_0^2-F_c^2)^2]/\Sigma[w(F_0^2)^2]\}^{1/2}$.

X-ray structure analysis. Crystal data and experimental conditions are listed in Table 6. The molecular structures are illustrated as ORTEP[62] plots in Figure 3-4. Selected bond lengths and angles with standard deviations in parentheses are presented below structure illustrations. Intensity data were collected with graphite monochromated Mo$_{K\alpha}$ (λ = 71.073 pm) for **1c**, **5** and Cu$_{K\alpha}$ radiation (λ = 154.178 pm) for **6**, respectively. The collected reflections were corrected for Lorentz and polarization effects. No absorption correction has been carried out. All structures were solved by direct methods and refined by full matrix least squares methods on F^2.[63] The correct determination of the absolute structure of **5** (R-configuration) is represented by a Flack parameter of -0.009(16). For **6** two symmetrically independent molecules were found in the asymmetric unit. Hydrogen atom positions were calculated and isotropically refined.[64]

References

(1)   a) C. Moberg, *Angew. Chem.* **1998**, *110*, 260-281; *Angew. Chem. Int. Ed. Engl.* **1998**, *37*, 248-268; b) C. Moberg, *Acta Chem. Scand.* **1996**, *50*, 195-202.

(2)   R. Noyori, *Asymmetric Catalysis in Organic Synthesis*, Wiley, New York, **1994**.

(3)   D. Hoppe, F. Hintze, P. Tebben, *Angew. Chem.* **1990**, *102*, 1457-1459; *Angew. Chem. Int. Ed. Engl.* **1990**, *29*, 1424-1426.

(4)   a) K. Ito, T. Katsuki, *Tetrahedron Lett.* **1993**, *34*, 2661-2664; b) A. von Zelewsky, *Coord. Chem. Rev.* **1999**, *190-192*, 811-825.

(5)   a) R. E. Lowenthal, A. Akibo, S. Masamune, *Tetrahedron Lett.* **1990**, *31*, 6005-6008; b) R. E. Lowenthal, S. Masamune, *Tetrahedron Lett.* **1991**, *32*, 7373-7376.

(6)   a) D. A. Evans, K. A. Woerpel, M. M. Hinman, M. M. Faul, *J. Am. Chem. Soc.* **1991**, *113*, 726-728; b) D. A. Evans, M. M. Faul, M. T. Bilodeau, *J. Org. Chem.*, **1991**, *56*, 6744-6746; c) D. A. Evans, M. M. Faul, M. T. Bilodeau, B. A. Anderson, D. M. Barnes, *J. Am. Chem. Soc.* **1993**, *115*, 5328-5329; d) D. A. Evans, M. T. Bilodeau, M. M. Faul, *J. Am. Chem. Soc.* **1994**, *116*, 2742-2753; e) J. S. Johnson, D. A. Evans, *Acc. Chem. Res.* **2000**, *33*, 325-335.

(7)   G. Helmchen, A. Pfaltz, *Acc. Chem. Res.* **2000**, *33*, 336-345.

(8)   a) A. Pfaltz, *Acc. Chem. Res.* **1993**, *26*, 339-345; b) A. Pfaltz, *Acta Chem. Scand.* **1996**, *50*, 189-194; c) A. Pfaltz, *Synlett.* **1999**, 835-842.

(9)   a) Z. Li, K. R. Conser, E. N. Jacobsen, *J. Am. Chem. Soc.*, **1993**, *115*, 5326-5327; b) W. Zhang, N. H. Lee, E. N. Jacobsen, *J. Am. Chem. Soc.*, **1994**, *116*, 425-426; c) Z. Li, R. W. Quan, E. N. Jacobsen, *J. Am. Chem. Soc.* **1995**, *117*, 5889-5890; d) K. B. Hansen, N. S. Finney, E. N. Jacobsen, *Angew. Chem.* **1995**, *107*, 750-752; *Angew. Chem. Int. Ed. Engl.* **1995**, *34*, 676-678.

(10)   a) H. Wittmann, A. Schorm, J. Sundermeyer, *Z. Anorg. Allg. Chem.* **2000**, *626*, 1583-1590; b) H. Wittmann, V. Raab, A. Schorm, J. Plackmeyer, J. Sundermeyer, *Eur. J. Inorg. Chem.* **2001**, 1937-1948; c) V. Raab, J. Kipke, J. Sundermeyer, *Inorg. Chem.* **2001**, *40*, 6964-6971.

(11)   a) A. I. Meyers, A. Price, *J. Org. Chem.* **1998**, *63*, 412-413; b) G. Sekar, A. DattaGupta, V. K. Singh, *J. Org. Chem.* **1998**, *63*, 2961-2967; c) D. A. Evans, C. S. Burgey, N. A. Paras, T. Vojkovsky, S. W. Tregay, *J. Am. Chem. Soc.* **1998**, *120*, 5824-5825; d) D. A. Evans, M. C. Kozlowski, J. S. Tedrow, *Tetrahedron Lett.*, **1996**, *37*, 7481-7484.

(12)   a) P. Müller in: *Transition Metal Catalyzed Nitrene Transfer: Aziridination and Insertion in Asymmetric Catalysis*, *Vol. 2*, M. P. Doyle (Ed.), Greenwich, Conn., **1997**, pp. 113-151; b) P. Müller, *Adv. Catal. Proc.* **1997**, *2*, 113-151; c) Y. L. Bennani, S. Hanessian, *Chem. Rev.* **1997**, *97*, 3161-3195; d) H. M. I. Osborn, J. Sweeney, *Tetrahedron: Asymmetry* **1997**, *8*, 1693-1715; e) E. N. Jacobsen in: *Aziridination in Comprehensive Asymmetric Catalysis*, E. N. Jacobsen, A. Pfaltz, H. Yamamoto (Eds.), Springer, Berlin, **1999**, pp. 607-621.

(13)   a) M. P. Doyle, M. N. Protopopova, *Tetrahedron* **1998**, *54*, 7919-7946; b) M. P. Doyle, D. C. Forbes, *Chem. Rev.* **1998**, *98*, 911-935; c) M. T. Reetz, E. Bohres, R. Goddard, *Chem. Comm.* **1998**, 935-936; d) T. Aratani, *Pure & Appl. Chem.* **1985**, *57*, 1839-1844; U. Leutenegger, G. Umbricht, C. Fahrni, P. von Matt, A. Pfaltz, *Tetrahedron* **1992**, *48*, 2143-2156; e) S. Kanemasa, S. Hamura, E. Harada, H. Yamamoto, *Tetrahedron Lett.* **1994**, *35*, 7985-7988; f) F. Adrián, M. I. Burguete, J. M. Fraile, J. I. García, J. García, E. García-España, S. V. Luis, J. A. Mayoral, A. J. Royo, M. C. Sánchez, *Eur. J. Inorg. Chem.* **1999**, 2347-2354.

(14)   a) V. K. Singh, A. DattaGupta, G. Sekar, *Synthesis* **1997**, 137-149; b) H. Fritschi, U. Leutenegger, A. Pfaltz, *Helv. Chim. Acta* **1988**, *71*, 1553-1565.

(15) a) J. A. Deyrup in *The Chemistry of Heterocyclic Compounds*, *Vol. 42*, A. Hassner (Ed.), Wiley, New York, **1983**, pp. 1-214; b) A. Padwa, A. D. Woolhouse in *Comprehensive Heterocyclic Chemistry*, *Vol. 7*, W. Lwowski (Ed.), Pergamon, Oxford, **1984**, pp. 47-93; c) W. H. Pearson, B. W. Lian, S. C. Bergmeier in *Comprehensive Heterocyclic Chemistry II*, *Vol. 1A*, A. Padwa (Ed.), Pergamon, Oxford, **1996**, pp. 61-96.

(16) M. Kasai, M. Kono, *Synlett* **1992**, 778-790.

(17) H. Nozaki, S. Moriuti, H. Takaya, R. Noyori, *Tetrahedron Lett.* **1966**, 5239-5244.

(18) a) D. Tanner, *Angew. Chem.* **1994**, *106*, 625-646; *Angew. Int. Ed. Engl.* **1994**, *33*, 599-619; b) D. Tanner, P. G. Andersson, A. Harden, P. Somfai, *Tetrahedron Lett.* **1994**, *35*, 4631-4634; c) A. M. Harm, J. G. Knight, G. Stemp, *Synlett* **1996**, 677-678; d) V. K. Aggarwal, A. Thompson, R. V. H. Jones, M. C. H. Standen, *J. Org. Chem.* **1996**, *61*, 8368-8369; e) L. Casarrubios, J. A. Pérez, M. Brookhart, J. L. Templeton, *J. Org. Chem.* **1996**, *61*, 8358-8359; f) A.-H. Li, L.-X. Dai, V. K. Aggarwal, *Chem. Rev.* **1997**, *97*, 2341-2372; g) D.-J. Cho, S.-J. Jeon, H.-S. Kim, *Synlett.* **1998**, *6*, 617-618; h) S. K. Bertilsson, L. Tedenborg, D. A. Alonso, P. G. Andersson, *Organometallics* **1999**, *18*, 1281-1286; i) W. Adam, K. J. Roschmann, C. R. Saha-Möller, *Eur. J. Org. Chem.* **2000**, *3*, 557-561.

(19) a) D. Mansuy, J. Mahy, A. Duréault, G. Bedi, P. Battioni, *J. Chem. Soc. Chem. Comm.* **1984**, 1161-1163; b) K. Noda, N. Hosoya, R. Irie, Y. Ito, T. Katsuki, *Synlett* **1993**, 469-471; c) H. Nishikori, T. Katsuki, *Tetrahedron Lett.* **1996**, *37*, 9245-9248; d) P. Müller, C. Baud, Y. Jacquier, M. Moran, I. Nägeli, *J. Phys. Org. Chem.* **1996**, *9*, 341-347; e) P. Müller, C. Baud, Y. Jacquier, *Tetrahedron* **1996**, *52*, 1543-1548; f) T.-S. Lai, H.-L. Kwong, C.-M. Che, S.-M. Peng, *Chem. Comm.* **1997**, 2373-2374.

(20) D. A. Evans, D. M. Barnes in *Encyclopedia of Reagents for Organic Synthesis*, *Vol. 7*, L. A. Paquette (Editor-in-Chief), J. Wiley & Sons, New York, **1995**, pp. 4958-4960.

(21) R. W. Quan, Z. Li, E. N. Jacobsen, *J. Am. Chem. Soc.* **1996**, *118*, 8156-8157.

(22) a) M. M. Díaz-Requejo, P. J. Pérez, M. Brookhart, J. L. Templeton, *Organometallics* **1997**, *16*, 4399-4402; b) P. J. Pérez, M. Brookhart, J. L. Templeton, *Organometallics* **1993**, *12*, 261-262.

(23)   P. Brandt, M. J. Södergren, P. G. Andersson, P.-O. Norrby, *J. Am. Chem. Soc.* **2000**, *122*, 8013-8020.

(24)   a) B. F. Straub, P. Hofmann, *Angew. Chem.* **2001**, *113*, 1328-1330; *Angew. Chem. Int. Ed. Engl.* **2001**, *40*, 1288-1290; b) M. Bühl, F. Terstegen, F. Löffler, B. Meynhardt, S. Kierse, M. Müller, C. Näther, U. Lüning, *Eur. J. Org. Chem.* **2001**, 2151-2160; c) L. Cavallo, M. E. Cucciolito, A. DeMartino, F. Giordano, I. Orabona, A. Vitagliano, *Chem. Eur. J.* **2000**, *6*, 1127-1139; d) H.-L. Kwong, L.-S. Cheng, W.-S. Lee, W.-L. Wong, W.-T. Wong, *Eur. J. Inorg. Chem. 2000*, 1997-2002; e) R. G. Salomon, J. K. Kochi, *J. Am. Chem. Soc.* **1973**, *95*, 3300-3310.

(25)   A. M. Harm, J. G. Knight, G. Stemp, *Tetrahedron Lett.* **1996**, *37*, 6189-6192.

(26)   a) M. J. Södergren, D. A. Alonso, P. G. Andersson, *Tetrahedron: Asymmetry* **1997**, *8*, 3563-3565; b) M. J. Södergren, D. A. Alonso, A. V. Bedekar, P. G. Andersson, *Tetrahedron Lett.* **1997**, *38*, 6897-6900.

(27)   B. V. Meprathu, S. Diltz, P. J. Walsh, J. D. Protasiewicz, *Tetrahedron Lett.* **1999**, *40*, 5459-5460.

(28)   P. Dauban, R. H. Dodd, *J. Org. Chem.* **1999**, *64*, 5304-5307.

(29)   a) S. I. Ali, M. D. Nikalje, A. Sudalai, *Org. Lett.* **1999**, *1*, 705-707; b) K. B. Sharpless, J. U. Jeong, *US Pat. 5,929,252* to The Scripps Research Institute (USA), **1999**; c) T. Ando, S. Minakata, I. Ryu, M. Komatsu, *Tetrahedron Lett.* **1998**, *39*, 309-312; d) D. P. Albone, P. S. Aujla, P. C. Taylor, S. Challenger, A. M. Derrick, *J. Org. Chem.* **1998**, *63*, 9569-9571.

(30)   B. M. Chanda, R. Vyas, A. V. Bedekar, *J. Org. Chem.* **2001**, *66*, 30-34.

(31)   A. V. Gontcharov, H. Liu, K. B. Sharpless, *Org. Lett.* **1999**, *1*, 783-786.

(32)   a) J. DuBois, C. S. Tomooka, J. Hong, E. M. Carreira, *Acc. Chem. Res.* **1997**, *30*, 364-372; b) S. Minakata, T. Ando, M. Nishimura, I. Ryu, M. Komatsu, *Angew. Chem.* **1998**, *110*, 3596-3598; *Angew. Chem. Int. Ed. Engl.* **1998**, *37*, 3392-3394.

(33)   a) G. J. Hutchings, C. Langham, P. Piaggio, S. Taylor, P. McMorn, D. J. Willock, D. Bethell, P. C. B. Page, C. Sly, F. Hancock, F. King, *Stud. Surf. Sci. Catal.* **2000**, *130A* (International Congress on Catalysis, 2000, Pt. A), 521-526; b) C. Langham, S. Taylor, D. Bethell, P. McMorn, P. C. Bulman Page, D. J. Willock, C. Sly, F. E. Hancock, F. King, G. J. Hutchings, *J. Chem. Soc. Perkin Trans. 2* **1999**, 1043-1049; c) C. Langham,

P. Piaggio, P. McMorn, D. J. Willock, G. J. Hutchings, D. Bethell, D. F. Lee, G. J. Hutchings, P. C. Bulman Page, C. Sly, F. E. Hancock, F. King, *Chem. Commun.* **1998**, 1601-1602; d) D. Bethell, G. J. Hutchings, C. Langham, P. C. Bulman Page, D. F. Lee, *Eur. Pat. Appl. EP 831086 A1* **1998**; e) D. Bethell, G. J. Hutchings, C. Langham, P. C. B. Page, D. F. Lee, *US Pat. 5,852,205* to Imperial Chemical Industries PLC (GB), **1998**.

(34) a) Wieland, G.; Simchen, G. *Liebigs Ann. Chem.* **1985**, 2178-2193; b) Barton, D. H. R.; Elliot, J. D.; Géro, S. D. *J. Chem. Soc., Perkin Trans. I* **1982**, 2085-2090; c) Barton, D. H. R.; Kervagoret, J. K.; Zard, S. Z. *Tetrahedron* **1990**, *46*, 7587-7598.

(35) a) Smith, P. A. S. *The Chemistry of Open-Chain Organic Nitrogen Compounds, Vol. 1*, Benjamin, W. A. Inc., New York, 1965, p. 277-290; b) Yamamoto, Y.; Kojima, S. *The Chemistry of Amidines and Imidates, Vol. 2*, J. Wiley & Sons, Chichester, 1991, p. 485-526; c) Schwesinger, R. *Nachr. Chem. Tech. Lab.* **1990**, *38*, 1214-1226.

(36) a) H. Eilingsfeld, M. Seefelder, H. Weidinger, *Angew. Chem.* **1960**, *72*, 836-845; b) H. Eilingsfeld, G. Neubauer, M. Seefelder, H. Weidinger, *Chem. Ber.* **1964**, *97*, 1232-1245.

(37) W. Kantlehner, E. Haug, W. W. Mergen, P. Speh, T. Maier, J. J. Kapassakalidis, H.-J. Bräuner, H. Hagen, *Liebigs Ann. Chem.* **1984**, 108-126.

(38) I. A. Cliffe in *Comprehensive Organic Functional Group Transformations, Vol. 6*, Elsevier Science Ltd., Oxford, **1987**, pp. 639-675.

(39) R. Knorr, A. Trzeciak, W. Bannwarth, D. Gillessen, *Tetrahedron Lett.* **1989**, *30*, 1927-1930.

(40) a) H. Kessler, D. Leibfritz, *Chem. Ber.* **1971**, *104*, 2158-2169; b) H. Kessler, *Angew. Chem.* **1970**, *82*, 237-253; *Angew. Chem. Int. Ed. Engl.* **1970**, *9*, 219-235; c) H. Kessler, D. Leibfritz, *Tetrahedron* **1970**, *26*, 1805-1820; d) H. Kessler, D. Leibfritz, *Liebigs Ann. Chem.* **1970**, *737*, 53-60.

(41) a) J. T. Groves, T. Takahashi, *J. Am. Chem. Soc.* **1983**, *105*, 2073-2074; b) K. J. O´Connor, S. Wey, C. J. Burrows, *Tetrahedron Lett.* **1992**, *33*, 1001-1004; c) E. Bohres,[13c] personal communication.

(42) Minimum ¹H NMR recording temperature in CD₃CN (mp. -44 °C).

(43) a) A. J. Papa, *J. Org. Chem.* **1966**, *31*, 1426-1430; b) W. Petz, *J. Organomet. Chem.* **1975**, *90*, 223-226.

(44) B. J. Hathaway in *Comprehensive Coordination Chemistry*, *Vol. 5*, G. Wilkinson (Ed.), Pergamon Press, **1987**.

(45) a) J. F. Modder, J.-M. Ernsting, K. Vrieze, M. de Wit, C. H. Stam, G. van Koten, *Inorg. Chem.* **1991**, *30*, 1208-1214; b) B. Neumann, U. Siemeling, H.-G. Stammler, U. Vorfeld, J. G. P. Delis, P. W. N. M. van Leeuwen, K. Vrieze, J. Fraanje, K. Goubitz, F. F. de Biani, P. Zanello, *J. Chem. Soc. Dalton Trans.* **1997**, 4705-4711.

(46) a) A. P. Cole, D. E. Root, P. Mukherjee, E. I. Solomon, T. D. P. Stack, *Science* **1996**, *273*, 1848-1850; b) V. Mahadevan, Z. Hou, A. P. Cole, D. E. Root, T. K. Lal, E. I. Solomon, T. D. P. Stack, *J. Am. Chem. Soc.* **1997**, *119*, 11996-11997.

(47) D. A. Evans, K. A. Woerpel, M. S. Scott, *Angew. Chem.* **1992**, *104*, 439-441; *Angew. Chem. Int. Engl.* **1992**, *31*, 430-432.

(48) C. Pariya, K. Panneerselvan, C.-S. Chung, T.-H. Lu, *Polyhedron* **1998**, *17*, 2555-2561.

(49) R. Boese, D. Bläser, W. Petz, *Z. Naturforsch.* **1988**, *43(B)*, 945-948.

(50) V. Raab, *Ph. D. Thesis* **2001**, *Ch. 3.1*, Phillips University Marburg, Germany.

(51) *ibid.*, *Ch. 5.1*.

(52) The ρ value of 0.99 in the $[C(NMe_2)_3]^+$ cation is due to crystal packing effects and assumes an ideal value of 1.00 in other complexes; W. Petz,[49] personal communication.

(53) W. L. F. Armarego, D. D. Perrin in *Purification of Laboratory Chemicals*, *4ᵗʰ Ed.*, Butterworth-Heinemann, Oxford, **1996**.

(54) J. F. Larrow, E. N. Jacobsen, *J. Org. Chem.* **1994**, *59*, 1939-1942.

(55) a) O. F. Williams, J. C. Bailer, Jr., *J. Am. Chem. Soc.* **1959**, *81*, 4464-4469; b) K. Saigo, N. Kubota, S. Takebayashi, M. Hasegawa, *Bull. Chem. Soc. Jpn.* **1986**, *59*, 931-932.

(56) T. Cohen, R. J. Ruffner, D. W. Shull, E. R. Fogel, J. R. Flack in *Organic Synthesis*, *Collective Volume VI*, Wiley, New York, **1988**, pp. 737-744.

(57) G. J. Kubas, *Inorg. Synth.* **1979**, *19*, 90-92.

(58) R. N. Keller, H. D. Wycoff, in *Inorg. Synth.*, *Vol. 2*; W. C. Fernelius (Ed.), Mc Graw-Hill Book Company, Inc., New York, **1946**, p. 1-4.

(59) H. Hecht, *Z. Anorg. Ch.* **1947**, *254*, 37-51.

(60) Y. Yamada, T. Yamamoto, M. Okawara, *Chem. Lett.* **1975**, 361-362.

(61) T. P. Seden, T. W. Turner, *J. Chem. Soc. (C)* **1968**, 876-878.

(62) Burnett, M. N.; Johnson, C. K. *ORTEP-III, Oak Ridge Thermal Ellipsoid Plot Program for Crystal Structure Illustrations*, Oak Ridge National Laboratory Report ORNL-6895, **1996**.

(63) a) Sheldrick, G. M. *SHELXS-97, Program for Crystal Structure Solution* and *SHELXL-97, Program for Crystal Structure Refinement* **1997**, University of Göttingen, Germany; b) Siemens Analytical X-ray Instruments Inc. *SHELXTL 5.06* **1995**, Madison, WI, USA.

(64) Crystallographic data (excluding structure factors) for the structures reported in this paper have been deposited with the Cambridge Crystallographic Data Centre as supplementary publication no. CCDC-179987 (**1c**), CCDC-179985 (**5**) and CCDC-179986 (**6**). Copies of the data can be obtained free of charge on application to CCDC, 12 Union Road, Cambridge CB2 1EZ, UK (fax: (+ 44) 1223 336-033; email: deposit@ccdc.cam.ac.uk).

— Chapter 2 —

Ligand Effects in the Copper Catalyzed Aerobic Oxidative Carbonylation of Methanol to Dimethyl Carbonate (DMC)

Keywords: Dimethyl carbonate synthesis • Oxidative carbonylation • Copper catalysts • N-ligands • Corrosion resistance.

Abstract

The influence of the type and amount of added N-donor ligand, of the anion and the oxidation state of copper in the catalytic aerobic oxidative carbonylation of methanol to dimethyl carbonate (DMC) is systematically studied. A surprising increase in activity and selectivity compared to the plain copper halides CuX_n (X = Cl, Br, I, n = 1, 2) is found for catalyst complexes with three or four *N*-methylimidazole (NMI) ligands at $Cu^{+/2+}$, a ligand regime reminiscent of the oxygen activating copper enzymes in nature. However, a large excess of NMI inhibits the catalysis. The NMI complexes turned out to be more active and selective as redox catalysts and less active in the competing undesired hydrolytic cleavage of DMC into methanol and carbon dioxide by the unavoidable byproduct water. Furthermore, corrosion of stainless steel autoclaves is efficiently inhibited in the presence of ≥2 eq. of NMI per copper halide.

1 Introduction

Due to the increasing number of applications for organic carbonates their production on an industrial scale is of current interest [1,2,3]. They are substances of low toxicity and good biodegradability which may in some cases replace toxic synthons such as phosgene in fine chemical and polymer syntheses [4,5]. They have a potential in the preparation of urethanes from aliphatic amines, which can in turn be cleaved to the corresponding isocyanates. The dimethyl carbonate (DMC) can also act as a non-toxic high-temperature methylating agent, as an alternative to dimethyl sulfate in the quaternization of reactive amines or in the methylation of phenol and naphthols [6]. The DMC technology may contribute to "Green Chemistry" replacing toxic or high waste technology. Transesterification of DMC leads to diphenyl carbonate, an important component in condensation reactions yielding

1

polycarbonates [1]. Finally, DMC gained interest as dipolar aprotic solvent and as fuel additive improving the octane number and replacing more toxic or less biodegradable additives [3].

For many years, the reaction of methanol and phosgene - or chlorine and carbon monoxide - in the presence of bases such as pyridine has been applied for DMC production [7]. Alternative oxidants for carbon monoxide are alkyl nitrites in palladium and platinum catalyzed methanol carbonylations [8,9]. However, these processes have rather high E-factors [10] and will probably be replaced by catalytic low-waste ("green") technologies using CO_2 as feedstock or using air as oxidant for CO. An example for the first strategy is the Lewis acid catalyzed two-step conversion of carbon dioxide and ethylene oxide into ethylene carbonate followed by its methanolysis to DMC and ethylene glycol [11,12]. The second strategy is laid out in numerous patents claiming the use of basic copper salts [13,14,15,16,17] in the oxidative carbonylation of methanol under various reaction conditions in batch reactors with catalyst slurries or molten salts [18]. The immobilization of copper salts on solid support [19,20,21,22,23] and the addition of bases as promoters such as hydroxides [24] and amines or pyridines [19,25,26] has been claimed, but the specific function of the nitrogen bases remained obscure. It has been proven by a number of carefully designed experiments that the stoichiometric comprehensible redox reactions [27,28] shown in Scheme 1 are most probably involved in the catalytic cycle [29].

$$2\ MeOH + 2\ CuCl + 0.5\ O_2 \longrightarrow 2\ Cu(OMe)Cl + H_2O$$

$$2\ Cu(OMe)Cl + CO \longrightarrow (MeO)_2CO + 2\ CuCl$$
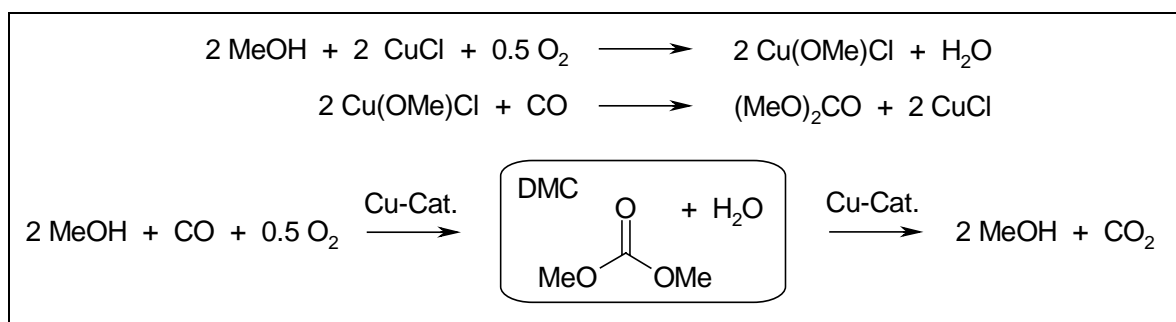
Scheme 1. Redox reactions involved in the oxidative carbonylation of MeOH to DMC and net result.

There are a number of unresolved problems in the patent literature. Despite of the use of substoichiometric amounts of copper catalysts, only low conversions of up to 30% per batch were observed [13]. Further problems are low selectivities due to undesired byproducts [30] and reactor corrosion [31,32,33]. In a recent paper by Sato et al., it was shown that copper chloride on polyvinyl pyridine loses much of its aggressive behavior in stainless steel corrosion [23]. However, there still remains an intrinsic problem in the oxidative

2

carbonylation process: the same copper catalyst, that is performing the redox reaction to DMC and water as by-product appears to catalyze as a Lewis acid the hydrolysis of DMC to CO_2 and MeOH. The net result of this second undesired process is the oxidation of carbon monoxide to carbon dioxide by oxygen. In an attempt to overcome many of these drawbacks we followed a very simple concept of coordination chemistry: in complexes of a Lewis base L (e.g. N-donor) and a Lewis acid Cu^{2+} the acidity of the metal cation is reduced depending on the type and number of coordinated ligands L of certain donor strength. Mixtures of such complexes of different Lewis acidity $[CuL]^{2+}$, $[CuL_2]^{2+}$, $[CuL_3]^{2+}$, $[CuL_4]^{2+}$ with coordinating (or non-coordinating) anions X^- may be regarded as a ligand buffered catalytic system, that may be more selective in redox reactions and less active in hydrolysis reactions. Therefore, the focus of the present study is a systematic investigation of the influence of the type of applied N-donor ligand, the equivalents of ligand employed per copper as well as the oxidation state and the counter anion of the copper salt on the performance of the oxidative carbonylation of methanol to DMC.

2 Experimental

2.1 General

   All reactions were carried out in a 100 mL V4A stainless steel autoclave, sealed with an EPDM O-ring, equipped with a teflon coated magnetic stirring bar, a 100 bar manometer and a Pt-100 thermoelement in the outer aluminum heating block as temperature control unit (±1°C).
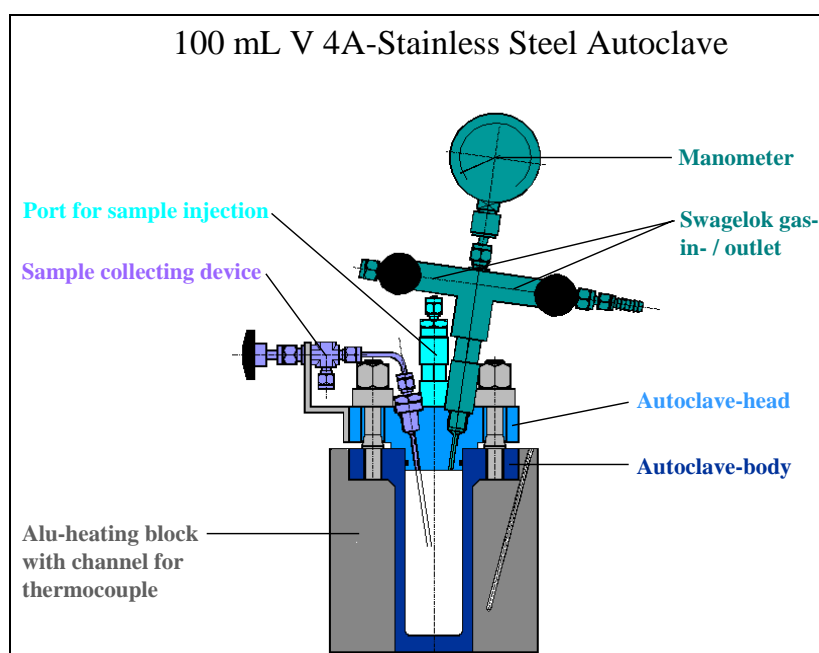
The organic products were analyzed by quantitative gas chromatography on a HRGC 5300 (Carlo Erba Instruments) equipped with a fused silica guard column (5 m × 0.53 mm) and a Rtx®-200 analytical column (30 m × 0.53 mm × 0.50 μm; Restek); split injector (1:20); FID temperature 200 °C, isothermic at 30 °C, toluene as internal standard (IS). GC-MS analyses were carried out on a VG Masslab TRIO-2. Melting points were determined in capillary tubes on a Büchi MP B-540 apparatus and are uncorrected. IR spectra were recorded on a Bruker IFS 88 FT and elemental analyses on a Heraeus CHN-Rapid analyzer.

2.2 Equations for the calculation of conversions, selectivities and yields

Straight calibration lines were established by GC analyses of mixtures of authentic samples with a composition range of 0 to 30 mmol substrate, the corresponding amount of product (0 to 15 mmol), 5 mmol of internal standard (toluene), and diethyl ketone as diluting solvent (10 mL).

k   = Gradient of straight calibration line $A_S(t)$ = Area of substrate signal

$n_S(t)$ = Amount of substrate at time (t) $A_P(t)$ = Area of product signal

$n_P(t)$ = Amount of product at time (t) $A_{IS}(t)$ = Area of internal standard

n_{IS} = Amount of internal standard

$$\frac{n_{S,P}}{n_{IS}} = k \cdot \frac{A_{S,P}}{A_{IS}} \quad \rightarrow \quad n_S(t) = k \cdot \frac{A_S(t)}{A_{IS}(t)} \cdot n_{IS} \quad / \quad n_P(t) = k \cdot \frac{A_P(t)}{A_{IS}(t)} \cdot n_{IS}$$

$$Conversion(t) = \frac{n_S(t_0) - n_S(t)}{n_S(t_0)} \cdot 100\% \qquad Yield(t) = \frac{n_P(t)}{n_S(t_0)} \cdot 100\%$$

$$Selectivity(t) = \frac{n_P(t)}{n_S(t=0) - n_S(t)} \cdot 100\% = \frac{Yield}{Conversion} \cdot 100\%$$

2.3 Materials

Methanol, toluene (IS), diethyl ketone as diluting solvent for GC samples and the ligands *N*-methylimidazole (NMI), 4-methylpyridine were freshly distilled prior to use. The following chemicals were prepared and purified by literature methods: *N*-methylpyrazole [34], CuCl [35], $CuCl_2$ and $CuBr_2$ [36], $Cu(ClO_4)_2$ [37], $[Cu(C_6H_6)]_{1/2}OTf$ [38], $Cu(OTf)_2$ [39], $[Cu(CH_3CN)_4]PF_6$ [40]. Commercially available chemicals were used as received from

Aldrich and Fluka: 4-dimethylaminopyridine (DMAP), CuI, CuBr, [Me$_4$N]OH × 5 H$_2$O; [Et$_4$N]$_2$CO$_3$; [Et$_4$N]CN; [Me$_4$N]F; [Et$_4$N]Cl; [Et$_4$N]Br; [Et$_4$N]I. The CO (3.5), O$_2$ (4.8), and synthetic air (20.5 % O$_2$ in N$_2$) were obtained from Messer Griesheim.

2.4 Catalyst preparation

The following complexes were synthesized according to known literature methods and analyzed by IR spectroscopy and elemental analyses (L = *N*-methylimidazole, NMI): LCuCl$_2$, L$_4$CuCl$_2$, L$_4$CuBr$_2$, L$_4$CuI$_2$ [41]; L$_2$CuCl$_2$, L$_2$CuBr$_2$ [41,42]; L$_3$CuCl$_2$, LCuBr$_2$, L$_3$CuBr$_2$ [33].

2.4.1 [(NMI)$_4$Cu]PF$_6$, *1*

[Cu(CH$_3$CN)$_4$]PF$_6$ (1.86 g, 5 mmol) is dissolved in 35 mL dry MeOH and NMI (1.66 g, 1.61 mL, 20.25 mmol) is added to the vigorously stirred solution. After 24 h, the reaction mixture is evaporated to half of its volume. A thick colorless precipitate is filtered off, washed with dry ether and dried in vacuo to give [(NMI)$_4$Cu]PF$_6$ (2.63 g, 4.90 mmol) in 98 % yield. Elemental analysis (%) calc. for C$_{16}$H$_{24}$N$_8$CuF$_6$P (536.99 g/mol): C, 35.79; H, 4.51; N, 20.87; Cu, 11.84; found: C, 36.13; H, 4.65; N, 20.58; Cu, 11.52. M.p.: 113 °C. IR (Nujol): $\tilde{\nu}$ = 3154 s, 3127 s, 1620 m, 1512 s, 1464 s, 1285 s, 1231 s, 1086 s, 1026 s, 932 s, 808 s, 760 s, 658 s, 557 s cm^{-1}.

2.4.2 (NMI)$_4$Cu(OTf)$_2$, *2*

Cu(OTf)$_2$ (723 mg, 2 mmol) is dissolved in 15 mL dry EtOH and *N*-methylimidazole (723 mg, 8.8 mmol) is added to the vigorously stirred solution. After 24 h, 15 mL of dry ether is added. The precipitate is filtered, washed with dry ether and dried in vacuo to yield 1.325 g (1.92 mmol, 96 %) (NMI)$_4$Cu(OTf)$_2$ as a purple powder. Elemental analysis (%) calc. for C$_{18}$H$_{24}$N$_8$O$_6$CuF$_6$S$_2$ (690.16 g/mol): C, 31.33; H, 3.51; N, 16.24; Cu, 9.21; found: C, 31.23; H, 3.64; N, 15.84; Cu, 9.76. M.p.: 170 °C (dec.). IR (Nujol): $\tilde{\nu}$ = 3136 w, 2967 w, 2851 vs, 1542 s, 1428 m, 1257 s, 1224 s, 1166 s, 1098 m, 1030 s, 952 m, 839 m, 757 m, 660 s, 638 s cm^{-1}.

2.5 Catalytic runs

The values for conversion and selectivity given in the charts and tables are based on an average of three experiments that have been reproduced within an experimental error of 2%.

2.5.1 Typical experimental procedure with isolated catalyst

The copper complex (0.3 mmol, 1 mol% relative to MeOH) is placed into the autoclave and methanol (30 mmol, 961 mg, 1215μL) is added via a syringe. In order to avoid the risk of working within the explosion area of the mixture CO/O_2 [43], the autoclave is filled at 20°C first with 2.65 bar oxygen (12.5 or 23 bar synthetic air, respectively, see Table 2), then with additional 50 bar carbon monoxide. After disconnecting the autoclave from the gas supply it is inserted into an aluminum heating block preheated to 150°C. Within 5 min, the autoclave reaches the reaction temperature of 120°C that is held constant. After a reaction time of 4 h, the autoclave is depressurized over a period of 10 min via a liquid nitrogen trap and finally all volatiles at $150°C/10^{-2}$ mbar are collected in that trap as well. To the condensate 5 mmol (461 mg) of toluene as internal standard (IS) is added. After diluting the condensate with 10 mL of diethyl ketone the homogenous mixture was analyzed via quantitative capillary gas chromatography. Products were identified and quantified by comparison of retention times and calibrated integrals with authentic samples.

2.5.2 Typical experimental procedure with catalyst prepared in situ

The copper salt (0.3 mmol, 1 mol% relative to MeOH or EtOH), N-ligand (molar quantities with respect to the desired equivalents, e.g. NMI, 99 mg, 96 μL, 1.2 mmol, 4 eq.) and methanol (30 mmol, 961 mg, 1215μL) are placed into the autoclave and the procedure described above is followed.

The same procedure is followed with 1.5 mmol (5 mol%) and 3 mmol (10 mol%) copper salt relative to MeOH and the corresponding equivalents of ligand (see 3.4.2).

2.5.3 Added ammonium salts to Cu(I)

161 mg (0.3 mmol, 1 mol% relative to MeOH) of copper complex [(NMI)$_4$Cu]PF$_6$ (**1**), 961 mg (30 mmol, 1215μL) MeOH, and equimolar amounts of tetraalkyl ammonium salts (see 3.4.1) containing the desired anion are placed together into the autoclave and the procedure described above is followed.

2.5.4 DPC experiment; Poly-p-phenylene oxide (PPO):

PhOH (2.82 g, 30 mmol) is treated under the same reaction conditions as in 2.5.2, catalyst: L$_4$CuCl$_2$ (L = N-methylimidazole). The autoclave is depressurized, the red-brown polymer is washed with MeCN (30 mL) and Et$_2$O (30 mL), and dried in vacuo at 100 °C. Yield: 2.65 g (29 mmol, 96 %).

M.p.: > 410 °C; IR (KBr): $\tilde{v}$ = 3427 m, 3061 w, 1589 m, 1489 s, 1345 w, 1201 s, 1097 m, 1023 w, 969 w, 830 m, 750 m, 690 m cm^{-1}; MS (70 eV, EI): *m/z* (%) = 94.1 (6) $[C_6H_5OH]^+$, 65 (1) $[C_5H_5]^+$; 31.0 (22) $[CH_3O]^+$, 28.0 (100) $[CO]^+$; elemental analysis calcd (%) for $(C_6H_4O)_n$ $(92.10)_n$: C 78.25, H 4.38, O 17.37; found C 73.10, H 4.34.

2.5.5 Hydrolysis experiments

15 mmol DMC (1351 mg, 1263 μL) and 15 mmol H_2O (271 mg, 271 μL) are placed together into the autoclave and then pressurized with 2.15 bar O_2 and 40 bar CO (the consumption of reaction gases under catalytic conditions is taken into account). After a reaction time of 1 h (30 min. 20°C→120°C followed by 30 min. at 120°C), the content of the autoclave is analyzed in the same way as described before.

2.5.6 Catalysis in the presence of molecular sieves 3 Å

The experiments were carried out by applying exactly the procedure described above for catalyst preparation in situ (2.5.2), however, 2.7 g 3 Å molecular sieves as beads (Fluka, ∅ ~2 mm) were added together with the catalyst and substrate.

3 Results and discussion

3.1 Influence of the type of N-ligand

As already mentioned, some patents are claiming the addition of bases such as hydroxides, amines or pyridines as promoters for the formation of basic copper catalysts in the presence of water and as corrosion inhibitors. In our first experiments, we tested the performance of isolated complexes L_4CuCl_2 (L = *N*-methylimidazole (NMI) and 4-methylpyridine) versus the blank sample of anhydrous $CuCl_2$ under identical conditions in DMC production: 1 mol% Cu catalyst in MeOH, 2.5 bar O_2, 50 bar CO, 120°C, 4 h. We observed that conversion of MeOH and selectivity in DMC synthesis did not deviate within the limits of experimental error (±2%) from those experiments obtained from in situ prepared complexes. There is even a tendency, that injection of the 4 eq. of the corresponding ligand to a methanol solution of $CuCl_2$ gave slightly better results (+ 1-2%) than the use of isolated and analytically characterized complexes L_4CuCl_2. Therefore, whenever possible we preferred the in situ generation of the catalytically active complexes.

Fig. 1 demonstrates that under the given conditions of our batch experiment the blank sample of $CuCl_2$ leads to a MeOH conversion of 15% and a DMC selectivity of 46%; this corresponds to a theoretical yield of 7% DMC. A number of added N-donor ligands including pyrazole, *N*-methylpyrazole and 4-methylpyridine did not increase the conversion whereas the selectivity drops to 20-30%. With respect to the DMC yields, it is clearly unfavorable to add 4 eq. of such ligands. However, we were surprised to find that addition of very basic N-donors such as TMG_3tren, 1,1,1-tris{2-[N^2-(1,1,3,3-tetramethylguanidino)]ethyl}amine (Fig. 2) [44,45], a superbasic peralkylguanidine derivative of tren (1 eq. of tetradentate ligand added), DMAP (4-dimethylaminopyridine) and NMI did significantly increase both, conversion and selectivity. It is noteworthy that the typical byproducts of the oxidative carbonylation of MeOH such as dimethoxy methane $CH_2(OCH_3)_2$ (DMM) and methyl formate $HCOOCH_3$ (MF) [22] could not be detected by means of GC-MS and by comparison with authentic samples.
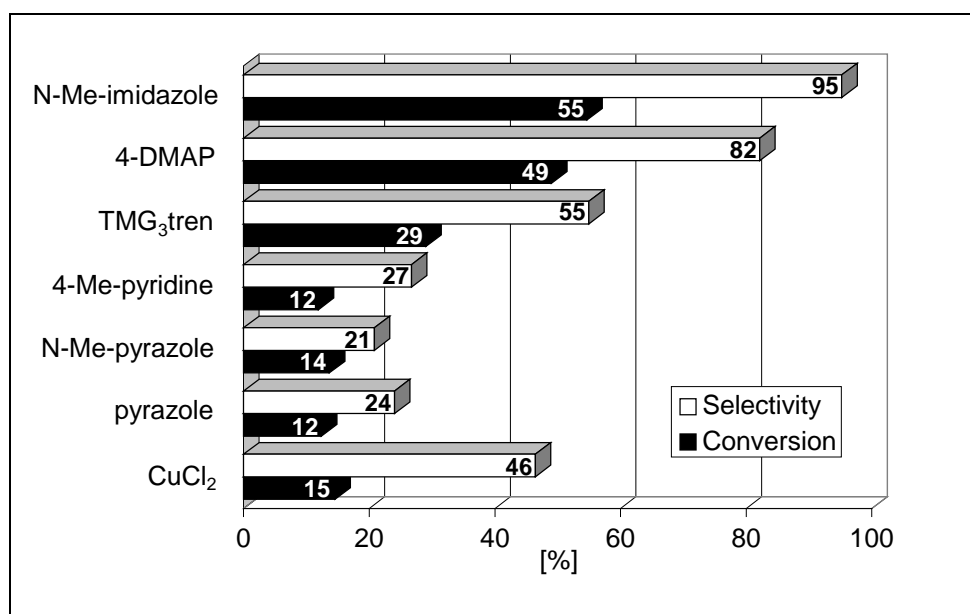

Fig. 1. $CuCl_2$ catalyst with added 4 eq. of various N-ligands. Reaction conditions: 1 mol% catalyst, 2.5 bar O_2, 50 bar CO, 120 °C, 4 h.

The best performance (55% conversion and 95% selectivity) is achieved by addition of 4 eq. of NMI. For technical reasons, the consumption of oxygen has not been monitored. However, the initial partial pressure of oxygen (2.5 bar O_2 in a 100 mL reactor) has been chosen to assure theoretically a full conversion of methanol even in the presence of the large excess of carbon monoxide ($CO:O_2 = 91:9$ mol%) being employed in order to stay outside the upper explosion area. It is expected that conversion and selectivity will become even better, if

the technical requirements of the reactor would allow us to hold the oxygen concentration constant and to monitor the undesired CO oxidation to CO_2. It is important to note that corrosion of the stainless steel autoclave is most striking with the blank $CuCl_2$ sample, however the corrosion is perfectly inhibited in each experiment with 4 eq. of added N-ligand.
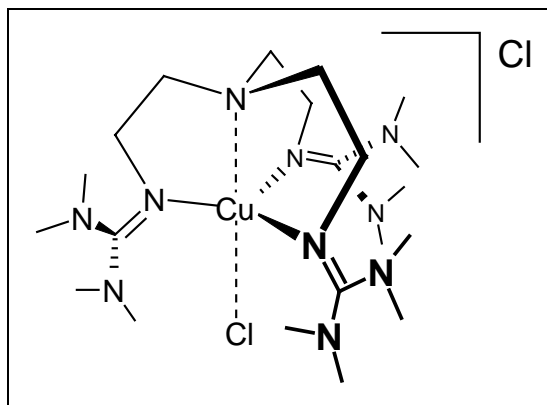

Fig. 2. Complex of TMG_3tren and $Cu^{II}Cl_2$.

3.2 Influence of the number of equivalents NMI at CuCl₂ and CuBr₂

The question arose how many equivalents of added *N*-methylimidazole would give the best performance. Fig. 3 presents the results of a series of experiments with 1, 2, 3, 4, and 10 eq. NMI added. We observe a continuous increase in MeOH conversion with a peak of 55% at 4 eq. If more than one ligand NMI is added to the catalytic reaction the selectivity is increasing significantly, at the same time the corrosion is efficiently inhibited. It is interesting to note that a large excess of 10 eq. added NMI tends to inhibit the catalytic cycle.
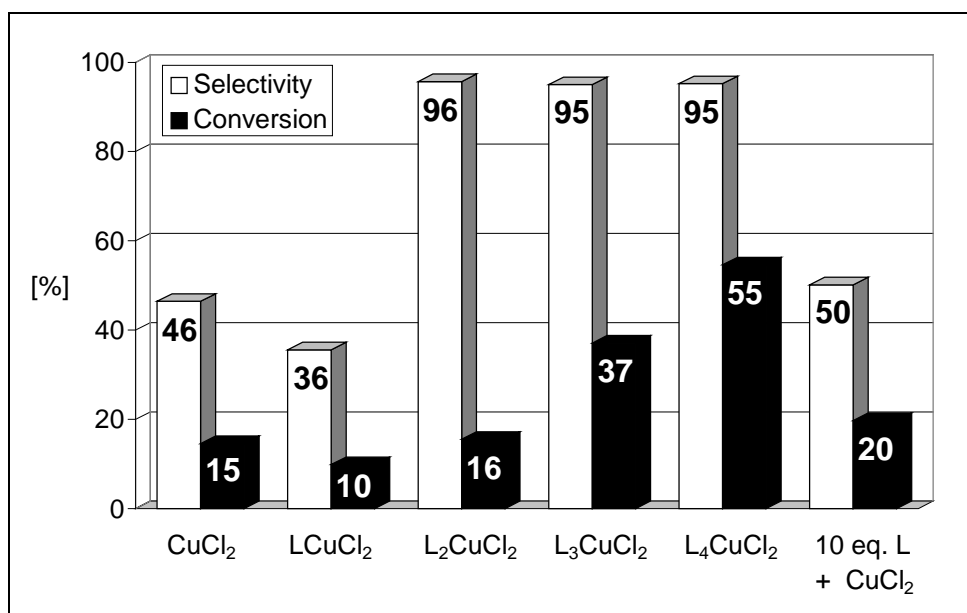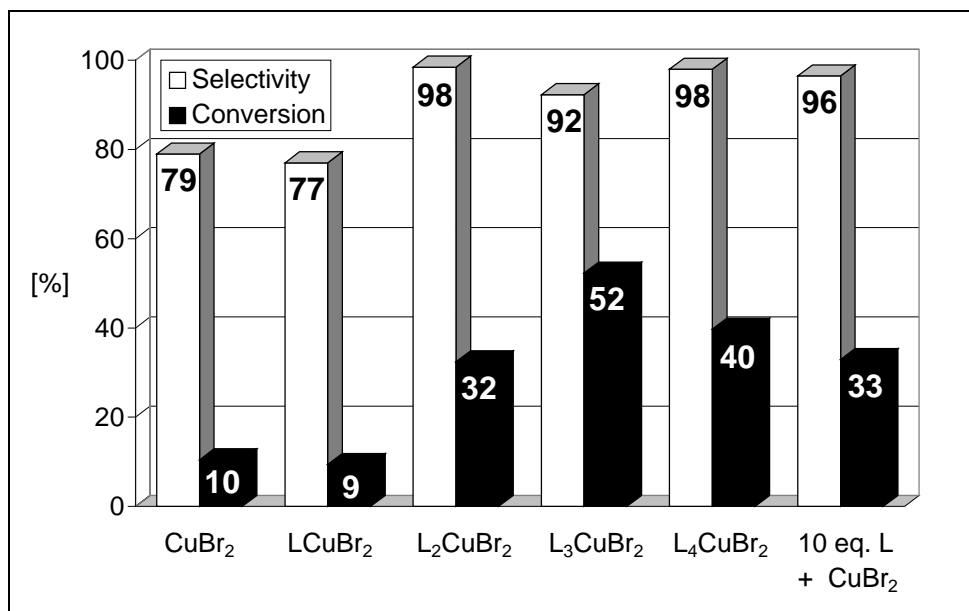

Fig. 3. $CuCl_2$ catalyst with various added equivalents of *N*-methylimidazole (L). Reaction conditions: 1 mol% catalyst, 2.5 bar O_2, 50 bar CO, 120 °C, 4 h.

A similar but not identical trend is observed for the corresponding $CuBr_2$ complexes (Fig. 4). They tend to be slightly more selective than their chloro counterparts and interestingly the peak of performance is found for the complex $(NMI)_3CuBr_2$. We observe the trend, that more than three added ligands NMI tend to inhibit the catalysis.

Fig. 4. $CuBr_2$ catalyst with various added equivalents of *N*-methylimidazole (L). Reaction conditions: 1 mol% catalyst, 2.5 bar O_2, 50 bar CO, 120 °C, 4 h.

Inhibition of catalysis by an excess of NMI may be taken as an indication that an important step of the catalytic cycle might involve the dissociation of a $[(NMI)_4Cu]^{n+}$ complex into a $[(NMI)_3Cu]^{n+}$ species. Even though, nature does not know the problem of DMC synthesis from CO, we were very surprised to learn that our best results were obtained with a copper center coordinated by three or four imidazole ligands. The $[(NMI)_3Cu]^{n+}$ core is reminiscent of the coordination site of the oxygen activating non-blue copper proteins in nature and the oxygen carrier hemocyanine. In the latter, copper is coordinated by three histidine ligands (Fig. 5). It is occurring in molluscs and arthropods in order to make oxygen available for their metabolism [46,47].
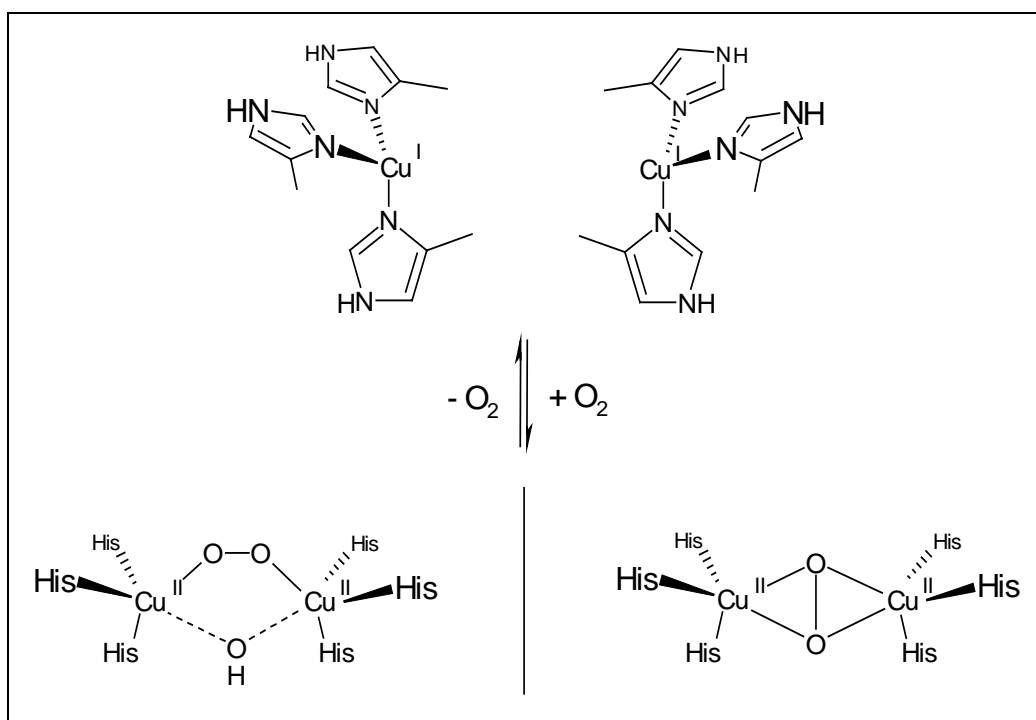
Fig. 5. Binding and transport of dioxygen in hemocyanine.

3.3 Anion influence on Cu(II) and Cu(I)

Stimulated by the slightly different results of $CuCl_2$ vs. $CuBr_2$ and by the fact that copper proteins in nature are using the Cu(I) oxidation state in their desoxy form we prepared a series of known and comparable Cu(I) and -(II) complexes $(NMI)_4CuX_n$ (n = 1, 2; X = Cl, Br, I, OTf) in order to investigate the anion effect on the catalysis more thoroughly. This series includes iodide as anion which is not oxidized by Cu(II) within the ligand regime of $[(NMI)_4Cu]^{2+}$ and triflate as a weakly or non-coordinating anion. The results with Cu(II) are shown in Fig. 6. The triflate is not competitive with respect to conversion and selectivity. The best conversion (58%) is achieved with the iodo complex, however, at the expense of selectivity (77%), thus, the theoretical yield of DMC is not exceeding 44%. The top performance with respect to the DMC yield (49%) is shown by the chloro complex (52% conversion and 95% selectivity) and the top performance with respect to selectivity by the bromo complex (98% selectivity at a conversion of 40% corresponding to 39% yield).
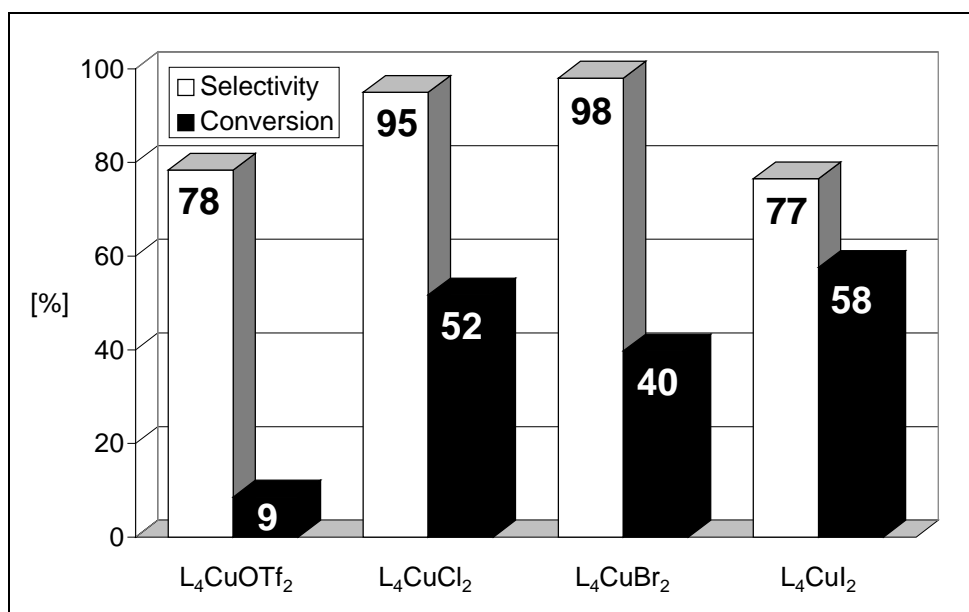
Fig. 6. Influence of various anions X^- (= OTf^-, Cl^-, Br^-, I^-) on the performance of isolated *N*-methylimidazole (L) complexes of Cu(II) L_4CuX_2. Reaction conditions: 1 mol% catalyst, 2.5 bar O_2, 50 bar CO, 120 °C, 4 h.

The results under identical catalytic conditions but with Cu(I) as the coordination center are shown in Fig. 7. Again the triflate shows the lowest conversion and selectivity. Most interestingly, the Cu(I) halide complexes follow the same trend in activity (conversion Cl^- > Br^- << I^-) as the corresponding Cu(II) halide complexes. There is a tendency that Cu(II) complexes are slightly more active and selective than the corresponding Cu(I) complexes. The same order of magnitude and the same trend with respect to their catalytic performance is in accord with the assumption that the same catalytic species is formed by both catalyst precursors. If both, Cu(I) and Cu(II) centers, are involved in the catalytic cycle, it seems not to be relevant, whether we start with one or the other, but obviously it appears to be much more relevant, how many equivalents of a strong N-donor are present per copper atom.
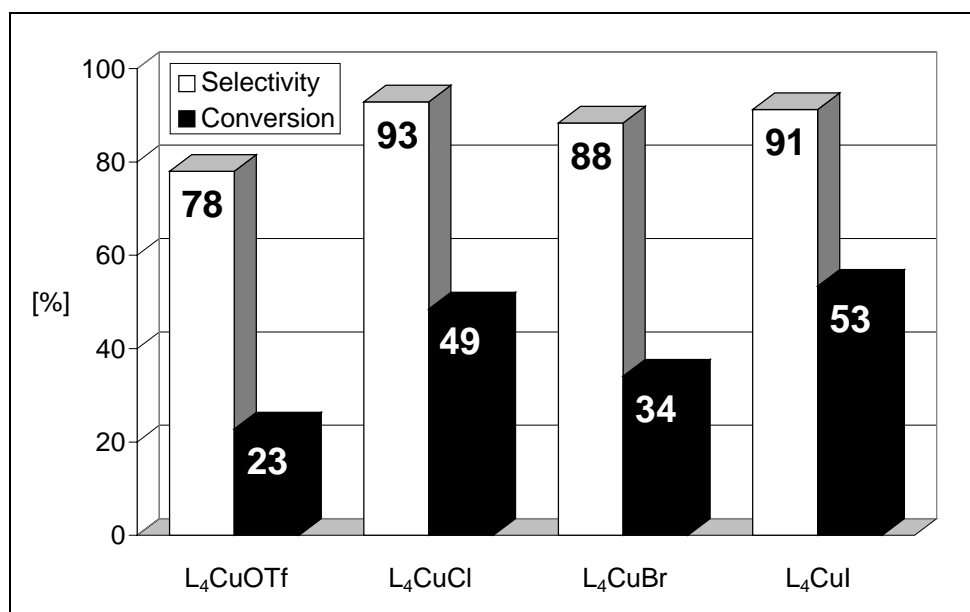
Fig. 7. Influence of various anions X^- (= OTf^-, Cl^-, Br^-, I^-) on the performance of isolated *N*-methylimidazole (L) complexes of Cu(I) L_4CuX. Reaction conditions: 1 mol% catalyst, 2.5 bar O_2, 50 bar CO, 120 °C, 4 h.

3.4 Influence of other parameters

3.4.1 Added ammonium salts to [Cu(NMI)$_4$]PF$_6$

Because of the strong impact of the anion on this catalysis, we were interested to evaluate a much greater number of anions in their effect on the catalytic performance of $[(NMI)_4Cu]^{n+}$ centers. Is was found that a combination of equimolar amounts of $[Cu(NMI)_4]PF_6$ with a non-coordinating anion and a quaternary ammonium salt of coordinating anions Cl^-, Br^-, and I^- gave nearly the same results (Fig. 8) as the use of the isolated complexes of these anions (Fig. 7). Therefore, we set out to test carbonate, hydroxide, fluoride, cyanide and other anions which were added as ammonium salts. We learned, that activity and selectivity is increasing dramatically if chloride, bromide, and iodide is added to the standard catalyst with PF_6^- counter anion (same trend $PF_6^- << Cl^- > Br^- < I^-$). However, activity and selectivity is decreasing with a trend $PF_6^- > F^- > CN^- > CO_3^{2-} > OH^-$ if these anions were added as corresponding ammonium salts. In patent literature, basic copper halides are made responsible for catalytic activity. Therefore, it is surprising, that added hydroxide shows one of the lowest conversions and the lowest selectivity. However, it has to be noted that in our experiment added ammonium salt $[Me_4N]OH \times 5\ H_2O$ was added as hydrate. Now it

becomes evident that water obviously inhibits an important step of the catalytic cycle, furthermore, it seems to lower the selectivity, e.g. by hydrolysis and formation of carbon dioxide.
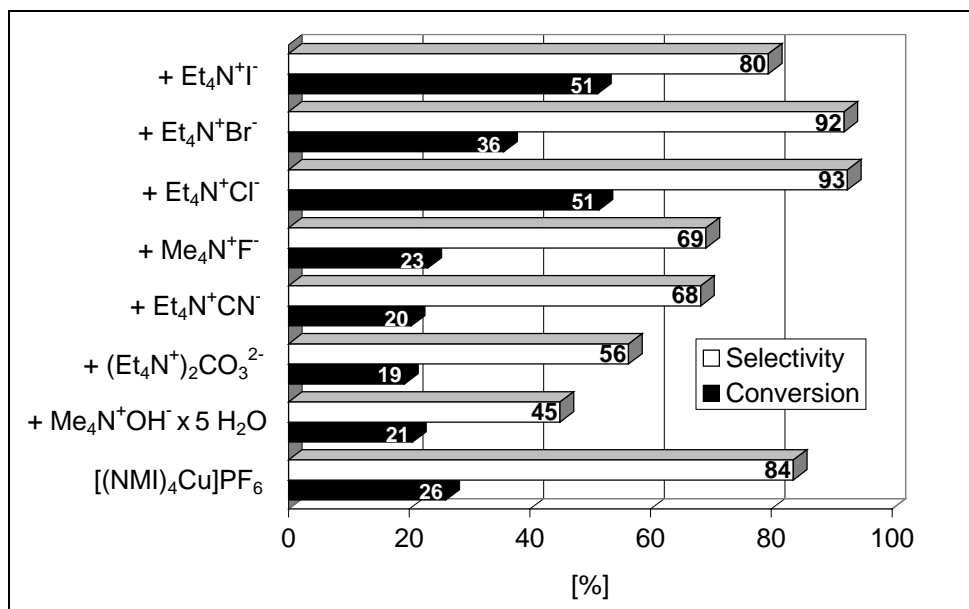

Fig. 8. Added ammonium salts equimolar to $[(NMI)_4Cu]PF_6$. Reaction Conditions: 1 mol% $(NMI)_4CuPF_6$ (+ 1 mol% X^-; + 0.5 mol% X^{2-}), 2.5 bar O_2, 50 bar CO, 120 °C, 4 h.

3.4.2 Concentration of catalyst

In many patents, substoichiometric (or even stoichiometric) amounts of copper catalysts were employed. This led us to the question whether our well-defined complexes may show even higher yields of DMC if the catalyst concentration is increased. We had to learn, that higher catalyst concentrations result only in moderate increases of conversion but at the expense of selectivity (Table 1). Consequently, the yields are not increasing very much.

Table 1. Variation of catalyst concentration.

Catalyst [mol%]	1	5	10
Conversion	55	61	67
Selectivity	95	90	87
DMC yield	52	55	58

Catalyst $(NMI)_4CuCl_2$, 2.5 bar O_2, 50 bar CO, 120 °C, 4 h.

3.4.3 Oxygen versus synthetic air as oxidant

With respect to industrial applications in DMC synthesis the use of synthetic air instead of pure oxygen was tested. In a comparative study, the best catalyst $(NMI)_4CuCl_2$ and 12.5 bar synthetic air representing an equivalent partial pressure of 2.5 bar pure oxygen was investigated. However, the conversion and particularly the selectivity is significantly lower, even if the effect of diluting oxygen by nitrogen was in part compensated with an even higher pressure (23 bar) of synthetic air (Table 2).

Table 2. Comparison oxygen vs. synthetic air.

Partial press. [bar]	Synthetic air: 12.5	Synthetic air: 23	O_2: 2.5
Conversion	43	40	55
Selectivity	76	88	95
DMC yield	33	35	52

1 mol% $(NMI)_4CuCl_2$, 50 bar CO, 120 °C, 4 h.

3.4.4 Reaction time

A rough kinetic profile of the catalysis is given in Fig. 9. After a reaction time of 4 h, a maximum of conversion and selectivity is achieved. Longer reaction times result in a formal decrease of conversion and selectivity as more and more methanol is produced by hydrolysis of DMC by the unavoidable byproduct water. With decreasing conversion and selectivity, the yields of DMC are going down from the maximum of 52% (after 4 h) via 42% (after 8 h) to 41% (after 16 h). At longer reaction times, the system appears to approach an equilibrium state between DMC production and DMC hydrolysis.
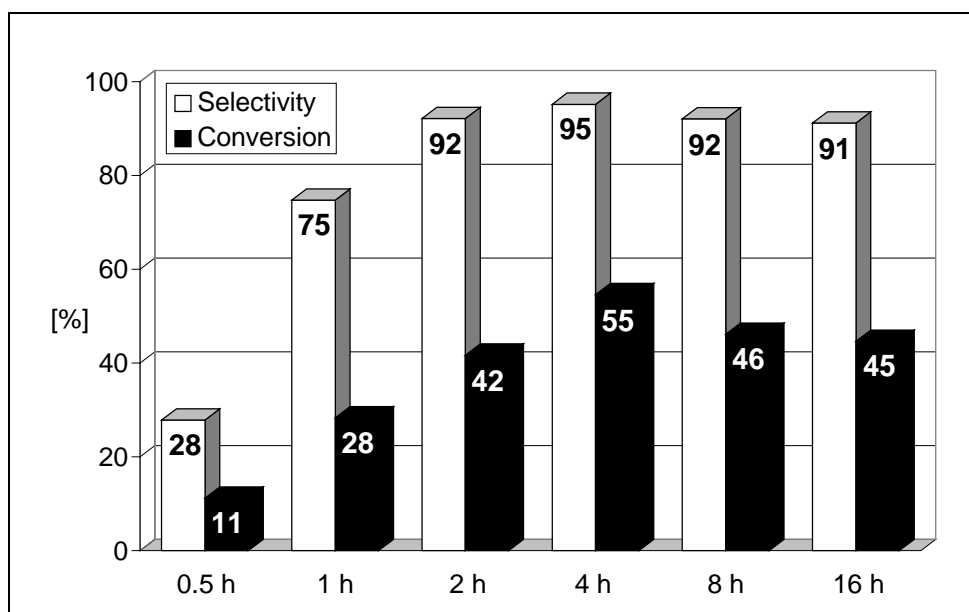
Fig. 9. Variation of reaction times. 1 mol% $(NMI)_4CuCl_2$, 2.5 bar O_2, 50 bar CO, 120 °C.

3.4.5 Ethanol as substrate

In order to evaluate whether our catalyst system is applicable to other substrates we carried out experiments using EtOH producing diethylcarbonate (DEC). Under the previously established optimized conditions (1 mol% $(NMI)_4CuCl_2$; 2.5 bar O_2; 50 bar CO; 4 h; 120 °C), DEC was formed with a conversion of 35% EtOH and in 79% selectivity. Apparently, the steric requirement and pK_s of the alcohol are responsible for the lower yield of 28% DEC.

3.4.6 PhOH as substrate

We further investigated the catalytic system in the oxidative carbonylation of PhOH to diphenylcarbonate (DPC) - the highly desired building block in polycarbonate production. Cu(II) phenoxo complexes [48] play an important role [49] in the selective catalytic oxidation of phenols. Unfortunately, no DPC was formed during the catalysis applying the previously established optimized conditions (catalyst: 1 mol% L_4CuCl_2 (L = *N*-methylimidazole); 2.5 bar O_2; 50 bar CO; 4 h; 120 °C). Instead of DPC a red-brown, high melting (m.p. > 410 °C) and absolutely insoluble polymer could be isolated in almost quantitative yield (96%). In a second catalyst system consisting of 0.5 mol% L_4CuCl_2 and 0.5 mol% L_4PdCl_2 (L = *N*-methylimidazole) the same observation was made. Besides, a metallic film on the glass insert of the autoclave developed due to reduction of Pd^{2+} to Pd^0.
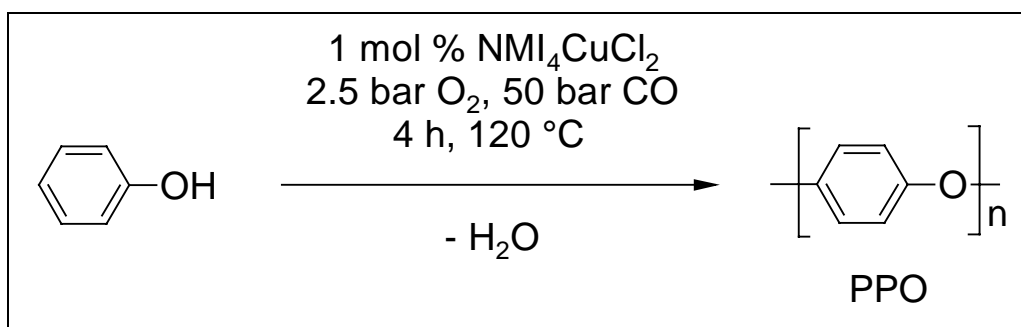
Fig. 10. Polymerization of PhOH to poly-*p*-phenylene oxide (PPO).

Although the polymer produced in the catalysis does somewhat differ from analytically pure poly-*p*-phenylene oxide (PPO) ($T_m \approx 290$ °C) [50] this is the most reasonable interpretation from its IR spectrum and high melting point which is typical for PPO´s [51]. IR absorption bands at 690 and 750 cm^{-1} (C-H out of plane bending vibrations) indicate mono- and at 830 cm^{-1} parasubstitued [52] benzene nuclei with a small amount of cross-linkage (weak absorption at 969 cm^{-1}). This is consistent with the only weakly pronounced absorption at 1023 cm^{-1} for *ortho*-linked phenylene ethers. The deviation of the elementary analysis from the theoretical values is mainly ascribed to impurities within the PPO of not homogeneously polymerized product as well as enclosed copper catalyst and PhOH. EI mass spectra are only little indicative but do contain a peak at 94.1 for phenylethers but could also be interpreted as enclosed substrate PhOH.

This polymerization of PhOH was hitherto only known for disubstituted aryl alcohols [49,51,53] despite several attempts [54] to polymerize 2,6 unsubstituted phenols. Only very recently a regioselective oxidative polymerization via Cu-OAr radicals has been reported [55].

3.5 Hydrolysis of DMC

With the aim to compare the redox versus hydrolytic activity of our catalyst complex (NMI)$_4$CuCl$_2$ with anhydrous CuCl$_2$ an experiment was designed where the starting point of the observation of hydrolytic activity is set at theoretical 100% conversion of MeOH and 100% selectivity to yield DMC and H$_2$O. An equimolar mixture of DMC and water is exposed to the same conditions as in the catalytic runs. After a reaction time of 60 minutes (30 min. 20°C→120°C followed by 30 min. at 120°C), the content of the autoclave is analyzed. Indeed, CuCl$_2$ buffered by 4 eq. of NMI leads to only 10% hydrolysis of DMC

compared to 27% for $CuCl_2$ without any N-donor ligands (Table 3). This fact clearly emphasizes that a catalyst system containing N-donor ligands such as NMI is not only superior in catalyzing the redox reaction with oxygen but also in retarding the DMC hydrolysis back to MeOH. It is plausible that for example intermediate species with a $[Cu(\mu\text{-}OH)Cu]^{n+}$ core are stronger protic acids and stronger Lewis acids when the copper centers are not coordinated by a set of 3-4 strong N-donor ligands. With respect to the better redox activity we already noted that imidazole coordination mimics histidine coordination of the oxygen activating copper redox enzymes of nature.

Table 3. Ratio DMC / MeOH as a consequence of hydrolysis.

Catalyst	DMC / MeOH [%]	
	t = 0 h	t = 1 h
$CuCl_2$	100 / 0	73 / 27
$(NMI)_4CuCl_2$	100 / 0	91 / 9

DMC:H_2O (1:1), 1 mol% catalyst, 2.15 bar O_2, 40 bar CO, t = 30 min. 20°C→120°C followed by 30 min. at 120°C.

Finally, experiments employing 3 Å molecular sieves as water withdrawing agent in order to reduce the risk of hydrolysis were carried out and the conversion as well as selectivity was compared with the blank experiment without added molecular sieves and the catalyst $(NMI)_4CuCl_2$.

In the presence of molecular sieves, the conversion is rising from 55% to 87% whereas the selectivity is decreasing from 95 % to 75%. Nevertheless, the DMC yield of 65% (compared to 52%) is the highest achieved in our experiments. Our current investigations are aimed at the extraction of water by different strategies.

3.6 Structural aspects

A short review of selected catalyst complexes that are structurally characterized or are isostructural with the proposed catalysts is presented in Fig. 11-14 [56].

3.6.1 L_4CuX_2

The coordination geometry of L_4CuX_2 complexes is best described as square planar with two additional distant axial ligands due to Jahn-Teller distortion. The N-donor molecules occupy the equatorial plane while the anionic ligands (X) are located in the axial positions. Structurally characterized complexes are: (*N*-vinylimidazole)$_4$CuCl$_2$ [57], (imidazole)$_4$CuBr$_2$ [58], (imidazole)$_4$Cu(BF$_4$)$_2$ [59]. The [(*N*-methylimidazole)$_4$Cu]$^{2+}$ cation has been subject to TRIPOS 5.2 force field calculations [60]. All compounds possess similar structures with two equally out of plane twisted imidazole molecules turned opposite to the other two imiadazoles in order to minimize steric repulsion.
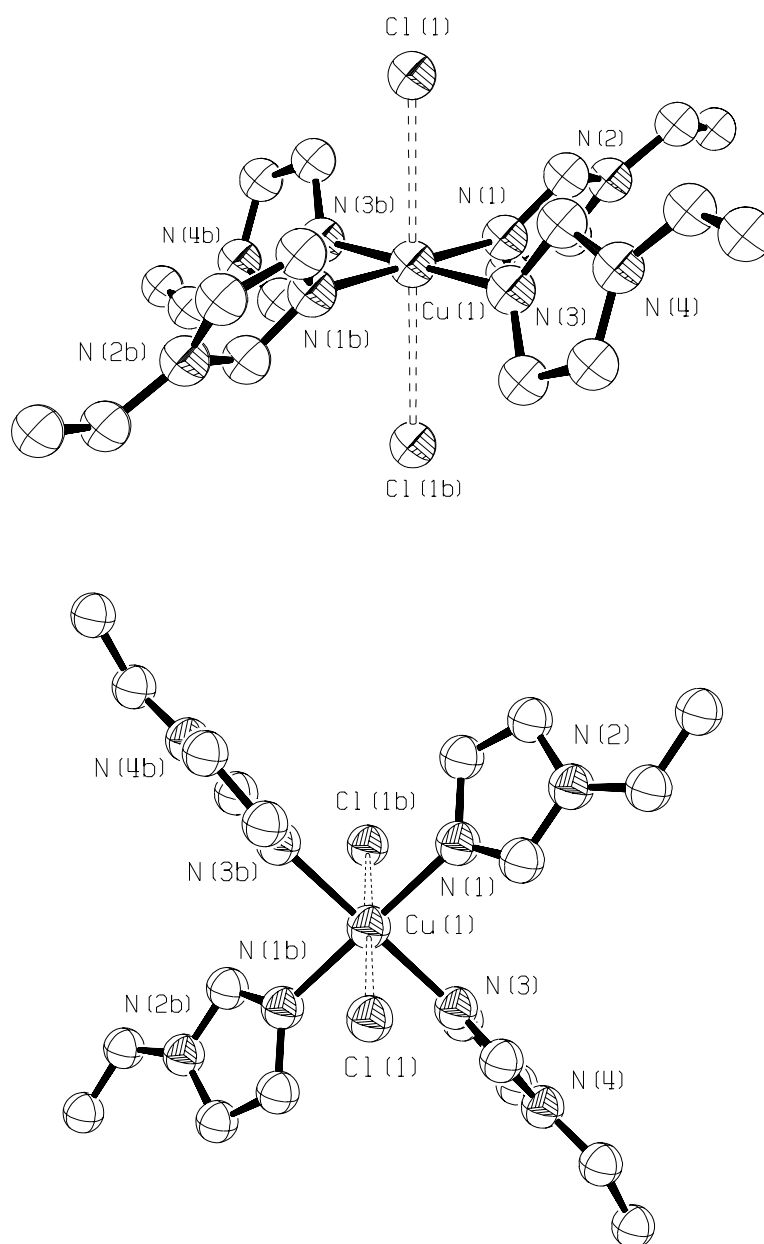

Fig. 11. ORTEP [61] plots of (*N*-vinylimidazole)$_4$CuCl$_2$ as representative for L_4CuX_2 complexes.

3.6.2 L₃CuX₂

There is only one example of a L_3CuX_2 complex, namely (1,2-dimethylimidazole)$_3$CuCl$_2$ [62]. It reveals a trigonal bipyramidal molecular structure. Two halogen anions and one imidazole ligand lie in the equatorial plane. The two axial imidazole ligands are nearly coplanar, while the equatorial imidazole ring is perpendicular to them, which gives the complex a close to C_s-symmetry.
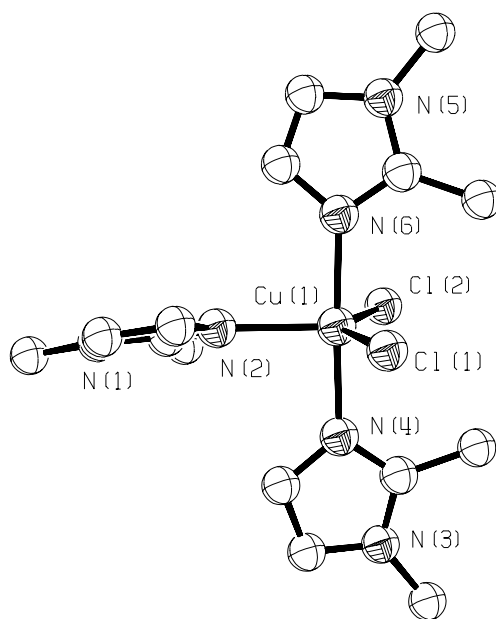

Fig. 12. ORTEP [61] plot of (1,2-dimethylimidazole)$_3$CuCl$_2$ as illustration for L_3CuX_2 complexes.

3.6.3 L₂CuX₂

Three structurally characterized complexes of the type L_2CuX_2 are known: (NMI)$_2$CuCl$_2$ [63], (NMI)$_2$CuBr$_2$ [64] and (imidazole)$_2$CuCl$_2$ [65]. The structural features differ only by variations in the degree of distortion from the ideal square planar coordination. The imidazole and halogen ligands are *trans* to one another.
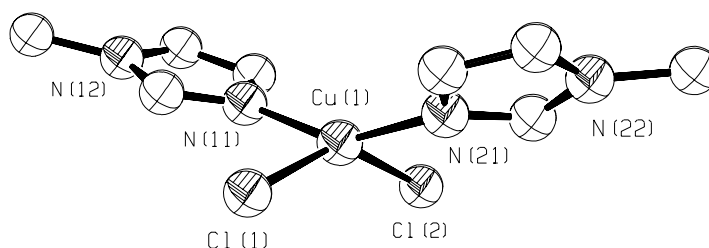

Fig. 13. Representative ORTEP [61] plot of (NMI)$_2$CuCl$_2$ to display L_2CuX_2 complexes.

3.6.4 LCuX$_2$

There is no structurally characterized example for LCuX$_2$ comparable to the complex used as catalyst.

3.6.5 L$_x$CuX

Solely one structurally characterized example for a Cu(I) complex regardless of the number of imidazole ligands is found in the literature: [Cu$_2$Cl(imidazole)$_4$]Cl [66]. In this complex the copper atoms show a trigonal coordination and are joined by a Cl bridge. The second chloride anion lies between the two hinged Cu coordination planes with the imidazole fragments in staggered manner.
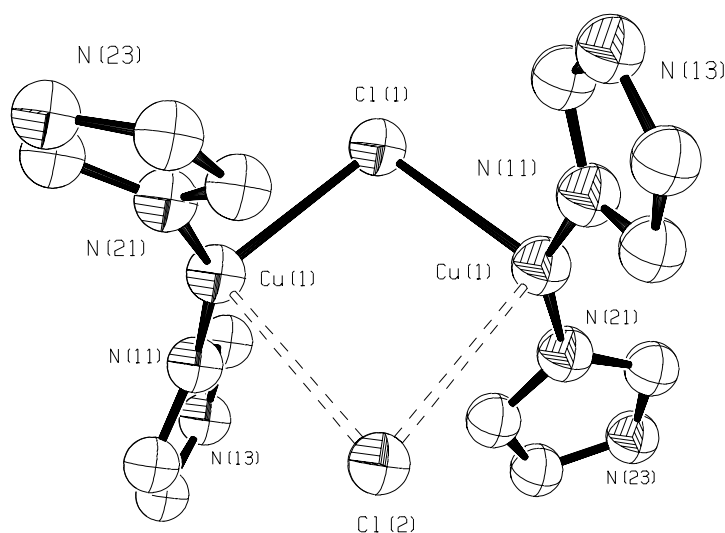

Fig. 14. ORTEP [61] view of [Cu$_2$Cl(imidazole)$_4$]Cl.

3.7 Mechanistic aspects

The mechanism of the copper catalyzed oxidative carbonylation of methanol to DMC has been the focus of some detailed studies. First insight was published by Saegusa et al. [27,28]. More detailed studies have been performed by Romano et al. including an investigation on the effect of water on DMC formation [29]. Extensive FTIR studies were performed by King gaining further evidence for certain intermediates such as Cu^I(CO), Cu^{II}(OMe) and a copper methoxycarbonyl intermediate [67]. In order to exclude a mechanism via radical coupling of Cl (from CuCl$_2$) and CO to phosgene and its methanolysis to DMC, we have investigated the reaction of anhydrous CuCl$_2$ with carbon monoxide in chlorobenzene as solvent. After 4 h / 120°C at a pressure of 50 bar CO a first fraction of volatiles (ca. 10 mL condensate) was

collected in a liquid nitrogen trap. We were not able to detect any phosgene in that condensate. As a most sensitive test for phosgene we used the trapping reaction with an equimolar mixture of methanol / pyridine, but could not detect any DMC via GC.

   Based on the previous mechanistic proposals and taking our own observation into account that it is not critical whether to start with Cu(I) or Cu(II) salts we propose a slightly modified mechanism involving a path of reductive oxygen activation, a path of carbon monoxide activation, an equilibrium of competing methanolysis versus hydrolysis of a copper oxo complex, and finally, two consecutive C-O-bond forming steps, the first performed in a mixed valence Cu(I,II) cluster, the second in a Cu(II) cluster. A proposed catalytic cycle is shown in Scheme 2.
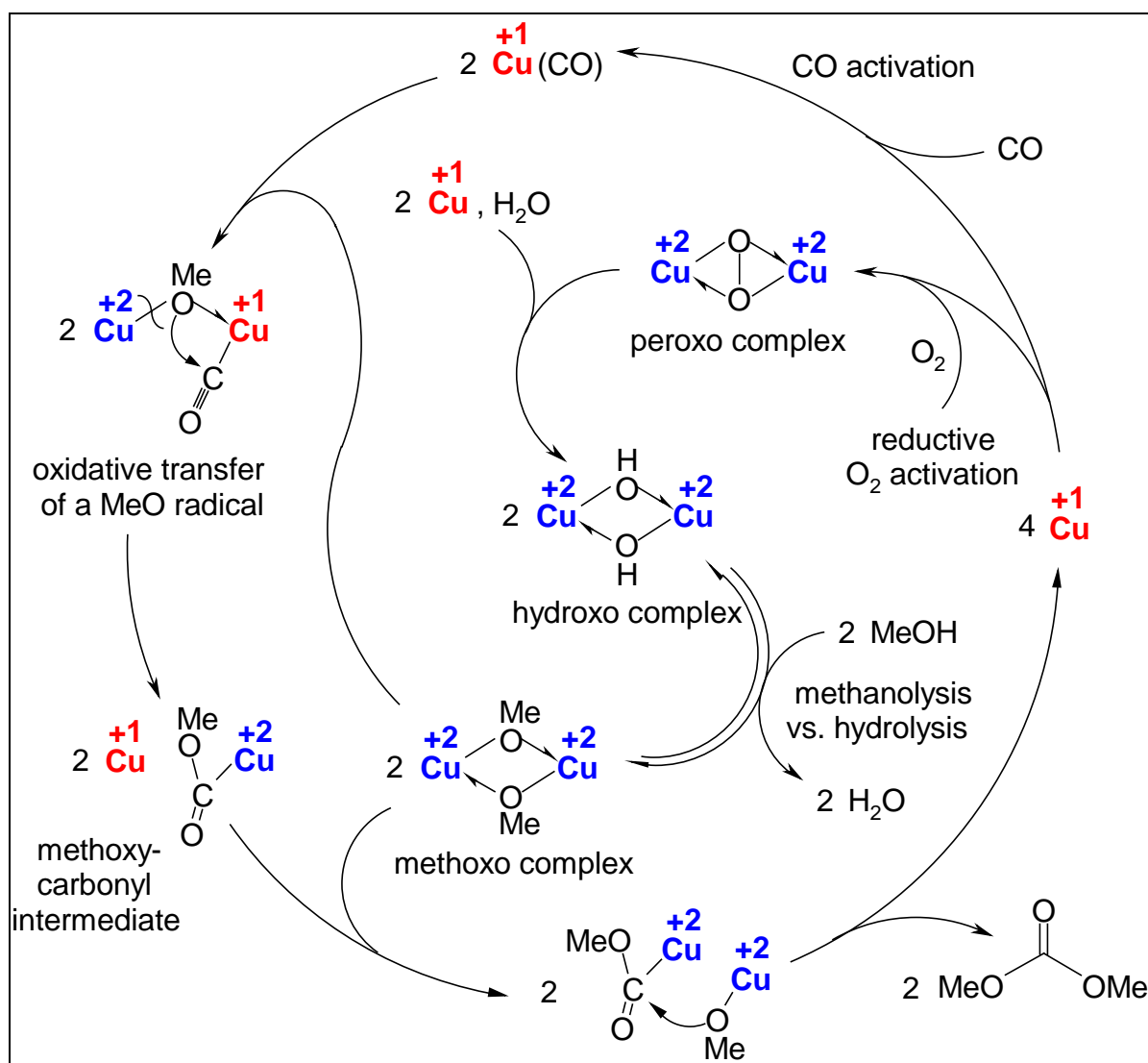
Scheme 2. Proposed catalytic reaction cycle for the oxidative carbonylation of methanol to DMC.

In Scheme 2, neither the anion - preferably chloride - nor the neutral N-donor ligand - preferably NMI - is taken into account. We learned from our experiments, that both ligands play an important part. It is assumed that chloride is providing the ideal three-electron donor ligand (μ-Cl) for the formation of mixed valent Cu(I,II)-chloro- and -methoxo-bridged clusters that may be involved in the cycle. Furthermore, imidazole is providing a perfect ligand regime for the activation of molecular oxygen [68,69] in a dinuclear or even higher-nuclear Cu(I) complex environment. If we assume that Cu(III) species are not involved in the O_2 reduction process, which is plausible at high concentrations of Cu(I), triplet oxygen will be reduced by 4 eq. of Cu(I) via a peroxo intermediate to give either 2 eq. of $[Cu(\mu\text{-OH})_2Cu]^{2+}$ (in the presence of water) or 2 eq. of $[Cu(\mu\text{-OMe})_2Cu]^{2+}$ (in the presence of excess methanol). Both structural units may be in equilibrium via competing methanolysis / hydrolysis processes, respectively. Hydrolysis may be even the preferred process, if the water content of the mixture becomes significant. Structural evidence for the existence of μ-peroxo, μ-hydroxo, and μ-oxo complexes stabilized by chelating N-donor ligands has been provided by Karlin [70,71], Kitajima [72,73], Tolman [74] and other authors [75]. A structurally characterized example for a dinuclear μ-methoxo complex is $[Cu(C_5H_5N)(OCH_3)Cl]_2$ [76]. The second reaction path of Scheme 2 illustrates the CO activation at a Cu(I) site. It is known that strong N-donor ligands render Cu(I) more electron rich and more capable for CO coordination [77]. We propose that a Cu(I) site for CO coordination and a Cu(II)-methoxo / -chloro species may form a mixed valent cluster via bridging ligands. In such clusters a latent methoxy radical may be formally transferred from Cu(II) to a CO ligand coordinated at an adjoining Cu(I) center. As a result, a new Cu(I) and a new Cu(II) methoxycarbonyl species would be generated. Equally, the nucleophilic attack of a methoxide anion at CO activated at Cu(I) followed by an electron transfer from Cu(I) to Cu(II) may be discussed. Coupling of a methoxycarbonyl radical and a methoxy radical should occur at a multinuclear Cu(II) cluster as there is no conceivable pathway which would allow the reductive elimination of both radicals [MeO] and [C(O)OMe] at a mononuclear Cu(II) site.

While it is known that a certain amount of water is required in the catalytic cycle [78], it is evident that larger amounts of water lead to unselective oxidation of CO to CO_2. The water sensitive spot in our mechanistic proposal is the equilibrium between the copper methoxo and hydroxo complex. Transfer of an OH radical would generate a carbonic acid monoester, which would decompose to carbon dioxide [79] and MeOH. On the other hand, hydrolysis of the methoxycarbonyl intermediate would generate a carbonic acid monoester and formally a

copper hydrido species, methanolysis of the methoxycarbonyl species would generate the carbonic acid diester and a copper hydrido species. As long as there are no model reactions available it can only be speculated that there might be even more or other mechanistic pathways involved in this DMC synthesis, e.g. involving reoxidation of such copper hydrido species by either oxygen or Cu(II)-peroxo / -oxo species. We are currently working on these model reactions.

4 Conclusion

The present paper describes a systematic study of ligand effects of anions and neutral N-donors on the oxidative carbonylation of methanol to dimethyl carbonate. Whereas in a qualitative manner the preference for copper halides has been reported before, a most surprising impact of NMI coordination to copper has been discovered here. The activity in methanol conversion and selectivity in DMC production is drastically increased if three or four strong N-donor ligands of the pentaalkylguanidine type, 4-dimethylaminopyridine (DMAP), and preferably NMI are coordinated at the catalytically active copper center. The imidazole coordination mimics the histidine coordination in oxygen activating copper enzymes of nature. Surprisingly, the number and type of coordinated N-ligands has a much higher impact on the catalytic performance, than the oxidation state of the copper complex and its counter anion - as long as it belongs to the group of heavier halides (chloride, bromide and iodide). All other anions including fluoride, hydroxide, carbonate, and cyanide (cyanate) give only poor results. The three top catalyst complexes $(NMI)_4CuCl_2$, $(NMI)_3CuBr_2$, and $(NMI)_4CuI$ show selectivities exceeding 90% in DMC production at methanol conversions exceeding 50 % under our standard batch reaction conditions (1 mol% catalyst, 2.5 bar O_2, 50 bar CO, 120°C, 4 h). The great advantage of these complexes is their higher activity and selectivity in oxygen activation and redox catalysis combined with their lower hydrolytic activity in the undesired DMC hydrolysis by the unavoidable byproduct water. Catalytic runs with such complexes require only low catalyst concentrations of 1 mol% compared to substoichiometric or even higher amounts of copper halides without N-ligand support. Finally, corrosion of the stainless steel reactors is efficiently inhibited if ≥2 eq. of N-donor ligand are present.

References

[1]   A.G. Shaikh, S. Sivaram, Chem. Rev. 96 (1996) 951-976 and cited references.

[2]   F. Rivetti, U. Romano, D. Delledonne, in: Proceedings of the ACS Symposium Series 626 on Green Chemistry: Designing Chemistry for the Environment (Chapter 6), Am. Chem. Soc. (1996) 70-80 and cited references.

[3]   M.A. Pacheco, C.L. Marshall, Review of dimethyl carbonate manufacture and its characteristics as a fuel additive", Energy & Fuels 11 (1997) 2-29 and cited references.

[4]   Y. Ono, Appl. Catal. A 155 (1997) 133-166.

[5]   G. Illuminati, U. Romano, R. Tesei, German Patent 2,528,412 (1979).

[6]   F. Merger, F. Towee, L. Shroff, EP 0,000,162 (1979).

[7]   H.J. Buysch, H. Krimm, H. Böhm, EP 21,211 (1979), to Bayer AG.

[8]   T. Matsuzaki, A. Nakamura, Catal. Surv. Jpn. 1 (1997) 77-88.

[9]   U. Romano, Chim. Ind. 75(4) (1993) 303-306.

[10]   R.A. Sheldon, Chem. Ind. 1 (1997) 12-15.

[11]   T. Sakakura, J.C. Choi, Y. Saito, T. Masuda, T. Sako, T. Oriyama, J. Org. Chem. 64 (1999) 4506-4508.

[12]   W. McGhee, D. Riley, J. Org. Chem. 60 (1995) 6205-6207.

[13]   U. Romano, R. Tesei, G. Cipriani, L. Micucci, US Pat. 4,218,391 (1980), to Anic S.p.A.

[14]   E. Hallgren, G. M. Lucas, US Pat. 4,360,477 (1982), to General Electric Co.

[15]   F. Rivetti, U. Romano, EP 534,545 (1993), to ENI Group Co.

[16]   N. Di Muzio, F. Rivetti, C. Fusi, G. Sasseli, US Pat. 5,210,269 (1993), to Enichem Synthesis S.p.A.

[17]   Z. Kricsfalussy, H. Waldmann, H.-J. Traenckner, EP 0,636,601 A1 (1995), to Bayer AG.

[18]   Z. Kricsfalussy, H. Waldmann, H.J. Traenckner, Ind. Eng. Chem. Res. 37 (1998) 865-866.

[19]   G. L. Curnutt, US Pat. 5,004,827 (1991), to Dow Chemical Co.

[20]   S.T. King, Catal. Today 33 (1997) 173-182.

[21]   K. Otsuka, T. Yagi, I. Yamanaka, Chem. Lett. (1994) 495-498.

[22]   K. Tomishige, T. Sakaihori, S. Sakai, K. Fujimoto, Appl. Catal. A 181 (1999) 95-102.

[23]   Y. Sato, M. Kagotani, T. Yamamoto, Y. Souma, Appl. Catal. A 185 (1999) 219-226.

[24]   Y. Toshima, K. Mori, H. Nakamura, JP Pat. 06,210,181 (1994), to Nikki Co.

[25]   E. Perotti, G. Cipriani, US Pat. RE 29,338 (1977), to Snam Progetti S.p.A.

[26]   G. Stammann, R. Becker, J. Grolig, H. Waldmann, US Pat. 4,370,275 (1983), to Bayer AG.

[27]   T. Saegusa, T. Tsuda, K. Isayama, K. Nishijima, Tetrahedron Lett. 7 (1968) 831-833.

[28]   T. Saegusa, T. Tsuda, K. Isayama, J. Org. Chem. 35(9) (1970) 2976-2978.

[29]   U. Romano, R. Tesei, M.M. Mauri, P. Rebora, Ind. Eng. Chem. Prod. Res. Dev. 19 (1980) 396-403.

[30]   B.K. Nefedov, N.S. Sergeeva, Y.T. Eidus, Izv. Akad. Nauk SSSR Ser. Khim. 4 (1973) 804-806.

[31]   T. Yamamoto, K. Imaizumi, Y. Maeda, Corrosion 45(6) (1989) 506-509.

[32]   D.M. Fenton, P.J. Steinwand, J. Org. Chem. 39 (1974) 701-704.

[33]   J.A. Welleman, F.B. Hulsbergen, J. Verbiest, J. Reedijk, J. Inorg. Nucl. Chem. 40 (1978) 143-147.

[34]   R. Hüttel, M.E. Schön, Liebigs Ann. Chem. 625 (1959) 55-65.

[35]   R.N. Keller, H.D. Wycoff, in: W.C. Fernelius (Ed.), Inorganic Syntheses, Vol. 2, Mc Graw-Hill, New York, 1946, pp. 1-4.

[36]   H. Hecht, Z. Anorg. Ch. 254 (1947) 37-51.

[37]   P.W.N.M van Leeuwen, W.L. Groeneveld, Inorg. Nucl. Chem. Lett. 3 (1967) 145-146.

[38]   R.G. Salomon, J.K. Kochi, J. Am. Chem. Soc. 95 (1973) 1889-1897.

[39]   C.L. Jenkins, J.K. Kochi, J. Am. Chem. Soc. 94 (1972) 843-855.

[40]   G.J. Kubas, Inorg. Synth. 19 (1979) 90-92.

[41]   D.M.L. Goodgame, M. Goodgame, G.W. Rayner-Canham, Inorg. Chim. Acta 3 (1969) 406-410.

[42]   J.A.C. van Ooijen, J. Reedijk, J. Chem. Soc. Dalton (1978) 1170-1175.

[43]   Chemsafe Database Recherche BAM-II.201 (1997), Bundesanstalt für Materialforschung und -prüfung; H. Warrink, Masters Thesis, Universität Gesamthochschule Paderborn, 1993.

[44]   H. Wittmann, V. Raab, A. Schorm, J. Plackmeyer, J. Sundermeyer, Eur. J. Inorg. Chem. (2001) 1937-1948.

[45]   V. Raab, J. Kipke, O. Burghaus, J. Sundermeyer, Inorg. Chem. 40 (2001) 6964-6971.

[46]   W. Kaim, Angew. Chem. 108 (1996) 47-64.

[47] K.A. Magnus, H. Ton-That, J.E. Carpenter, Chem. Rev. 94 (1994) 727-735.

[48] J.F. Harrod, Can. J. Chem. 47 (1969) 637-645.

[49] A.S. Hay, H.S. Blanchard, G.F. Endres, J.W. Eustance, J. Am. Chem. Soc. 81 (1959) 6335-6336.

[50] H.M. van Dort, C.A.M. Hoefs, E.P. Magré, A.J. Schöpf, K. Yntema, Eur. Polym. J. 4 (1968) 275-287.

[51] D. Braun, H. Cherdron, H. Ritter, in: Praktikum der Makromolekularen Stoffe, J. Wiley, VCH, Weinheim, 1999, pp. 264-289.

[52] M. Hesse, H. Meier, B. Zeeh, in: Spektoskopische Methoden in der organischen Chemie, 4. Aufl., Thieme Verlag, Stuttgart, New York, 1991.

[53] a) R. Ikeda, J. Sugihara, H. Uyama, S. Kobayashi, Macromolecules 29 (1996) 8702-8705; b) W. Chen, G. Challa, Eur. Polym. J. 26 (1990) 1211-1216; c) A.S. Hay, Macromolecules 2 (1969) 107-108; d) H. Finkbeiner, A.S. Hay, H.S. Blanchard, G.F. Endres, J. Org. Chem. 31 (1966) 549-555.

[54] H. Uyama, H. Kurioka, I. Kaneko, S. Kobayashi, Chem. Lett. (1994) 423-426.

[55] H. Higashimura, K. Fujisawa, Y. Moro-oka, M. Kubota, A. Shiga, A. Terahara, H. Uyama, S. Kobayashi, J. Am. Chem. Soc. 120 (1998) 8529-8530.

[56] CCDC recherche, January 2001.

[57] A.A. Kashaev, E.A. Zel´bst, M.P. Demidov, Y.L. Frolov, N.N. Chipanina, E.S. Domnina, G. G. Skvortsova, Koord. Khim. 4 (1978) 785-790.

[58] O.J. Parker, G.L. Breneman, Acta Cryst. C51 (1995) 1097-1099.

[59] C.-C. Su, T.-T. Hwang, O.Y.-P. Wang, S.-L. Wang, F.-L. Liao, Transition Met. Chem. 17 (1992) 91-96.

[60] F. Wiesemann, S. Teipel, B. Krebs, U. Höweler, Inorg. Chem. 33 (1994) 1891-1898.

[61] M.N. Burnett, C.K. Johnson, *ORTEP-III, Oak Ridge Thermal Ellipsoid Plot Program for Crystal Structure Illustrations*, Oak Ridge National Laboratory Report ORNL-6895, (1996).

[62] F. Huq, A.C. Skapski, J. Chem. Soc. (A) (1971) 1927-1931.

[63] J.A.C. van Ooijen, J. Reedijk, A.L. Spek, J. Chem. Soc. Dalton Trans. (1979) 1183-1186.

[64] J.C. Jansen, H. van Koningsveld, J.A.C. van Ooijen, Cryst. Struct. Comm. 7 (1978) 637-641.

[65] B.K.S. Lundberg, Acta Chem. Scand. 26 (1972) 3977-3983.

[66] W. Clegg, S.R. Acott, C.D. Garner, J. Chem. Soc. Dalton Trans. (1984) 2581-2583.

[67] S.T. King, J. Catal. 161 (1996) 530-538.

[68] I. Sanyal, R.W. Strange, N.J. Blackburn, K.D. Karlin, J. Am. Chem. Soc. 113 (1991) 4692-4693.

[69] I. Sanyal, K.D. Karlin, R.W. Strange, N.J. Blackburn, J. Am. Chem. Soc. 115 (1993) 11259-11270.

[70] K.D. Karlin, J. Am. Chem. Soc. 110 (1988) 3690-3692.

[71] K.D. Karlin, J. Am. Chem. Soc. 115 (1993) 2677-2689.

[72] N. Kitajima, J. Am. Chem. Soc. 114 (1992) 1277-1291.

[73] N. Kitajima, Y. Moro-oka, Chem. Rev. 94 (1994) 737-757.

[74] W.B. Tolman, Acc. Chem. Res. 30(6) (1997) 227-237.

[75] S. Schindler, Chem. Eur. J. Microrev. (2000) 2311-2326 and cited references.

[76] R.D. Willett, G.L. Breneman, Inorg. Chem. 22 (1983) 326-329.

[77] M. Pasquali, C. Floriani, A. Gaetani-Manfredotti, Inorg. Chem. 20 (1981) 3382-3388.

[78] U. Romano, EP 365,083 (1989), to ENI Chem.

[79] J.J. Byerley, J.Y.H. Lee, Can. J. Chem. 45 (1967) 3025-3030.

— Chapter 3.1 —

Copper Complexes of Novel Superbasic Peralkylguanidine Derivatives of Tris(2-aminoethyl)amine (tren) as Constraint Geometry Ligands

Keywords: N ligands • Tripodal ligands • Guanidines • Coordination chemistry • Copper

Abstract

The coordination chemistry of copper(I) and copper(II) ions with novel tripodal peralkylguanidine derivatives of the tris(2-aminoethyl)amine (tren) backbone TMG$_3$tren (tetramethylguanidino-tren) N{CH$_2$CH$_2$N=C(NMe$_2$)$_2$}$_3$ (**1**) and cyclic DMPG$_3$tren (dimethylpropyleneguanidino-tren) N[CH$_2$CH$_2$N=C{NMe(CH$_2$)$_3$NMe}]$_3$ (**2**) is reported. These sterically demanding ligands form complexes of constraint trigonal geometry. Their superbasic character with estimated pK_{BH+} values 6 orders of magnitude higher than that of the known Me$_6$tren and their softer N-donor character compared to *tert*-amine ligands stabilize cationic mononuclear Cu(I) and Cu(II) ions by delocalization of charge into the guanidine functionalities. The crystal structures and spectroscopic features of two cationic copper(I) complexes with an uncommon trigonal-pyramidal [N$_4$Cu]$^+$ coordination sphere and a sterically protected open coordination site and of two cationic copper(II) complexes with the characteristic trigonal-bipyramidal coordination geometry [N$_4$CuCl]$^+$ and [N$_5$Cu]$^{2+}$ are reported. A structural parameter ρ is introduced as a measure for delocalization of positive charge in guanidines.

Introduction

Copper complexes with multidentate tripodal alkylamine, Schiff base, or aza aromatic ligands or hybrids thereof have been extensively used to model the structure and reactivity of active sites in copper proteins that transport oxygen, transfer oxygen after O-O bond cleavage, or use oxygen as H atom acceptor, such as hemocyanine,[1] tyrosinase,[2] and galactose oxidase.[3] The ligands of the tris(2-aminoethyl)amine (tren) family shown in Figure 1 may be the most prominent representatives among the tripods that force a metal cation into a trigonal-bipyramidal coordination geometry.[4] Coordination chemistry of copper has been mainly

developed with H$_6$tren (tris(2-aminoethyl)amine),[5] Me$_6$tren (tris(2-dimethylamino)amine),[5b,6] and tmpa (tris(2-pyridylmethyl)amine),[7] also with Schiff bases[8] as well as with mixed[9] pyrazole[10] and imidazole[11] or tris(pyrazolylborate)[1h,i,12] derived tripod ligands.

R = R' = Me   TMG$_3$tren (1)
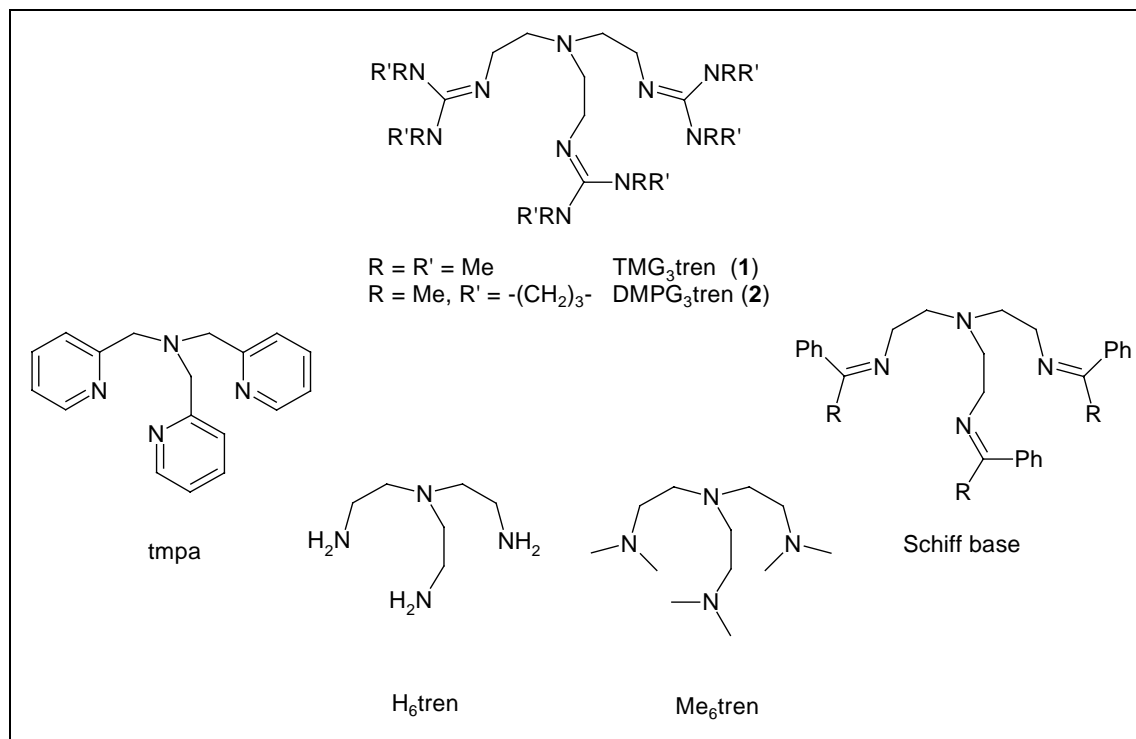R = Me, R' = -(CH$_2$)$_3$-   DMPG$_3$tren (2)

Figure 1. Structural relationship between the novel peralkylguanidino-tren ligands and the most prominent tripods of the tren ligand family.

One approach to influence the catalytic metal properties is the variation of the bite angle of these tripods and of their steric demand by introducing different armlengths;[7a,b,10,13] another approach is the variation of the basicity, softness, and π-acceptor ability of the N-donor, e.g., by alkylation of the primary amine functionality of H$_6$tren or converting it to an sp^2 N-donor (Schiff base, tmpa).[7,8] Peralkylated guanidines belong to the strongest organic neutral bases known.[14] They are several magnitudes superior in basicity than tertiary amines due to the excellent stabilization of the positive charge in their resonance stabilized cations.[15] This trend may be demonstrated by the pK_{BH+} (MeCN) values of the 1,2,2,6,6-pentamethyl piperidinium cation (18.62), the parent guanidinium cation (23.3), and the pentamethyl guanidinium cation (25.00).[15c] However, despite of their prominent proton affinity, surprisingly little is known about their capability to bind Lewis acidic metal cations. There are a few reports on coordination compounds of monoguanidines HN=C(NRR')$_2$.[16,17,18,19,20] The first complexes

of chelating bisguanidines have been reported by Kuhn[21] and ourselves.[22] Coordination compounds of biologically relevant transition metals Zn, Fe, Mn, and Mo with tripodal trisguanidine TMG$_3$tren (N{CH$_2$CH$_2$N=C(NMe$_2$)$_2$}$_3$; **1**) are currently being investigated by us.[23] The pronounced tendency of biguanides to stabilize unusually high oxidation states of metals, e.g., in Ag(III)[24] and Ni(III)[25] complexes (Figure 2), attracted our attention, since highly oxidized copper(III) centers are involved in the activation and cleavage of dioxygen.[1,2,3,26]
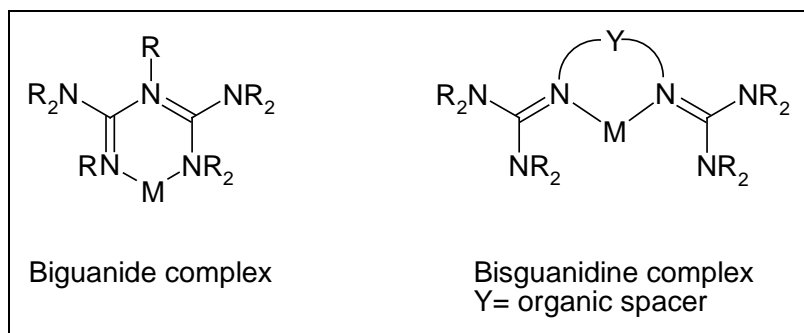

Figure 2. Guanidine-based complexes.

In proteins the H$_5$-guanidinium functionality of arginine serves as anion receptor.[27] The focus of this investigation is the largely unexplored capability of multidentate R$_5$-guanidines to serve as receptors for copper(I) and copper(II) cations. The basicity of these neutral ligands lies between that of tertiary amines and amido ligands; they are expected to be softer in character than amines. The question arises whether guanidines may be π-acidic like Schiff bases or π-basic like amido ligands. Many more aspects in guanidine coordination chemistry are unexplored such as fine-tuning of the basicity, donor strength, sterical demand, and bite of chelating ligands by variation of the substituents at the guanidine function. Following our study on guanidine coordination compounds with the en and tame backbone,[22] we wish to introduce the one with the tren type ligand regime and copper in oxidation states +1 and +2.

Results and Discussion

Synthetic Studies. Multidentate alkyl tetramethyl guanidines are synthesized by treating primary polyamines with Vilsmeyer salts, a method described earlier by Eilingsfeld and Seefelder[28] and improved by Kantlehner et al.[29] for monoguanidines. Because of difficulties in purification of bis- and trisguanidines, there is a need for selective reactions in this synthesis. A close to quantitative transformation of a primary amine functionality into the

guanidine may be accomplished by the reaction with the Vilsmeyer salt [(Me$_2$N)$_2$C-Cl]Cl obtained by reaction of tetramethylurea with phosgene,[30] trichloromethylchloroformate (diphosgene),[31a] or oxalyl chloride in toluene.[32] Cyclic guanidines may be prepared by a similar strategy.[31] The corresponding guanidinium salt is then deprotonated in THF/NaH or in a two-phase system of 50% NaOH(aq)/MeCN to yield the free base. By using this protocol 1,1,1-tris{2-[N^2-(1,1,3,3-tetramethylguanidino)]ethyl}amine (**1**) (TMG$_3$tren) has been obtained in a yield of 86%.[23] We were interested to create a ligand with cyclic guanidine functionalities, as in five- and six-membered cyclic guanidines the lone pairs at the nitrogen atoms are forced into better conjugation; thus an enhanced N-basicity and a better donor strength than that of non cyclic counterparts may be anticipated. Treatment of commercially available *N,N'*-dimethylpropyleneurea (DMPU) with phosgene leads to the corresponding chloro amidinium salt (the synthesis of the 5-membered ring analogue in a similar manner to our method has been reported[31]), which is condensed with H$_6$tren to finally yield the new ligand 1,1,1-tris{2-[N^2-(1,3-dimethylpropyleneguanidino)]ethyl}amine (**2**) (DMPG$_3$tren).
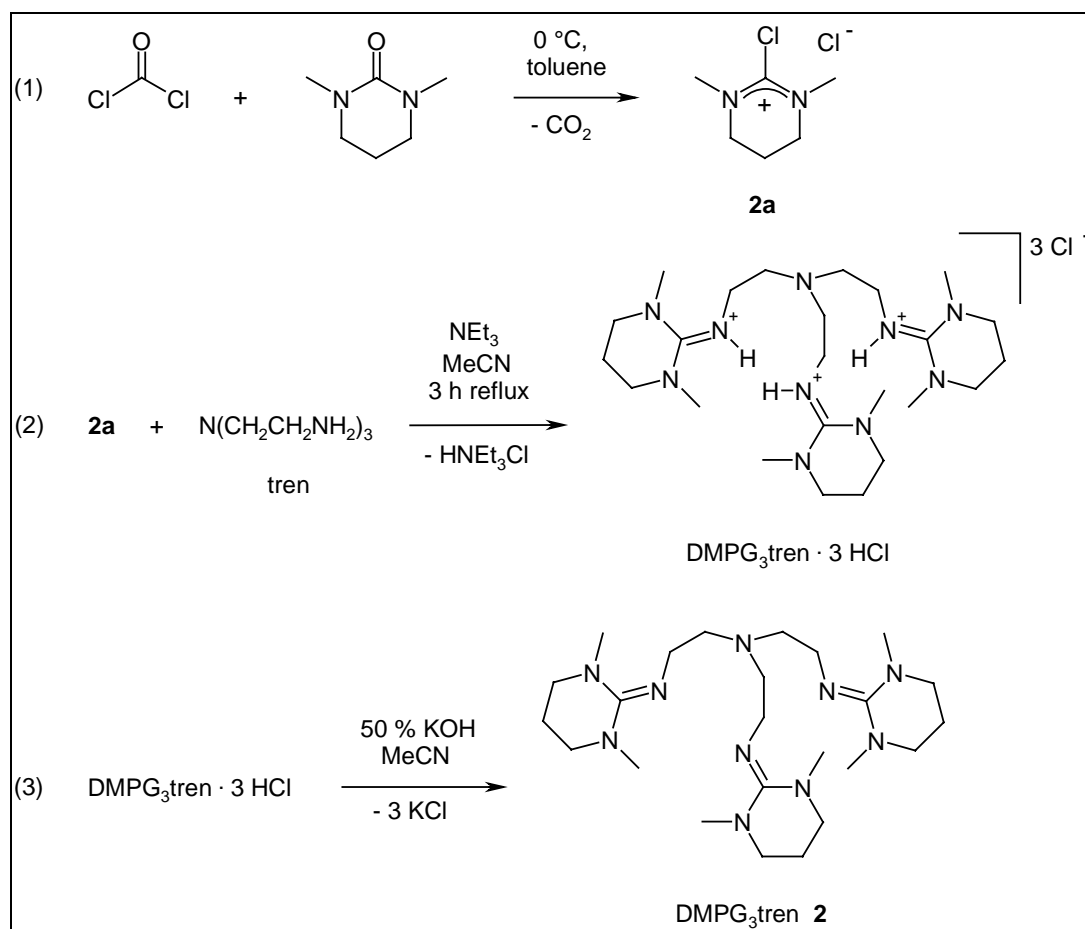

Figure 3. Preparation of peralkylated oligoguanidines, e.g., DMPG$_3$tren (**2**).

4

Both ligands **1** and **2** have been used in the synthesis of stable and highly crystalline copper complexes **3-6**. It is remarkable that guanidines as very strong but polarizable bases stabilize both copper(I) and copper(II) centers in the same N$_4$-donor regime. This is in contrast to the known instability for some copper(I) complexes of H$_6$tren ligands, which are harder in character and sterically less shielded: their complexes tend to disproportionate to copper(0/II).[6c] Due to the high proton affinity of our guanidines, the dominant species in aqueous solution are hydrated guanidinium hydroxides. Therefore, these ligands tend to form basic copper(II) salts from aqua complexes. To overcome the tendency of protolysis, the Cu(II) salts were dehydrated by the ortho ester method[33] prior to their use as starting material. The complexes are synthesized in good yields by combining the dehydrated metal salts with 1.05 equivalents of **1** and **2** in dry acetonitrile. Surprisingly, all complexes **3-6** are ionic, even those of copper(I) such as **5** that contains a nonsolvated chloride ion in the solid state structure (vide infra). Consequently, **3-6** are soluble in polar aprotic media such as MeCN and acetone or CH$_2$Cl$_2$ but insoluble in diethyl ether and hydrocarbons.
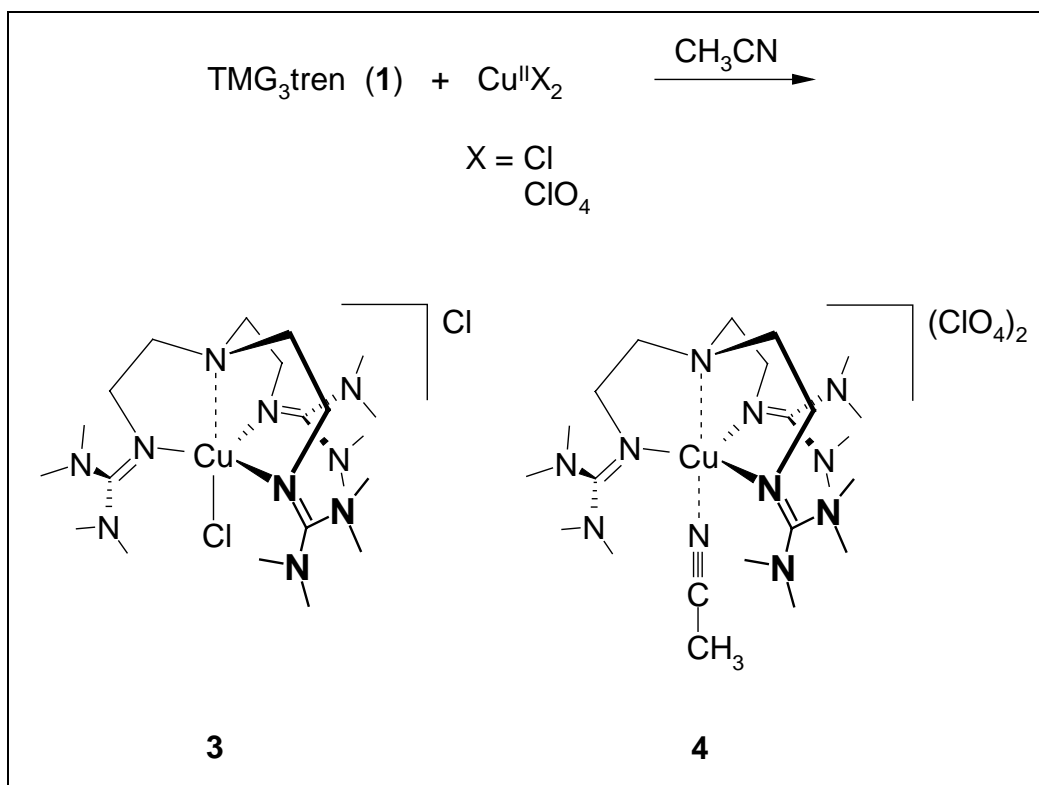

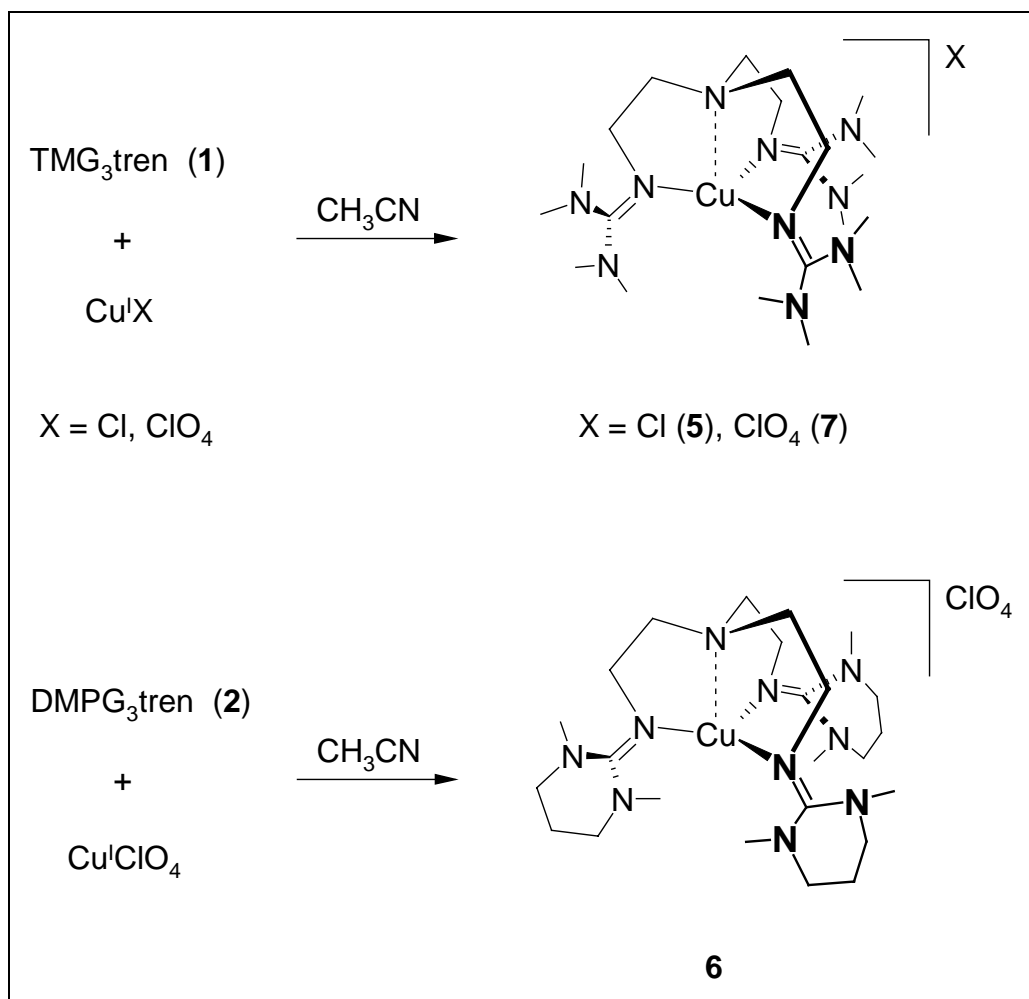**Figure 4.** Complex formation of copper(II) perchlorate and chloride with TMG$_3$tren (**1**).

TMG$_3$tren (**1**)

+

Cu^{I}X

$\xrightarrow{\text{CH}_3\text{CN}}$

X = Cl, ClO$_4$

X = Cl (**5**), ClO$_4$ (**7**)

DMPG$_3$tren (**2**)

+

Cu^{I}ClO$_4$

$\xrightarrow{\text{CH}_3\text{CN}}$

6

Figure 5. Complex formation of Cu(I) salts with TMG$_3$tren (**1**) and DMPG$_3$tren (**2**).

All complexes **3**-**6** are sensitive to moisture. It is observed that metal hydroxides and protonated ligand are formed when **3**-**6** are exposed to aqueous solvent mixtures. These findings are explained by the high proton affinity of guanidines: deprotonation of an aqua ligand irreversibly induces the hydrolytic cleavage of the metal-nitrogen bond, a pattern resembling hydrolysis of amido complexes (Figure 6).
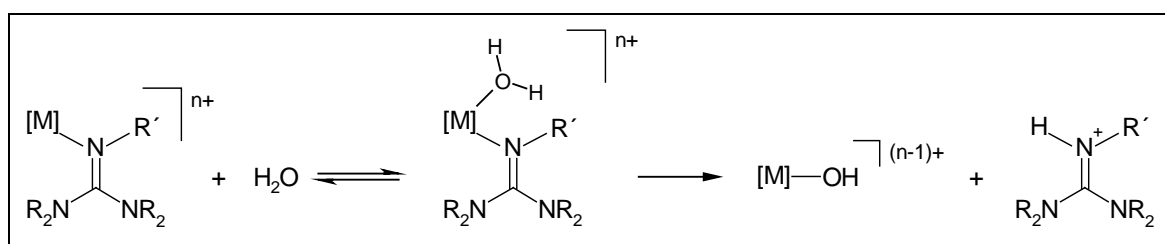

Figure 6. Hydrolytic cleavage of the metal-nitrogen bond.

The copper(I) complexes are highly sensitive to oxygen. We are currently investigating this reaction by means of UV-vis and Raman spectroscopies.[34]

Spectroscopic Studies. All complexes show the parent molecular ions in the APCI mass spectra obtained from MeCN solutions. Their composition is confirmed by the characteristic isotopic patterns which are in accord with simulated ones.

A difference between the free guanidine base and in metal coordination or protonation, respectively can be recognized in the infrared spectra where the free ligands show a single absorption ν(C=N) at wavenumbers of 1620 (TMG$_3$tren) and 1595 (DMPG$_3$tren) cm^{-1} (KBr pellet). In complexes with Lewis acids this absorption shows fine structure which is a typical feature due to lowering of the molecular symmetry in guanidinium cations. It is also found in the hexamethylguanidinium cation.[35] As a consequence to weakening of the double bond, the absorption for the C=N stretching frequency is shifted to lower wavenumbers by 60 cm^{-1} in Cu(II) and 50 cm^{-1} in Cu(I) complexes.

As expected, the Cu(I) complexes **5**, **6**, and **7** are diamagnetic and colorless. Their 200 MHz room temperature ^{1}H and ^{13}C NMR spectra in CD$_3$CN reveal two sets of chemically inequivalent *N*-methyl protons. This behavior is explained by a rigid >C=N- bonding axis on the NMR time scale rendering one NMe$_2$ group cis and the other one trans with respect to the Cu substituent (Figure 14). By raising the temperature, coalescence of the proton signals is cannot be observed up to temperatures of 336 K for **7** at 500 MHz in CD$_3$CN,[36] which is probably due to the sterically congested situation of the coordinated tren ligand. The barrier to rotation about the C=N bond should be higher than the estimated 71 kJ/mol.[37]

The magnetic susceptibilities of the paramagnetic Cu(II) complexes were determined by the Evans method[38] for [(TMG$_3$tren)Cu^{II}Cl]Cl (**3**), μ_{eff} = 1.9 ± 0.1 μ_B, and [(TMG$_3$tren)Cu^{II}(NCMe)](ClO$_4$)$_2$ (**4**), μ_{eff} = 1.8 ± 0.1 μ_B. The values are well in accordance with literature values[39] of known tren complexes: μ_{eff}[(Me$_6$tren)Cu^{II}X]X (X = Br, ClO$_4$), 1.86 μ_B;[4] μ_{eff}[(H$_6$tren)Cu^{II}Cl]$_2$(BPh$_4$)$_2$, 2.01 μ_B; μ_{eff}[(H$_6$tren)Cu^{II}Br]$_2$(BPh$_4$)$_2$, 1.94 μ_B.[5f]

EPR spectra of the two copper(II) complexes **3** and **4** were recorded in frozen solution of acetonitrile (120 K) at 9.2608 GHz (X-Band) and values for *g* and *A* were estimated from simulated spectra.[40]

Complex **3** shows a single unresolved line at g_{iso} = 2.141(5) with 13.68 mT peak-to-peak distance. The absence of any resolution by substituting one nitrogen with a chlorine atom in the first ligand sphere is mainly caused by the two magnetic isotopes (^{35}Cl 75.8%, ^{37}Cl 24.2%) with spin $^3/_2$ (2 × 4 = 8 instead of 3 lines), the 4.0 (^{35}Cl) and 4.9 (^{37}Cl) times higher quadrupole moments, the slightly higher gyromagnetic moments (1.35 and 1.13 times greater than for ^{14}N), and the 8 times higher spin orbit constants.[41] The latter causes a faster spin relaxation via the spin orbit coupling and therefore broadens the lines more at the same temperature. The higher spin orbit constants are probably also responsible for reduction of the *g*-anisotropy of complex **3** compared to complex **4**, visible by comparing the spectral width of both spectra (13.68 mT for **3**$_{exp}$, 18.57 mT for **4**$_{exp}$).[42] The latter is speculative because it is not possible to exclude a reduction of ^{63,65}Cu hyperfine interaction as a reason for the more narrow overall spectral width.
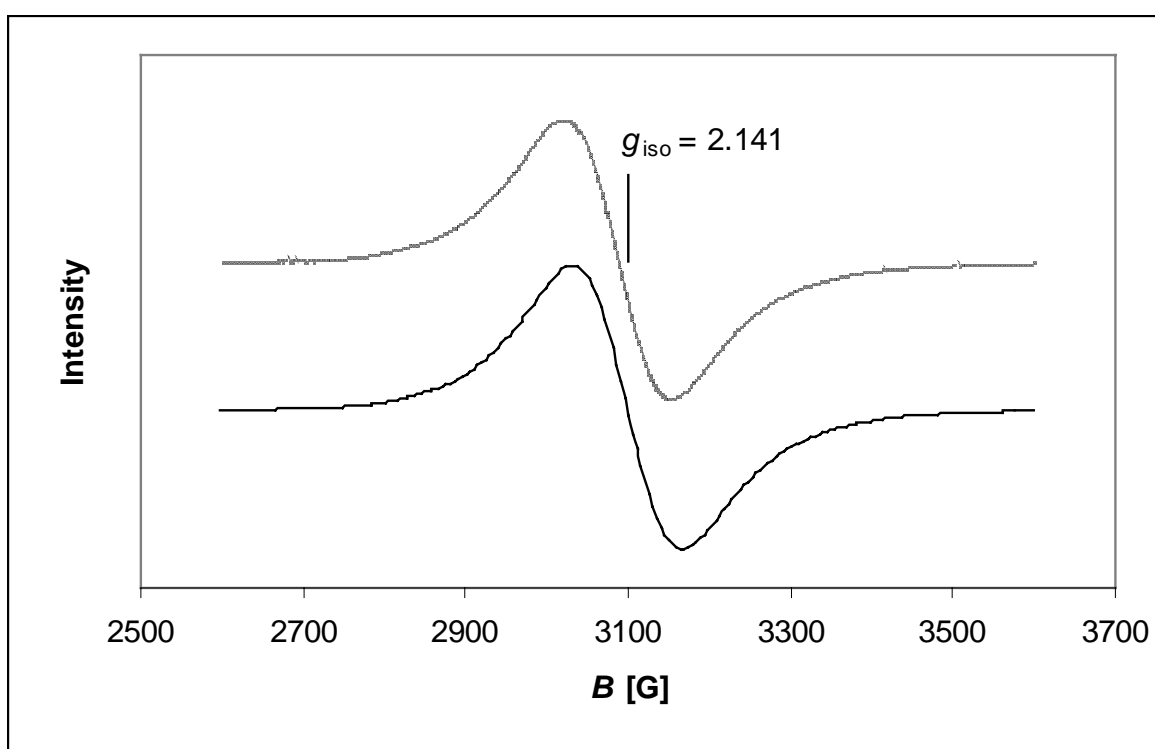

Figure 7. Experimentally determined (bottom, —) and simulated (top, ⋯⋯) EPR spectra (X-band) of complex [(TMG$_3$tren)Cu^{II}Cl]Cl (**3**) in frozen solution of acetonitrile (120 K), microwave frequency = 9.2608 GHz.

8

The EPR spectrum of complex **4** has been analyzed by least-squares fits to an orthorhombic spin Hamiltonian. The g-tensor with $g_1 = 2.201(5)$, $g_2 = 2.050(5)$, and $g_3 = 2.033(5)$ obtained by best fit is in the expected range for Cu(II) complexes.[1c,5a,c,f,43,44] The small but detectable deviation from axial symmetry ($g_2 - g_3 = 0.02$) is in agreement with the crystallographic data (vide infra). Overall, the spectrum is consistent with trigonal-bipyramidal geometry for d^9 configurations[1c] with elongated axial ligands due to Jahn-Teller distortion ($g_{\parallel}$ (g_1) > $g_{\perp}$ (g_2, g_3) ≈ 2.04).[45,46] The poor resolution is caused by inhomogeneous broadening due to hyperfine interaction with the nitrogen atoms in the first ligand sphere. The individual hyperfine tensors are most likely magnetically inequivalent with respect to the g-tensor axes because of symmetry reasons.
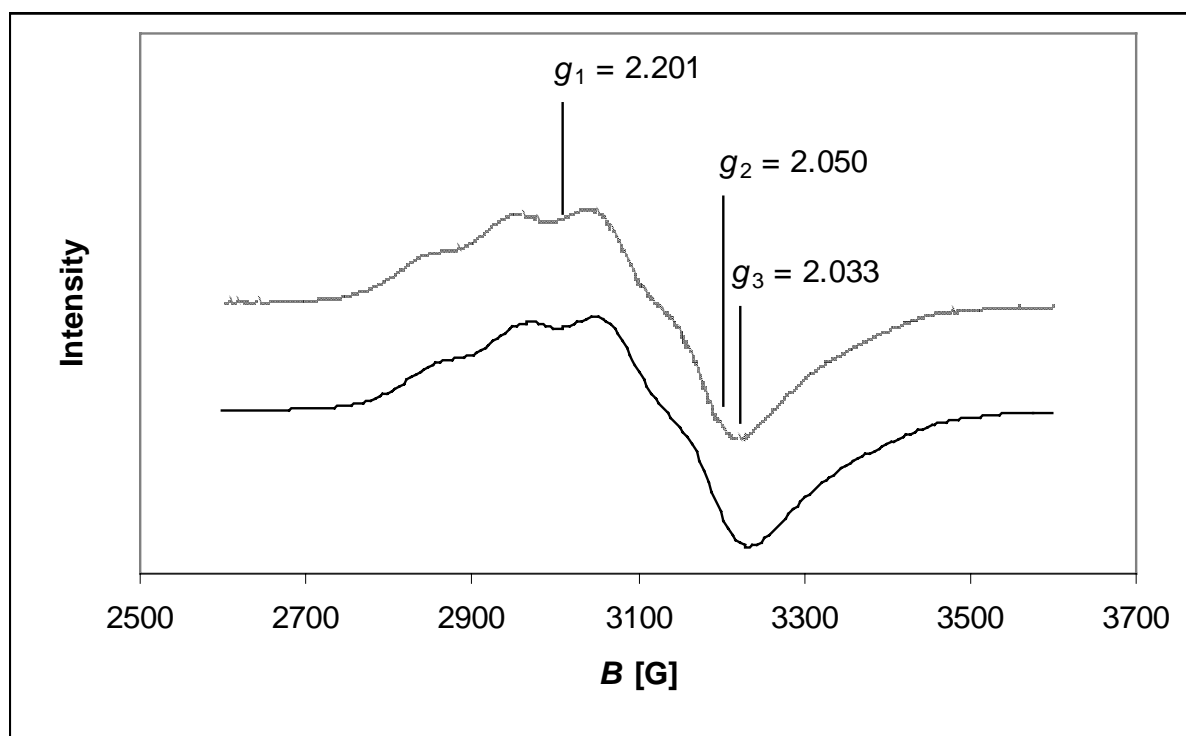

Figure 8. Experimentally determined (bottom, —) and simulated (top, ·····) EPR spectra (X-band) of complex [(TMG$_3$tren)Cu^{II}(NCMe)](ClO$_4$)$_2$ (**4**) in frozen solution of acetonitrile (120 K), microwave frequency = 9.2608 GHz ($A_1 = 98$; $A_2 = 32$; $A_3 = 58 \times 10^{-4}$cm^{-1}).

Molecular Structures. The crystal structures of complexes **3**-**6** were established by X-ray crystallography. Single crystals were grown by slow diffusion of ether into saturated acetonitrile solutions. The results are displayed in Figure 9-12, selected bonding distances and angles are collected in Table 1, and parameters of the data collection and refinement are shown in Table 4. All complexes possess a nearly trigonal molecular geometry with the tertiary amine nitrogen atom located in the apical and three guanidine nitrogens in the equatorial positions. **5** has crystallographically imposed C_3 symmetry. The copper(II) complexes **3** and **4** have a trigonal-bipyramidal core with a chloro ligand for monocationic **3** or an acetonitrile ligand for dicationic **4** occupying the axial position trans to the *tert*-amine functionality. This is the expected coordination geometry also known from Cu(II)-tren complexes even with rather weakly coordinating anions such as triflate[5b] or perchlorate.[4b] In the copper(I) complexes **5** and **6**, however, the axial position trans to the amine functionality remains unoccupied regardless of the coordinative ability of an anion such as chloride or acetonitrile as solvent. In contrast, Karlin´s 18 valence electron [(tmpa)Cu(NCMe)]$^+$ complex coordinates an additional axial nitrile ligand.[7c] As a consequence, the axial amine ligand is released into a weaker bonding interaction (Table 2). Tetracoordination was also observed for [L^{4}Cu]$^+$[BPh$_4$]$^-$,[8a] a Schiff base derivative of tren, if noncoordinating anions and noncoordinating solvent such as acetone were applied.
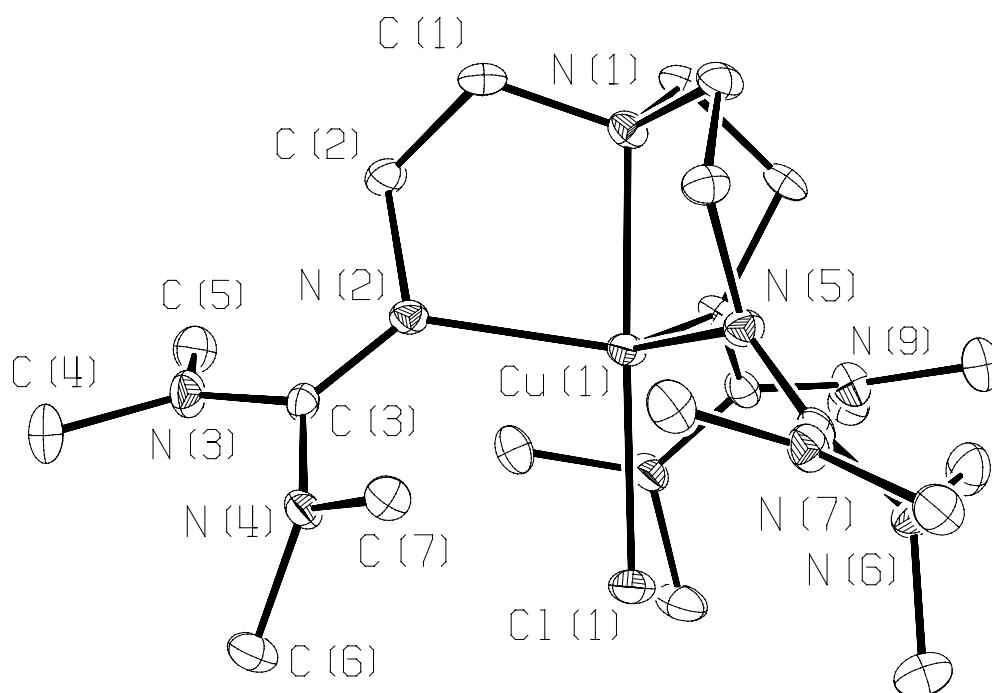

Figure 9. An ORTEP view of [(TMG$_3$tren)Cu^{II}Cl]Cl (**3**). Thermal ellipsoids are at 30% probability level; second peripheral chloride anion and hydrogen atoms omitted for clarity.

10

Figure 10. An ORTEP view of [(TMG₃tren)Cu^{II}(NCMe)](ClO₄)₂ (**4**). Thermal ellipsoids are at 30% probability level; second peripheral perchlorate anion and hydrogen atoms omitted for clarity.
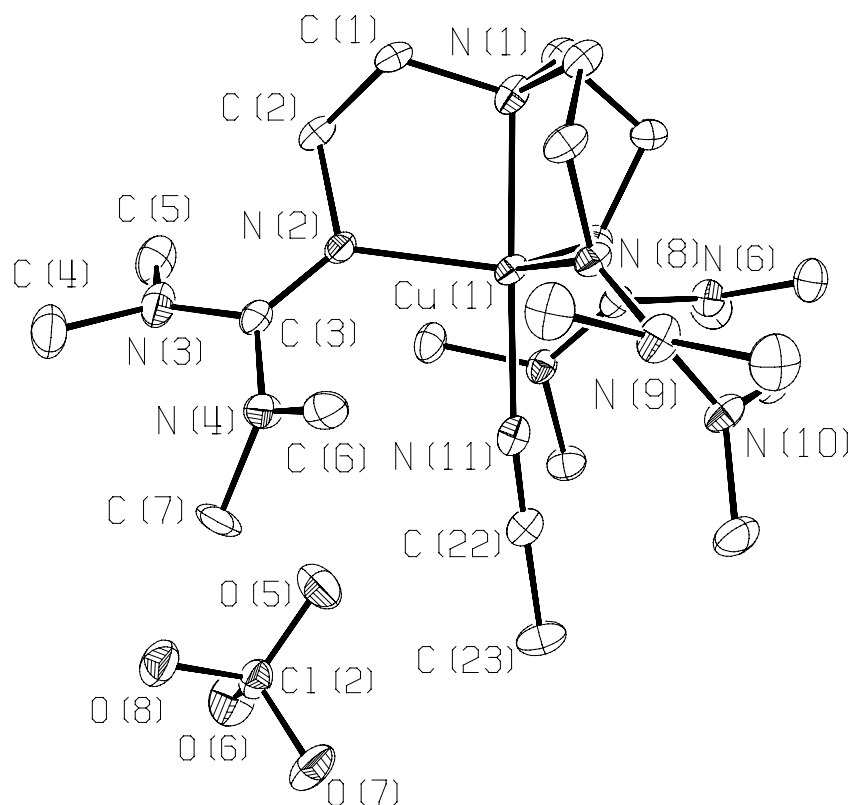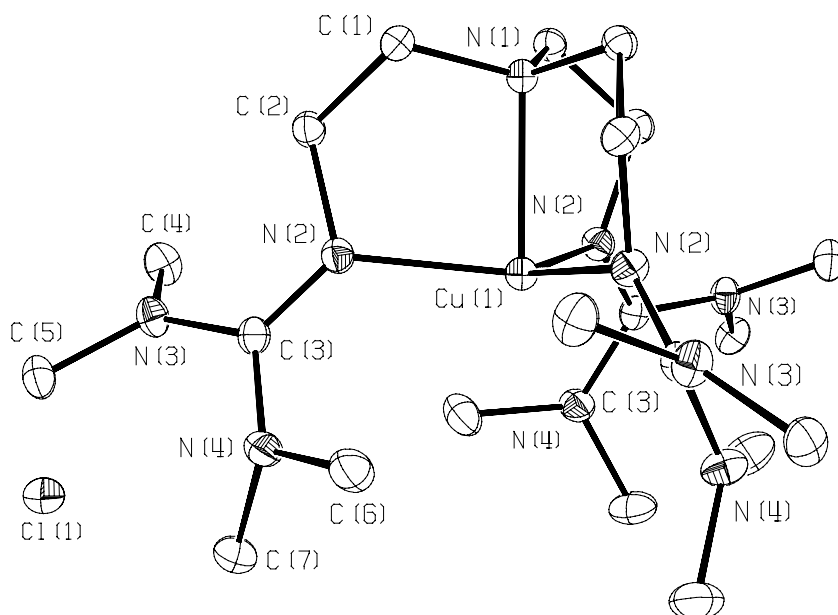

Figure 11. An ORTEP view of [(TMG₃tren)Cu^{I}]Cl (**5**). Thermal ellipsoids are at 30% probability level; hydrogen atoms omitted for clarity.

11
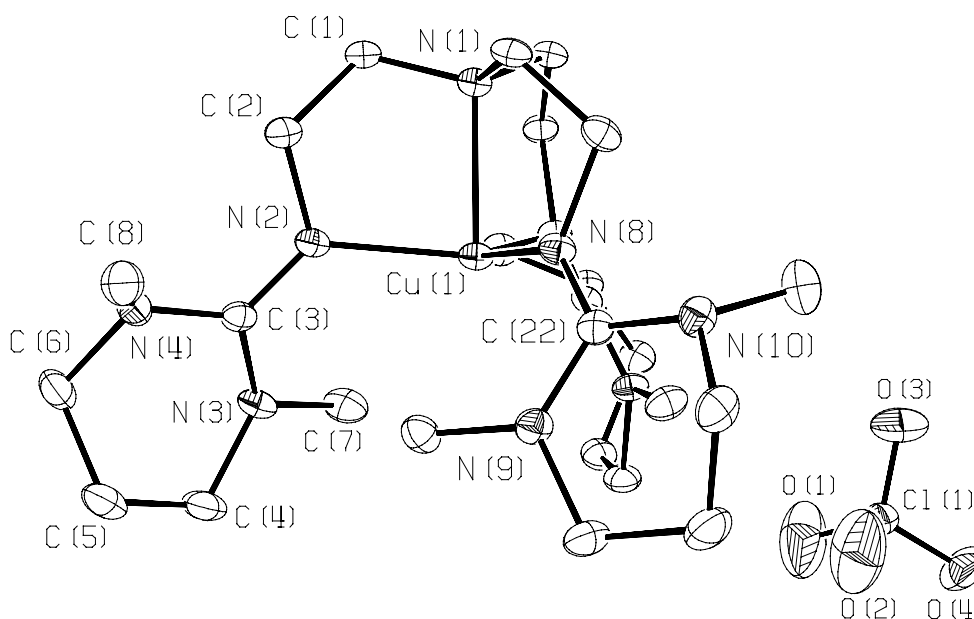
Figure 12. An ORTEP view of [(DMPG$_3$tren)Cu^I]ClO$_4$ (**6**). Thermal ellipsoids are at 30% probability level; hydrogen atoms omitted for clarity.

Table 1. Selected Bond Lengths [pm] and Bond Angles [deg] for Complexes **3** - **6**, Crystallographic Standard Deviations in Parentheses.[a]

	[(**1**)Cu^{II}Cl]Cl (**3**)	[(**1**)Cu^{II}(NCMe)] (ClO$_4$)$_2$ (**4**)	[(**1**)Cu^I]Cl (**5**)	[(**2**)Cu^I]ClO$_4$ (**6**)
Cu(1)-N(2)	210.4(3)	205.4(4)	205.2(2)	205.1(3)
Cu(1)-N(5)	209.1(3)	205.7(4)	205.2(2)	203.6(3)
Cu(1)-N(8)	210.9(3)	208.2(4)	205.2(2)	205.1(3)
Cu(1)-N(1)	211.1(3)	207.8(5)	219.0(3)	217.4(3)
Cu(1)-L$_{ax}$	228.5(1)	200.2(5)	-	-
∅ C-N$_{eq}$	131.4±0.3	130.8±0.7	129.4±0.0	130.3±0.5
∅ C-NR$_2$	136.4±0.5	136.3±0.8	137.6±0.6	137.8±1.6
N(1)-Cu(1)-N(11)	178.40(9)	177.62(17)	-	-
∅ N$_{eq}$-Cu-N$_{eq}$	118.1±2.6	118.6±1.4	119.0±0.0	119.2±1.6
∅ N$_{ax}$-Cu-N$_{eq}$	81.9±0.3	83.2±0.4	84.3±0.0	84.8±0.1
∅ Σ° CN$_3$	360.0±0.0	360.0±0.0	360.0±0.0	359.8±0.0
∅ Σ° N$_{eq}$	358.5±0.4	359.8±0.1	357.5±0.0	357.8±0.3
∅ Σ° NR$_2$	358.6±0.5	359.8±0.3	356.6±1.5	352.4±5.9

[a] Calculated average values are denoted with standard deviation (±).

The copper atom is slightly axially distorted, being localized below the equatorial plane defined by the guanidine nitrogen atoms. Consequently, the N_{ax}-Cu-N_{eq} angles are smaller than 90°. In complexes involving longer arm lengths of the tripod,[7a,b,10,13] copper can also be localized above the plane of the three equatorial nitrogen atoms, consequently the average N_{ax}-Cu-N_{eq} angles are larger than 90°. As a measure for the degree of trigonality, the structural index parameter $\tau = (\beta - \alpha)/60°$ [47] was established by Addison and Reedijk.[48] Table 2 compares the distortions from trigonality of our complexes with counterparts from literature of the tren family. The comparison reveals that our guanidine tripods **1** and **2** induce larger axial displacement of the copper atom from the equatorial plane than the purely amine based tren ligands H$_6$tren (L^1) and Me$_6$tren (L^2), although not as large as pyridine based tmpa (L^3).

Shorter Cu-N bonds and an increase in the contraction of the TMG$_3$tren ligand is observed for dicationic **4** when compared to monocationic **3**. This trend can be assigned to the higher effective charge at the metal center.[49] The axial distortion of Cu from the equatorial plane is dependent on ionic radii, electronic configuration, and the coordination number of the metal ions: it is larger for pentacoordinate d^9 Cu(II) (ionic radius 79 pm)[50] than for tetracoordinate d^{10} Cu(I) (74 pm).[50] Interestingly, d^9 Cu(II) ions show shorter bonds to the equatorial guanidine nitrogen atoms than to the axial amine nitrogen atom. The opposite trend - longer equatorial than axial Cu-N distances - has been found for other Cu(II) complexes of the tren ligand family with H$_6$tren, Me$_6$tren and even tmpa with sp^2 N-donor atoms (Table 2, first and second sections). Surprisingly, differences between long axial amine and short equatorial guanidine bonding distances become even more evident for diamagnetic tetracoordinate d^{10} Cu(I) complexes (Table 2, third section), and they are most prominent for isoelectronic pentacoordinate d^{10} Zn(II) ions (ionic radius 82 pm)[50] (Zn-N_{ax} 226.9(2) and Zn-N_{eq} 204.0 ± 0.8 pm).[23] With respect to the general trend of shorter M-N bonds, guanidine-based tren ligands have stronger metal ligand interactions than their amine or pyridine-based counterparts (L^1, L^2, L^3, Table 2). Their excellent donor quality can be attributed in part to their superbasic character 6 orders of magnitude higher than that of *tert*-amines and to their smaller steric hindrance at the sp^2 donor atom compared to neutral amine tripods. In their donor quality, in their hydrolytic lability of the M-N bond, in their bite indicated by the axial Cu displacement, and in their ability to stabilize some coordination compounds with unusual trigonal-monopyramidal geometry, our neutral guanidine ligands should in fact be placed

between the prominent ligand classes H$_6$tren, Me$_6$tren, and tmpa introduced by Karlin et al.[7a,b,c] and the tripodal secondary tren-amido(3-) ligands introduced by Schrock et al.[51]

Table 2. Structural Features of Complexes **3-6** and Literature Counterparts.

complex	axial distortion[a] [pm]	d (M-N$_{eq}$)[b] [pm]	d (M-N$_{ax}$) [pm]	d (M-L$_{ax}$) [pm]	τ[c]
(**3**) [(**1**)Cu^{II}Cl]$^+$	29.5	210.1±0.8	211.1(3)	228.5(1)	0.96
(**A**) [L^{2}Cu^{II}Cl]$^{+ \,6b}$	20.8	218.6±0.0	204.0(6)	223.4(2)	1.01
(**A´**) [L^{3}Cu^{II}Cl]$^{+ \,7a,d}$	31.8	206.5±0.5	205.0(6)	223.3(2)	1.00
(**4**) [(**1**)Cu^{II}(NCMe)]$^{2+}$	24.5	206.4±1.3	207.8(5)	200.2(5)	0.95
(**B**) [L^{1}Cu^{II}(NCMe)]$^{2+ \,5b}$	16.2	207.0±0.0	198(1)	200(2)	1.01
(**B´**) [L^{2}Cu^{II}(NCMe)]$^{2+ \,5b}$	16.3	214.2±1.1	200.4(6)	196.5(7)	0.97
(**5**) [(**1**)Cu^I]$^+$	20.5	205.2±0.0	219.0(3)	-	-
(**6**) [(**2**)Cu^I]$^+$	18.6	204.6±0.7	217.4(3)	-	-
(**C**) [L^{2}Cu^I(ClO$_4$)]$^{+ \,6c}$	19.1(8)	212.2±0.0	220.0(7)	353(1)	-
(**C´**) [L^{3}Cu^I(NCMe)]^{7c}	56.8	211.0±1.5	243.9(8)	199.9(9)	0.99
(**C´´**) [L^{4}Cu^I]^{8a}	20.8(1)	201.0±0.7	223.2(2)	-	-

[a] Distance of M to equatorial plane defined by the three equatorial nitrogen atoms. [b] Average bond distance of three equatorial nitrogen atoms to metal center. [c] $\tau = 1$ for ideal trigonal bipyramidal geometry, respectively $\tau = 0$ for ideal square pyramidal structure. Standard deviations in parentheses. L^1 = H$_6$tren, L^2 = Me$_6$tren, L^3 = tmpa, L^4 = S$_3$tren, Schiff base N(CH$_2$CH$_2$N=CH-Ph)$_3$.

Besides electronic effects, the steric congestion in the periphery of our multidentate guanidines is an important feature of all structures. Table 1 reveals average values for the sum of angles very close to 360° at the three coordinating guanidine nitrogen atoms $\Sigma° N_{eq}$, at all the other 3 × 2 guanidine nitrogen atoms $\Sigma° NR_2$, and finally at the central guanidine carbon atom $\Sigma° CN_3$. These planar building blocks are, however, twisted by approximately 40° into a propeller-like conformation in order to reduce steric repulsions. As a consequence, the methyl groups of the NMe$_2$ substituents are staggered (Figure 13) and the torsion angles Cu-N-C-N and N-C-N-C are in the range 20-45°, predominantly 35-45° out of plane (Figure 13). Similar dihedral angles out of ideal π-conjugation have been found for the ground state of the hexamethylguanidinium cation[52] and in complexes of **1** with Mn^{2+}, Fe^{2+}, and Zn^{2+} ions.[23] There is a trend that lone pairs at peripheral nitrogen atoms in the more rigid cyclic guanidine

14

system DMPG$_3$tren (**2**) are forced into better conjugation: the average dihedral angles (average value of all dihedral angles $\varnothing$ $\Sigma°$ N=C-N-C for *syn*-coplanar orientation: 34.1° ± 12.3 (complex **5**) vs. 25.4° ± 19.1 (complex **6**)) deviate less from the ideal coplanar conformation with the CN$_3$ guanidine unit, though these values are hampered by large deviations of the individual values. It is assumed that by better conjugation, delocalization of the positive charge is improved, and differences in the three guanidine CN$_3$ bond lengths are diminished, as is indicated by an increasing ρ factor (vide infra). Thus, ligand **2** should provide enhanced basicity compared to **1**. The equatorial and axial Cu-N bond distances of **2** are in fact smaller compared to **1**; however, they are not significantly smaller as the donor character includes both steric (rigidity) and electronic (basicity) effects.
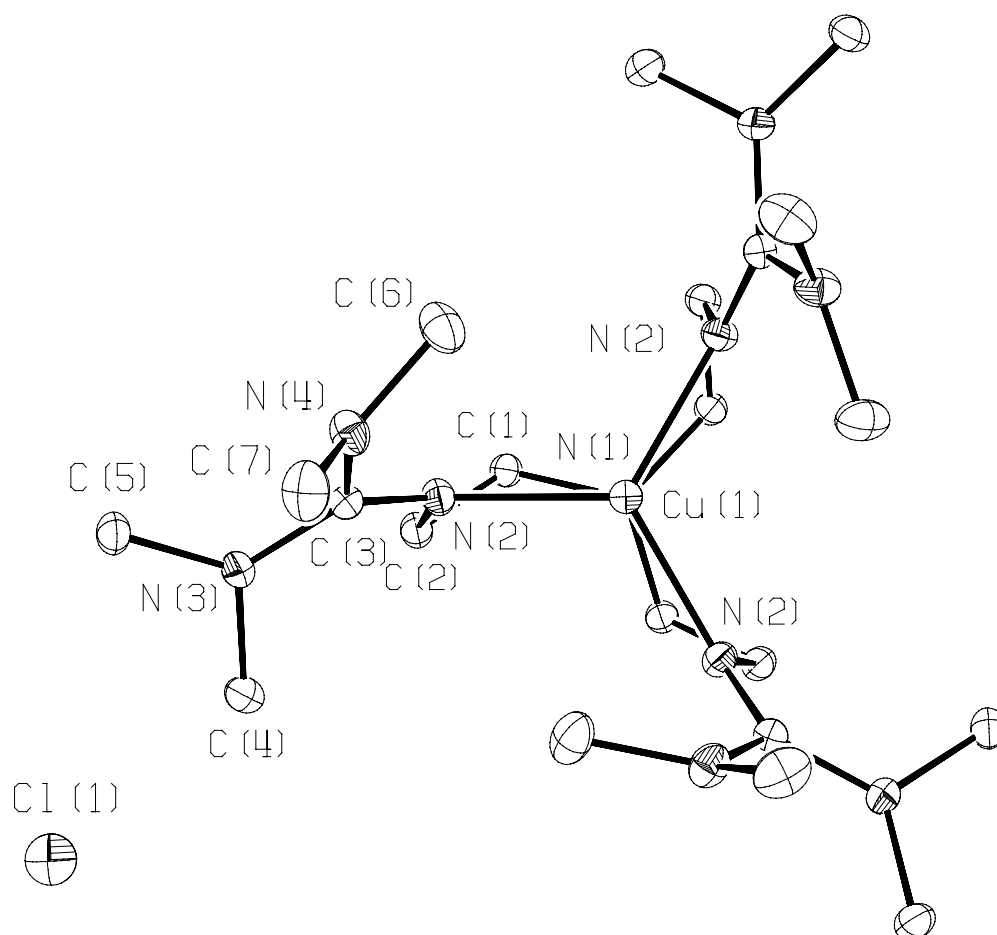

Figure 13. An ORTEP view of [(TMG$_3$tren)Cu^I]Cl (**5**) with crystallographically imposed C_3-symmetry, projection along the C_3 axis. Thermal ellipsoids are at 30% probability level; hydrogen atoms omitted for clarity.

Structural parameter ρ. ρ is defined as quotient of the shortest of the three C-N bonding distances of a guanidine functionality (typically the one coordinated by the weakest electrophile E, a Figure 14) and the average distance of the other two C-N bonds (b, c Figure 14): $\rho = 2a / (b + c)$. In the free guanidine (no E, first section Table 3), the quotient assumes a value of $\rho \approx 0.92$ which can be observed in structures with dangling guanidine arms, such as in [Mo(κ^2-TMG$_3$tren)(CO)$_3$].[23] If the delocalization of positive charge within the guanidine moiety becomes near ideal (bond lengths $\varnothing$ C=N vs. $\varnothing$ C-NR$_2$ become equal) $\rho \approx 1$ (last section in Table 3). For our guanidine complexes (E = M^{n+}, Table 3) of the tren type, the average C=N bonds are shorter by the factor $\rho = 0.94$ - 0.96 (94 - 96 %) than those to the peripheric NR$_2$ groups ($\varnothing$ C-NR$_2$). It is noteworthy that even the difference between different electrophiles Cu(I) and Cu(II) (0.94 vs. 0.96) as well as ligands of different donor strength (**1** and **2**, 0.94 vs. 0.95) can be recognized by reviewing ρ.

Table 3. Average C=N vs. C-NR$_2$ Distances [pm] and Quotient ρ; Standard Deviations ($\pm$).[a]

complex	$\varnothing$ C=N (a)	$\varnothing$ C-NR$_2$ (b,c)	ρ
[(**1**)Mo(CO)$_3$][b,23]	127.6±0.0	138.7±0.9	0.920
[(**3**)Zn^{II}Cl$_2$][b,c,22]	127.9±0.0	139.5±0.4	0.917
[(**1**)Cu^{II}Cl]Cl (**3**)	131.4±0.3	136.4±0.5	0.964
[(**1**)Cu^{II}(NCMe)](ClO$_4$)$_2$ (**4**)	130.8±0.7	136.3±0.8	0.960
[(**1**)Cu^{I}]Cl (**5**)	129.4±0.0	137.6±0.6	0.940
[(**2**)Cu^{I}]ClO$_4$ (**6**)	130.3±0.5	137.8±1.6	0.945
[(**1**)Mn^{II}Cl]Cl [23]	131.5±0.4	136.4±0.7	0.964
[(**1**)Mn^{II}(NCMe)](ClO$_4$)$_2$ [23]	131.1±0.5	136.1±0.2	0.963
[(**1**)Fe^{II}(NCMe)](ClO$_4$)$_2$ [23]	131.1±1.1	136.0±0.7	0.964
[(**1**)Zn^{II}(NCMe)](ClO$_4$)$_2$ [23]	131.8±0.6	136.1±0.5	0.963
[(**4**)H$_2$]Cl$_2$ [d,22]	133.6±0.0	134.0±0.2	0.997
[(**5**)][Fe(CO)$_4$C(O)NMe$_2$] [e,53]	132.9±0.0	133.7±0.7	0.994[54]

[a] Structural parameter $\rho = \varnothing$ C=N / $\varnothing$ C-NR$_2$. [b] Complex contains a free guanidine group in form of a noncoordinated „dangling" arm of a tripodal ligand. [c] Ligand (**3**) = 1,1,1-Tris[N^2-(1,1,3,3-tetramethyl-guanidino)methyl]ethane. [d] Ligand (**4**) = 1,2-Di[N^2-(1,1,3,3-tetramethylguanidinium)]ethane dichloride tetrahydrate (TMG$_2$en $\times$ 2 HCl). [e] Ligand (**5**) = [C(NMe$_2$)$_3$]$^+$.
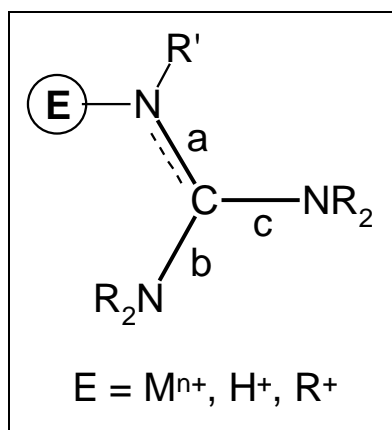
Figure 14. C-N bonds a, b and c for the determination of quotient ρ.

Conclusion

A novel tripod ligand with three superbasic pentaalkyl guanidine donor functions and a constraint geometry to stabilize cationic metal ions in a trigonal-bipyramidal coordination has been introduced. Peralkyl oligoguanidines such as **1** and **2** are in fact a new class of N-donor ligands within the large family of multidentate N-donors that typically contain multidentate amines, imines (Schiff bases), and azaaromatic building blocks. Due to its ability to delocalize positive charge into the three guanidinium moieties, TMG$_3$tren (**1**) and DMPG$_3$tren (**2**) stabilize cationic and dicationic complexes. With the parameter ρ a value is introduced which allows estimation of the donor ability and charge delocalization in guanidines. Our current interest is focused on the activation of small molecules such as dioxygen and their transformations in the molecular pocket imposed by the guanidine ligand regime.

Experimental Section

Materials and Methods. All experiments were carried out in hot assembled and under vacuum cooled glassware under an inert atmosphere of argon (99.998%) dried with P$_4$O$_{10}$ granulate. Solvents and triethylamine were purified according to literature procedures and also kept under inert atmosphere. Tris(2-aminoethyl)amine (Fluka) and *N,N´*-dimethylpropyleneurea (DMPU) (Aldrich) were used as purchased. Copper(II) perchlorate was dehydrated by the ortho ester method,[33] CuCl$_2$ was dehydrated by treatment with SOCl$_2$,[55] [Cu(CH$_3$CN)$_4$]ClO$_4$ was synthesized[56] and CuCl purified[57] according to literature methods. Substances sensitive to moisture and air were kept in a nitrogen-flushed glovebox (Braun, Type MB 150 BG-I).

Spectra were recorded on the following spectrometers: NMR, Bruker ARX 200; IR, Bruker IFS 88 FT; MS(EI, 70 eV), Varian MAT CH-7a; MS(APCI), Hewlett-Packard HP 5989 B; elemental analysis, Heraeus CHN-Rapid; melting points, Büchi MP B-540 (uncorrected); X-ray, ENRAF-Nonius CAD4 and Stoe IPDS; ESR, Bruker ESP 300 E (X-Band); magnetic moment: Evans method.[38]

Caution! Phosgene is a severe toxic agent that can cause pulmonary embolism and in case of heavy exposure may be lethal. Use only at a well-ventilated fume hood. Perchlorate salts are potentially explosive and should be handled with care.

The preparation of *N,N,N´,N´*-tetramethylformamidinium chloride and 1,1,1-tris{2-[*N^2*-(1,1,3,3-tetramethylguanidino)]ethyl}amine (**1**) is described elsewhere.[23]

N,N´-Dimethylpropylenechlorformamidinium Chloride (2a):[58]

Analogous to a literature method[30] phosgene was passed through a solution of *N,N´*-dimethylpropyleneurea (DMPU) (103.8 g, 97 mL, 810 mmol) in toluene (300 mL) kept at 0 °C in a flask equipped with a reflux condenser cryostated to -30 °C for 2 h. After that time the phosgene inlet was cut off and the solution was allowed to warm to room temperature stirring for 24 h; after that period the formed suspension was warmed to 35 °C for 3 h, still maintaining the reflux condensor at -30 °C. The light yellow precipitate was filtered off, washed three times with dry ether, and dried in vacuo. Yield: 93% (138 g, 754 mmol).

18

^{1}H NMR (200.1 MHz, CD$_3$CN, 25 °C): δ = 3.65 (t, $^3J_{HH}$ = 5.9 Hz, 4 H, N-CH_2), 3.29 (s, 6 H, CH_3), 2.07 (quint, $^3J_{HH}$ = 5.8 Hz, 2 H, ring-CH_2-) ppm; ^{13}C NMR (50.3 MHz, CD$_3$CN, 25 °C): δ = 152.8 (CN$_3$), 50.7 (CH$_3$), 42.7 (N-CH$_2$), 19.0 (-CH$_2$-) ppm; elemental analysis: calcd (%) for C$_6$H$_{12}$N$_2$Cl$_2$ (183.1): C 39.36, H 6.61, N 15.30; found C 39.31, H 6.53, N 14.96.

1,1,1-Tris{2-[N^2-(1,3-dimethylpropyleneguanidino)]ethyl}amine (DMPG$_3$tren = 2):

To a solution of tris(2-aminoethyl)amine (4.39 g, 4.5 mL, 30 mmol) and triethylamine (9.1 g, 12.5 mL, 90 mmol) in 75 mL acetonitrile 16.5 g (90 mmol) of [{NMe(CH$_2$)$_3$NMe}C-Cl]Cl (**B**) dissolved in 75 mL of the same solvent was slowly added under cooling in an ice bath. After the exothermic reaction took place, the mixture was refluxed for 3 h. Afterward 3.6 g (90 mmol) of NaOH in 20 mL of water was added under vigorous stirring in order to deprotonate the HNEt$_3$Cl. After removal of the solvent as well as excess NEt$_3$ the precipitate was washed three times with dry ether to remove unreacted amine and dried in vacuo. DMPG$_3$tren (**2**) was obtained by complete deprotonation of the tris(hydrochloride) with 50 mL of 50% KOH and extraction of the aqueous phase with MeCN (3 × 50 mL). The combined filtrates were evaporated to dryness and taken up in a mixture of 50 mL of Et$_2$O and 10 mL of MeCN. The solution was dried over Na$_2$SO$_4$, stirred with activated charcoal to eliminate impurities and filtered warm through Celite. After drying in vacuo, DMPG$_3$tren was obtained as a beige solid in 90% yield (12.9 g, 27.1 mmol).

mp 73 °C; ^{1}H NMR (200.1 MHz, CD$_3$CN, 25 °C): δ = 3.19-3.15 (m, 6 H, N-CH_2), 3.03 (t, $^3J_{HH}$ = 6.4 Hz, 12 H, ring-N-CH_2), 2.68 (s, 18 H, CH_3), 2.58-2.52 (m, 6 H, =N-CH_2), 1.83 (quint, $^3J_{HH}$ = 6.3 Hz, 6 H, ring-CH_2) ppm; ^{13}C NMR (50.3 MHz, CD$_3$CN, 25 °C): δ = 156.9 (CN$_3$), 59.1 (N-CH$_2$), 48.5 (ring-N-CH$_2$), 47.8 (=N-CH$_2$), 38.2 (CH$_3$), 20.3 (ring-CH$_2$-) ppm; IR (KBr): $\tilde{\nu}$ = 3410 m(br), 2940 s, 1595 s, 1438 s, 1320 m, 1234 m, 1161 m, 1109 m, 1041 m, 1013 m, 875 w, 738 w cm^{-1}; MS (EI, 70 eV): m/z (%) = 477 (9) [(**2**)]$^+$, 336 (24) [(**2**)-C$_7$H$_{14}$N$_3$]$^+$, 140 (100) [C$_7$H$_{14}$N$_3$]$^+$; elemental analysis: calcd (%) for C$_{24}$H$_{48}$N$_{10}$ (476.7): C 60.47, H 10.15, N 29.38; found C 60.35, H 10.15, N 28.76.

General Procedure for the Synthesis of the Copper Complexes:

Equimolar amounts of dehydrated metal salt and ligand were each dissolved in 5 mL of dry MeCN under argon. The solutions were combined and stirred for 30 min at 40-50 °C, filtered through Celite, and reduced in volume to approximately 2 mL. The complex was then

precipitated by the addition of 10 mL of dry ether, washed with absolute ether, and dried in vacuo. Single crystals suitable for X-ray analysis can be grown by slow diffusion of ether into the acetonitrile solution.

Chloro{1,1,1-tris-[N^2-(1,1,3,3-tetramethylguanidino)ethyl]amine}copper(II) Chloride (3).

General procedure with dehydrated $CuCl_2$ (134 mg, 1.0 mmol), 450 mg (1.05 mmol) of **1**. Yield: 553 mg (0.96 mmol), 96% yellow-green crystals.

mp 175 °C (dec); IR (KBr): $\tilde{\nu}$ = 3415 m(br), 2883 m, 1578 s, 1556 s, 1534 s, 1479 m, 1463 m, 1424 m, 1392 s, 1344 m, 1329 m, 1232 m, 1163 m, 1148 m, 1078 m, 1066 m, 1037 m, 1007 m, 940 m, 902 m, 763 m cm^{-1}; MS (APCI, MeCN): m/z = 537 [M-Cl]$^+$, 503 [(**1**)Cu]$^+$, 441 [(**1**)]$^+$; μ_{eff} (Evans method, 5% [D₆]-benzene in CD₃CN, 25 °C): μ_B/mol = 1.9 ± 0.1; elemental analysis: calcd (%) for $C_{21}H_{48}N_{10}Cl_2Cu$ (575.1): C 43.86, H 8.41, N 24.35; found C 43.61, H 9.10, N 23.13.

Acetonitrile(1,1,1-tris{2-[N^2-(1,1,3,3-tetramethylguanidino)]ethyl}amine)copper(II) Diperchlorate (4).

General procedure with dehydrated $Cu(ClO_4)_2$ (262 mg, 1.0 mmol), 450 mg (1.05 mmol) of **1**. Yield: 707 mg (0.95 mmol), 95% emerald crystals.

IR (KBr): $\tilde{\nu}$ = 3439 w(br), 2890 m, 1579 s, 1559 s, 1534 s, 1461 m, 1426 m, 1395 s, 1347 w, 1332 w, 1256 w, 1163 m, 1094 s, 902 m, 765 m, 623 s cm^{-1}; MS (APCI, MeCN): m/z = 642 [M-ClO₄]$^+$, 502 [(**1**)Cu]$^+$, 441 [(**1**)]$^+$; μ_{eff} (Evans method, 5% [D₆]-benzene in CD₃CN, 25 °C): μ_B/mol = 1.8 ± 0.1; elemental analysis: calcd (%) for $C_{21}H_{48}N_{10}O_8Cl_2Cu \times CH_3CN$ (744.2): C 37.12, H 6.91, N 20.70; found C 37.10, H 6.46, N 20.50.

{1,1,1-tris-[N^2-(1,1,3,3-tetramethylguanidino)ethyl]amine}copper(I) Chloride (5).

General procedure with CuCl (99 mg, 1.0 mmol), 450 mg (1.05 mmol) of **1**. Yield: 490 mg (0.91 mmol), 91% pale green crystals.

mp 98 °C (dec); ^{1}H NMR (200.1 MHz, CD₃CN, 25 °C): δ = 3.18 (t, $^3J_{HH}$ = 5.2 Hz, 6 H, N-CH_2), 2.68 (s, 18 H, CH_3), 2.62 (s, 18 H, CH_3), 2.56 (t, $^3J_{HH}$ = 5.2 Hz, 6 H, =N-CH_2) ppm; ^{13}C NMR (50.3 MHz, CD₃CN, 25 °C): δ = 161.8 (CN_3), 52.5 (=N-CH₂), 48.8 (N-CH₂), 39.1 (CH_3), 39.0 (CH_3) ppm; IR (KBr): $\tilde{\nu}$ = 3432 w(br), 2878 m, 1580 s, 1568 s, 1517 s, 1462 m, 1427 s, 1388 s, 1348 m, 1327 m, 1279 m, 1246 m, 1229 m, 1157 m, 1144 m, 1070 m, 1045

m, 1018 m, 999 m, 900 m, 880 m, 757 m cm^{-1}; MS (APCI, MeCN): m/z = 540 [M]$^+$, 502 [(**1**)Cu]$^+$, 441 [(**1**)]$^+$; elemental analysis: calcd (%) for C$_{21}$H$_{48}$N$_{10}$ClCu (539.7): C 46.74, H 8.96, N 25.95; found C 46.43, H 9.06, N 25.13.

{1,1,1-Tris-[N^2-(1,3-dimethylpropyleneguanidino)ethyl]amine}copper(I) Perchlorate (6).

General procedure with [Cu(CH$_3$CN)$_4$]ClO$_4$ (327 mg, 1.0 mmol), 490 mg (1.05 mmol) of **2**. Yield: 555 mg (0.87 mmol), 87% colorless crystals.

^{1}H NMR (200.1 MHz, CD$_3$CN, 25 °C): δ = 3.21 (t, $^3J_{HH}$ = 5.2 Hz, 6 H, N-CH_2), 3.05 (t, $^3J_{HH}$ = 6.4 Hz, 12 H, ring-N-CH_2), 2.75 (s, 18 H, CH_3), 2.58 (t, $^3J_{HH}$ = 5.2 Hz, 6 H, =N-CH_2), 1.85 (quint, $^3J_{HH}$ = 6.4 Hz, 6 H, ring-CH_2) ppm; ^{13}C NMR (50.3 MHz, CD$_3$CN, 25 °C): δ = 159.3 (CN$_3$), 53.1 (N-CH$_2$), 48.6 (=N-CH$_2$), 47.8 (ring-N-CH$_2$), 38.5 (CH$_3$), 21.1 (ring-CH$_2$-) ppm; IR (KBr): $\tilde{\nu}$ = 3436 w(br), 2948 m, 2882 m, 1602 s, 1577 s, 1507 s, 1438 m, 1422 m, 1365 m, 1341 m, 1322 m, 1276 m, 1243 m, 1167 m, 1096 s(br), 1041 m, 744 m, 715 m, 622 m cm^{-1}; MS (APCI, MeCN): m/z = 639 [M]$^+$, 540 [(**2**)Cu]$^+$, 477 [(**2**)]$^+$; elemental analysis: calcd (%) for C$_{24}$H$_{48}$N$_{10}$O$_4$ClCu (639.7): C 45.06, H 7.56, N 21.90; found C 45.36, H 7.94, N 21.78.

{1,1,1-Tris-[N^2-(1,1,3,3-tetramethylguanidino)ethyl]amine}copper(I) Perchlorate (7).

General procedure with [Cu(CH$_3$CN)$_4$]ClO$_4$ (327 mg, 1.0 mmol), 450 mg (1.05 mmol) of **1**. Yield: 535 mg (0.89 mmol), 89% colorless crystals.

^{1}H NMR (200.1 MHz, CD$_3$CN, 25 °C): δ = 3.19 (t, $^3J_{HH}$ = 5.4 Hz, 6 H, N-CH_2), 2.70 (s, 18 H, CH_3), 2.64 (s, 18 H, CH_3), 2.58 (t, $^3J_{HH}$ = 5.2 Hz, 6 H, =N-CH_2) ppm; ^{13}C NMR (50.3 MHz, CD$_3$CN, 25 °C): δ = 161.8 (CN$_3$), 52.5 (=N-CH$_2$), 48.8 (N-CH$_2$), 39.1 (CH$_3$), 39.0 (CH$_3$) ppm; IR (KBr): $\tilde{\nu}$ = 3437 w(br), 2876 m, 1588 s, 1570 s, 1518 m, 1456 m, 1428 m, 1389 s, 1343 w, 1326 w, 1248 w, 1229 w, 1158 m, 1142 m, 1092 s, 883 w, 757 w, 621 w cm^{-1}; MS (APCI, MeCN): m/z = 602 [M]$^+$, 502 [(**1**)Cu]$^+$, 441 [(**1**)]$^+$; elemental analysis: calcd (%) for C$_{21}$H$_{48}$N$_{10}$O$_4$ClCu (603.7): C 41.78, H 8.01, N 23.20; found C 42.48, H 7.60, N 22.80.

Table 4. Crystal Data and Structure Refinement for **3** and **4**.

complex	[(TMG$_3$tren)Cu^{II}Cl]Cl (**3**)	[(TMG$_3$tren)Cu^{II}(NCMe)](ClO$_4$)$_2$ (**4**)
empirical formula	C$_{21}$H$_{48}$N$_{10}$Cl$_2$Cu	C$_{23}$H$_{51}$N$_{11}$O$_8$Cl$_2$Cu
formula weight [g mol^{-1}]	575.1	744.2
temperature [K]	203(2)	193(2)
crystal system	triclinic	monoclinic
space group	P$\bar{1}$	P2$_1$/c
a [pm]	1310.4(1)	1137.2(2)
b [pm]	1310.7(1)	1491.2(1)
c [pm]	2921.0(2)	1154.5(3)
α [deg]	89.985(8)	90
β [deg]	89.599(11)	94.194(19)
γ [deg]	60.428(7)	90
volume [Å^3]	4363.2(6)	1819.5(7)
Z	2	4
ρ [mg m^{-3}]	1.321	1.422
μ [mm^{-1}]	0.935	0.841
F(000)	1860	1572
crystal size [mm^3]	0.70 x 0.70 x 0.20	1.20 x 0.30 x 0.15
diffractometer	Stoe IPDS	Enraf Nonius CAD4
scan technique	ω-scan	ω-scan
θ-range for data collection [deg]	1.91...25.95	2.40...24.97
index ranges	-16≤h≤16,	-19≤h≤19,
	-16≤k≤16,	-15≤k≤0,
	-35≤l≤35	0≤l≤19
reflections collected	50906	6641
independent refl.	15843	6091
R_{int}	0.0570	0.0298
observed reflections [$F \geq 4\sigma(F)$]	9893	5019
data/restraints/parameters	15843/0/965	6091/0/418
goodness of fit on F^2	0.805	1.198
$R1$ [$F_0 \geq 4\sigma(F)$][a]	0.0434	0.0618
wR_2 (all data) [a]	0.1198	0.2073
transmission (max./min.)	0.8351 / 0.5607	0.8842 / 0.4319
largest diff. Peak and hole [eÅ^{-3}]	1.056 / -1.692	0.626 / -1.349

[a] $R_1 = \Sigma||F_0|-|F_c||/\Sigma|F_0|$; $wR_2 = \{\Sigma[w(F_0^2 - F_c^2)^2]/\Sigma[w(F_0^2)^2]\}^{1/2}$.

Table 5. Crystal Data and Structure Refinement for **5** and **6**.

Complex	[(TMG$_3$tren)Cu^I]Cl (**5**)	[(DMPG$_3$tren)Cu^I]ClO$_4$ (**6**)
empirical formula	C$_{21}$H$_{48}$N$_{10}$ClCu × O	C$_{24}$H$_{48}$N$_{10}$O$_4$ClCu
formula weight [g mol^{-1}]	539.7 × 16.0	639.7
temperature [K]	203(2)	193(2)
crystal system	hexagonal	monoclinic
space group	R$\bar{3}$	P2$_1$/n
a [pm]	1181.3(2)	1512.2(2)
b [pm]	1181.3(2)	1179.0(1)
c [pm]	3505.6(2)	1742.3(2)
α [deg]	90	90
β [deg]	90	104.458(12)
γ [deg]	120	90
volume [Å^3]	4236.6(11)	3007.9(6)
Z	3	4
ρ [mg m^{-3}]	1.307	1.413
μ [mm^{-1}]	0.900	0.863
$F(000)$	1787	1360
crystal size [mm^3]	0.72 x 0.51 x 0.06	0.54 x 0.45 x 0.15
diffractometer	Enraf Nonius CAD4	Enraf Nonius CAD4
scan technique	ω-scan	ω-scan
θ-range for data collection [deg]	2.31...25.00	2.22...24.96
index ranges	-12≤h≤0,	0≤h≤17,
	-12≤k≤0,	0≤k≤13,
	-41≤l≤41	-20≤l≤20
reflections collected	1916	5477
independent refl.	1649	5265
R_{int}	0.0491	0.0303
observed reflections [$F \geq 4\sigma(F)$]	1544	4368
data/restraints/parameters	1649/0/167	5265/0/361
goodness of fit on F^2	1.055	1.052
$R1$ [$F_0 \geq 4\sigma(F)$][a]	0.0432	0.0518
wR$_2$ (all data) [a]	0.1206	0.1489
transmission (max./min.)	0.9480 / 0.5633	0.8814 / 0.6529
largest diff. Peak and hole [eÅ^{-3}]	0.894 / -0.788	1.217 / -0.548

[a] $R_1 = \Sigma||F_0|-|F_c||/\Sigma|F_0|$; wR$_2 = \{\Sigma[w(F_0^2-F_c^2)^2]/\Sigma[w(F_0^2)^2]\}^{1/2}$.

X-ray Structure Analysis. Crystal data and experimental conditions are listed in Table 4. and 5. The molecular structures are illustrated as ORTEP[59] plots in Figure 9-13. Selected bond lengths and angles with standard deviations in parentheses are presented in Table 1. Intensity data were collected with graphite monochromated Mo K$_\alpha$ radiation (λ = 71.073 pm). The collected reflections were corrected for Lorentz and polarization effects. Structures **4**, **5** and **6** were solved by direct methods and refined by full-matrix least-squares methods on F^2 while **3** was solved with SIR92.[60] Hydrogen atoms were calculated and isotropically refined.[61]

References

(1)   Selected references: a) Magnus, K. A.; Ton-That, H.; Carpenter, J. E. *Chem. Rev.* **1994**, *94*, 727-735; b) Kaim, W. *Angew. Chem.* **1996**, *108*, 47-64, *Angew. Chem. Int. Ed. Engl.* **1996**, *35*, 43-60; c) Kaim, W.; Schwederski, B. *Bioanorganische Chemie*, *2. Aufl.*, Teubner, Stuttgart, **1995**, pp 193-220; d) Jacobson, R. R.; Tyeklár, Z.; Farooq, A.; Karlin, K. D.; Liu, S.; Zubieta, J. *J. Am. Chem. Soc.* **1988**, *110*, 3690-3692; e) Karlin, K. D.; Tolman, W. B.; Kaderli, S.; Zuberbühler, A. D. *J. Mol. Catal. A: Chem.* **1997**, *117*, 215-222; f) Tolman, W. B. *Acc. Chem. Res.* **1997**, *30*, 227-237; g) Schindler, S. *Eur. J. Inorg. Chem.* **2000**, Microreview, 2311-2326; h) Kitajima, N; Moro-oka, Y. *Chem. Rev.* **1994**, *94*, 737-757; i) Kitajima, N.; Fujisawa, K.; Fujimoto, C.; Moro-oka, Y.; Hashimoto, S.; Kitagawa, T.; Toriumi, K.; Tatsumi, K.; Nakamura, A. *J. Am. Chem. Soc.* **1992**, *114*, 1277-1291; j) Baldwin, M. J.; Root, D. E.; Pate, J. E.; Fujisawa, K.; Kitajima, N.; Solomon, E. I. *J. Am. Chem. Soc.* **1992**, *114*, 10421-10431; k) Solomon, E. I.; Tuczek, F.; Root, D. E.; Brown, C. A. *Chem. Rev.* **1994**, *94*, 827-856.

(2)   Selected references: a) Holland, P. L.; Rodgers, K. R.; Tolman, W. B. *Angew. Chem.* **1999**, *111*, 1210-1213; *Angew. Chem. Int. Ed. Engl.* **1999**, *38*, 1139-1142; b) Becker, M.; Schindler, S.; Karlin, K. D.; Kaden, T. K.; Kaderli, S.; Palanché, T.; Zuberbühler, A. *Inorg. Chem.* **1999**, *38*, 1989-1995; c) Fujisawa, K.; Tanaka, M.; Moro-oka, Y.; Kitajima, N. *J. Am. Chem. Soc.* **1994**, *116*, 12079-12080; d) Wada, A.; Harata, M.; Hasegawa, K.; Jitsukawa, K.; Masuda, H.; Mukai, M.; Kitagawa, T.; Einaga, H. *Angew. Chem.* **1998**, *110*, 874-875; *Angew. Chem. Int. Ed. Engl.* **1998**, *37*, 798-799; e) Reim, J.; Werner, R.; Haase, W.; Krebs, B. *Chem. Eur. J.* **1998**, *4*, 289-298.

(3)   a) Y. Wang, T. D. P. Stack, *J. Am. Chem. Soc.* **1996**, *118*, 13097-13098; b) Jazdzewski, B. A.; Young, Jr., V. G.; Tolman, W. B. *J. Chem. Soc. Chem. Comm.* **1998**, 2521-2522; c) Müller, J.; Weyhermüller, T.; Bill, E.; Hildebrandt, P.; Ould-Moussa, L.; Glaser, T.; Wieghardt, K. *Angew. Chem.* **1998**, *110*, 637-640; *Angew. Chem. Int. Ed. Engl.* **1998**, *37*, 616-619; d) Chaudhuri, P.; Hess, M.; Müller, J.; Hildenbrand, K.; Bill, E.; Weyhermüller, T.; Wieghardt, K. *J. Am. Chem. Soc.* **1999**, *121*, 9599-9610.

(4)   a) Ciampolini, M.; Nardi, N. *Inorg. Chem.* **1966**, *5*, 41-44; b) Ciampolini, M.; Nardi, N.; Speroni, G. P. *Coord. Chem. Rev.* **1966**, *1*, 222-233.

(5)   a) Duggan, M.; Noel, R.; Hathaway, B.; Tomlinson, G.; Brint, P.; Pelin, K. *J. Chem. Soc. Dalton* **1980**, 1342-1348; b) Scott, M. J.; Lee, S. C., Holm, R. H. *Inorg. Chem.* **1994**, *33*, 4651-4662; c) Su, C.-C.; Lu, W.-S.; Hui, T.-Y.; Chang, T.-Y.; Wang, S.-L.; Liao, F.-L. *Polyhedron* **1993**, *12*, 2249-2259; d) Stibrany, R. T.; Potenza, J. A.; Schugar, H. J. *Acta Cryst.* **1993**, *C49*, 1561-1564; e) Jain, P. C.; Lingafelter, E. C. *J. Am. Chem. Soc.* **1967**, *89*, 6131-6136; f) Laskowski, E. J.; Duggan, D. M.; Hendrickson, D. N. *Inorg. Chem.* **1975**, *14*, 2449-2459.

(6)   a) Di Vaira, M.; Orioli, P. L. *Acta Cryst.* **1968**, *B24*, 595-599; b) Anderegg, G.; Gramlich, V. *Helv. Chim. Acta* **1994**, *77*, 685-690; c) Becker, M.; Heinemann, F. W.; Schindler, S. *Chem. Eur. J.* **1999**, *5*, 3124-3129.

(7)   a) Karlin, K. D.; Hayes, J. C.; Juen, S; Hutchinson, J. P.; Zubieta, J. *Inorg. Chem.* **1982**, *21*, 4106-4108; b) Karlin, K. D.; Hayes, J. C.; Hutchinson, J. P.; Hyde, J. R.; Zubieta, J. *Inorg. Chim. Acta* **1982**, *64*, L219-L220; c) Tyeklár, Z.; Jacobson, R. R.; Wei, N.; Murthy, N. N.; Zubieta, J.; Karlin, K. D. *J. Am. Chem. Soc.* **1993**, *115*, 2677-2689; d) Allen, C. S.; Chuang, C.-L.; Cornebise, M.; Canary, J. W. *Inorg. Chim. Acta* **1995**, *239*, 29-37; e) Nagao, H.; Komeda, N.; Mukaida, M.; Suzuki, M.; Tanaka, K. *Inorg. Chem.* **1996**, *35*, 6809-6815.

(8)   a) Alyea, E. C.; Ferguson, G.; Jennings, M. C.; Xu, Z. *Polyhedron* **1990**, *9*, 739-741; b) Walther, D.; Hamza, K.; Görls, H.; Imhof, W. *Z. Anorg. Allg. Chem.* **1997**, *623*, 1135-1143.

(9)   G. Tabbi, W. L. Driessen, J. Reedijk, R. P. Bonomo, N. Veldman, A. L. Spek, *Inorg. Chem.* **1997**, *36*, 1168-1175.

(10)   Sorrell, T. N.; Jameson, D. L. *Inorg. Chem.* **1982**, *21*, 1014-1019.

(11)   Lynch, W. E.; Kurtz, D. M.; Wang, S.; Scott, R. A. *J. Am. Chem. Soc.* **1994**, *116*, 11030-11038.

(12)   a) Janiak, C.; Temizdemir, S.; Dechert, S.; Deck, W.; Girgsdies, F.; Heinze, J.; Kolm, M. J.; Scharmann, T. G.; Zipffel, O. M. *Eur. J. Inorg. Chem.* **2000**, 1229-1241; b) Janiak, C.; Scharmann, T. G.; Günther, W.; Hinrichs, W.; Lentz, D. *Chem. Ber.* **1996**, *129*, 991-995.

(13)   a) Dittler-Klingemann, A. M.; Hahn, F. E.; Orvig, C. *Bioanorganische Chemie: Übergangsmetalle in der Biologie und ihre Koordinationsverbindungen*, Trautwein, A. (Ed.), Wiley VCH, Weinheim, **1997**, p. 552-569; b) Dittler-Klingemann, A. M.; Hahn, F. E. *Inorg. Chem.* **1996**, *35*, 1996-1999; c) Dittler-Klingemann, A. M.; Orvig, C.; Thaler, F.; Hubbard, C. D.; van Eldik, R.; Schindler, S.; Fábián, I. *Inorg. Chem.* **1996**, *35*, 7798-7803; d) Dittler-Klingemann, A. M.; Hahn, F. E.; Orvig, C.; Rettig, S. J. *Acta Cryst.* **1996**, *C52*, 1957-1959.

(14)   a) Wieland, G.; Simchen, G. *Liebigs Ann. Chem.* **1985**, 2178-2193; b) Barton, D. H. R.; Elliot, J. D.; Géro, S. D. *J. Chem. Soc., Perkin Trans. I* **1982**, 2085-2090; c) Barton, D. H. R.; Kervagoret, J. K.; Zard, S. Z. *Tetrahedron* **1990**, *46*, 7587-7598.

(15)   a) Smith, P. A. S. *The Chemistry of Open-Chain Organic Nitrogen Compounds, Vol. 1*, Benjamin, W. A. Inc., New York, **1965**, p. 277-290; b) Yamamoto, Y.; Kojima, S. *The Chemistry of Amidines and Imidates, Vol. 2*, J. Wiley & Sons, Chichester, **1991**, p. 485-526; c) Schwesinger, R. *Nachr. Chem. Tech. Lab.* **1990**, *38*, 1214-1226.

(16)   Ratilla, E. M. A.; Scott, B. K.; Moxness, M. S.; Kostic, N. M. *Inorg. Chem.* **1990**, *29*, 918-926.

(17)   a) Hessler, A.; Stelzer, O.; Dibowski, H.; Worm, K.; Schmidtchen, F. P. *J. Org. Chem.* **1997**, *62*, 2362-2369; b) Schmidtchen, F. P.; Berger, M. *Chem. Rev.* **1997**, *97*, 1609-1646.

(18)   a) Ratilla, E. M. A.; Kostic, N. M. *J. Am. Chem. Soc.* **1988**, *110*, 4427-4428; b) Przybyla, A. E.; Robbins, J.; Menon, N.; Peck Jr., H. D. *FEMS Microbiol. Rev.* **1992**, *88*, 109-136; c) Fairlie, D. P.; Jackson, W. G.; Skelton, B. W.; Wen, H.; White, A. H.; Wickramasinghe, W. A.; Woon, T. C.; Taube, H. *Inorg. Chem.* **1997**, *36*, 1020-1028.

(19)   a) Longhi, R.; Drago, R. S. *Inorg. Chem.* **1965**, *4*, 11-14; b) Snaith, R.; Wade, K.; Wyatt, B. K. *J. Chem. Soc. A* **1970**, 380-383; c) Mehrotra, R. C. *Comprehensive*

Coordination Chemistry, Vol. 2, Pergamon, Oxford, 1987, pp 269-291; d) de Vries, N.; Costello, C. E.; Jones, A. G.; Davison, A. *Inorg. Chem.* **1990**, *29*, 1348-1352; e) Fehlhammer, W. P.; Metzner, R.; Sperber, W. *Chem. Ber.* **1994**, *127*, 829-833; f) Bailey, P. J.; Grant, K. J.; Pace, S.; Parsons, S.; Stewart, L. J. *J. Chem. Soc. Dalton Trans.* **1997**, 4263-4266; g) Schneider, W.; Bauer, A.; Schier, A.; Schmidbaur, H. *Chem. Ber./Recueil* **1997**, *130*, 1417-1422.

(20) Schneider, W.; Bauer, A.; Schier, A.; Schmidbaur, H. *Chem. Ber./Recl.* **1997**, *130*, 1417-1422.

(21) Kuhn, N.; Grathwohl, M.; Steimann, M.; Henkel, G. *Z. Naturforsch. Teil B* **1998**, *53*, 997-1003.

(22) Wittmann, H.; Schorm, A.; Sundermeyer, J. *Z. Anorg. Allg. Chem.* **2000**, *626*, 1583-1590.

(23) Wittmann, H.; Raab, V.; Schorm, A.; Plackmeyer, J.; Sundermeyer, J. *Eur. J. Inorg. Chem.* **2001**, 1937-1948.

(24) Simms, M. L.; Atwood, J. L.; Zatko, D. A. *J. Chem. Soc., Chem. Commun.* **1973**, 46-47.

(25) Sen, D.; Saha, C. *J. Chem. Soc., Dalton Trans.* **1976**, 776-779.

(26) a) Mahadevan, V; Hou, Z.; Cole, A. P.; Root, D. E.; Lal, T. K.; Solomon, E. I.; Stack, T. D. P. *J. Am. Chem. Soc.* **1997**, *119*, 11996-11997; b) Itoh, S; Taki, M.; Nakao, H.; Holland, P. L.; Tolman, W. B.; Que Jr., L.; Fukuzumi, S. *Angew. Chem.* **2000**, *112*, 409-411; *Angew. Chem. Int. Ed. Engl.* **2000**, *39*, 398-400.

(27) Representative examples: a) Muche, M. S.; Göbel, M. W. *Angew. Chem.* **1996**, *108*, 2263-2265; *Angew. Chem. Int. Ed. Engl.* **1996**, *35*, 2126-2129 and references cited; b) Deslongchamps, G.; Galán, A.; de Mendoza, J.; Rebek, Jr., J. *Angew. Chem. Int. Ed. Engl.* **1992**, *31*, 61-63 and references cited.

(28) a) Eilingsfeld, H.; Seefelder, M.; Weidinger, H. *Angew. Chem.* **1960**, *72*, 836-845; b) Eilingsfeld, H.; Neubauer, G.; Seefelder, M.; Weidinger, H. *Chem. Ber.* **1964**, *97*, 1232-1245.

(29) Kantlehner, W.; Haug, E.; Mergen, W. W.; Speh, P.; Maier, T.; Kapassakalidis, J. J.; Bräuner, H.-J.; Hagen, H. *Liebigs Ann. Chem.* **1984**, 108-126.

(30)   Cliffe, I. A. In *Comprehensive Organic Functional Group Transformations, Vol. 6*, Elsevier Science Ltd., Oxford, **1987**, pp 639-675.

(31)   a) Isobe, T.; Ishikawa, T. *J. Org. Chem.* **1999**, *64*, 6984-6988; b) Isobe, T.; Fukuda, K.; Ishikawa, T. *Tetrahedron: Asymmetry* **1998**, *9*, 1729-1735.

(32)   Knorr, R.; Trzeciak, A.; Bannwarth, W.; Gillessen, D. *Tetrahedron Lett.* **1989**, *30*, 1927-1930.

(33)   van Leeuwen, P. W. N. M.; Groeneveld, W. L. *Inorg. Nucl. Chem. Lett.* **1967**, *3*, 145-146.

(34)   Sundermeyer, J.; Raab, V.; Schindler, S.; Schatz, M., Work in progress.

(35)   a) Papa, A. J. *J. Org. Chem.* **1966**, *31*, 1426-1430; b) Petz, W. *J. Organomet. Chem.* **1975**, *90*, 223-226.

(36)   Maximum ^{1}H NMR recording temperature in CD$_3$CN (bp. 81 °C) due to field inhomogeneity.

(37)   Value calculated by $\Delta G^{\ddagger} = 19.1 \times 10^{-3} \times T_c\,(9.97 + \log T_c - \log|\nu_A - \nu_B|)$, $\Delta\nu$ obtained from experimental 300 K spectrum. Hesse, M.; Meier, H.; Zeeh, B. In *Spektoskopische Methoden in der organischen Chemie*, *4. Aufl.*, Thieme Verlag, Stuttgart, New York, **1991**.

(38)   a) Evans, D. F. *J. Chem. Soc.* **1953**, 2003-2005; b) Fritz, H. P.; Schwarzhans, K.-E. *J. Organomet. Chem.* **1964**, *1*, 208-211; c) Crawford, T. H.; Swanson, J. *J. Chem. Educ.* **1971**, *48*, 382-386; d) Löliger, J.; Scheffold, R. *J. Chem. Educ.* **1972**, *49*, 646-647; e) Grant, D. H. *J. Chem. Educ.* **1995**, *72*, 39-40.

(39)   Riedel, E. *Anorganische Chemie*, *2. Aufl.*, W. de Gruyter, Berlin, New York, **1990**, p 586.

(40)   Burghaus, O. *SIMEPR, Program for Simulation of EPR-Spectra* **1985**, Philipps-University, Marburg, Germany.

(41)   Carrington, A.; McLachlan, A. D. In *Introduction to Magnetic Resonance*, Chapman & Hall, London, New York, **1980**.

(42)   a) Kurreck, H.; Kirste, B.; Lubitz, W. In *Electron Nuclear Double Resonance Spectroscopy of Radicals in Solution*, VCH, Weinheim, **1988**; b) Atherton, N. M. In *Principles of Electron Spin Resonance*, E. Horwood Ltd., Chichester, **1993**.

(43) a) Comba, P.; Hambley, T. W.; Hilfenhaus, P.; Richens, D. T. *J. Chem. Soc. Dalton Trans.* **1996**, 533-539; b) Klein Gebbink, R. J. M.; Bosman, A. W.; Feiters, M. C.; Meijer, E. W.; Nolte, R. J. M. *Chem. Eur. J.* **1999**, *5*, 65-69.

(44) a) Solomon, E. I.; Sundaram, U. M.; Machonkin, T. E. *Chem. Rev.* **1996**, *96*, 2563-2605; b) Tani, F.; Matsumoto, Y.; Tachi, Y.; Sasaki, T.; Naruta, Y. *J. Chem. Soc. Chem. Commun.* **1998**, 1731-1732; c) Yokoi, H. *Bull. Chem. Soc. Jpn.* **1974**, *47*, 3037-3040; d) Sakaguchi, U.; Addison, A. W. *J. Am. Chem. Soc.* **1977**, *99*, 5189-5190; e) Yokoi, H.; Addison, A. W. *Inorg. Chem.* **1977**, *16*, 1341-1349.

(45) Reinen, D.; Friebel, C. *Structure and Bonding* **1979**, *37*, 1-60.

(46) For examples of compressed trigonal bipyramidal geometry ($g_\perp > g_\parallel$), see ref. 5 a), c) and Lu, Z.-L.; Duan, C.-Y.; Tian, Y.-P.; You, X.-Z.; *Inorg. Chem.* **1996**, *35*, 2253-2258.

(47) β and α are defined as the largest and second largest metal centered angles between two donors A and B in a pentacoordinated molecule ($\beta \geq \alpha$).

(48) Addison, A. W.; Rao, T. N.; Reedijk, J.; van Rijn, J.; Verschoor, G. C. *J. Chem. Soc. Dalton Trans.* **1984**, 1349-1356.

(49) Deeth, R. J.; Gerloch, M. *Inorg. Chem.* **1985**, *24*, 4490-4493.

(50) Huheey, J. E.; Keiter, E. A.; Keiter, R. L. *Inorganic Chemistry*, 4th ed., Harper Collins, New York, **1993**.

(51) Cummins, C. C.; Lee, J.; Schrock, R. R.; Davis, W. M. *Angew. Chem.* **1992**, *104*, 1510-1512; *Angew. Chem. Int. Ed. Engl.* **1992**, *31*, 1501-1503.

(52) Gobbi, A.; Frenking, G. *J. Am. Chem. Soc.* **1993**, *115*, 2362-2372.

(53) Boese, R.; Bläser, D.; Petz, W. *Z. Naturforsch.* **1988**, *43(B)*, 945-948.

(54) The ρ-value of 0.994 in the $[C(NMe_2)_3]^+$ cation is due to crystal packing effects and assumes the ideal value of 1.00 in other complexes; W. Petz,[53] personal communication.

(55) Hecht, H. *Z. Anorg. Ch.* **1947**, *254*, 37-51.

(56) Kubas, G. J. *Inorg. Synth.* **1979**, *19*, 90-92.

(57) Keller, R. N.; Wycoff, H. D. *Inorganic Syntheses, Vol. 2*; Fernelius, W. C. (Ed.), McGraw-Hill Book Company, Inc., New York, **1946**, pp 1-4.

(58) Kaneko, T.; Wong, H.; Doyle, T. W. *Tetrahedron Lett.* **1985**, *26*, 3923-3926.

(59) Burnett, M. N.; Johnson, C. K. *ORTEP-III, Oak Ridge Thermal Ellipsoid Plot Program for Crystal Structure Illustrations*, Oak Ridge National Laboratory Report ORNL-6895, **1996**.

(60) a) Sheldrick, G. M. *SHELXS-97, Program for Crystal Structure Solution* and *SHELXL-97, Program for Crystal Structure Refinement* **1997**, Göttingen, Germany; b) Siemens Analytical X-ray Instruments Inc. *SHELXTL 5.06* **1995**, Madison, WI, USA; c) Giacovazzo, C. *SIR-92, Program for Crystal Structure Solution* **1992**, Bari, Italy.

(61) Crystallographic data (excluding structure factors) for the structures reported in this paper have been deposited with the Cambridge Crystallographic Data Centre as Supplementary Publication No. CCDC-161187 (**3**), CCDC-161186 (**4**), CCDC-161184 (**5**) and CCDC-161185 (**6**). Copies of the data can be obtained free of charge on application to CCDC, 12 Union Road, Cambridge CB2 1EZ, UK (fax: (+ 44) 1223 336-033; email: deposit@ccdc.cam.ac.uk).

— Chapter 3.2 —

The Reactivity of (TMG₃tren)Cu Complexes

The reactivity of the copper precursor complexes introduced in Chapter 3 has been studied in the reaction with various oxene and nitrene sources.

3.2.1 Reaction with O_2[1]

[(TMG₃tren)Cu]ClO₄ was exposed to dioxygen at -78 °C in either acetone or propionitrile solution (Scheme 1). An immediate change of color could be observed, turning from light yellow to emerald green, and vanishing upon warming to room temperature with recovery of a greenish yellow color. This behaviour could be reversibly observed several times before the complex decomposed.
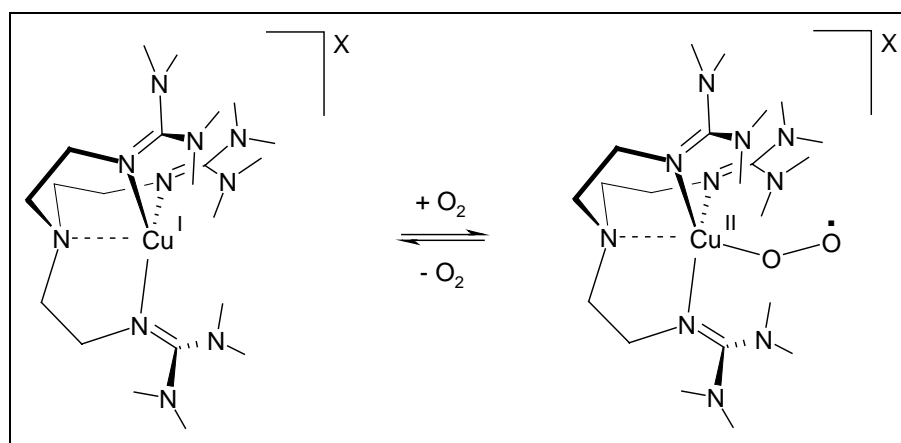
Scheme 1. Reversible reaction of [(TMG₃tren)Cu]ClO₄ with dioxygen in acetone at -78 °C to a mononuclear end-on superoxo complex.

Copper oxo complexes are usually only stable at temperatures below ca. -30 °C with very few exceptions.[2,3] This circumstance makes it difficult to detect these species with conventional spectroscopic methods. Low temperature stopped-flow UV/Vis and resonance raman spectroscopy proved to be the method of choice to gain evidence about the formation of copper oxo complexes.[4] Indeed, when subjected to a stopped-flow apparatus which allows recording of UV/Vis spectra on a millisecond time scale, the reversible development of absorptions at wavelengths of 440 and 680 nm become visible, either in acetone or propionitrile solution (Figure 1 and Figure 2). Both bands indicate the formation of a Cu(II) superoxo complex.[5] The band at 440 nm is assigned to the strong L→M charge transfer of the superoxo ligand.
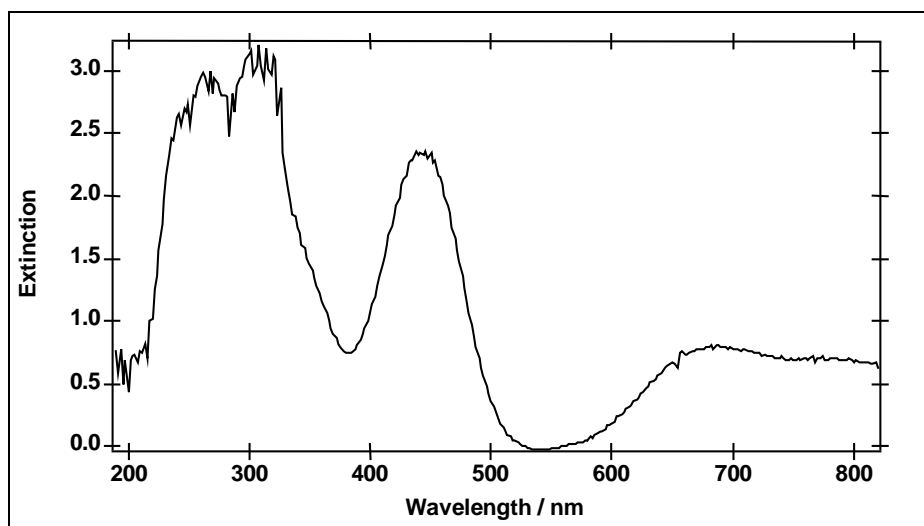
Figure 1. Low temperature (-70 °C) UV/Vis spectrum of [(TMG₃tren)Cu]ClO₄ ([complex] = 5 mM) after reaction with O_2 in acetone.

Our concept of providing superbasic donor ligands that should be able to stabilize transition metals in unusually high oxidation states also proved to be effective. Where the bulk of copper complexes with other N-donor ligands applied in the oxygenation reaction had undergone reasonable decay at temperatures above -50 to -30 °C, our complex showed a fairly stable constitution, expressed by the conservation of the characteristic UV/Vis absorption at 440 nm over a period of time at -30 °C.
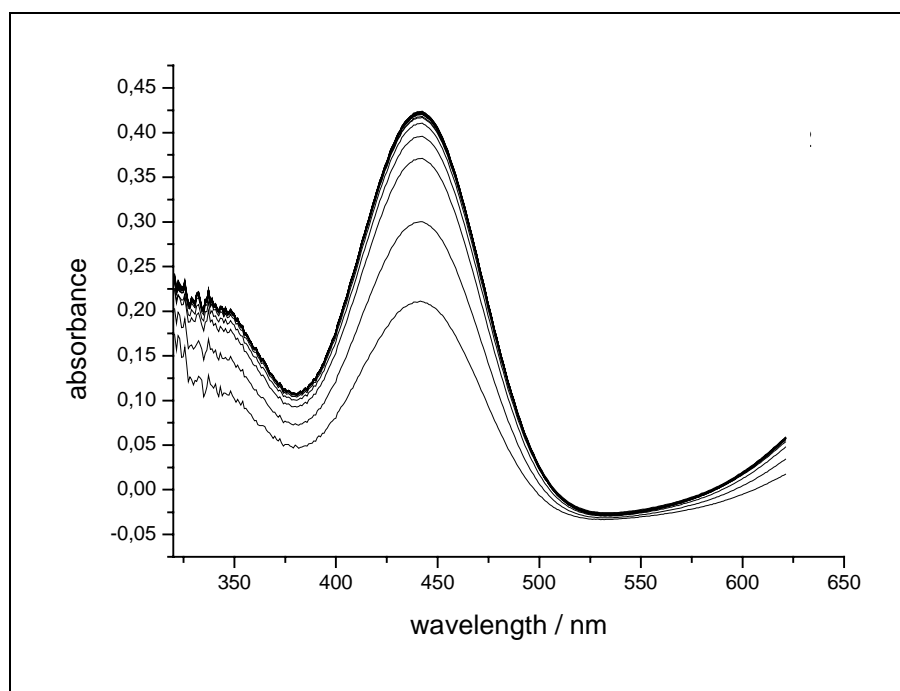

Figure 2. Formation of the superoxo complex at -90 °C, stopped-flow UV/Vis spectrum in EtCN ([complex] = 5 mM, t = 0.33 s, 5 % O_2 saturation).

2

Further proof for the formation of a superoxo copper complex was obtained by its resonance raman spectrum (Figure 3). A comparative sweep at different temperatures (room temperature: bottom, -70 °C: top) in acetone resulted in a reversible absorption at 1122 cm^{-1} which is attributed to the ν(O-O) vibration of a superoxo species.[4,5] Additional evidence is received by recording the spectra after reaction with $^{18}O_2$ instead of $^{16}O_2$, which resulted in a shift of the absorption to 1060 cm^{-1}.
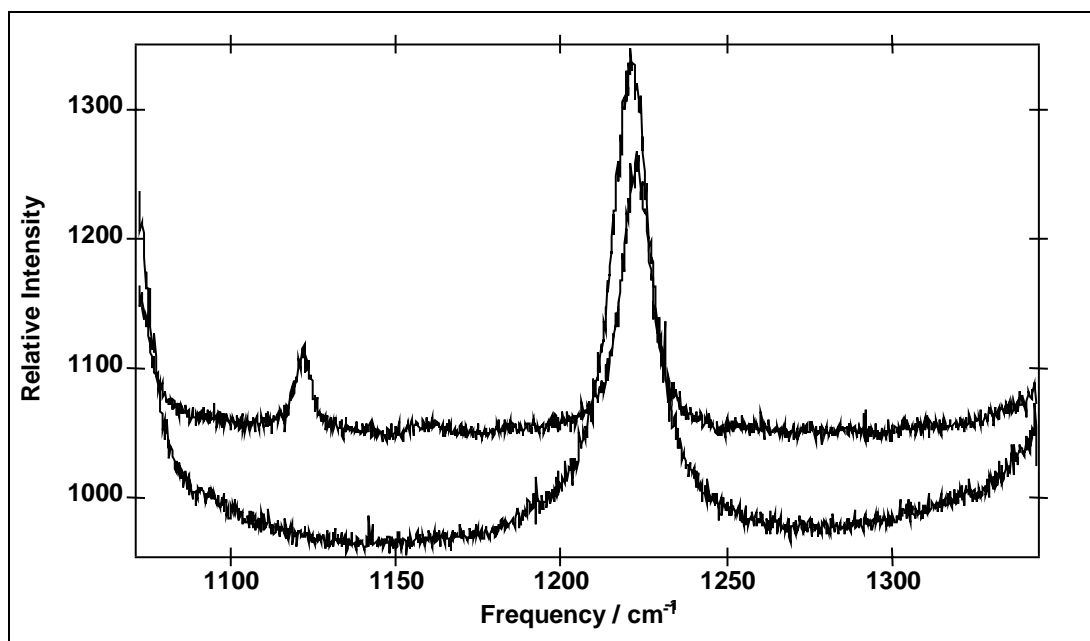

Figure 3. Resonance raman spectra of [(TMG$_3$tren)Cu]ClO$_4$ (2.5 mM) after reaction with ^{16}O in acetone (top: -70 °C, bottom: room temperature).

From the structure of the copper precursor it is suggested that a mononuclear complex is formed (Scheme 1). The methyl groups of the guanidine units provide a molecular pocket of high steric demand (Figure 4) that efficiently prevents the superoxo complex to further reduced by a second Cu(I) equivalent to yield a bis-μ-peroxo complex.[5,6] The crystal structure of a supposed monomeric side-on superoxo copper(II) complex with a tris(pyrazolylborate) ligand was reported by Kitajima et al., its dimerization was also prevented by bulky groups in the ligand periphery.[7] However, this complex turned out to be a hydroperoxo species. Furthermore, it is assumed that only a superoxo complex with end-on bonded dioxygen could be realized due to the steric demand provided by the ligand. This is envisaged in a space filling illustration with view into the molecular pocket imposed by the precursor complex (Figure 5). However, crystal growth experiments have to be continued in order to avoid speculations.
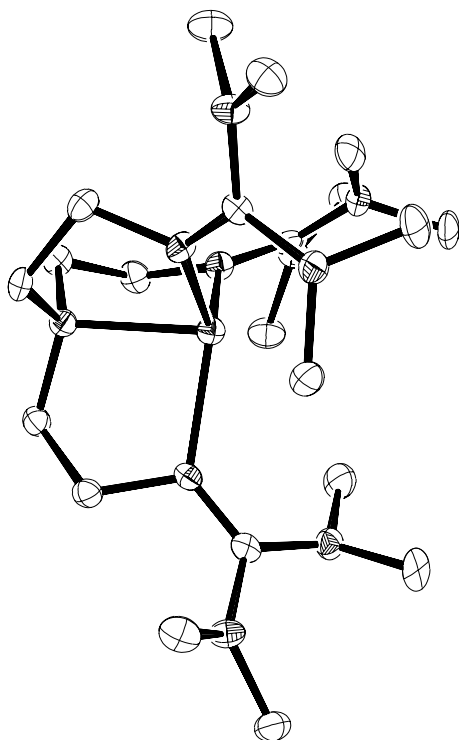
Figure 4. ORTEP plot of the molecular structure of [(TMG$_3$tren)Cu]ClO$_4$, view into the molecular pocket imposed by the ligand; thermal ellipsoids are at 30 % probability level, perchlorate anion and hydrogen atoms omitted for clarity.
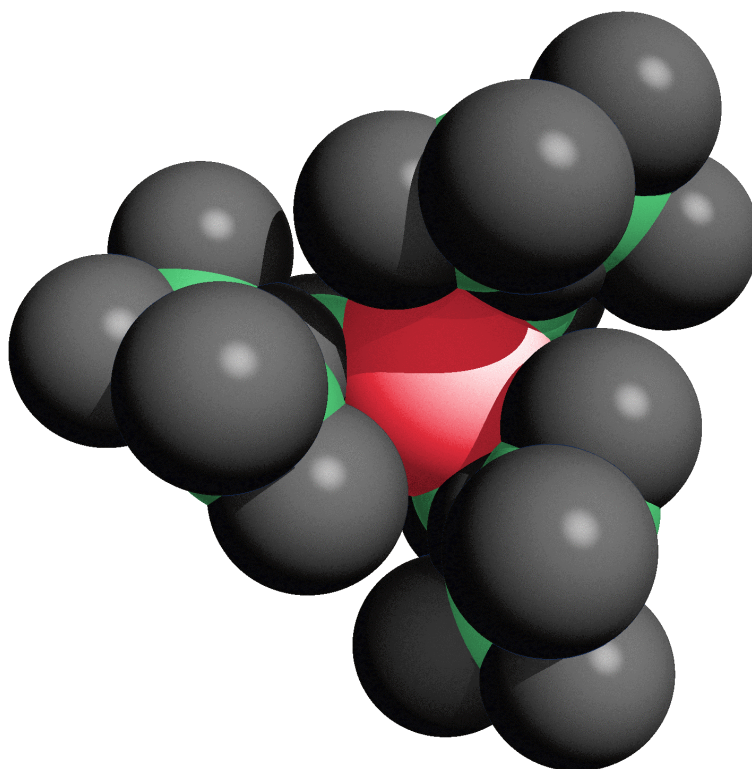

Figure 5. Space filling illustration[8] of [(TMG$_3$tren)Cu]ClO$_4$, view along the C_3 axis Cu-N$_{tert}$.

3.2.2 Reaction with CO, ethylene, and acetylene

All attempts to react the complex [(TMG$_3$tren)Cu]ClO$_4$ with CO or ethylene in acetone or propionitrile solution at -78 °C failed (Scheme 2). Only the precursor could be isolated which was evident from FD mass spectra, elemental analysis and IR spectra. No CO or ethylene complex was formed as is known for other structurally characterized examples of copper complexes.[6a,9,10]
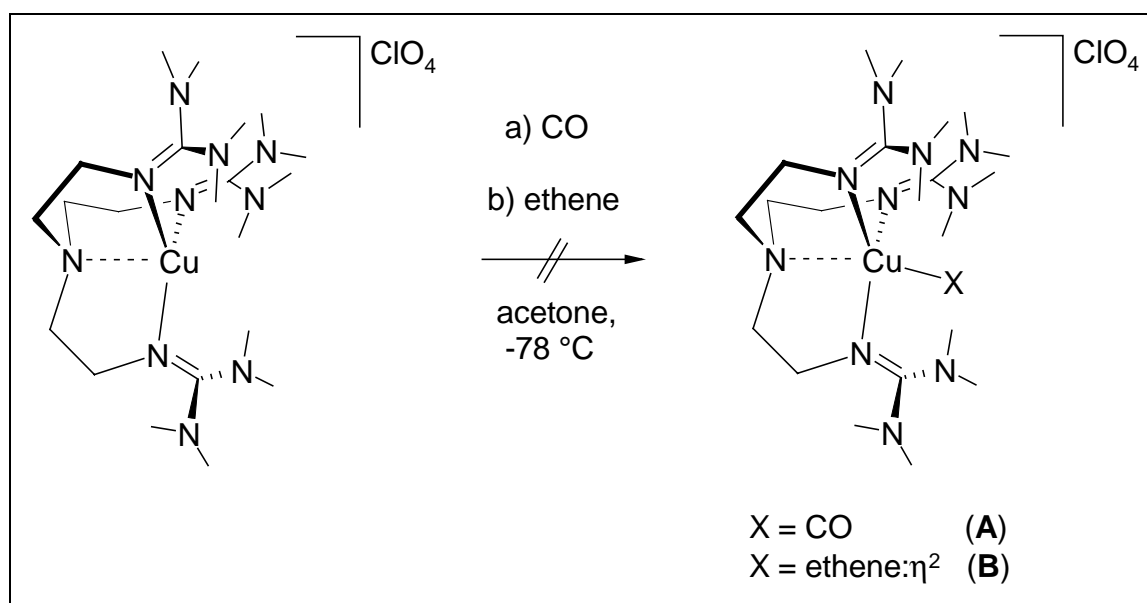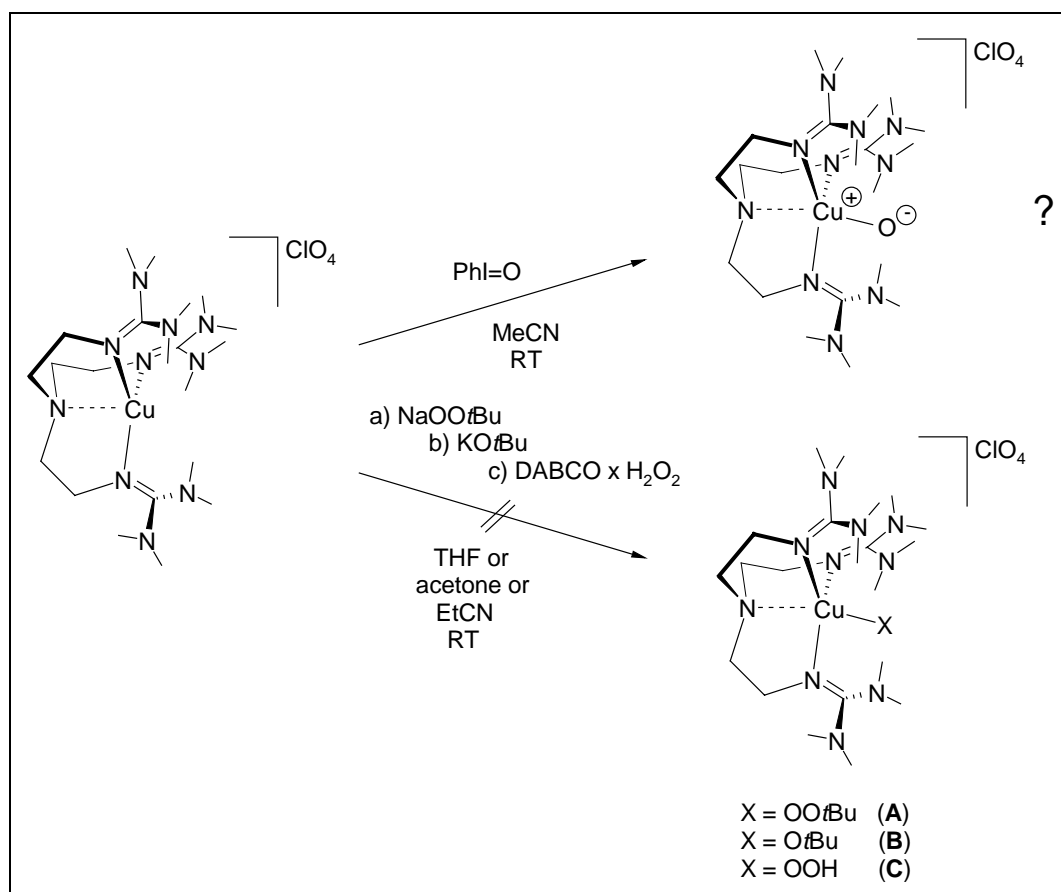

Scheme 2. Reaction of [(TMG$_3$tren)Cu]ClO$_4$ with CO and ethene.

However, when acetylene was bubbled through a solution of [(TMG$_3$tren)Cu]ClO$_4$ in acetone at -78 °C, and was allowed to warm to room temperature, the development of a precipitate with a change of color from bright yellow via orange to red, and finally red-brown was observed. Isolation of the precipitate gave a dark red-brown powder that detonated upon scratching, the formation of a copper acetylide was most probable.

3.2.3 Reaction with NaOO*t*Bu, KO*t*Bu, DABCO × 2 H₂O₂, and PhI=O

Attempts to react the complex [(TMG₃tren)Cu]ClO₄ or its Cu(II) analogue with NaOO*t*Bu, KO*t*Bu and DABCO × 2 H₂O₂ in various solvents (THF, acetone, EtCN) at -78 °C resulted only in re-isolation of the precursor, which was evident from FD mass spectra, elemental analysis and IR spectra. No copper alkoxide was formed (Scheme 3).[11]
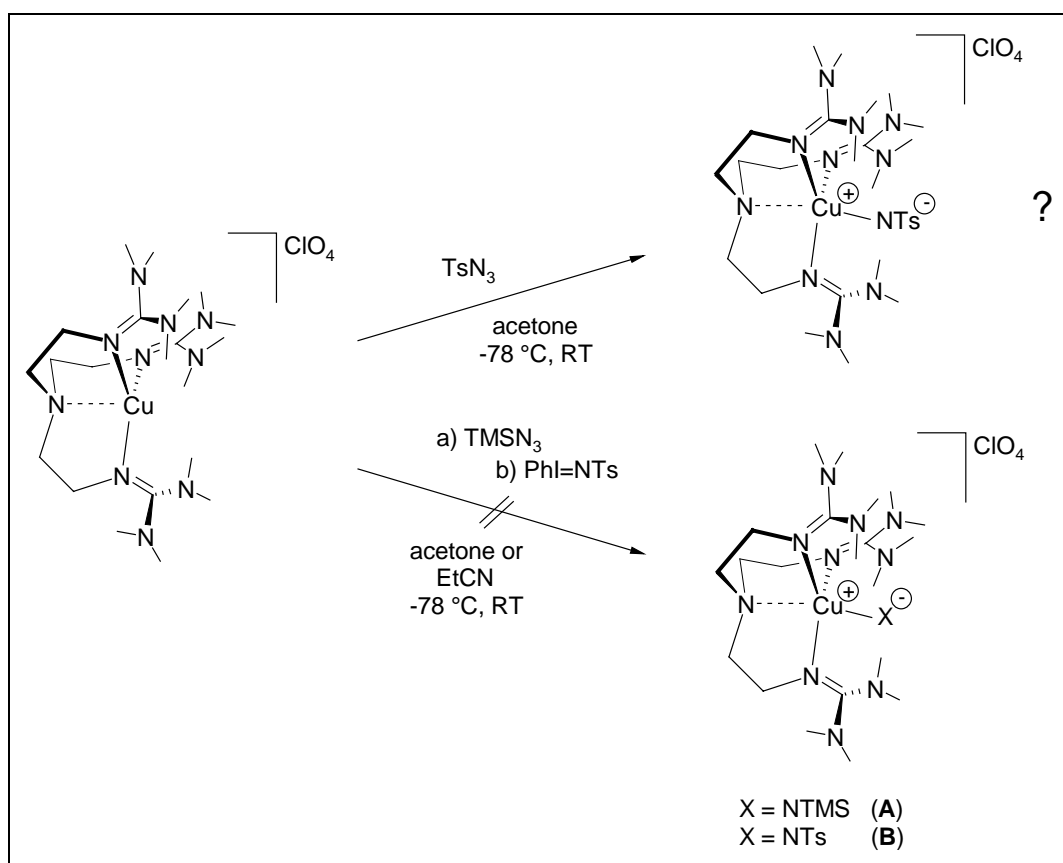

Scheme 3. Reaction of [(TMG₃tren)Cu]ClO₄ with NaOO*t*Bu, KO*t*Bu and DABCO × 2 H₂O₂.

When PhI=O was employed in the reaction as oxidizing reactant, layering of the acetonitrile solution with dry Et₂O resulted in part in the development of turquoise crystals. Analysis of the crystals and separate analysis of the bulk green residue gave identical results. IR spectra showed only the absorptions of the precursor complex. Elemental analysis matched a terminal copper oxo complex [(TMG₃tren)Cu(O)]ClO₄ and are supported by a signal in the FD mass spectrum at $m/z = 518$ [(TMG₃tren)Cu(O)]. Endeavours to receive a crystal structure are set out to confirm the formation of the postulated complex.

3.2.4 Reaction with TMSN₃, PhI=NTs and TsN₃

Reactions with TMSN₃, PhI=NTs and TsN₃ as nitrene precursors for the isolation of a possible copper nitrene intermediate were carried out (Scheme 4). In the case of TMSN₃ and PhI=NTs, no reaction was observed and only the copper complex [(TMG₃tren)Cu]ClO₄ could be isolated.

Employing TsN₃ resulted in a signal at the FD mass spectrum at $m/z = 671$, which can be assigned to the copper nitrene complex [(TMG₃tren)Cu(NTs)]. However, IR spectra revealed only the bands of the precursor complex, and elemental analysis showed a best fit for [(TMG₃tren)Cu(NTs)]ClO₄. Certainly, no copper azide complex was formed.[12] Endeavours to receive a crystal structure are set out to confirm the formation of the postulated complex.

Scheme 4. Reaction of [(TMG₃tren)Cu]ClO₄ with TMSN₃, PhI=NTs and TosN₃.

Experimental

Materials and methods: (see parent chapter 5.1)

UV/Vis spectra were recorded on a HP 89090 A spectrometer, resonance raman spectra were obtained from excitation with a titan-saphire laser at 785.0 nm with a Spex 1402 monochromator and an ISA CCD camera (2000 × 800 pixel) at 140 K.

Potassium-*tert*-butylate (KO*t*Bu) was used as purchased from MERCK. Sodium-*tert*-butylperoxide (NaOO*t*Bu),[13] 1,4-diazabicyclo[2.2.2]octane (DABCO) × 2 H$_2$O$_2$,[14] and iodosylbenzene (PhI=O)[15] were prepared according to literature methods.

Trimethylsilyl azide (TMSN$_3$) was used as purchased from Fluka. [*N*-(*p*-toluenesulfonyl)imino]phenyliodinane (PhI=NTs) [16] was prepared by a published method and recrystallized from methanol/water at 5 °C, and *p*-toluenesulfonyl azide (TsN$_3$)[17] was prepared by a literature method.

Caution! Perchlorate salts are potentially explosive and should be handled with care.

Dioxygen activation:

[Cu(CH$_3$CN)$_4$]ClO$_4$ (327 mg, 1.0 mmol) and TMG$_3$tren (**1**) (450 mg, 1.05 mmol) were dissolved in dry acetone (5 mL) or EtCN (5 mL), respectively, at room temperature and the solution was concentrated to a volume of ca. 2 mL. The solution was then cooled to -78 °C, and the color turned emerald green, immediately after dioxygen was bubbled through. After 1 min. the oxygen inlet was cut off and the reaction solution was placed into a freezer at -83 °C for crystallization.

Reaction with CO, ethylene and acetylene:

The procedure described above was followed. After the gas inlet was cut off the solution was allowed to warm to room temperature. In the case of the copper acetylide, the supernatant was decanted, the residue washed with dry acetone and diethyl ether, and dried in vacuo.

Reaction with NaOO*t*Bu, KO*t*Bu and DABCO × 2 H$_2$O$_2$ and PhI=O:

[Cu(CH$_3$CN)$_4$]ClO$_4$ (327 mg, 1.0 mmol) and TMG$_3$tren (**1**) (450 mg, 1.05 mmol) were dissolved in dry THF (5 mL), MeCN (5 mL) or acetone (5 mL), respectively, at room temperature. NaOO*t*Bu (112 mg, 1.00 mmol), KO*t*Bu (112 mg, 1.00 mmol), DABCO × 2 H$_2$O$_2$ (90 mg, 0.50 mmol) or PhI=O (220 mg, 1.00 mmol), respectively, was added and stirred at ca. 50 °C for 1 hour. All solutions turned green upon addition of the reactant and were concentrated in volume to ca. 2 mL. The products were precipitated by the addition of dry diethyl ether and the resulting residues were washed with the same solvent (3 × 10 mL) and dried in vacuo.

Yield from the reaction with PhI=O: 460 mg.

IR (KBr): $\tilde{v}$ = 3434 w(br), 2875 m, 1582 s, 1524 s, 1484 w, 1462 m, 1427 m, 1392 s, 1160 m, 1143 m, 1091 s, 763 w, 622 w cm^{-1}; MS (FD, MeCN): m/z = 518 [(**1**)Cu(O)]$^+$, 503 [(**1**)Cu]$^+$; elemental analysis found (%) C 40.97, H 7.67, N 20.90, calcd. for C$_{21}$H$_{48}$N$_{10}$O$_5$ClCu [(**1**)Cu(O)]ClO$_4$ (619.7) C 40.70, H 7.81, N 22.60, calcd. for C$_{21}$H$_{48}$N$_{10}$OCu [(**1**)Cu(O)] (520.2): C 48.49, H 9.30, N 26.92.

Reaction with TMSN$_3$, PhI=NTs and TsN$_3$:

[Cu(CH$_3$CN)$_4$]ClO$_4$ (327 mg, 1.0 mmol) and TMG$_3$tren (**1**) (450 mg, 1.05 mmol) were dissolved in dry THF (5 mL), or EtCN (5 mL) or acetone (5 mL), respectively, at room temperature. Then, the solution was cooled to -78 °C and TMSN$_3$ (115 mg, 1.00 mmol), PhI=NTs (373 mg, 1.00 mmol), or TsN$_3$ (197 mg, 1.00 mmol) was added and the reaction mixture was allowed to warm to room temperature. All solutions turned green upon addition of the reactant and were concentrated in volume to ca. 2 mL. The solutions were precipitated by the addition of dry diethyl ether and the resulting residues were washed with the same solvent (3 × 10 mL) and dried in vacuo.

Yield from the reaction with TosN$_3$: 510 mg.

IR (KBr): $\tilde{v}$ = 3427 w(br), 2893 m, 1582 s, 1566 s, 1527 m, 1460 w, 1427 w, 1394 m, 1263 w, 1137 m, 1093 s, 622 w cm^{-1}; MS (FD, MeCN): m/z = 671 [(**1**)Cu(NTs)]$^+$, 503 [(**1**)Cu]$^+$, 441 [(**1**)]$^+$; elemental analysis found (%) C 43.74, H 7.06, N 18.52, calcd. for C$_{28}$H$_{55}$N$_{11}$ClCuO$_6$S [(**1**)Cu(NTs)]ClO$_4$ (772.9): C 43.51, H 7.17, N 19.93, calcd. for C$_{28}$H$_{55}$N$_{11}$ClCuO$_2$S [(**1**)Cu(NTs)] (673.4) C 49.94, H 8.23, N 22.88.

References

[1]   Collaboration with S. Schindler, M. Schatz, Institute for Inorganic Chemistry, Friedrich-Alexander-University, Erlangen-Nürnberg, **2000** / **2001**.

[2]   a) K. D. Karlin, J. C. Hayes, J. Zubieta in: *Copper Coordination Chemistry: Biochemical and Inorganic Perspectives*, K. D. Karlin, J. Zubieta (Eds.), Adenine Press, Guilderland, New York, **1983**, pp. 457-472; b) K. D. Karlin, D.-H. Lee, S. Kaderli, A. D. Zuberbühler, *J. Chem. Soc. Chem. Comm.* **1997**, 475-476.

[3]   a) K. D. Karlin, D.-H. Lee, S. Kaderli, A. D. Zuberbühler, *J. Chem. Soc. Chem. Comm.* **1997**, 475-476; b) H. Börzel, P. Comba, C. Katsichtis, W. Kiefer, A. Lienke, V. Nagel, H. Pritzkow, Chem. Eur. J. 1999, 5, 1716-1721.

[4]   a) J. E. Pate, R. W. Cruse, K. D. Karlin, E. I. Solomon, *J. Am. Chem. Soc.* **1987**, *109*, 2624-2630; b) K. D. Karlin, P. Gosh, R. W. Cruse, A. Farooq, Y. Gultneh, R. R. Jacobson, N. J. Blackburn, R. W. Strange, J. Zubieta, *J. Am. Chem. Soc.* **1988**, *110*, 6769-6780; c) Baldwin, M. J.; Root, D. E.; Pate, J. E.; Fujisawa, K.; Kitajima, N.; Solomon, E. I. *J. Am. Chem. Soc.* **1992**, *114*, 10421-10431; d) Solomon, E. I.; Tuczek, F.; Root, D. E.; Brown, C. A. *Chem. Rev.* **1994**, *94*, 827-856; e) K. D. Karlin, W. B. Tolman, S. Kaderli, A. D. Zuberbühler, *J. Mol. Catal. A: Chem.* **1997**, *117*, 215-222; f) S. Schindler, C. D. Hubbard, R. van Eldik, *Chem. Soc. Rev.* **1998**, *27*, 387-393.

[5]   S. Schindler, *Eur. J. Inorg. Chem.* **2000**, 2311-2326.

[6]   a) N. Kitajima, K. Fujisawa, C. Fujimoto, Y. Moro-oka, S. Hashimoto, T. Kitagawa, K. Toriumi, K. Tatsumi, A. Nakamura, *J. Am. Chem. Soc.* **1992**, *114*, 1277-1291; b) N. Kitajima, Y. Moro-oka, *Chem. Rev.* **1994**, *94*, 737-757; c) W. B. Tolman, *Acc. Chem. Res.* **1997**, *30*, 227-237.

[7]   K. Fujisawa, M. Tanaka, Y. Moro-oka, N. Kitajima, *J. Am. Chem. Soc.* **1994**, *116*, 12079-12080.

[8]   M. N. Burnett, C. K. Johnson, *ORTEP-III, Oak Ridge Thermal Ellipsoid Plot Program for Crystal Structure Illustrations*, Oak Ridge National Laboratory Report ORNL-6895, **1996**.

[9]   M. Pasquali, C. Floriani, G. Venturi, A. Gaetani-Manfredotti, A. Chiesi-Villa, *J. Am. Chem. Soc.* **1982**, *104*, 4092-4099.

[10] a) J. S. Thompson, R. L. Harlow, J. F. Whitney, *J. Am. Chem. Soc.* **1983**, *105*, 3522-3527; b) P. J. Pérez, M. Brookhart, J. L. Templeton, *Organometallics* **1993**, *12*, 261-262.

[11] Yamashita, H. Ito, T. Ito, *Inorg. Chem.* **1983**, *22*, 2102-2104.

[12] C. J. Harding, F. E. Mabbs, E. J. L. MacInnes, V. McKee, J. Nelson, *J. Chem. Soc. Dalton Trans.* **1996**, 3227-3230.

[13] M. Bold, *Masters Thesis* **1998**, Philipps University Marburg, Germany.

[14] A. A. Osswald, D. L. Guertin, *J. Org. Chem.* **1963**, *28*, 651-657.

[15] H. Saltzmann, J. G. Sharefkin, *Org. Synth.* **1963**, *43*, 60-61.

[16] Y. Yamada, T. Yamamoto, M. Okawara, *Chem. Lett.* **1975**, 361-362.

[17] D. S. Breslow, M. F. Sloan, N. R. Newberg, W. B. Renfrow, *J. Am. Chem. Soc.* **1969**, *91*, 2273-2279.

— Chapter 3.3 —

Cu Complexes with HMPI₃tren as Ligand

Results and discussion

A ligand analogue based on iminophosphorane rather than peralkyl guanidine groups should possess even more basic properties and a higher donor character (also see Chapter 5.2). HMPI₃tren was synthesized and complex formation with Cu(I/II) salts was attempted. Copper ligand complexes of a 1:1 ratio with Cu(I/II) perchlorate salts could not be isolated. Copper complexes of Cu(I) and Cu(II) were obtained from the chloride salts with equimolar amounts of HMPI₃tren ligand. Both resulted in red-brown amorphous substances. The formation of the complexes was confirmed by ESI mass spectra revealing the parent molecular ions. However, correct elemental analysis could not be received. So far, single crystals could not be obtained from MeCN, acetone or toluene and any solvent mixtures of the prementioned with diethyl ether.
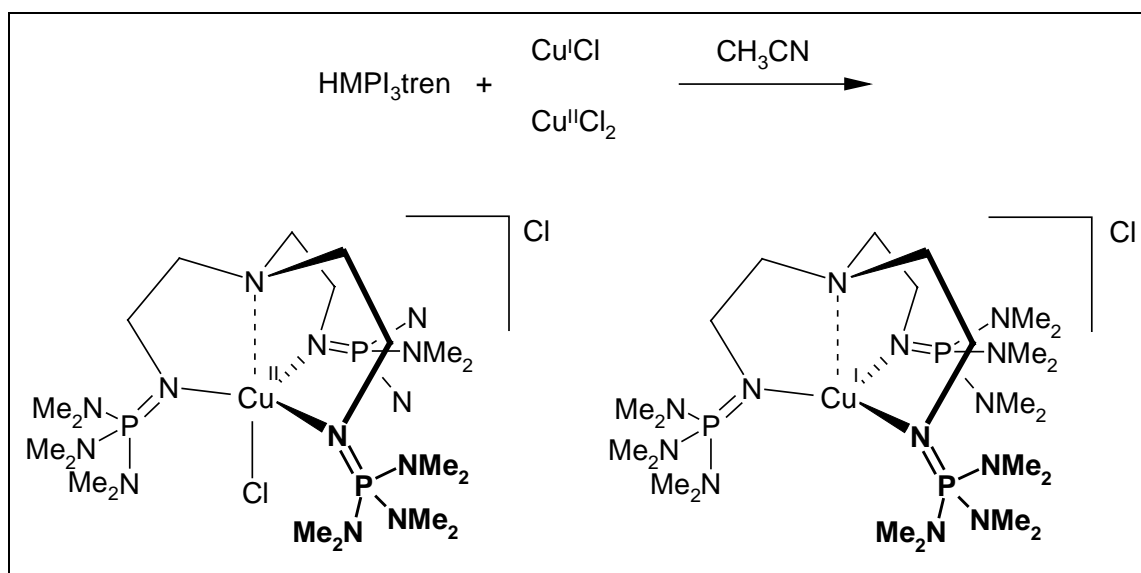

Figure 1. Complex formation of Cu(I/II)-chloride with HMPI₃tren.

Experimental

Materials and methods: (see parent chapter 5.1)

1,1,1-Tris{2-[N^3-(dimethylamino)phosphoranylideneamino]ethyl}amine (HMPI$_3$tren) was prepared according to a published method.[1]

Complex formation of HMPI$_3$tren with copper(I) Chloride:

CuCl (99 mg, 1.00 mmol) and HMPI$_3$tren (L) (629 mg, 1.00 mmol) were dissolved in dry MeCN (5 mL). The solution was concentrated to ca. 2 mL and layered with diethyl ether. A deep red colored crystalline appearing solid was isolated which became a brown amorphous material upon drying in vacuo. Yield: 390 mg.

^{1}H NMR (200.1 MHz, CD$_3$CN, 25 °C): δ = 3.25-3.00 (m, 6 H, CH$_2$), 2.93-2.68 (m, 6 H, CH$_2$), 2.66 (d, $^3J_{HP}$ = 9.2 Hz, 54 H, CH$_3$) ppm; ^{13}C NMR (50.3 MHz, CD$_3$CN, 25 °C): δ = 37.4 (CH$_3$) ppm; IR (KBr): $\tilde{\nu}$ = 3431 w(br), 2924 s, 2887 s, 2847 s, 1493 m, 1463 m, 1455 m, 1293 s, 1170 s, 1124 m, 1064 m, 981 vs, 853 w, 820 w, 749 m, 735 m cm^{-1}; MS (ESI, MeCN): m/z (%) = 728 [LCuCl]$^+$, 692 [LCu]$^+$, 630 [L]$^+$; elemental analysis found (%) C 29.24, H 8.02, N 17.30; (1:1 complex) calcd. C$_{24}$H$_{66}$N$_{13}$CuClP$_3$ (728.8): C 39.55, H 9.13, N 24.98.

Complex formation of HMPI$_3$tren with copper(II) Chloride:

CuCl$_2$ (134 mg, 1.00 mmol) and HMPI$_3$tren (L) (629 mg, 1.00 mmol) were dissolved in dry MeCN (5 mL). The solution was concentrated to ca. 2 mL and layered with diethyl ether. A deep red colored crystalline appearing solid was isolated which became a brown amorphous material upon drying in vacuo. Yield: 450 mg.

IR (KBr): $\tilde{\nu}$ = 3435 m(br), 2999 m, 2902 m, 1621 m(br), 1460 m, 1304 s, 1188 s, 1126 m, 1069 m, 996 s, 750 m cm^{-1}; MS (ESI, MeCN): m/z (%) = 728 [LCuCl]$^+$, 692 [LCu]$^+$, 630 [L]$^+$; elemental analysis found (%) C 37.11, H 9.09, N 22.29; (1:1 complex) calcd. C$_{24}$H$_{66}$N$_{13}$CuCl$_2$P$_3$ (764.3): C 37.72, H 8.70, N 23.83.

References

[1] H. Wittman, *Ph. D. Thesis* **1999**, Philipps-University Marburg, Germany.

— Chapter 4 —

Complexes of Manganese, Iron, Zinc, and Molybdenum with a Superbasic Trisguanidine Derivative of Tris(2-aminoethyl)amine (Tren) as Tripod Ligand

Keywords: Ligand design • N ligands • Tripodal ligands • Coordination chemistry • Manganese • Iron • Zinc • Molybdenum

Abstract

The synthesis of a novel tripod ligand N{CH$_2$CH$_2$N=C(NMe$_2$)$_2$}$_3$, based on the tris(2-aminoethyl)amine (tren) backbone and having a set of three superbasic tetramethyl guanidine (TMG) donor atoms instead of the primary amine functionalities, is described. This ligand has been prepared by treating tren with the Vilsmeyer-Salt [(Me$_2$N)$_2$CCl]Cl in the presence of triethylamine as an auxiliary base and NaOH. Complexes of manganese(II), iron(II) and zinc(II) as biologically relevant transition metal ions as well as of molydenum(0) have been synthesized and spectroscopically and structurally characterized. The electrochemical properties of selected complexes have been studied.

Introduction

Peralkylguanidines belong to the strongest organic neutral bases known.[1] They are several orders of magnitude more basic than tertiary amines due to the excellent stabilization of the positive charge over their resonance-stabilized cations.[2] This trend is illustrated by the pK_{BH+} values (MeCN) of the 1,2,2,6,6-pentamethylpiperidinium cation (18.62), the parent guanidinium cation (23.3), and the pentamethylguanidinium cation (25.00).[2c] Therefore, in aqueous media, guanidines exist almost exclusively in the protonated form.[3] Guanidines are currently attracting attention as anion receptors,[4] both in enzymes and in model systems. Due to their hydrophilic nature, they also play an important role in the mediation of solubility of natural products[5] and the stabilization of protein conformations through hydrogen bonding.[5,6,7] However, surprisingly little is known about the coordination chemistry of guanidines. There is some indication that the guanidine functionality of arginine may play a role as neutral donor towards various metal cations in the hydrophobic domains of cytochrom

c enzymes and other such systems.[2,5,6,8] There have been a few reports on coordination compounds of monoguanidines HN=C(NRR')$_2$.[5,6,8,9] The first complexes of chelating bis(guanidine)s have been reported by Kuhn[10] and ourselves.[11a] We became interested in the coordination chemistry of bis-, tris- and oligoguanidines because of the marked tendency of biguanides to stabilize unusually high oxidation states of metals, e.g. in Ag(III)[12] and Ni(III)[13] complexes (Scheme 1).
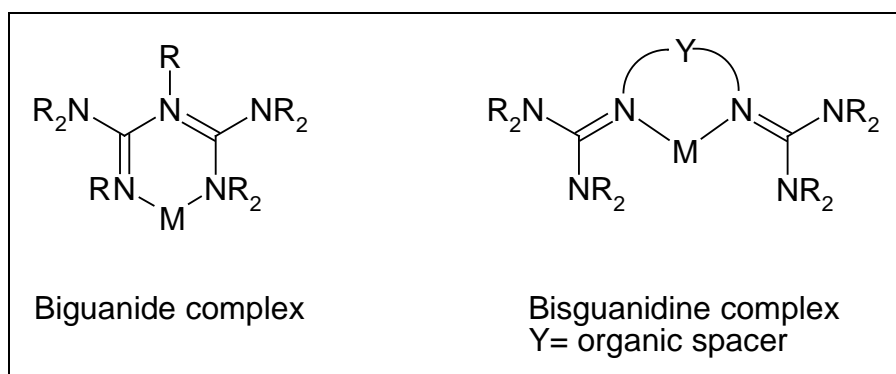
Scheme 1. Guanidine-based complexes.

The focus of this investigation is to evaluate the donor capability of tetradentate pentaalkyl guanidine derivatives. The basicities of these neutral ligands are intermediate between that of tertiary amines and amido ligands, but the question remains as to how well they interact with Lewis acids. Indeed, the question arises as to whether, in addition to their strong σ-donor interaction sp^2-N$\rightarrow$ M, guanidines may also be π-acidic like Schiff bases or π-basic like amido ligands. Various aspects of guanidine coordination chemistry remain unexplored, such as fine the tuning of the basicity, donor strength, steric demand and control of the solubility by variation of the substituents at the guanidine function. Following our study on guanidine derivatives of the tmeda and tame backbones,[11a] we wish to report our first results on the synthesis and coordination chemistry of guanidine derivatives of the tren ligand family (Scheme 2). The target molecule 1,1,1-tris{2-[N^2-(1,1,3,3-tetramethylguanidino)]ethyl} amine (**1**) (TMG$_3$tren) is structurally related to known Schiff bases,[14] tris(pyridylmethyl) amine (tmpa)[15] and other tripodal ligands[16] based on the well-known tren backbone (Scheme 2).
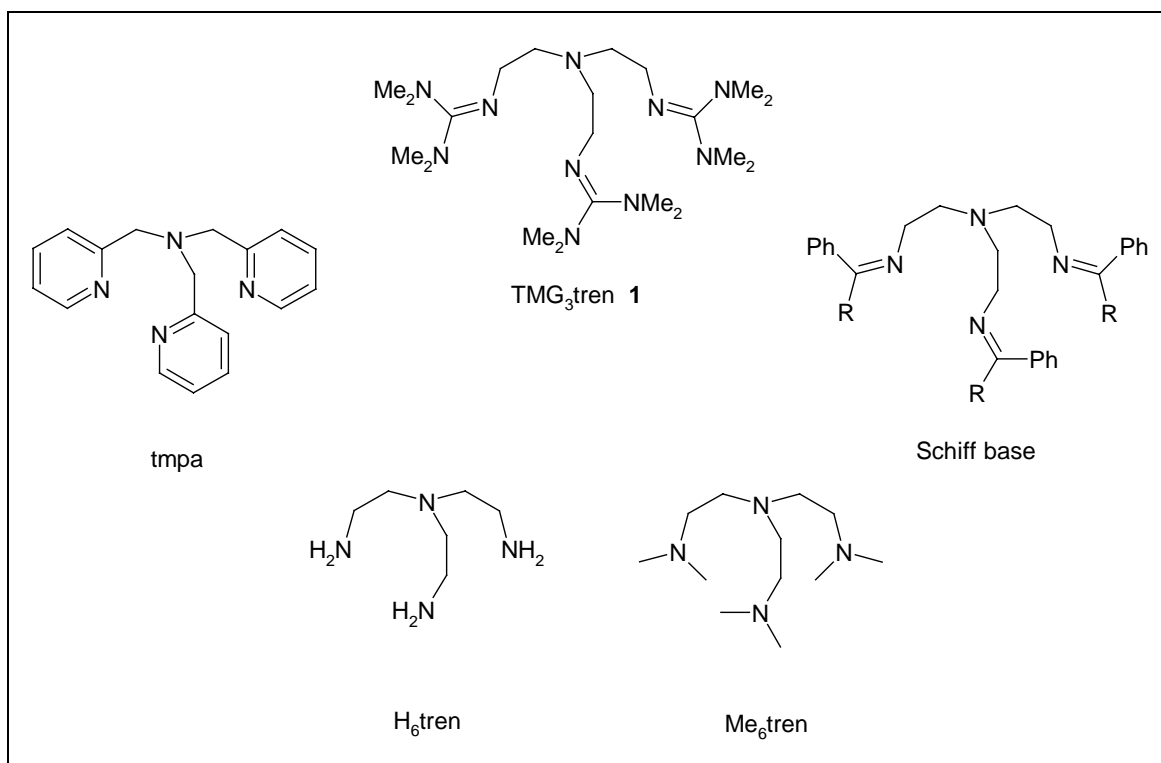
Scheme 2. Structural relationship between the target **1** and known tripods of the tren ligand family.

Results and Discussion

Ligand synthesis

The synthesis of the target ligand **1** was accomplished following our general procedure that allows the transformation of primary bis-, tris- or polyamines into the corresponding tetramethylguanidino derivatives.[11] The main problem associated with this synthesis is that polyguanidines as well as their hydrochlorides are extremely hygroscopic. Typically, they cannot be distilled/sublimed without decomposition and may not be purified by column chromatography on polar phases (SiO$_2$, Al$_2$O$_3$). Because of these purification difficulties, it was imperative that the synthesis involved selective reactions. A nearly quantitative transformation of a primary amine functionality into the guanidine may be accomplished by reaction with the Vilsmeyer salt [(Me$_2$N)$_2$CCl]Cl, a method first described by Eilingsfeld and Seefelder[17] and later improved by Kantlehner et al.[18] for *mono*guanidines. The Vilsmeyer salt is obtained by reaction of tetramethylurea with phosgene[19] or oxalyl chloride in toluene.[20] Reaction of the latter with tren in the presence of triethylamine as an auxiliary base leads to the corresponding hydrochloride **1A** (Scheme 3). Separation from the by-product HNEt$_3$Cl is accomplished by adding one equiv. of NaOH per guanidine functionality

and removing the resulting NEt_3 and NaCl by crystallization from acetonitrile / diethyl ether. In the present case, the free base **1** was obtained as a yellow oil that crystallized upon standing in an overall yield of up to 86% by deprotonation of the tris(hydrochloride) using a two-phase system MeCN/50% aqueous KOH.
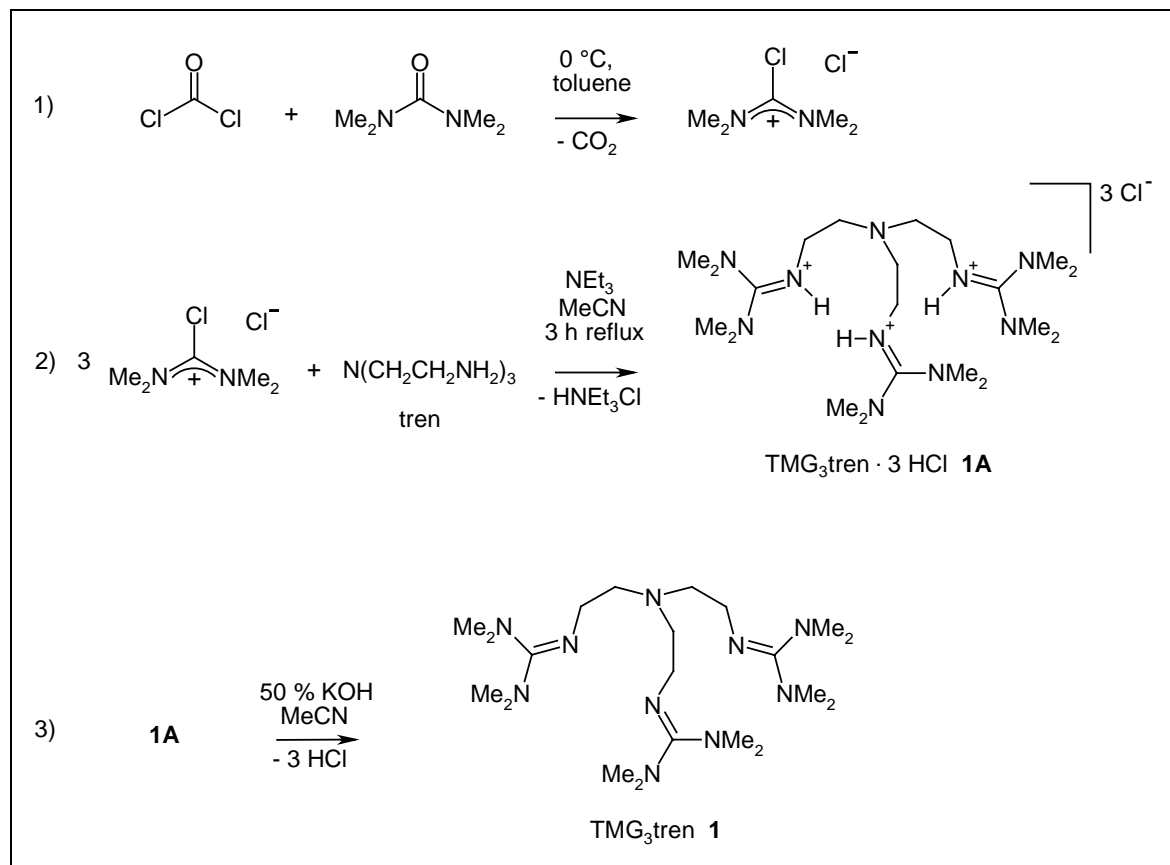
Scheme 3. Preparation of peralkylated oligoguanidines.

The spectroscopic features of the protonated ligand **1A** are very similar to those of the free guanidine base **1**. A difference can be seen in the IR spectra, where TMG₃tren shows a single absorption at $\nu(C=N) = 1620$ cm^{-1} while the corresponding absorption of the tris(hydrochloride) is split into two separate bands at 1627 and 1584 cm^{-1}. This splitting is a typical feature due to the decreased molecular symmetry in guanidinium cations. It is also observed for the hexamethylguanidinium cation.[21] In order to avoid steric interactions the NMe₂ substituents adopt a mutually twisted propeller-like conformation[21,22] rather than a coplanar one. The UV/Vis spectrum of **1** in MeCN shows an absorption of 216 nm with a molar extinction coefficient ε of approximately 1×10^4 for each guanidinium unit, attributable to the $\pi \rightarrow p^*$ transition of the C=N bond.[23] The ¹H-NMR spectrum of **1** features

4

only one signal due to the methyl groups, while the ^{13}C NMR reveals the presence of two chemically non-equivalent methyl groups. It is known from the literature that the barrier to rotation about the C=N double bond of pentaalkylguanidines (Scheme 4) leading to a *syn-anti* isomerization.[2b,24] is markedly lowered by protonation or by increased steric demand of the alkyl groups. The bulkiness of the tren backbone leads to a lower barrier, which is manifested in the equivalence seen in the ^{1}H NMR spectrum.
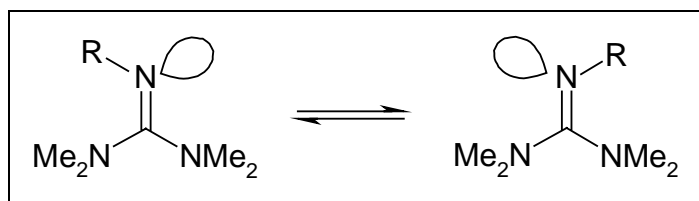

Scheme 4. The *syn-anti* isomerization of pentasubstituted guanidines.

Metal complex synthesis

The free guanidine base **1** is moderately stable in D_2O. Due to slow hydrolysis, tetramethylurea is formed over a period of several days by decomposition of the guanidinium hydroxide. In contrast, the hydrochloride **1A** is perfectly stable in D_2O. In order to avoid side reactions due to hydrolysis of the ligand and of the metal salts, the latter were dehydrated by the orthoester method[25] prior to complexation. The complexes were synthesized in good yields by combining the dehydrated metal salts with 1.05 equiv. of TMG₃tren (**1**) in dry acetonitrile and stirring for 30 min (Scheme 5 and 6). The resulting ionic complexes **2-5** proved to be soluble in polar aprotic media such as MeCN, CH_2Cl_2 or acetone, but insoluble in diethyl ether and hydrocarbons.
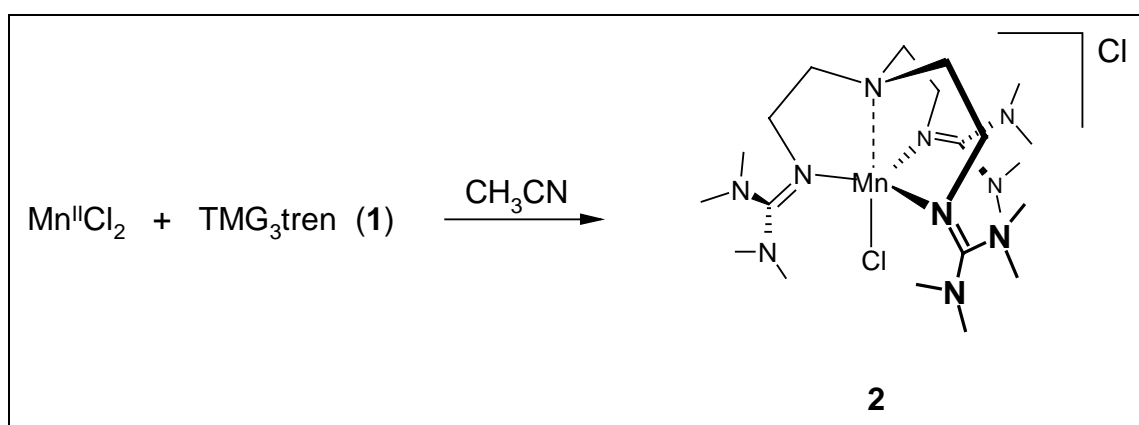
Scheme 5. Complex formation of MnCl₂ with TMG₃tren (**1**).
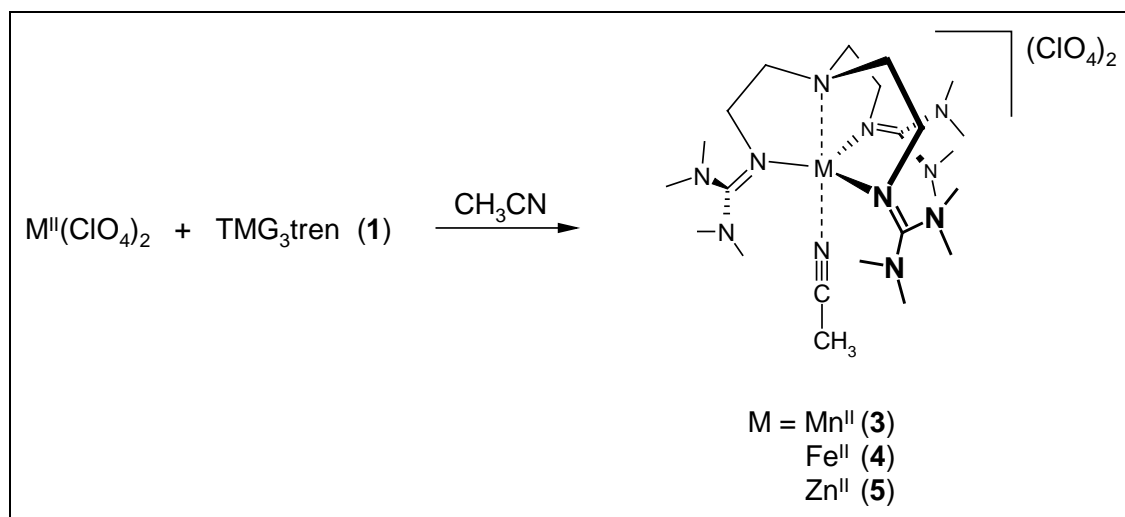
Scheme 6. Complexation of M^{2+} perchlorate salts with TMG$_3$tren.

The spectroscopic properties of the complexes resemble those of the protonated ligand (**1A**). For example, two IR absorptions are seen in the 1600 cm^{-1} IR region due to ν(C=N). The UV/Vis maxima are shifted 5 - 10 nm to lower wavelengths. While the zinc(II) complex (**5**) is diamangnetic, the manganese(II) (**2**, **3**) and iron(II) (**4**) complexes are paramagnetic with spin-only values of the order expected for d^5 and d^6 high-spin complexes[26] comparable to those of known complexes: μ_{eff}[Mn(Me$_6$tren)Br]Br: 6.01 B.M.; μ_{eff}[Fe(Me$_6$tren)Br]Br: 5.34 B.M.;[27] μ_{eff}[Mn(ntb)Cl]Cl (ntb = tris(2-benzimidazolylmethyl) amine): 5.83 B.M..[28] Their magnetic susceptibilities μ_{eff} **2**: 5.9 B.M.; μ_{eff} **3**: 5.8 B.M.; μ_{eff} **4**: 5.4 B.M.; all with an uncertainty of ± 0.1, were determined by the Evans method.[29]

Attempts to prepare well-defined complexes of **1** with Fe^{III} and Mn^{III} salts have hitherto proved unsuccessful. It seems that, due to steric repulsion, the bite of the ligand is better matched with larger ions than with smaller, highly charged ions. This interpretation is in accordance with the electrochemical results discussed below, which reveal the rapid decomposition of the oxidized iron species.

The stabilities of compounds **2-5** towards hydrolysis were examined. All the complexes were found to be sensitive to air and moisture, despite the extreme steric shielding provided by the ligand. In general, it was observed that metal hydroxides along with the protonated ligand were formed when **2-5** were exposed to aqueous solvent mixtures. These findings may be explained by the extremely high proton affinity of guanidines. Deprotonation of an aqua

ligand irreversibly induces the hydrolytic cleavage of the metal-nitrogen bond, a pattern that is also typical for amido complexes (Scheme 7).
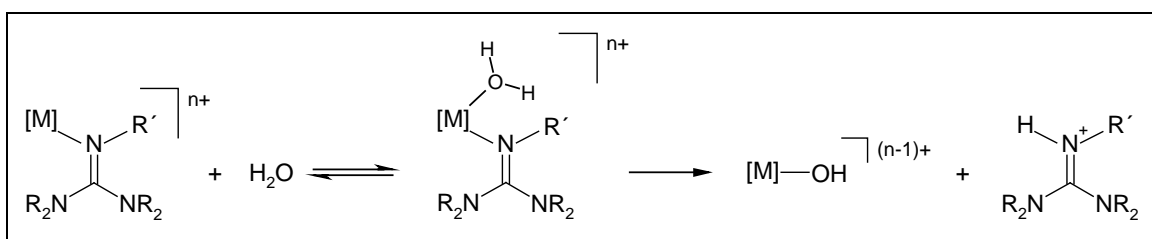
Scheme 7. Hydrolytic cleavage of the metal-nitrogen bond.

Structural Characterization

Single crystals of all the ionic complexes suitable for X-ray crystallography were grown by slow diffusion of diethyl ether into acetonitrile solutions. The results of the structure analyses are presented in Figures 1-5, while selected bond lengths and angles are collected in Table 1 and parameters relating to the data collection and refinement are listed in Tables 7 and 8. Complexes **2** (Figure 1), **3** (Figure 2), **4** (Figure 3), and **5** (Figure 4) each possess a nearly C_3 symmetric trigonal-bipyramidal molecular geometry, with the amine nitrogen atom located in one of the axial positions, and *N*-coordinated acetonitrile (**3**, **4**, **5**) or chloride ion (**2**) occupying the other.
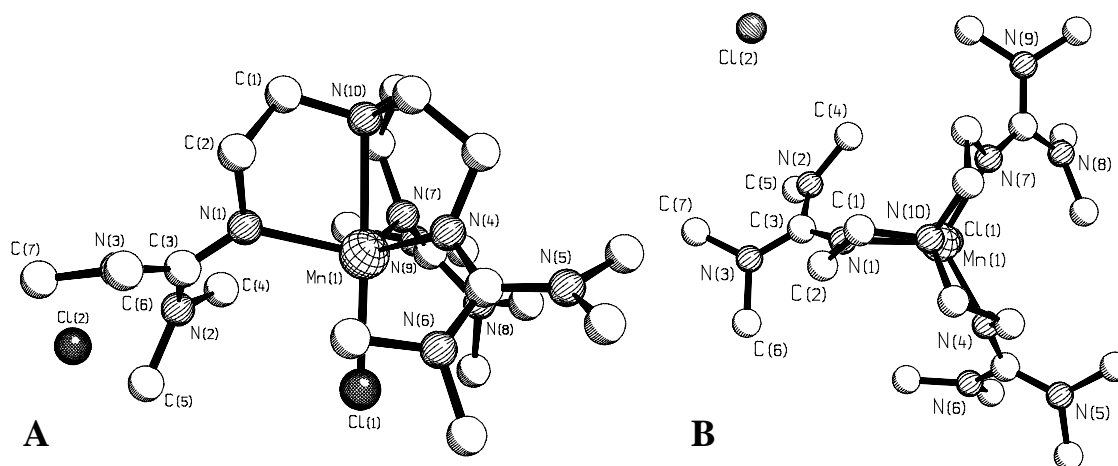
Figure 1. Molecular structure of [(TMG$_3$tren)Mn^{II}Cl]Cl (**2**) (**A**), Schakal plot of a projection along the local C_3 axis (**B**).[47]
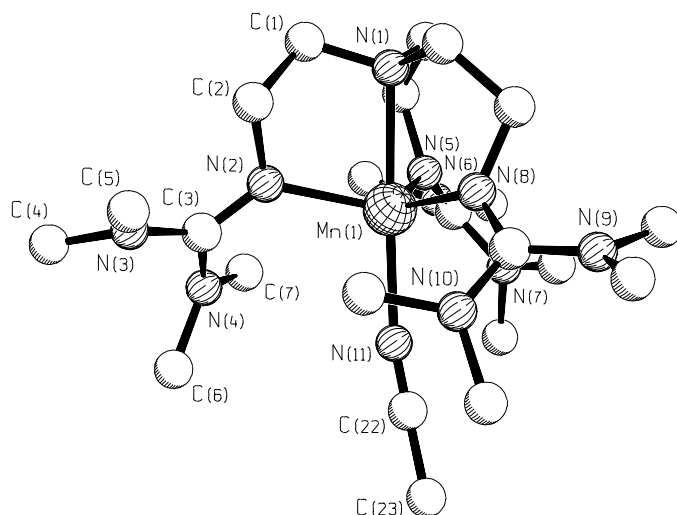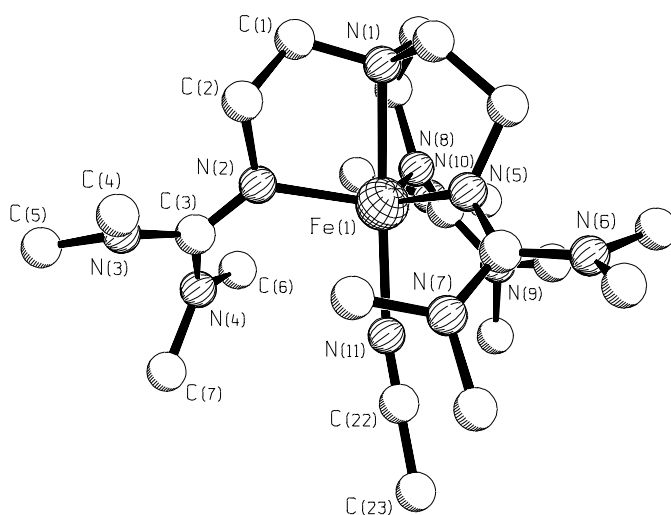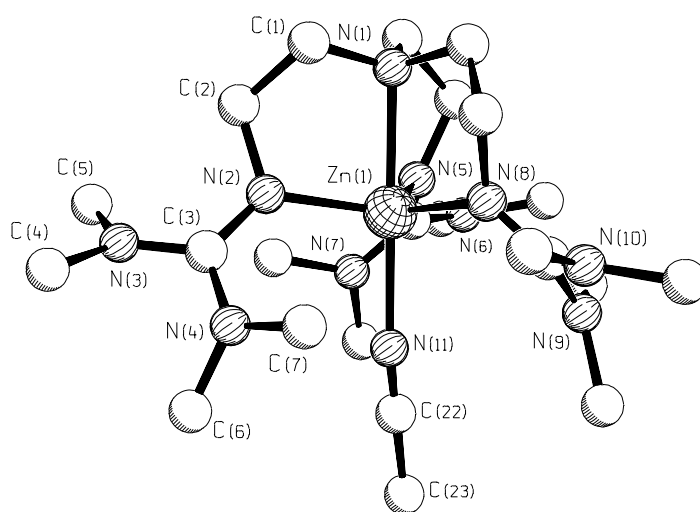
Figure 2. Molecular stucture of **3**.[47]

Figure 3. Molecular stucture of **4**.[47]

Figure 4. Molecular stucture of **5**.[47]

Table 1. Selected bond lengths [pm] and bond angles [°] in complexes **2**-**6**, with standard deviations in parentheses.

[(TMG$_3$tren)Mn^{II}Cl]Cl (**2**)					
Mn(1)-N(1)	218.2(2)	Mn(1)-N(4)	217.7(1)	Mn(1)-N(7)	219.1(2)
Mn(1)-N(10)	237.8(1)	Mn(1)-Cl(1)	243.0(1)		
∅ N$_{eq}$-Mn-N$_{eq}$	114.63(6)	∅ N$_{ax}$-Mn-N$_{eq}$	76.38(5)	N(10)-Mn(1)-Cl(1)	177.57(4)
[(TMG$_3$tren)Mn^{II}(NCMe)](ClO$_4$)$_2$ (**3**)					
Mn(1)-N(2)	212.7(3)	Mn(1)-N(5)	214.8(3)	Mn(1)-N(8)	213.1(3)
Mn(1)-N(1)	232.8(3)	Mn(1)-N(11)	221.5(3)		
∅ N$_{eq}$-Mn-N$_{eq}$	115.79(11)	∅ N$_{ax}$-Mn-N$_{eq}$	78.00(10)	N(1)-Mn(1)- N(11)	175.64(11)
[(TMG$_3$tren)Fe^{II}(NCMe)](ClO$_4$)$_2$ (**4**)					
Fe(1)-N(2)	207.3(3)	Fe(1)-N(5)	206.1(4)	Fe(1)-N(8)	208.4(4)
Fe(1)-N(1)	225.4(3)	Fe(1)-N(11)	215.1(4)		
∅ N$_{eq}$-Fe-N$_{eq}$	116.95(14)	∅ N$_{ax}$-Fe-N$_{eq}$	79.85(14)	N(1)-Fe(1)- N(11)	176.62(14)
[(TMG$_3$tren)Zn^{II}(NCMe)](ClO$_4$)$_2$ (**5**)					
Zn(1)-N(2)	203.4(2)	Zn(1)-N(5)	203.4(2)	Zn(1)-N(8)	205.1(3)
Zn(1)-N(1)	226.9(2)	Zn(1)-N(11)	218.7(3)		
∅ N$_{eq}$-Zn-N$_{eq}$	117.46(10)	∅ N$_{ax}$-Zn-N$_{eq}$	80.74(9)	N(1)-Zn(1)- N(11)	177.25(9)
[(TMG$_3$tren)Mo^{0}(CO)$_3$] (**6**)					
Mo(1)-N(1)	235.4(2)	Mo(1)-N(2)	233.6(2)	Mo(1)-N(5)	231.9(2)
Mo(1)-C(22)	193.0(3)	Mo(1)-C(23)	192.4(3)	Mo(1)-C(24)	192.4(3)
N(2)-C(3)	131.7(3)	C(3)-N(3)	136.4(4)	C(3)-N(4)	137.7(4)
N(5)-C(10)	131.1(3)	C(10)-N(6)	137.2(4)	C(10)-N(7)	137.2(4)
N(8)-C(17)	127.6(4)	C(17)-N(9)	139.6(4)	C(17)-N(10)	137.8(4)
N(1)-Mo(1)- C(23)	175.64(10)	N(2)-Mo(1)- C(24)	174.64(10)	N(5)-Mo(1)- C(22)	167.41(10)

The imino nitrogen atoms of the guanidine groups define the equatorial plane. The metal atom is slightly axially distorted from the equatorial plane towards the acetonitrile molecule. As is evident from Table 2, this deviation is accompanied by a change in ionic radius of the metal center. It also has an effect on the bond lengths between the amine and guanidine nitrogen atoms and the metal ion, whereas the distance to the acetonitrile nitrogen atom remains essentially the same. Other compounds containing Mn, Fe and Zn in similar tren

ligand coordination spheres are included in the table in order to correlate our results. However, an absolute comparison remains difficult because the ligand properties differ significantly, e.g. in terms of steric hindrance or considering the different neutral and anionic coligands which lead to different effective charges at the metal atoms and hence to different bond lengths to the equatorial nitrogen atoms.[30]

Table 2. Ionic radii of Mn, Fe and Zn; structural features of complexes **2**-**5** and literature counterparts.

Com plex	Metal atom	Ionic radius[31] [pm]	Axial distortion[a] [pm]	d (M-N$_{ax}$) [pm]	d (M-N$_{eq}$)[b] [pm]	d (M-L$_{ax}$) [pm]
A	[L^{1}Mn^{II}-Br]$^{+[32]}$	89	36	219	227	249
A´	[L^{2}Mn^{II}-Cl]$^{+[28]}$	89	63	252	216	236
B	[L^{1}Fe^{II}-Br]$^{+[32]}$	85	32	221	215	248
C	[L^{1}Zn^{II}-Br]$^{+[32]}$	82	27	219	211	245
C´	[L^{2}Zn^{II}-Cl]$^{+[33]}$	82	64	248	205	225
C´´	[L^{3}Zn^{II}-Cl]$^{+[34]}$	82	39	232	206	231
2	[(**1**)Mn^{II}-Cl]$^+$	89	51	237.8(1)	218.3(2)	243.0(1)
3	[(**1**)Mn^{II}(NCMe)]$^{++}$	89	44	232.8(3)	213.5(3)	221.5(3)
4	[(**1**)Fe^{II}(NCMe)]$^{++}$	85[c]	37	225.4(3)	207.3(4)	215.1(4)
5	[(**1**)Zn^{II}(NCMe)]$^{++}$	82	33	226.9(2)	204.0(2)	218.7(3)

[a] Distance of M from the equatorial plane defined by the three equatorial nitrogen atoms. - [b] Average distance of the three equatorial nitrogen atoms from the metal center. - [c] Average radius of Fe^{2+} for coordination numbers 4 and 6 (high spin).[31] Standard deviations in parentheses. L^1 = Me$_6$tren, L^2 = Tris(2-benzimidazolyl-methyl)amine (ntb), L^3 = H$_6$tren.

Comparing complex **2**, which bears an anionic chloro ligand, with dicationic **3**, which has a neutral acetonitrile ligand instead, the increased contraction of the TMG$_3$-tren ligand can be directly attributed to the higher effective charge at the metal center. As expected, the axial distortion decreases with decreasing ion radius of the central atom.

A comparison of **2** with [(Me$_6$tren)Mn^{II}Br]Br$^{[32]}$ (**A**) as regards the relative donor abilities of the amine and guanidine ligands is made difficult by the different steric requirements of the two ligand regimes. In the case of **1**, steric repulsion is greatest at the periphery. Since donor ability incorporates basicity and steric hindrance, the TMG$_3$tren ligand can be estimated to be

superior to Me$_6$tren in its donor ability. The guanidine sp^2-nitrogen atom is much more basic than the amine sp^3-nitrogen of Me$_6$tren and is also sterically less hindered. The net result is that the average bond length between the equatorial guanidine nitrogen atoms and the metal center is much smaller (218 pm) than the corresponding amine-metal distance in [(Me$_6$tren)Mn^{II}Br]Br (**A**) (227 pm). A stronger donor component by the equatorial guanidines is also consistent with the longer distance to the axial amine in **2** (238 pm) compared to that in the corresponding Me$_6$tren complex **A** (219 pm). In the latter donor acceptor-complex, the axial amine has to provide more electron density towards the overall charge compensation. As a consequence, the displacement of the manganese cation out of the equatorial plane is significantly greater in **2** (51 pm) compared to that in [(Me$_6$tren)Mn^{II}Br]Br (**A**) (36 pm).

A characteristic structural feature of all the complexes **2-5** is shown in Figure 1 (**B**). In order to reduce steric repulsion, the guanidine dimethylamino units are twisted by approximately 40° into a propeller-like conformation. The dimethylamino groups are not coplanar within the planar guanidine CN$_3$ unit but show out-of-plane torsion angles of 20-45° (Table 3). A similar distortion has been found for the hexamethyl guanidinium cation in its ground state.[35]

Table 3. Torsion angles [°] in complex [(TMG$_3$tren)Mn^{II}Cl]Cl (**2**).

Mn(1)-N(1)-C(3)-N(2/3)	N(1)-C(3)-N(2)-C(4/5)	N(1)-C(3)-N(3)-C(6/7)
-42.7 / 140.3	-22.4 / 139.9	-40.6 / 147.2

In spite of these steric limitations to perfect π-conjugation in the outer ligand sphere, the superbasic tripod **1** efficiently stabilizes dicationic complexes by delocalizing the charge over the three perfectly planar guanidinium cations (sum of angles in representative **2**: see Table 5).

According to a CCDC search (September 2000), no structurally characterized complexes of iron and manganese with pentacoordination by five neutral N-donor ligands have hitherto been reported. On the other hand, for d^{10} Zn^{2+},[36] Cd^{2+},[37] Ag$^+$,[38] and d^9 Cu^{2+},[39] this coordination mode is more common. Just a few representatives involving the tren ligand or its *N*-methyl derivatives and an anionic ligand have been reported, for example the halide complexes of Di Vaira et al.[32] and Templeton et al.,[34] and the pseudohalide (OCN$^-$ and SCN$^-$) investigated by Laskowski and co-workers.[40]

The Question of π-Bonding Contributions of Guanidine Ligands

Because the C=N valence vibrations of coordinated guanidines do not seem to give a reliable measure of the donor and acceptor qualities of TMG$_3$tren, we set out to synthesize a complex containing CO as a an indicator ligand for electronic interactions of the coligands. The tris(acetonitrile) complex [(CH$_3$CN)$_3$Mo(CO)$_3$] was found to react cleanly with **1** to give compound **6** in 79 % yield (Scheme 7). The IR spectrum of **6** features more than two ν(C=N) absorptions in the region 1515-1580 cm^{-1}, while in the ^{13}C NMR spectrum two resonances due to guanidine CN$_3$ moieties are observed. Complex **6** proved to be stable under atmospheric conditions for a short period of time, but ultimately turned from yellow to brown. It showed a similar sensitivity to oxidation in solution. While the TMG$_3$-tren ligand is able to displace even an anionic chloro ligand from **2**, it is incapable of displacing more than three carbon monoxide ligands from [Mo(CO)$_6$] or derivatives thereof. It bonds in a facial manner, leaving one guanidine functionality as a dangling arm. This may be taken as an indication that **1** is not a good π-acceptor, and furthermore that it is a ligand of constraint geometry, not being able to stabilize geometries other than trigonal-bipyramidal in its tripodal coordination mode. Figure 5 shows the results of a X-ray analysis of single crystals of **6** obtained from acetonitrile / diethyl ether.
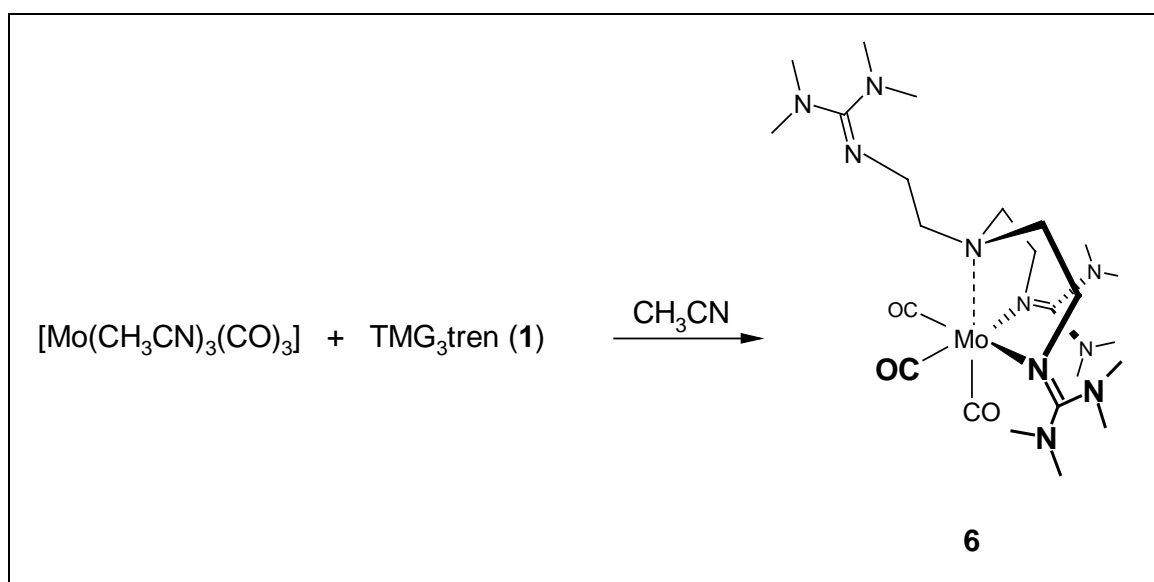
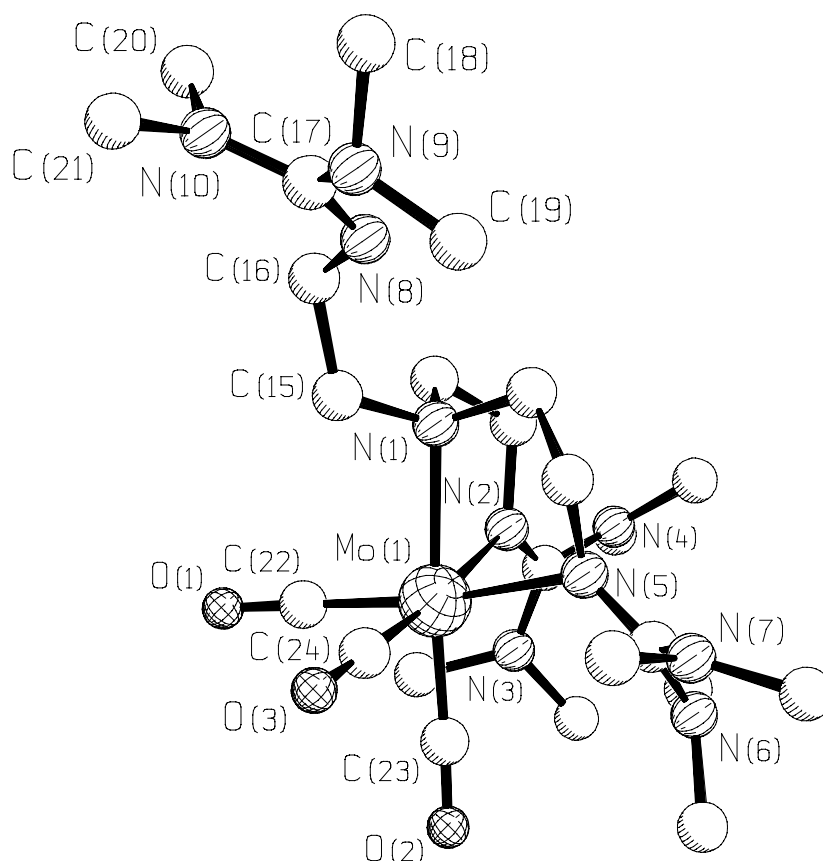Scheme 8. Facial coordination of TMG$_3$tren to [Mo(CO)$_3$] in **6**.

Figure 5. Molecular stucture of **6**.[47]

The molecule of **6** exhibits local C_s symmetry in the crystalline state with a mirror plane defined by C(15), N(1), Mo(1), C(23), and O(2). The molybdenum atom is coordinated in a distorted octahedral manner. The inner ligand core is defined by three facial carbonyl ligands, one amine, and two guanidine ligands. One dangling guanidine arm points away from the inner core. The amine is bonded with a slightly longer Mo-N(1) distance [235.4(2) pm] than the two guanidines Mo-N(2) [233.6(2) pm] and Mo(1)-N(5) [231.9(2) pm]. However, this difference in bonding is not reflected in specific bonding differences of the *trans*-CO ligands. On the other hand, a comparison of structural parameters of the closely related complexes **6** and [Mo(CO)$_3$(dien)],[41] in which *cis*-(diethylenetriamine) (dien) acts as a pure σ-donor, indicates slightly stronger donation by the guanidine ligand. Back-donation in **6** is slightly stronger; the Mo-C bonds tend to be shorter and the C-O bonds tend to be slightly longer as compared to those in the amine complex [(dien)Mo(CO)$_3$] (Table 4).

Table 4. Comparison of bond lengths in **6** and [(dien)Mo(CO)₃]; dien = *cis*-diethylenetriamine.

	6	[(dien)Mo(CO)₃][41]
$\varnothing$(Mo-N$_{amine}$) [pm]	235.4	232.3
$\varnothing$(Mo-N$_{imine}$) [pm]	232.7	-
$\varnothing$(Mo-C) [pm]	192.6	194.3
$\varnothing$(C-O) [pm]	117.8	115.3
$\varnothing$(C-Mo-C) [°]	84.8	85.3

Carbonyl stretching frequencies are often used as an additional criterion for evaluating the donor / acceptor qualities of coligands. There is no clear trend when guanidine **6** (1883 cm^{-1}) is compared to complexes of amines that act as pure σ-donors such as [(tacn)Mo(CO)₃] (1850 cm^{-1})[42] or [(dien)Mo(CO)₃] (1887 cm^{-1}).[41] On the basis of structural and IR spectroscopic evidence, it appears that there is no π-interaction between the metal center and ligand **1**.

Finally, the comparison of C-N bond lengths in guanidines, guanidinium hydrochlorides, and guanidine complexes (Lewis acid adducts) allows us to estimate the extent of electron density donation to a proton or a Lewis acid, respectively. The greater the donation, the more the imino nitrogen-carbon bond length should become equivalent to the peripheral C-NMe₂ bond lengths. In the dangling guanidine group of **6**, a short bond C-N$_{guanidine}$ bond [127.6(4) pm] and two long bonds to the peripheral C-NMe₂ groups [139.6(4) and 137.8(4) pm] are observed. The differences between these three guanidine C-N bond lengths become much smaller when the guanidine is coordinated to a Lewis acid (e.g. **2**), and become negligible upon protonation as a result of complete charge perfect delocalization (Table 5).

Table 5. Bond angle sums [°] and selected guanidine C-N distances [pm] in the non-coordinated guanidine of **6**, the coordinated guanidine in **2**, and protonated guanidine in bis(tetramethylguanidino)ethane hydrochloride.

		[(TMG$_3$tren)Mo(CO)$_3$] (**6**)			
Σ° N(8)	-	Σ° N(9/10)	344.5 / 358.8	Σ° C(17)	359.9
C(17)-N(8)	127.6(4)	C(17)-N(9)	139.6(4)	C(17)-N(10)	137.8(4)
		[(TMG$_3$tren)Mn^{II}Cl]Cl (**2**)			
Σ° N(1)	359.4	Σ° N(2/3)	357.8 / 359.6	Σ° C(3)	359.9
C(3)-N(1)	131.9(2)	C(3)-N(2)	135.5(2)	C(3)-N(3)	136.9(2)
		TMG$_2$en · 2 HCl [11a]			
Σ° N(3)	358.1	Σ° N(1/2)	359.9 / 359.9	Σ° C(5)	360.0
C(5)-N(3)	133.6(2)	C(5)-N(1)	134.2(2)	C(5)-N(2)	133.8(2)

Cyclic Voltammetric Measurements

In order to gain additional information about the synthesized compounds, cyclic voltammetry experiments were carried out. A reversible Mn$^{+3/+2}$ couple could be observed for **2** ($E_{1/2}$ = +0.47 V, $\Delta E_{1/2}$ = 0.11 V, i_a / i_c = 1), along with an additional wave ($E_{1/2}$ = +0.92 V, $\Delta E_{1/2}$ = 0.22 V, i_a / i_c = 4) for the couple Mn$^{+4/+3}$. The latter was irreversible, pointing to rapid decomposition of the oxidized species (Figure 7).
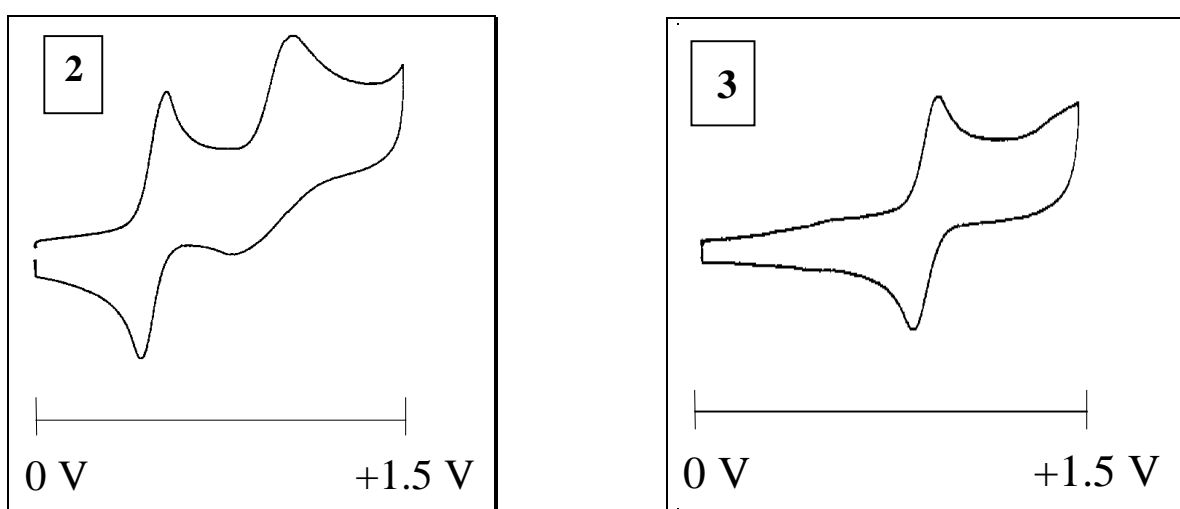

Figure 6. Cyclic voltammograms of **2** and **3** (CH$_3$CN / TBAP, 2 mm glassy carbon / SCE / Pt, ν = 100 mV s^{-1}, 20 °C).

Compound **3** shows only a single wave in the anodic region at $E_{1/2} = +0.88$ V ($\Delta E_{1/2} = 0.09$ V, $i_a / i_c = 1$) corresponding to the reversible couple Mn$^{+3/+2}$. The Mn$^{II} \rightarrow$ Mn^{III} transition for compound **2** was found to occur at a lower oxidation potential than the corresponding step for **3** owing to the presence of the anionic chloro ligand, which facilitates the oxidation of **2**. The oxidation potential of Mn$^{III} \rightarrow$ Mn^{IV} does not lie in the window of 0 to 1.5 V.
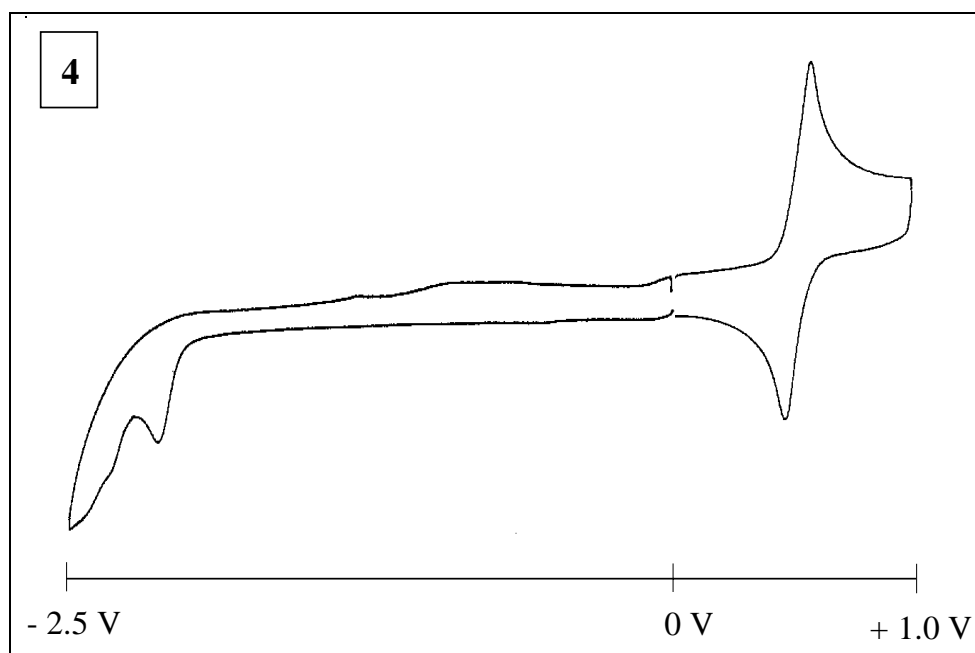
Figure 7. Cyclic voltammogram of **4** (CH$_3$CN / TBAP, 2 mm glassy carbon / SCE / Pt, $\nu = 100$ mV s^{-1}, 20 °C).

Complex **4** displays a potential of $E_{1/2} = +0.52$ V ($\Delta E_{1/2} = 0.11$ V) for the Fe$^{II} \rightarrow$ Fe^{III} electron transfer, $i_a / i_c = 1$ (Figure 8). The irreversible wave in the cathodic region (-2.09 V) can only cautiously be assigned to an Fe$^{II} \rightarrow$ Fe^{I} reduction because of its low intensity and position near the border of the electrochemical window.

The values of the normal potentials can only be compared indirectly due to the different recording conditions (solvent, temperature) but can still be used to draw qualitative conclusions. All the complexes display lower oxidation potential compared to the redox potentials of the aqua complexes Mn (II $\rightarrow$ III): +1.54 V; Fe (II $\rightarrow$ III): +0.77 V[43] as a result of the electron-donating TMG$_3$tren ligand. As expected, the monocationic complex **2** is more easily oxidized than the dicationic compound **3** (Table 6).

16

Table 6. Selected redox potentials.

Metal complex	$E_{1/2}$[43] [V]
[Mn(H$_2$O)$_6$]$^{2+}$ (+3/+2)[a]	+1.54
[(**1**)Mn(NCMe)]$^{2+}$ (+3/+2)[b]	+0.88
[(**1**)Mn-Cl]$^+$ (+3/+2)[b]	+0.47
[Fe(H$_2$O)$_6$]$^{2+}$ (+3/+2)[a]	+0.77
[(**1**)Fe(NCMe)]$^{2+}$ (+3/+2)[b]	+0.52

[a] Recorded in H$_2$O. - [b] Recorded in MeCN.

Besides the inherent donor abilities of a ligand, steric factors cannot be neglected with regard to the resulting oxidation potential and stability of the oxidized species.[44] This statement is related to the investigations of Ray[45] and Schrock,[46] who commented on the oxidation potentials of various transition metal complexes with tren-like amido ligands possessing varying degrees of steric strain. We believe that the instability of our oxidized complexes is due to the steric strain of the ligand periphery imposed by the reduced radius of the cation in its oxidized form.

Conclusions

Peralkyloligoguanidines are an unexplored class of mulitdentate nitrogen ligands within the large family chelating N-donors typically containing amines, imines (Schiff bases), and azaaromatic building blocks. The novel tripod ligand TMG$_3$tren (**1**), a derivative of tren with three superbasic pentaalkylguanidine donor functions and a geometry constrained to coordinate metal ions only in a trigonal-bipyramidal mode, has been introduced. Due to its ability to delocalize positive charge over the three guanidinium moieties, **1** stabilizes cationic and even dicationic complexes, which are not so common for the corresponding parent compounds with tren ligands. However, increasing steric strain on the ligand periphery as a consequence of the decreased ionic radii of highly oxidized metal cations seems to limit the stability of such high-valent species. Initial evidence that larger cations are coordinated more favourably than smaller ones was provided by the bite angle and steric constraints of the tripodal ligand sphere of **1**. Our current interest is focused on the Lewis acid activation of small molecules other than acetonitrile and their transformations in the molecular pocket imposed by the guanidine ligand environment. Furthermore, we are extending our investigation of this class of ligands to other metals and other guanidine building blocks.

Experimental Section

Materials and methods:

All experiments were carried out in glassware that was assembled while hot and cooled under inert atmosphere of argon 4.8 dried with P_4O_{10} granulate. Solvents were purified according to literature procedures and were also kept under inert gas. Tris(2-aminoethyl)amine and the metal salts were used as purchased from Fluka. Triethylamine was freshly distilled and stored under argon prior to use. Substances sensitive to moisture and air were kept in nitrogen-flushed glove-box (Braun, Type MB 150 BG-I). - Spectra were recorded with the following spectrometers: - NMR: Bruker AM 400 (^{13}C: gated-decoupled), - IR: Bruker IFS 88 FT, - MS(EI, 70 eV): Varian MAT CH-7a, Elemental Analysis: Heraeus CHN-Rapid, Melting points: Büchi MP B-540 (uncorrected), X-ray crystallography: ENRAF-Nonius CAD4 and Siemens P4, - Magnetic susceptibility: Evans-method.[29]

Electrochemical Measurements: Cyclic voltammetry (CV) was performed with electrochemical equipment from AMEL (Milano) consisting of a Model 552 potentiostat, Model 563 multipurpose unit, Nicolet Model 3091 storage oscilloscope and Kipp & Zonen Model BD 90 x / y recorder. The electrochemical cell was operated under argon, with glassy carbon, platinum rod, and saturated calomel (SCE) serving as working, counter, and reference electrodes, respectively. For temperature control the cell was immersed in a thermostated cooling bath. CV curves were obtained at a scan rate of 100 mV s^{-1} working at 20 °C in MeCN / 0.1 M nBu$_4$NClO$_4$.

Caution! Phosgene is a severe toxic agent that can cause pulmonary embolism and in case of heavy exposition may be lethal. It should only be used in a well-ventilated fume hood. Perchlorate salts are potentially explosive and should be handled with care.

Tetramethylchlorformamidiniumchloride:[19]

In a flask fitted with a reflux condenser cryostatted at -30 °C, phosgene was passed through a solution of tetramethylurea (50.00 g, 430 mmol) in toluene (200 mL) kept at 0 °C for 2 h. The phosgene inlet was then closed and the solution is allowed to warm to room temperature under stirring for a period of 24 h, with the reflux condensor being maintained at -30 °C. The precipitate formed was collected by filtration, washed three times with dry diethyl ether and, dried in vacuo. Yield: ca. 95 %.

1,1,1-Tris{2-[N^2-(1,1,3,3-tetramethylguanidino)]ethyl}amine (1):

To a solution of tris(2-aminoethyl)amine (14.62 g, 100 mmol) and triethylamine (30.36 g, 41.6 mL, 300 mmol) in acetonitrile (50 mL), a solution of [(Me$_2$N)$_2$CCl]Cl (51.32 g, 300 mmol) in acetonitrile (150 mL) was slowly added under cooling in an ice bath. After the exothermic reaction had occurred, the mixture was refluxed for 3 h, in the course of which a clear solution was produced. NaOH (12.00 g, 300 mmol) in water (30 mL) was subsequently added under vigorous stirring in order to deprotonate the NEt$_3$HCl. After evaporation of the solvents and excess NEt$_3$, TMG$_3$tren (**1**) was obtained by deprotonation of **1A** [tris(hydrochloride)] with 50 % KOH (50 mL) and extracting the aqueous phase MeCN (3 × 50 mL). The combined extracts were concentrated to dryness and the residue was taken up in warm hexane. The resulting solution was dried with MgSO$_4$, stirred with activated charcoal while still warm to eliminate impurities, and then filtered through Celite. Finally, removal of the solvent and drying of the residue in vacuo gave TMG$_3$tren (**1**) as yellow oil that crystallized upon standing in 86 % yield (38.03 g, 86.3 mmol).

M.p.: 59-60 °C; ^{1}H NMR (200.1 MHz, CDCl$_3$, 25 °C, CDCl$_3$): δ = 3.23 (m, 6 H, CH$_2$), 2.84-2.59 (m, 42 H, CH$_2$+CH$_3$) ppm; ^{13}C NMR (50.3 MHz, CDCl$_3$, 25 °C, CDCl$_3$): δ = 160.37 (CN$_3$), 58.18, 48.35 (CH$_2$), 39.61, 38.84 (CH$_3$) ppm; IR (Film): $\tilde{\nu}$ = 2880 s, 2839 sh, 1620 s [ν(C=N)], 1495 m, 1453 w, 1364 s, 1236 w, 1130 m, 1062 w, 989 w cm^{-1}; UV/Vis (MeCN): λ_{max} (ε) = 216 nm (24000 mol^{-1} dm^3 cm^{-1}); MS (EI, 70 eV): m/z (%) = 439.0 (1) [M–H]$^+$, 312.0 (100) [C$_{15}$H$_{34}$N$_7$]$^+$, 210.0 (73) [C$_{11}$H$_{22}$N$_4$]$^+$, 142.0 (43) [C$_7$H$_{16}$N$_3$]$^+$, 128.0 (54) [C$_6$H$_{14}$N$_3$]$^+$, 85.0 (82) [C$_4$H$_9$N$_2$]$^+$, 72.0 (26) [C$_3$H$_8$N$_2$]$^+$, 58.0 (80) [C$_2$H$_6$N$_2$]$^+$; elemental analysis calcd. (%) for C$_{21}$H$_{48}$N$_{10}$ (440.7): C 57.24, H 10.98, N 31.78; found C 56.87, H 10.83, N 31.45.

1,1,1-Tris-{2-[N^2-(1,1,3,3-tetramethylguanidinium)]ethyl}amine Trichloride (1A; 1 × 3 HCl):

The Hydrochloride salt could be obtained by treating the free oligoguanidine base (0.57 g, 1.13 mmol) dissolved in EtOH (10 mL) with the requisite amount of 1 M HCl (3.5 mL). Recrystallization from EtOH/Et$_2$O gave strongly hygroscopic, colorless crystals that analyzed as the trihydrate. Yield 0.51 g (0.84 mmol, 74 %). Following our synthesis of **1**, the TMG$_3$tren tris(hydrochloride) **1A** could also be obtained without isolation of the free base. After deprotonation of NEt$_3$HCl with an equimolar amount of NaOH dissolved in the minimum volume of water and removing all volatiles in vacuo, the crude tris(hydrochloride) was redissolved in warm MeCN. The resulting solution was dried with MgSO$_4$, treated with

activated charcoal, passed through Celite, and the solvent was evaporated. The residue was washed with dry diethyl ether and dried in vacuo to yield the tris(hydrochloride) **1A** as a colorless, strongly hygroscopic solid analyzed as the trihydrate.

M.p. 153 °C (dec.); ^{1}H NMR (200.1 MHz, CD$_3$CN, 25 °C, CD$_3$CN): δ = 8.91 (s, br, 3 H, NH), 3.76 (br, 12 H, CH$_2$), 2.92 (s, 36 H, CH$_3$), 2.55 (br, 6 H, H$_2$O) ppm; ^{13}C-NMR (50.3 MHz, CD$_3$CN, 25 °C, CD$_3$CN): δ = 161.31 (CN$_3$), 51.70 (CH$_2$), 39.51 (CH$_3$), 39.35 (CH$_2$) ppm; IR (KBr): $\tilde{v}$ = 3431 s, 1627 s, 1584 s [v(C=N)], 1457 m, 1406 s, 1311 w, 1233 w, 1176 w, 1136 w, 1067 w, 900 m, 668 m(br) cm^{-1}; UV/Vis (H$_2$O): λ_{max} (ε) = 213 nm (34000 mol^{-1} dm^3 cm^{-1}); MS (EI, 70 eV): m/z (%) = 440.0 (1) [M–3HCl]$^+$, 312.0 (95) [C$_{15}$H$_{34}$N$_7$]$^+$, 255.0 (28) [C$_{12}$H$_{27}$N$_6$]$^+$, 222.0 (17) [C$_{10}$H$_{18}$N$_6$]$^+$, 210.0 (67) [C$_{11}$H$_{22}$N$_4$]$^+$, 197.0 (28) [C$_{10}$H$_{21}$N$_4$]$^+$, 142.0 (91) [C$_7$H$_{16}$N$_3$]$^+$, 128.0 (94) [C$_6$H$_{14}$N$_3$]$^+$, 97.0 (45) [C$_6$H$_{11}$N]$^+$, 85.0 (94) [C$_4$H$_9$N$_2$]$^+$, 71.0 (64) [C$_3$H$_7$N$_2$]$^+$, 58.0 (95) [C$_2$H$_6$N$_2$]$^+$, 36.0 (100) [HCl]$^+$; elemental analysis calcd. (%) for C$_{21}$H$_{51}$Cl$_3$N$_{10}$ × 3 H$_2$O (604.1): C 41.75, H 9.51, N 23.19; found C 41.69, H 9.86, N 22.83.

General Procedure for the synthesis of the TMG$_3$tren complexes:

The metal salts were first dehydrated by the orthoester method.[25] Thus, the hydrated salts were stirred in dry EtOH containing twice the molar amount, with respect to water present in the salt, of triethyl orthoformate at 60 °C for 1 h. Equimolar amounts of the dehydrated metal salt and **1** were separately dissolved in 5 mL portions of dry MeCN under argon. These solutions were then combined and the resulting mixture was stirred for 30 min. at 40-50 °C, filtered through Celite, and concentrated to a volume of ca. 3 mL. The complex was then precipitated by the addition of 10 mL dry diethyl ether, washed with absolute diethyl ether, and dried in vacuo. Single crystals suitable for X-ray analysis could be grown by slow diffusion of diethyl ether into the respective acetonitrile solutions.

Chloro{1,1,1-tris-[N^2-(1,1,3,3-tetramethylguanidino)ethyl]amine}manganese(II) Chloride (2):

The general procedure was followed using MnCl$_2$ (0.15 g, 1.12 mmol) and **1** (0.66 g, 1.15 mmol). Yield: 0.59 g (1.04 mmol) 93 % as colorless crystals.

M.p. 230 °C (dec.); IR (KBr): $\tilde{v}$ = 2947 m, 2881 m, 1618 s, 1573 s [v(C=N)], 1553 vs, 1427 m, 1395 m, 1342 w, 1164 sh, 1151 s, 1075 m, 891 m, 764 m cm^{-1}; UV/Vis (MeCN): λ_{max} (ε) = 226 nm (49000 mol^{-1} dm^3 cm^{-1}); MS (EI, 70 eV): m/z = 312.0 (60) [C$_{15}$H$_{34}$N$_7$]$^+$, 210.0 (33)

[C$_{11}$H$_{22}$N$_4$]$^+$, 142.0 (32) [C$_7$H$_{16}$N$_3$]$^+$, 128.0 (43) [C$_6$H$_{14}$N$_3$]$^+$, 85.0 (100) [C$_4$H$_9$N$_2$]$^+$, 71.0 (31) [C$_3$H$_7$N$_2$]$^+$, 58.0 (74) [C$_2$H$_6$N$_2$]$^+$, 28.0 (80) [CH$_2$N]$^+$; μ$_{eff}$ (Evans method, 5 % [D$_6$]-benzene in CD$_3$CN, 25 °C): μ_B/mol = 5.9 ± 0.1; CV (MeCN / TBAP, 2 mm GC / SCE / Pt, ν = 100 mV s^{-1}, 20 °C): $E_{1/2}$ (+3/+2) 0.47 V, $\Delta E_{1/2}$ (+3/+2) 0.11 V, $I_{pa/pc}$ 1, $E_{1/2}$ (+4/+3) 0.92 V, $\Delta E_{1/2}$ (+4/+3) 0.22 V, $I_{pa/pc}$ 4; elemental analysis calcd. (%) for C$_{21}$H$_{48}$Cl$_2$N$_{10}$Mn (566.5): C 44.52, H 8.54, N 24.72; found C 44.06, H 8.53, N 23.73.

Acetonitrile(1,1,1-tris{2-[N^2-(1,1,3,3-tetramethylguanidino)]ethyl}amine)manganese(II)-Diperchlorate (3):

The general procedure was followed using Mn(ClO$_4$)$_2$ (0.47 g, 1.86 mmol) and **1** (0.84 g, 1.90 mmol). Yield: 1.30 g (1.77 mmol) 95 % as colorless crystals.

IR (KBr): $\tilde{\nu}$ = 2893 m, 2275 w [ν(C≡N)], 1616 sh, 1565 vs, 1535 s [ν(C=N)], 1463 m, 1427 m, 1398 s, 1346 w, 1257 w, 1164 m, 1092 vs [ν(Cl=O)], 906 w, 892 w, 769 m, 624 s cm^{-1}; MS (EI, 70 eV): m/z (%) = 128.0 (24) [C$_6$H$_{14}$N$_3$]$^+$, 85.0 (100) [C$_4$H$_9$N$_2$]$^+$, 71.0 (25) [C$_3$H$_7$N$_2$]$^+$, 44.0 (46) [C$_2$H$_6$N]$^+$; μ$_{eff}$ (Evans method, 5 % [D$_6$]-benzene in CD$_3$CN, 25 °C): μ_B/mol = 5.8 ± 0.1; CV (MeCN / TBAP, 2 mm GC / SCE / Pt, ν = 100 mV s^{-1}, 20 °C): $E_{1/2}$ (+3/+2) 0.88 V, $\Delta E_{1/2}$ (+3/+2) 0.09 V, $I_{pa/pc}$ 1; elemental analysis calcd. (%) for C$_{23}$H$_{51}$Cl$_2$MnN$_{11}$O$_8$ (735.6): C 37.56, H 6.99, N 20.95; found C 37.42, H 6.95, N 20.62

Acetonitrile(1,1,1-tris{2-[N^2-(1,1,3,3-tetramethylguanidino)]ethyl}amine)iron(II)-Diperchlorate (4):

The general procedure was followed using Fe(ClO$_4$)$_2$ (0.32 g, 1.26 mmol) and **1** (0.57 g, 1.30 mmol). Yield: 0.83 g (1.13 mmol) 89 % as light yellow crystals.

IR (KBr): $\tilde{\nu}$ = 2893 m, 2270 w [ν(C≡N)], 1614 sh, 1558 vs, 1533 sh [ν(C=N)], 1463 m, 1427 m, 1399 s, 1346 m, 1257 w, 1166 m, 1090 vs [ν(Cl=O)], 908 w, 894 m, 772 m, 623 s cm^{-1}; μ$_{eff}$ (Evans method, 5 % [D$_6$]-benzene in CD$_3$CN, 25 °C): μ_B/mol = 5.4 ± 0.1; CV (MeCN / TBAP, 2 mm GC / SCE / Pt, ν = 100 mV s^{-1}, 20 °C): $E_{1/2}$ (+3/+2) 0.52 V, $\Delta E_{1/2}$ (+3/+2) 0.11 V, $I_{pa/pc}$ 1, $E_{1/2}$ (+2/+1) - 2.09 V; elemental analysis calcd. (%) for C$_{23}$H$_{51}$Cl$_2$FeN$_{11}$O$_8$ (736.5): C 37.51, H 6.98, N 20.92; found C 36.90, H 7.03 ,N 20.52.

Acetonitrile(1,1,1-tris{2-[N^2-(1,1,3,3-tetramethylguanidino)]ethyl}amine)zinc(II)-Diperchlorate (5):

The general procedure was followed using Zn(ClO$_4$)$_2$ (0.41 g, 1.54 mmol) and **1** (0.71 g, 1.60 mmol). Yield: 0.96 g (1.29 mmol) 84 % as colorless crystals.

^{1}H NMR (200.1 MHz, CDCl$_3$, 25 °C, CDCl$_3$): δ = 3.02-2.77 (m, br, 48 H, CH$_3$+CH$_2$), 2.04 (s, 3 H, NCCH$_3$) ppm; ^{13}C NMR (50.3 MHz, CDCl$_3$, 25 °C, CDCl$_3$): δ = 165.95 (CN$_3$), 53.84 (CH$_2$), 46.59 (CH$_2$), 39.35 (CH$_3$) ppm; IR (KBr): $\tilde{v}$ = 2948 w, 2894 w, 2251 w [v(C≡N)], 1620 sh, 1571 s, 1555 s [v(C=N)], 1463 w, 1427 m, 1398 s, 1348 w, 1250 w, 1165 m, 1146 m, 1096 vs [v(Cl=O)], 894 w, 766 w, 625 m cm^{-1}; MS (EI, 70 eV): *m/z* (%) = 85.0 (100) [C$_4$H$_9$N$_2$]$^+$, 71.0 (33) [C$_3$H$_7$N$_2$]$^+$, 44.0 (60) [C$_2$H$_6$N]$^+$; elemental analysis calcd. (%) for C$_{23}$H$_{51}$Cl$_2$N$_{11}$O$_8$Zn (746.0): C 37.03, H 6.89, N 20.65; found C 36.88, H 7.09, N 20.53.

Tricarbonyl(*fac*-tris{2-[N^2-(1,1,3,3-tetramethylguanidino)]ethyl}amine)molybdenum(0) (6):

The general procedure was followed using [Mo(CH$_3$CN)$_3$(CO)$_3$] (0.42 g, 1.40 mmol) and **1** (0.88 g, 2.00 mmol). Yield: 0.689 g (1.11 mmol) 79 % as yellow powder.

^{1}H NMR (300.1 MHz, CD$_3$CN, 25 °C, CD$_3$CN): δ = 3.50 (m, 2 H, CH$_2$), 3.16 (m, 6 H, CH$_2$), 2.70 (m, 40 H, CH$_3$+CH$_2$) ppm; ^{13}C NMR (75.5 MHz, CD$_3$CN, 25 °C, CD$_3$CN): δ = 232.71, 230.11 (CO), 166.54 (CN$_3$, coordinated TMG), 160.82 (CN$_3$, free TMG), 66.08, 57.19, 50.70, 46.20 (CH$_2$), 39.79, 39.33 (CH$_3$) ppm; IR (KBr): $\tilde{v}$ = 2889 s, 1883 s, 1740 vs, 1730 sh [v(C=O)], 1619 s, 1577 s, 1553 sh, 1515 s [v(C=N)], 1455 m, 1424 w, 1390 s, 1236 m, 1142 m, 1060 w, 1026 w, 976 w, 895 w, 763 w cm^{-1}; MS (EI, 70 eV): *m/z* (%) = 621.0 (1) [*M*]$^+$, 594.0 (2) [*M*−CO]$^+$, 312.0 (98) [C$_{15}$H$_{34}$N$_7$]$^+$, 255.0 (17) [C$_{11}$H$_{25}$N$_7$]$^+$, 210.0 (52) [C$_{11}$H$_{22}$N$_4$]$^+$, 142.0 (60) [C$_7$H$_{16}$N$_3$]$^+$, 128.0 (64) [C$_6$H$_{14}$N$_3$]$^+$, 101.0 (40) [C$_5$H$_{13}$N$_2$]$^+$, 85.0 (96) [C$_4$H$_9$N$_2$]$^+$, 72.0 (53) [C$_3$H$_8$N$_2$]$^+$, 58.0 (100) [C$_2$H$_6$N$_2$]$^+$, 44.0 (37) [C$_2$H$_6$N]$^+$, 28.0 (72) [CH$_2$N]$^+$; elemental analysis calcd. (%) for C$_{21}$H$_{48}$MoN$_{10}$O$_3$ (620.7): C 46.45, H 7.80, N 22.57, found C 45.89, H 8.07, N 22.29.

Table 7. Crystal data and details of the structure refinement for **2**, **3**, and **4**.

Complex	[(**1**)Mn^{II}Cl]Cl (**2**)	[(**1**)Mn^{II}(NCMe)] (ClO$_4$)$_2$ (**3**)	[(**1**)Fe^{II}(NCMe)] (ClO$_4$)$_2$ (**4**)
Empirical formula	C$_{21}$H$_{48}$Cl$_2$MnN$_{10}$	C$_{23}$H$_{51}$Cl$_2$MnN$_{11}$O$_8$	C$_{23}$H$_{51}$Cl$_2$FeN$_{11}$O$_8$
Molecular mass [g mol^{-1}]	607.59	735.59	736.50
Temperature [K]	223(2)	198(2)	198(2)
Crystal system	triclinic	monoclinic	monoclinic
Space group	P$\bar{1}$	P2$_1$/c	P2$_1$/c
a [pm]	1174.6(3)	1619.1(1)	1614.4(1)
b [pm]	1227.4(2)	1333.6(1)	1329.3(1)
c [pm]	1298.1(2)	1651.1(1)	1641.7(1)
α [°]	92.451(9)	90	90
β [°]	96.182(10)	94.669(10)	94.460(10)
γ [°]	117.907(10)	90	90
Volume [Å^3]	1635.1(5)	3553.1(5)	3512.7(4)
Z	2	4	4
ρ [Mgm^{-3}]	1.234	1.375	1.393
μ [mm^{-1}]	0.598	0.580	0.640
F(000)	650	1556	1560
Crystal size [mm^3]	0.40 x 0.30 x 0.20	0.39 x 0.33 x 0.15	0.28 x 0.21x 0.10
Diffractometer	Siemens P4	Enraf Nonius CAD4	Enraf Nonius CAD4
Scan technique	ω-scan	ω-scan	ω-scan
θ-range for data collection [°]	1.89...27.71	2.48...24.99	3.06...24.98
Index ranges	0≤h≤13, -14≤k≤14, -14≤l≤14	0≤h≤19, 0≤k≤15, -19≤l≤19	-19≤h≤0, -15≤k≤0, -19≤l≤19
Reflections collected	5996	6462	6379
Independent refl.	5720	6227	6150
R_{int}	0.0461	0.0169	0.0309
Observed reflections [$F \geq 4\sigma(F)$]	5230	5272	3741
Data/restraints/ parameters	5720/0/ 366	6227/0/ 430	6150/0/ 430
Goodness of fit on F^2	1.033	1.106	1.032
$R1$ [$F_0 \geq 4\sigma(F)$][a]	0.0327	0.0487	0.0599
wR$_2$ (all data) [a]	0.0916	0.1655	0.1490
Transmission (min./max.)	0.8898 / 0.7959	0.9181 / 0.0855	0.9388 / 0.8412
Largest diff. Peak and hole [eÅ^{-3}]	0.364 / -0.316	0.532 / -0.448	0.529 / -0.364

[a] $R_1 = \Sigma||F_0|-|F_c||/\Sigma|F_0|$; wR$_2 = \{\Sigma[w(F_0^2 - F_c^2)^2]/\Sigma[w(F_0^2)^2]\}^{1/2}$.

Table 8. Crystal data and details of the structure refinement for **5** and **6**.

Complex	[(**1**)Zn^{II}(NCMe)](ClO$_4$)$_2$	[(**1**)Mo^0(CO)$_3$]
	(**5**)	(**6**)
Empirical formula	C$_{23}$H$_{51}$Cl$_2$N$_{11}$O$_8$Zn	C$_{21}$H$_{48}$MoN$_{10}$O$_3$
Molecular mass [g mol^{-1}]	746.02	661.72
Temperature [K]	193(2)	223(2)
Crystal system	monoclinic	triclinic
Space group	P2$_1$/c	P$\bar{1}$
a [pm]	1618.2(10)	1006.0(2)
b [pm]	1320.4(9)	1259.5(2)
c [pm]	1634.3(6)	1529.3(2)
α [°]	90	66.470(12)
β [°]	94.63(4)	75.237(9)
γ [°]	90	76.840(15)
Volume [Å^3]	3481(3)	1700.3(5)
Z	4	2
ρ [Mgm^{-3}]	1.424	1.292
μ [mm^{-1}]	0.918	0.429
F(000)	1576	700
Crystal size [mm^3]	0.25 x 0.25 x 0.25	0.45 x 0.35 x 0.25
Diffractometer	Enraf Nonius CAD4	Siemens P4
Scan technique	ω-scan	ω-scan
θ-range for data collection [°]	2.30...26.01	1.78...25.04
Index ranges	-19≤h≤19, -16≤k≤0, 0≤l≤20	0≤h≤11, -13≤k≤13, -14≤l≤14
Reflections collected	7086	5789
Independent refl.	6834	5483
R_{int}	0.0194	0.0281
Observed reflections [$F \geq 4\sigma(F)$]	5251	4982
Data/restraints/ parameters	6834/0/ 418	5483/0/ 403
Goodness of fit on F^2	1.038	1.010
$R1$ [$F_0 \geq 4\sigma(F)$][a]	0.0418	0.0334
wR$_2$ (all data) [a]	0.1192	0.0907
Transmission (min./max.)	0.8030 / 0.8030	0.9004 / 0.8305
Largest diff. Peak and hole [eÅ^{-3}]	0.595 / -0.537	0.722 / -0.619

[a] $R_1 = \Sigma||F_0|-|F_c||/\Sigma|F_0|$; wR$_2 = \{\Sigma[w(F_0^2-F_c^2)^2]/\Sigma[w(F_0^2)^2]\}^{1/2}$.

X-ray structure analysis: Crystal data and experimental conditions are listed in Tables 7 and 8. The molecular structures are illustrated as Schakal[47] plots in Figures 1-6. Selected bond lengths and angles with standard deviations in parentheses are presented in Table 1. Intensity data were collected with graphite monochromated Mo$_{K\alpha}$ radiation (λ = 71.069 pm). The collected reflections were corrected for Lorentz and polarization effects. Structures **2**, **5** and **6** were solved by direct methods and refined by full matrix least squares methods on F^2, while **3** and **4** were solved with SIR92.[48] Hydrogen atoms were calculated and isotropically refined except for those of H23A, B, C of **3** and **4**, which were found and then isotropically refined. An empirical absorption correction based on the psi-scans of 9 reflections (T_{min} = 0.4508, T_{max} = 0.5098) was performed for **4**.[49]

References

[1] a) G. Wieland, G. Simchen, *Liebigs Ann. Chem.* **1985**, 2178-2193; b) D. H. R. Barton, J. D. Elliot, S. D. Géro, *J. Chem. Soc., Perkin Trans. I* **1982**, 2085-2090; c) D. H. R. Barton, J. K. Kervagoret, S. Z. Zard, *Tetrahedron* **1990**, *46*, 7587-7598.

[2] a) P. A. S. Smith in *The Chemistry of Open-Chain Organic Nitrogen Compounds: Vol. 1*, W. A. Benjamin Inc. New York, **1965**, pp. 277-290, b) Y. Yamamoto, S. Kojima in *The Chemistry of Amidines and Imidates, Vol. 2*, J. Wiley & Sons, Chichester, **1991**, pp. 485-526; c) R. Schwesinger, *Nachr. Chem. Tech. Lab.* **1990**, *38*, 1214-1226.

[3] H. Dugas, C. Penney in *Bioorganic Chemistry*, Springer, New York, **1981**, p. 15.

[4] representative examples: a) M. S. Muche, M. W. Göbel, *Angew. Chem.* **1996**, *108*, 2263-2265; *Angew. Chem. Int. Ed. Engl.* **1996**, *35*, 2126-2129 and references cited; b) G. Deslongchamps, A. Galán, J. de Mendoza, J. Rebek, Jr., *Angew. Chem. Int. Ed. Engl.* **1992**, *31*, 61-63 and references cited.

[5] E. M. A. Ratilla, B. K. Scott, M. S. Moxness, N. M. Kostic, *Inorg. Chem.* **1990**, *29*, 918-926.

[6] a) A. Hessler, O. Stelzer, H. Dibowski, K. Worm, F. P. Schmidtchen, *J. Org. Chem.* **1997**, *62*, 2362-2369; b) F. P. Schmidtchen, M. Berger, *Chem. Rev.* **1997**, *97*, 1609-1646.

[7] a) P. D. Beer, D. K. Smith, *Prog. Inorg. Chem.* **1997**, *46*, 1-96; b) J. S. Albert, M. W. Peczuh, A. D. Hamilton, *Bioorg. Med. Chem.* **1997**, *5(8)*, 1455-1467; c) C. Schmuck, *Chem. Eur. J.* **2000**, *6(4)*, 709-718.

[8]   a) E. M. A. Ratilla, N. M. Kostic, *J. Am. Chem. Soc.* **1988**, *110*, 4427-4428; b) A. E. Przybyla, J. Robbins, N. Menon, H. D. Peck Jr., *FEMS Microbiology Reviews* **1992**, *88*, 109-136; c) D. P. Fairlie, W. G. Jackson, B. W. Skelton, H. Wen, A. H. White, W. A. Wickramasinghe, T. C. Woon, H. Taube, *Inorg. Chem.* **1997**, *36*, 1020-1028.

[9]   a) R. Longhi, R. S. Drago, *Inorg. Chem.* **1965**, *4*, 11-14; b) R. Snaith, K. Wade, B. K. Wyatt, *J. Chem. Soc. A* **1970**, 380-383; c) R. C. Mehrotra in *Comprehensive Coordination Chemistry, Vol. 2*, Pergamon, Oxford, **1987**, pp. 269-291; d) N. de Vries, C. E. Costello, A. G. Jones, A. Davison, *Inorg. Chem.* **1990**, *29*, 1348-1352; e) W. P. Fehlhammer, R. Metzner, W. Sperber, *Chem. Ber.* **1994**, *127*, 829-833; f) P. J. Bailey, K. J. Grant, S. Pace, S. Parsons, L. J. Stewart, *J. Chem. Soc. Dalton Trans.* **1997**, 4263-4266; g) W. Schneider, A. Bauer, A. Schier, H. Schmidbaur, *Chem. Ber./Recueil* **1997**, *130*, 1417-1422.

[10]   N. Kuhn, M. Grathwohl, M. Steimann, G. Henkel, *Z. Naturforsch. Teil B* **1998**, *53*, 997-1003.

[11]   a) H. Wittmann, A. Schorm, J. Sundermeyer, *Z. Anorg. Allg. Chem.* **2000**, *626*, 1583-1590; b) H. Wittmann, PhD Thesis, Philipps-Universität Marburg (GER), **1999**.

[12]   M. L. Simms, J. L. Atwood, D. A. Zatko, *J. Chem. Soc., Chem. Comm.* **1973**, 46.

[13]   D. Sen, C. Saha, *J. Chem. Soc., Dalton Trans.* **1976**, 776.

[14]   S. Djebbar-Sid, O. Benali-Baitich, J. P. Deloume, *Transition Met. Chem.* **1998**, *23(4)*, 443-447.

[15]   a) Y. Gultneh, A. Farooq, K. D. Karlin, S. Liu, J. Zubieta, *Inorg. Chim. Acta* **1993**, *211(2)*, 171-175; S. Fox, A. Nanthakumar, M. Wikstrom, K. D. Karlin, N. J. Blackburn, *J. Am. Chem. Soc.* **1996**, *118(1)*, 24-34; c) T. D. Ju, R. A. Ghiladi, D.-H. Lee, G. P. F. Van Strijdonck, A. S. Woods, R. J. Cotter, V. G. Young, K. D. Karlin, *Inorg. Chem.* **1999**, *38(10)*, 2244-2245.

[16]   a) M. Pascaly, M. Duda, A. Rompel, B. H. Shift, W. Meyer-Klaucke, B. Krebs, *Inorg. Chem.* **1999**, *291*, 289; b) M. Duda, M. Pascaly, B. Krebs, *J. Chem. Soc., Chem. Comm.* **1997**, 835.

[17]   a) H. Eilingsfeld, M. Seefelder, H. Weidinger, *Angew. Chem.* **1960**, *72*, 836-845; b) H. Eilingsfeld, G. Neubauer, M. Seefelder, H. Weidinger, *Chem. Ber.* **1964**, *97*, 1232-1245.

[18]   W. Kantlehner, E. Haug, W. W. Mergen, P. Speh, T. Maier, J. J. Kapassakalidis, H.-J. Bräuner, H. Hagen, *Liebigs Ann. Chem.* **1984**, 108-126.

[19]   I. A. Cliffe in *Comprehensive Organic Functional Group Transformations, Vol. 6*, Elsevier Science Ltd., Oxford, **1987**, pp. 639-675.

[20]   R. Knorr, A. Trzeciak, W. Bannwarth, D. Gillessen, *Tetrahedron Lett.* **1989**, *30*, 1927-1930.

[21]   a) A. J. Papa, *J. Org. Chem.* **1966**, *31*, 1426-1430; b) W. Petz, *J. Organomet. Chem.* **1975**, *90*, 223-226.

[22]   A. V. Santoro, G. Mickevicius, *J. Org. Chem.* **1979**, *44*, 117-120.

[23]   M. Hesse, H. Meier, B. Zeeh in *Spektoskopische Methoden in der organischen Chemie*, *4. Aufl.*, Thieme, Stuttgart **1991**, p. 9.

[24]   H. Kessler, D. Leibfritz, *Tetrahedron* **1970**, *26*, 1805-1820.

[25]   P. W. N. M. van Leeuwen, W. L. Groeneveld, *Inorg. Nucl. Chem. Lett.* **1967**, *3*, 145-146.

[26]   E. Riedel, „*Anorganische Chemie*" **1990**, *2. Aufl.*, W. de Gruyter, Berlin, 586.

[27]   M. Ciampolini, N. Nardi, *Inorg. Chem.* **1966**, *5(7)*, 1150-1154.

[28]   M. S. Lah, H. Chun, , *Inorg. Chem.* **1997**, *36*, 1782-1785.

[29]   a) D. F. Evans, *J. Chem. Soc.* **1953**, 2003-2005; b) H. P. Fritz, K.-E. Schwarzhans, *J. Organomet. Chem.* **1964**, *1*, 208-211; c) T. H. Crawford, J. Swanson, *J. Chem. Educ.* **1971**, *48*, 382-386; d) J. Löliger, R. Scheffold, *J. Chem. Educ.* **1972**, *49*, 646-647; e) D. H. Grant, *J. Chem. Educ.* **1995**, *72*, 39-40.

[30]   R. J. Deeth, M. Gerloch, *Inorg. Chem.* **1985**, *24*, 4490-4493.

[31]   a) J. E. Huheey, E. A. Keiter, R. L. Keiter in *Inorganic Chemistry*, 4th Ed., Harper Collins, New York, **1993**; b) U. Müller in *Anorganische Strukturchemie*, *3. Aufl.*, Teubner, Stuttgart, **1996**.

[32]   M. Di Vaira, P. L. Orioli, *Acta Crystallogr. Sect. B* **1968**, *24*, 1269-1272.

[33]   R. Gregorzik, U. Hartmann, H. Vahrenkamp, *Chem. Ber.* **1994**, *127*, 2117-2122.

[34]   R. J. Sime, R. P. Dodge, A. Zalkin, D. H. Templeton, *Inorg. Chem.* **1971**, *10*, 537-541.

[35]   A. Gobbi, G. Frenking, *J. Am. Chem. Soc.* **1993**, *115*, 2362-2372.

[36]   Representative examples: a) K. R. Adam, S. P. H. Arshad, D. S. Baldwin, P. A. Duckworth, A. J. Leong, L. F. Lindoy, B. J. McCool, M. McPartlin, B. A. Tailor, P. A. Tasker, *Inorg. Chem.* **1994**, *33*, 1194-1200; b) N. W. Alcock, F. McLaren, P. Moore, G.

A. Pike, S. M. Roe, *Chem. Comm.* **1989**, 629-632; c) L. Casella, M. E. Silver, J. A. Ibers, *Inorg. Chem.* **1984**, *23*, 1409-1418.

[37]   M. G. B Drew, S. Hollis, S. G. McFall, S. M. Nelson, *J. Inorg. Nucl. Chem.* **1978**, *40*, 1595-1596.

[38]   S. M. Nelson, S. G. McFall, M. G. B. Drew, A. H. bin Othman, *Chem. Comm.* **1977**, 370-371.

[39]   a) M. Duggan, N. Ray, B. Hathaway, G. Tomlinson, P. Brint, K. Pelin, *J. Chem. Soc., Dalton Trans.* **1980**, 1342-1348; b) L. Raehm, J. M. Kern, J.-P. Sauvage, *Chem. Eur. J.* **1999**, *5*, 3310-3317.

[40]   E. J. Laskowski, D. N. Hendrickson, *Inorg. Chem.* **1978**, *17*, 457-470.

[41]   F. A. Cotton, R. M. Wing, *Inorg. Chem.* **1965**, *4(3)*, 314-317.

[42]   P. Chaudhuri, K. Wieghardt, Y.-H. Tsai, C. Krüger, *Inorg. Chem.* **1984**, *23*, 427-432.

[43]   *Handbook of Chemistry & Physics, 1st Student Edition*, CRC Press, Boca Raton, **1988**.

[44]   M. G. B. Drew, C. J. Harding, V. McKee, G. G. Morgan, J. Nelson, *Chem. Commun.* **1995**, 1035-1038.

[45]   a) M. Ray, B. S. Hammes, G. P. A. Yap, A. L. Rheingold, A. S. Borovik, *Inorg. Chem.* **1998**, *37*, 1527-1532; b) M. Ray, A. P. Golombek, M. P. Hendrich, V. G. Young Jr., A. S. Borovik, *J. Am.Chem. Soc.* **1996**, *118*, 6084-6085; c) M. Ray, G. P. A. Yap, A. L. Rheingold, A. S. Borovik, *Chem. Commun.* **1995**, 1777-1778.

[46]   a) C. C. Cummins, J. Lee, R. R. Schrock, W. M. Davis, *Angew. Chem.* **1992**, *104*, 1510-1512; *Angew. Chem. Int. Ed. Engl.* **1992**, *31*, 1501-1503; b) J. S. Freundlich, R. R. Schrock, C. C. Cummins, W. M. Davis, *J. Am Chem. Soc.* **1994**, *116*, 6476-6477; c) R. R. Schrock, C. C. Cummins, T. Wilhelm, S. Lin, S. M. Reid, M. Kol, W. M. Davis, *Organometallics* **1996**, *15*, 1470-1476.

[47]   E. Keller, *Schakal-97, Program for the Graphic Representation of Molecule and Crystallographic Models* **1997**, Universität Freiburg, Germany.

[48]   a) G. M. Sheldrick, *SHELXS-97, Program for Crystal Structure Solution* and *SHELXL-97, Program for Crystal Structure Refinement* **1997**, Göttingen, Germany; b) Siemens Analytical X-ray Instruments Inc., *SHELXTL 5.06* **1995**, Madison, WI, USA; c) C. Giacovazzo, *SIR-92, Program for Crystal Structure Solution* **1992**, Bari, Italy.

[49] Crystallographic data (excluding structure factors) for the structures reported in this paper have been deposited with the Cambridge Crystallographic Data Centre as supplementary publication no. CCDC-148696 (**2**), CCDC-148700 (**3**), CCDC-148699 (**4**), CCDC-148698 (**5**) and CCDC-148697 (**6**). Copies of the data can be obtained free of charge on application to CCDC, 12 Union Road, Cambridge CB2 1EZ, UK (fax: (+ 44) 1223 336-033; email: deposit@ccdc.cam.ac.uk).

— Chapter 5.1 —

1,8-Bis(tetramethylguanidino)naphthalene (TMGN):

A New, Superbasic and Kinetically Active „Proton Sponge"

Keywords: Basicity • Dynamic NMR Spectroscopy • Peralkylated guanidines • Protonation • „Proton sponge"

Abstract

1,8-Bis(tetramethylguanidino)naphthalene (TMGN, **1**) is a new, readily accessible, and stable „proton sponge" with an experimental pK_{BH+} value of 25.1 in MeCN, which is nearly seven orders of magnitude higher in basicity than the classical „proton sponge" 1,8-bis(dimethylamino)-naphthalene (DMAN). Because of the sterically less crowded character of the proton-accepting sp^2-nitrogen atoms, TMGN also has a higher kinetic basicity than DMAN, which is shown by time resolved proton self-exchange reactions. TMGN is more resistant to hydrolysis and is a weaker nucleophile with the alkylating agent EtI in comparison to the commercially available guanidine 7-methyl-1,5,7-triazabicyclo[4.4.0]dec-5-ene (MTBD). Crystal structures of the free base, of the *mono-* and *bis*protonated base were determined. The dynamic behavior of all three species in solution was investigated by variable-temperature ^1H NMR experiments. $\Delta G^{\ddagger}$ values obtained by spectra simulation reveal a concerted mechanism of rotation about the C-N bonds of the protonated forms of TMGN.

Introduction

For over three decades, neutral organic bases with chelating proton-acceptor functionalities have attracted particular interest. On account of their high proton affinity, they are named „proton sponges" according to the classical example, 1,8-bis(dimethylamino)naphthalene (DMAN, Scheme 2), that was introduced by Alder et al.[1,2] The field has been reviewed by Staab and Saupe,[3] and more recently by Llamas-Saiz et al.,[4] as well as in a limited manner on 1,8-diaminonaphthalene derivatives by Pozharskii.[5] „Proton sponges" are still the focus of current research activity[6] and are also the subject of vivid interest of theoretical chemists.[7] A general feature of all „proton sponges" is the presence of two basic nitrogen centers in the molecule, which have an orientation that allows the uptake of *one* proton to yield a stabilized $[N{\cdots}H{\cdots}N]^+$ intramolecular hydrogen bond (IHB). Compared to ordinary

1

alkyl and aryl amines, amidines and guanidines such proton chelators present a dramatic increase in basicity on account of i) destabilization of the base as a consequence of strong repulsion of unshared electron pairs, ii) formation of an IHB in the protonated form, and iii) relief from steric strain upon protonation. Two general concepts to raise the thermodynamic basicity or proton affinity have been followed (Scheme 1). One is to replace the naphthalene skeleton by other aromatic spacers, such as fluorene,[8] heterofluorene,[9] phenanthrene[10] and biphenyl,[11] thus influencing the basicity by varying the nonbonding N···N distance of the proton-acceptor pairs. The other concept focuses on the variation of the basic nitrogen centers [6d,e,12,13,14,15] or its adjacent environment („buttressing effect").[2,3,5,16,17]
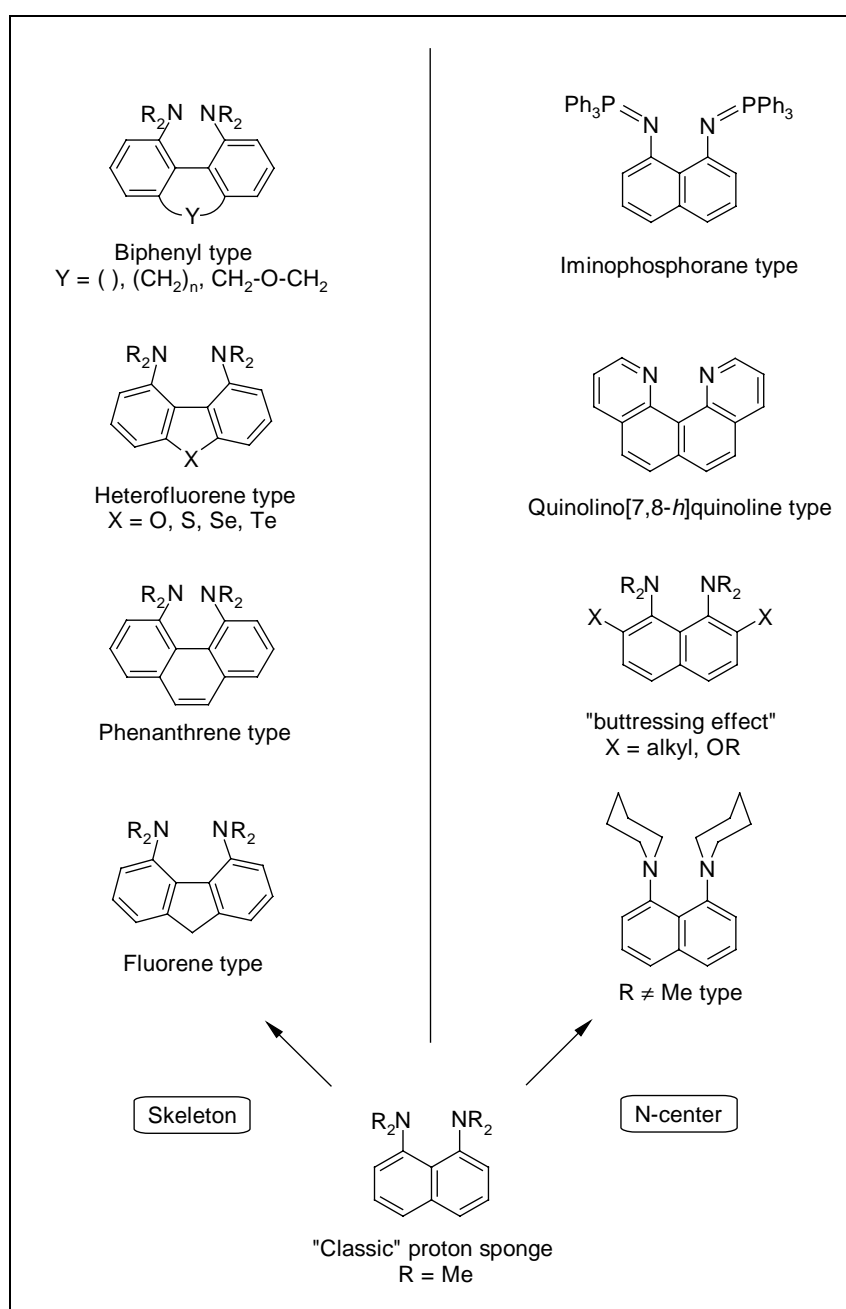
Scheme 1. Survey of strategies to influence the basicity of „proton sponges".

There is a trend that „proton sponges" with high thermodynamic basicity typically have a low kinetic basicity: The captured proton does not usually take part in rapid proton-exchange reactions, which would allow such neutral superbases to serve as catalysts in salt-free base-catalyzed reactions. A successful strategy to overcome the kinetic inertness has been presented by Schwesinger et al., who developed a thermodynamically strong and at the same time kinetically active superbase that incorporates the vinamidine structure (Scheme 2).[18] However, its multistep synthesis, moderate stability, and moderate solubility in aprotic solvents are some limitations of this „proton sponge", that proved to take up *two* protons in the presence of excess acid.
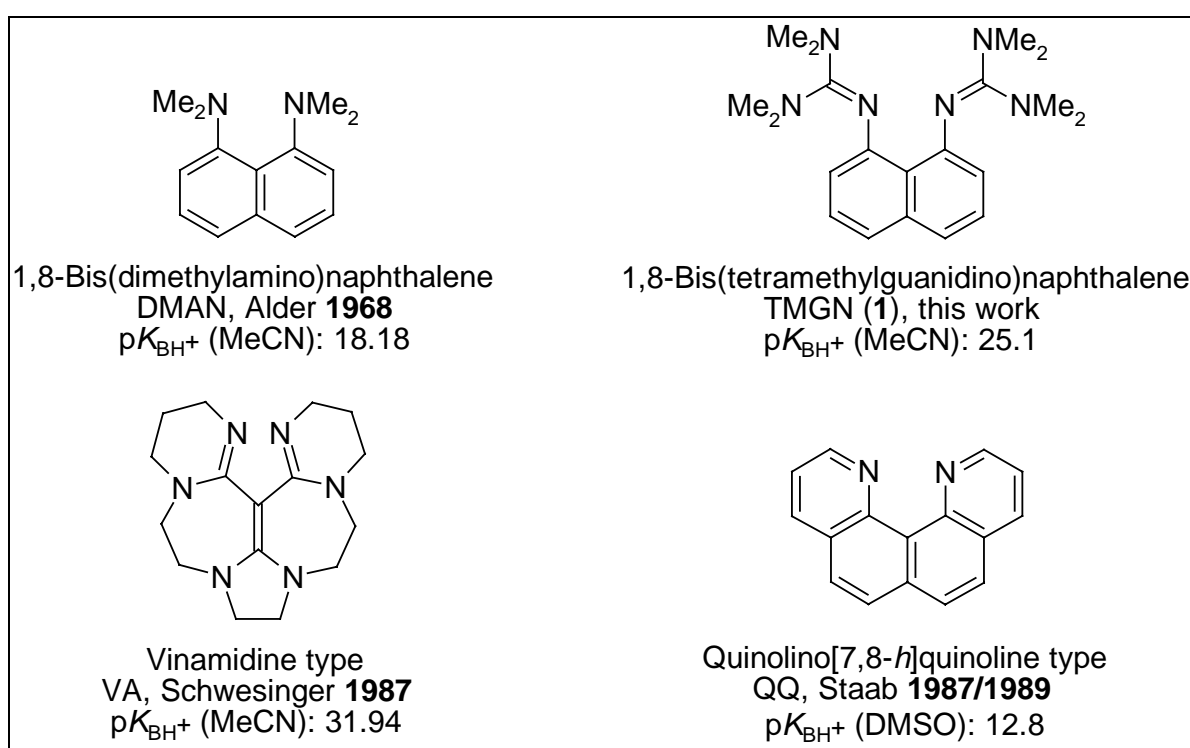
Scheme 2. Representative „proton sponges" in relation to TMGN (**1**).

After an examination of the reported strategies to increase the basicity of 1,8-diaminonaphthalene „proton sponges" and being aware that peralkyl guanidines belong to the strongest organic neutral bases known,[19] we decided to use the tetramethylguanidino group as an efficient and straightforward modification of the chelating proton-acceptor. Peralkylguanidines are several orders of magnitude higher in basicity than tertiary amines because of the excellent stabilization of the positive charge in their resonance-stabilized cations.[20] This trend may be demonstrated by the pK_{BH+} (MeCN) values of the 1,2,2,6,6-pentamethylpiperidinium cation (18.62), the parent guanidinium cation (23.3), and the

3

pentamethylguanidinium cation (25.00).[20c] It is interesting to note that pK_{BH+} values of a wide range of nonchelating *N*-aryl guanidines have been determined[21] and that one promising candidate for proton chelation, 2,2'-bis(tetramethylguanidyl)-1,1'-biphenyl, did not exhibit „proton sponge" properties, such as formation of an IHB.[22] Dissociation constants and kinetics of proton transfer reactions of nonchelating guanidine bases in acetonitrile[23] as well as DMAN systems[16a,b,24] have been the subject of previous detailed studies.

In the present paper, we report on the synthesis as well as the spectroscopic and structural properties of 1,8-bis(tetramethylguanidino)naphthalene (TMGN (**1**), Scheme 2) and its *mono-* and *bis*protonated forms. Surprisingly, this new „proton sponge", which has a basicity that is higher by the factor of more than 10^7 than Alder's classical DMAN, was successfully prepared by a one-step synthesis in high yield. It is relatively stable towards autoxidation, soluble in aprotic nonpolar solvents, and in contrast to DMAN, kinetically active in proton-exchange reactions.

Results and Discussion

Synthesis. TMGN (**1**) is synthesized by a method previously described by us for the synthesis of multidentate metal-chelating oligoguanidines.[25] Tetramethylchlorformamidinium chloride[26] is treated with 1,8-diaminonaphthalene in the presence of triethylamine as an auxiliary base and in MeCN as the solvent. After deprotonation of the guanidinium cation with 50% aqueous KOH and extraction into hexane, **1** is obtained in analytically pure form (Scheme 3). In comparison to other „proton sponges" of similar basicity, this represents a rather simple synthesis from convenient precursors, as the Vilsmeyer salt [Cl-C(NMe$_2$)$_2$]Cl and related electrophiles may be produced in large scale from ureas and phosgene or oxalyl chloride.
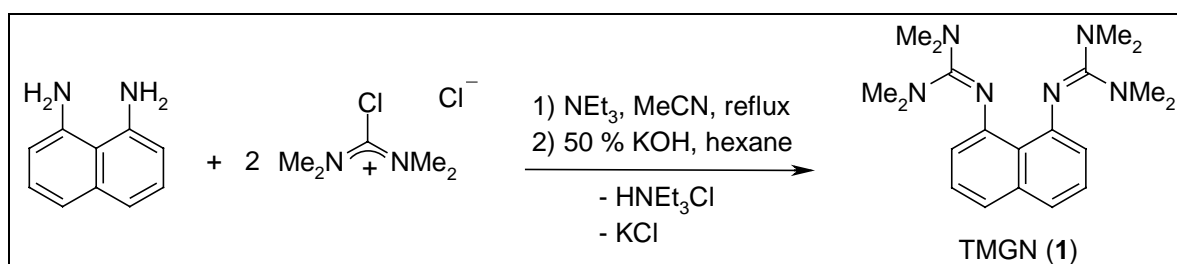
Scheme 3. Synthesis of TMGN (**1**).

4

Reactivity studies. TMGN (**1**) is cleanly *mono*protonated by an equimolar amount of NH$_4$PF$_6$ in MeCN to yield [**1**-H][PF$_6$] (**2a**). Colorless single crystals are obtained by slow diffusion of dry ether into the MeCN solution.

Surprisingly, *mono*protonated [**1**-H]$^+$ does not show the kinetic inertness with respect to *bis*protonation, that is typical for many „proton sponges". Similar to the kinetically active vinamidine „proton sponge" of Schwesinger,[18] it readily takes up a second proton when treated with an excess of strong acids, such as trifluormethanesulfonic acid, tetrafluoroboric acid etherate, trifluoroacetic acid, aqueous hexafluorophosphoric acid or gaseous HCl. However, complete *bis*protonation could not be achieved by excess NH$_4$PF$_6$ in MeCN. Colorless single crystals of [**1**-H$_2$][Cl, Cl$_2$H] (**3a**) were obtained after excess of hydrogen chloride was passed through a CH$_2$Cl$_2$ solution of **1** and crystallization from MeCN. *Bis*protonation is a rather unusual feature observed in only a small number of „proton sponges", which can be divided into „proton sponges" that bear a double set of basic centers (A)[5,6b,27] and a second class where the formation of the IHB is insufficiently strong or completely prevented (B) (Scheme 4).[17a,18,28,29]
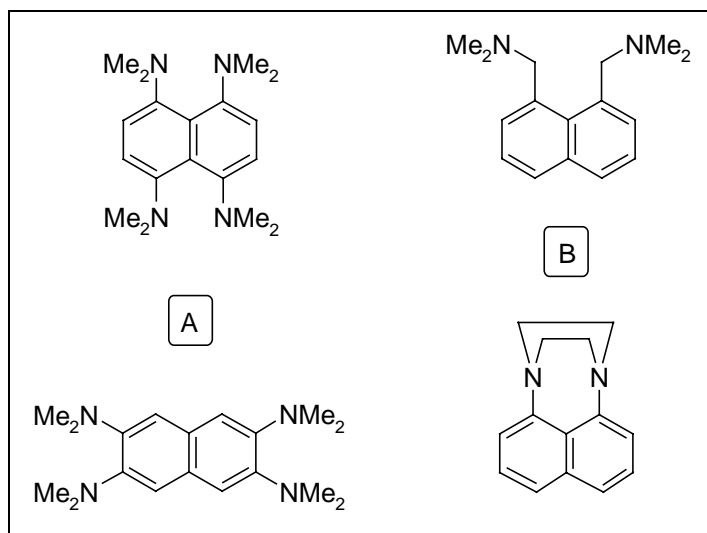
Scheme 4. „Proton sponges" that can be *bis*protonated, with two sets of basic centers (A) and forming insufficiently strong IHB´s (B).

TMGN (**1**) is perfectly stable towards hydrolysis under acidic conditions (1 M D$_3$O$^+$, 25 °C, 6 d). The hydrolysis of **1** in basic media was monitored by ^{1}H NMR (0.83 M NaOD in [D$_6$]DMSO/D$_2$O) and compared to the commercially available guanidine 7-methyl-1,5,7-triazabicyclo[4.4.0]dec-5-ene (MTBD). While **1** is stable at room temperature for 24 h,

MTBD hydrolysis is observed. At elevated temperatures (60 °C, 5 d), 44% of **1** and 73% of MTBD is hydrolyzed to the corresponding urea.

In order to evaluate the nucleophilicity of **1**, an alkylation reaction of **1** and MTBD with C_2H_5I was performed under identical conditions (2.5 eq C_2H_5I per guanidine function, 25 °C, CD_2Cl_2). While no conversion of **1** was observed after 15 min by means of ^{1}H NMR, ≈ 50% of MTBD was converted into the ethyl guanidinium salt. At longer reaction times (3 d, 25 °C) even less nucleophilic **1** was converted into a mixture of protonated and alkylated products, which however, could not be quantified because of signal overlap.

Structure of the base 1. Single crystals of TMGN suitable for X-ray crystallography were obtained by crystallization from hexane. The result of the structural analysis is shown in Figure 1, selected bond lengths and angles are given in Table 1. The molecular structure of **1** is close to C_2 symmetric molecular structure of **1** with only small deviations from ideal symmetry as a consequence of the strong repulsion of the two lone pairs centered at the proton-acceptor sp^2-nitrogen atoms N(1) and N(4) in an *anti*-orientation.
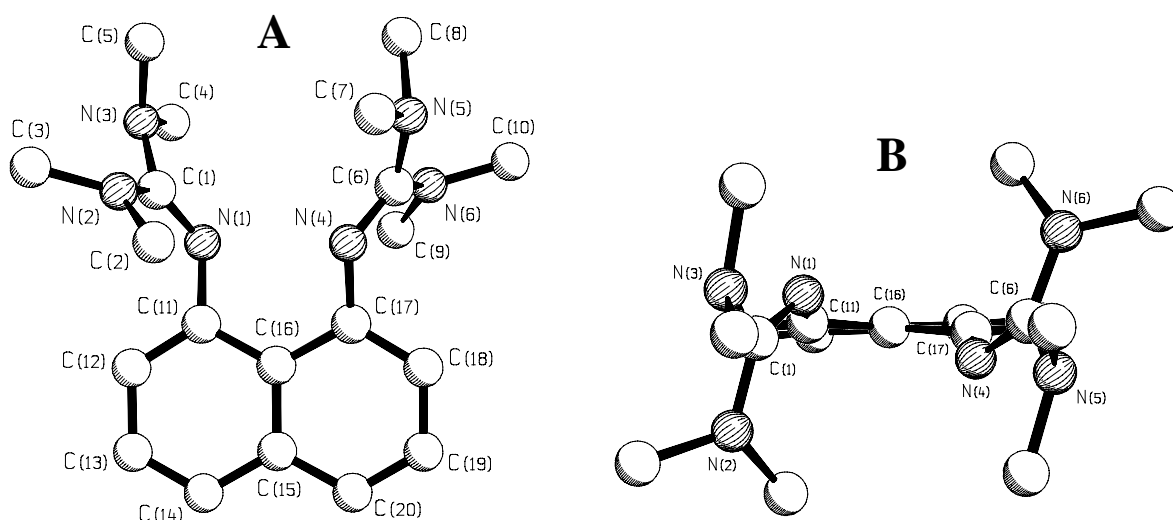

Figure 1. Molecular structure of TMGN (**1**), view perpendicular to the naphthalene ring plane (**A**) and projection along the C_2-axis C(16)-C(15) of the molecule (**B**).[71]

Both guanidine centers C(1) and C(6) are trigonal planar (Σ° 359.9°, Table 1). As found in other peralkyl oligoguanidines,[25a,b] the four dimethylamino groups in the periphery deviate from ideal conjugation with the $C(1)N_3$ and $C(6)N_3$ planes as indicated by torsion angles N-C-N-C of 8-45°. A similar propeller-like distortion as a result of steric repulsions has been

6

found for the ground state of the hexamethylguanidinium cation.[30] The guanidine double bonds C(1/6)-N(1/4) (128.2±0.1 pm) are shorter by the factor $\rho = 0.93$[25c,d] (*vide infra*) than the average bonding lengths of C(1) and C(6) to the peripheral NMe_2 nitrogen atoms (138.4±0.1 pm, Table 2). This demonstrates the effect of conjugation of the guanidine group with the aromatic naphthalene system, weakening the double bond in contrast to the situation in compounds **A** and **B** (Table 2).

Table 1. Selected bonding, nonbonding lengths [pm], angles, dihedral angles and bond angle sums [°] in TMGN (**1**), [**1**-H][PF_6] (**2a**), [**1**-H_2][Cl, Cl_2H] (**3a**), and [**1**-H_2][PF_6, BF_4] (**3b**).[a]

	TMGN (**1**)	[**1**-H][PF_6] (**2a**)	[**1**-H_2][Cl, Cl_2H] (**3a**)	[**1**-H_2][PF_6, BF_4] (**3b**)
C(1)=N(1)	128.1(3)	135.1(6)	136.6(3)	133.3(17)
C(6)=N(4)	128.3(3)	132.6(6)	136.5(3)	133.3(18)
C-NMe_2 (∅)	138.4±0.1	134.2±2.0	133.1±0.4	133.9±1.8
C(11)-N(1)	140.1(3)	140.9(6)	142.6(3)	143.7(14)
C(17)-N(4)	139.6(3)	141.4(6)	143.4(3)	143.6(15)
N(1)-H(1A)	-	91(6)	90(3)	87
N(4)-H(1A)/H(4)	-	175(6)	92(3)	87
N(1)···N(4)	271.7(3)	259.3(5)	288.1(3)	282.3
C(11)···C(17)	251.9(3)	255.3(7)	258.2(4)	256.0
C(11)-C(16)-C(17)	122.6(2)	124.6(4)	127.8(2)	126.6(10)
C(11/17)-C(16)-C(15)-C(20/14)	173.7(2) / 172.3(2)	178.7(4) / 178.9(4)	178.2(2) / 177.3(2)	179.4(11) / 179.9(12)
N(1/4)-C(11/17)-C(16)-C(15)	-161.6(2) / -161.2(2)	177.4(1) / -171.0(4)	-172.5(2) / -174.8(2)	-178.5(10) / 178.9(10)
C(16)-C(11/17)-N(1/4)-H(1A/4A)	- / -	-9(4) / -	62.58(1) / 68.66(0)	- / -
C(1/6)=N(1/4)-C(11/17)-C(12/18)	57.7(3) / 53.2(4)	-10.3(8) / 49.2(7)	31.4(3) / -34.1(3)	-37.6(15) / -27.7(18)
Σ° N(1)	-	360.0	350.6	proton calcd. -
Σ° N(4)	-	-	351.5	not found
Σ° C(1)	359.9	360.0	360.0	360.0
Σ° C(6)	359.9	359.9	360.0	359.9
Σ° N_{Me2} (∅)	353.2±3.9	359.0±1.1	359.7±0.3	358.7±0.6

[a] Crystallographic standard deviations in parentheses, calculated average values (∅) are denoted with standard deviation (±).

Table 2. Average C=N vs. C-NR$_2$ lengths [pm] and quotient ρ, standard deviations (±).[a]

Complex	$\varnothing$ C=N (a)	$\varnothing$ C-NR$_2$ (b, c)	ρ
TMGN (**1**)	128.2±0.1	138.4±0.1	0.927
[(**A**)Mo(CO)$_3$][b,c,[25b]]	127.6±0.0	138.7±0.9	0.920
[(**B**)Zn^{II}Cl$_2$][b,d,[25a]]	127.9±0.0	139.5±0.4	0.917
[(**C**)Cu^{II}Cl$_2$][e,[25d]]	131.4±0.8	136.8±2.2	0.960
[**1**-H][PF$_6$] (**2a**) (bridge)	132.6±0.0	135.8±0.4	0.977
[**1**-H][PF$_6$] (**2a**) (bond)	135.1±0.0	132.6±1.6	1.019
[**1**-H][Cl, Cl$_2$H] (**3a**)	136.6±0.0	133.1±0.4	1.026
[(**D**)H$_2$]Cl$_2$ [f,[25a]]	133.6±0.0	134.0±0.2	0.997
[(**E**)][Fe(CO)$_4$C(O)NMe$_2$] [g,[31]]	132.9±0.0	133.7±0.7	0.994[32]

[a] Structural parameter $\rho = \varnothing$ C=N / $\varnothing$ C-NR$_2$. [b] Complex bears a free guanidine group in form of a noncoordinated „dangling" arm of a tripodal ligand. [c] Ligand (**A**) = 1,1,1-Tris{2-[N^2-(1,1,3,3-tetramethylguanidino)]ethyl}amine (TMG$_3$tren). [d] Ligand (**B**) = 1,1,1-Tris[N^2-(1,1,3,3-tetramethyl guanidino)methyl]ethane. [e] Ligand (**C**) = (1R,2R)-(-)-1,2-Bis[N^2-(1,1,3,3-tetramethylguanidino)] cyclohexane (TMG$_2$CH). [f] Ligand (**D**) = 1,2-Di[N^2-(1,1,3,3-tetramethylguanidinium)]ethane dichloride tetrahydrate (TMG$_2$en × 2 HCl). [g] Ligand (**E**) = [C(NMe$_2$)$_3$]$^+$.

Some characteristic structural features reveal differences in the steric constraint of TMGN and the sterically more crowded DMAN[33] and less crowded Quinolino[7,8-*h*]quinoline (QQ, Scheme 2)[14a] (corresponding values in brackets). The indicators are the angle C(11)-C(16)-C(17) 122.6° (DMAN: 125.8°; QQ: 125.4°) of the naphthalene ring, the nonbonding distance C(11)···C(17) 251.9 pm (DMAN: 256.2; QQ: 258.3), and the very short nonbonding distance between the acceptor atoms N(1)···N(4) 271.7 pm (DMAN: 279.2; QQ: 272.7; 1,8-diaminonaphthalene: 272[5]). Additional evidence for the extent of distortion comes from the average *anti*-coplanar torsion angles within the naphthalene skeleton C(11/17)-C(16)-C(15)-C(20/14) 173.0° (DMAN: 170.3°; QQ: 178.9°) and with respect to the twisted N-donor atoms N(1/4)-C(11/17)-C(16)-C(15) 161.4° (DMAN: 168.2; QQ: 177.8). Because of the different hybridization of the N-atoms (sp^2) compared to typical „proton sponges" (sp^3) the *anti*-conformation of the unshared electron pairs is more easily realized, as can be seen at the position of the imine nitrogen atoms in Figure 1B. In addition, the average *syn*-coplanar torsion angle C(1/6)-N(1/4)-C(11/17)-C(12/18): 55.5° (**1**) reveals that the degree of possible conjugation between the π-systems of the naphthalene ring and the guanidine moiety is marginal. However, the quotient ρ discloses a noticeable influence of the aromatic system on

the guanidine group, the C=N bond is elongated compared to aliphatic guanidines (first section Table 2).

Structure of *mono*protonated 1. The result of the structural analysis is shown in Figure 2, selected bond lengths and angles are given in Table 1. In [**1**-H][PF$_6$] (**2a**), the C_2 symmetry of the corresponding base structure is not preserved. The naphthalene system is flattened and can be considered virtually planar with the captured proton located between the imine nitrogen atoms in the same plane. There are no significant interactions between the PF$_6^-$ anion and the cation of **2a**.
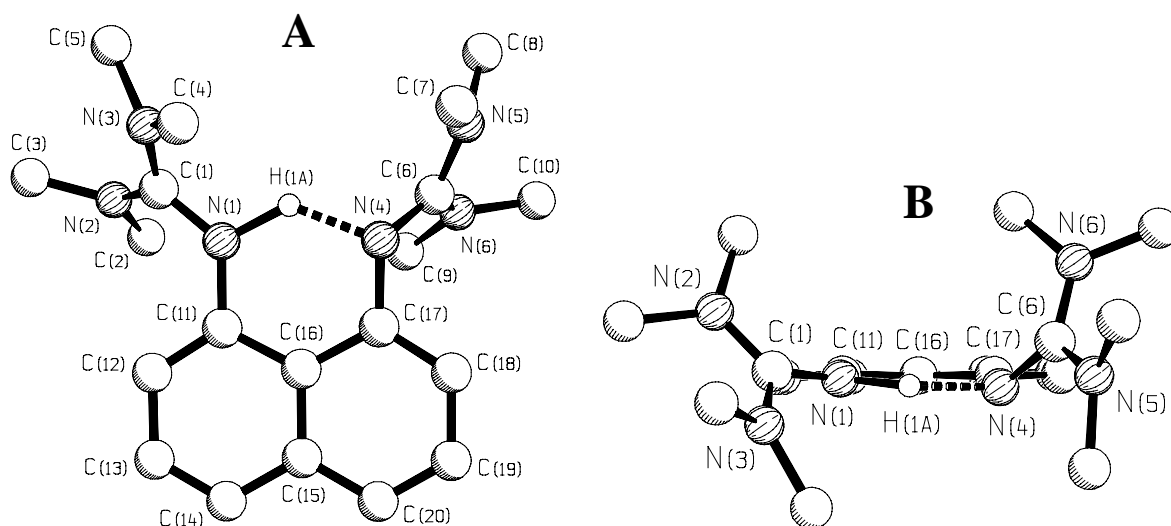
Figure 2. Molecular structure of [**1**-H][PF$_6$] (**2a**), view perpendicular to mean ring plane (**A**) and projection along C(15)-C(16) (**B**), anion omitted for clarity.[71]

In *mono*protonated TMGN, the bond lengths between C(1/6) and N(1/4) become elongated, in *bis*protonated species they become equivalent to the peripheral C-NR$_2$ bonds (Table 1). Indeed, ρ becomes 1.019 for the guanidine group with the smaller N-H distance within the IHB and is 0.977 for the one with the larger N-H distance. This is in agreement with the existence of a true IHB in the *mono*protonated form of TMGN (further evidence is raised by the results of dynamic NMR spectroscopy, *vide infra*).

The guanidine nitrogen atoms N(1)···N(4) of **2a** are found at a closer distance of 259.3 pm compared with **1** (271.7 pm), which is in the range of the average value of 258 pm in DMANH$^+$ structures.[5,34] The torsion angles for the evaluation of planarity within the naphthalene ring indicate that it is flattened to a large degree. On protonation, the angle C(11)-C(16)-C(17) is stretched to 124.6° in **2a**, while it remains essentially unchanged in DMANH$^+$ 125.6°.[34c] This trend is in agreement with an elongation of the C(11)···C(17) distance to 255.3 pm (DMANH$^+$: 253.9). Furthermore, the average *anti*-coplanar torsion angles C(11/17)-C(16)-C(15)-C(20/14) 178.8° (DMANH$^+$: 178.7) and the twisting of the donor atoms N(1)-C(11)-C(16)-C(15) and N(4)-C(17)-C(16)-C(15) 177.4° and 171.0°, respectively, (DMANH$^+$: 179.6° and 177.7°) and indicate the trend of planarization. The proton was found and isotropically refined. For confirmation of the exact position of the proton or differentiation of the imine nitrogen atoms, a neutron diffraction structure analysis[35] and ESCA spectroscopy,[36] respectively, would be the method of choice. The proton is localized unsymmetrically in a nonlinear hydrogen bridge N(1)-H(1A)···N(4) as indicated by the short N(1)-H(1A) distance of 91 pm, a long distance N(4)···H(1A) of 175 pm and an N(1)-H(1A)-N(4) angle of 152°. A similar geometry has been found in other „proton sponges" (Table 3).

Table 3. Comparison of N-H bond lengths [pm] and angles [°] in various „proton sponges" with [**1**-H][PF$_6$] (**2a**) and [**1**-H$_2$][Cl, Cl$_2$H] (**3a**).

compound	N···N	N-H	(N)H···N	N-H···N
[DMANH]ClMH^a	264.4(2)	110.6(5)	160.8(6)	153.3(5)
[DMANH]HS^b	258.3(2)	108(2)	155(2)	157(2)
[TDMANH$_2$]Br$_2$^{c}	256.7(5)	122(1)	139(1)	158(-)
[VAH](BPh$_4$)^d	254.1(-)	92.0(3)	178(1)	137.6(-)
[VAH$_2$](ClO$_4$)$_2$^{d}	284.5(-)	86.0(34) / 86.0(49)	-	-
[**1**-H][PF$_6$] (**2a**)	259.3(5)	91(6)	175(6)	152(5)
[**1**-H$_2$][Cl, Cl$_2$H] (**3a**)	288.1(3)	90(3) / 92(3)	-	-

^{a} 1-Dimethylamino-8-dimethylammonionaphthalene 1,2-dichloro maleate, determined via neutron diffraction.[35] ^{b} 1-Dimethylamino-8-dimethylammonionaphthalene hydrogen squarate.[34c] ^{c} 5,8-Bis(dimethylamino)-1,4-bis(dimethylammonio)naphthalene dibromide.[27] ^{d} Vinamidine.[18]

The *syn*-coplanar torsion angles, which indicate the probability of p-orbital overlap C(1/6)-N(1/4)-C(11/17)-C(12/18), differ significantly for both guanidine groups of **2a**. While the guanidine group with the smaller N-H bond length unfolds a torsion angle of only 10.3°, which permits conjugation, the other group remains at a disadvantageous angle of almost 50°, similar to the angles observed in **1**.

Structure of *bis*protonated 1. The X-ray structure of [**1**-H$_2$][Cl, Cl$_2$H] (**3a**) is shown in Figure 3, selected bond lengths and angles are given in Table 1, the hydrogen atoms H(1), H(4), and H(2) were found and isotropically refined. In the dication **3a**, the planarity of the naphthalene ring observed in **2a** is essentially maintained while the guanidinium units are increasingly twisted with respect to each other. The protons adopt a *syn*-conformation with hydrogen bonding to a bridging chloride anion so that the inner core of the molecule has almost C_s symmetry. The chelating hydrogen bonds lengths are 221(3) pm for N(1)-H(1)···Cl(1) and 229(3) pm for N(4)-H(4)···Cl(1). A solvate with hydrogen chloride is formed by second chloride anion. The resulting anion [Cl-H···Cl]⁻ reveals an unsymmetrical linear hydrogen bond similar to the structurally characterized example [H$_3$O•18-crown-6][Cl$_2$H][37] within a variety of characteristic bond lengths and angles that have been found for this anion (Table 4).

Table 4. Comparison of Cl-H···Cl bond lengths [pm] and angles [°] in [**1**-H$_2$][Cl, Cl$_2$H] (**3a**) with structurally characterized reference compounds containing the [Cl$_2$H]⁻ anion.

Compound	Cl-H	Cl···H	Cl-H···Cl
[**1**-H$_2$][Cl, Cl$_2$H] (**3a**)	145(5)	170(5)	177(2)
[AsPh$_4$][Cl$_2$H][38]	154.6	154.6	180.0
[H$_3$O•18-crown-6][Cl$_2$H][37]	147.1	164.9	168.2
[(Me$_3$NH)$_2$Cl][Cl$_2$H][39]	138.4	178.6	163.2

3a exhibits close to perfect delocalization of the positive charge within the guanidine moieties which is expressed by a ρ value of 1.026, again elongation of the former C=N bond ($\rho > 1.00$) in comparison to the last two entries in Table 2 is caused by the conjugative effect of the aromatic system.

As a result of the second protonation the angle C(11)-C(16)-C(17) is further enlarged to 127.8°, the nonbonding distances C(11)···C(17) 258.2 pm and N(1)···N(4) 288.1 pm are also elongated. These parameters reflect a dramatic increase in steric strain as a consequence of *bis*protonation: Both protons point towards the bridging chloride ion, the guanidine functions adopt a *syn*- and not an *anti*-conformation. As a result, the guanidine N-atoms lie almost in the same plane as the naphthalene ring, as indicated by the *anti*-coplanar torsion angles N(1/4)-C(11/17)-C(16)-C(15) 172.5° and 174.8°. It is plausible that this sterically congested conformation is stabilized through hydrogen bonds to the chloride anion (Figure 3).
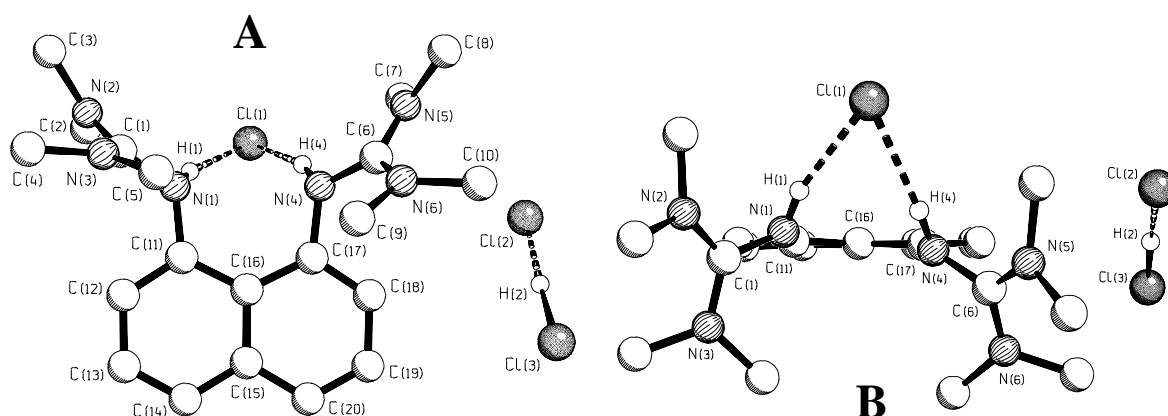
Figure 3. Molecular structure of [**1**-H$_2$][Cl, Cl$_2$H] (**3a**), view perpendicular to mean ring plane (**A**) and front view along C(15)-C(16) (**B**).[71]

The planarity of the naphthalene ring is expressed by its average *anti*-coplanar torsion angle C(11/17)-C(16)-C(15)-C(20/14) 177.8°. In **3a**, the *syn*-coplanar torsion angles (C(1/6)-N(1/4)-C(11/17)-C(12/18) relevant to evaluate a conjugation are approximately 33°. A ρ value of 1.03 indicates that the former C=N bond is even elongated in comparison to the C-NR$_2$ bonds, which is effected by the naphthalene ring.

The reaction of **1** with aqueous hexafluorophosphoric acid gave light brown crystals, which were subjected to an X-ray analysis that identified the product as [**1**-H$_2$][PF$_6$, BF$_4$] (**3b**). This surprising result arises from an HBF$_4$ impurity in the HPF$_6$ introduced in the manufacturing process, as has been previously reported.[40] Further evidence for the BF$_4^-$ anion is provided by NMR (^{19}F, ^{31}P, ^{11}B) as well as ESI mass spectrometry (see experimental). Even though the *R* values of its structure resolution were rather poor because of twinning and disorder of the anions, the proportions in the naphthalene cation can be considered accurate according to the temperature factors of cation vs. anion. Without going into a detailed discussion of structural parameters, one specific difference between **3a** and **3b** should be pointed out:

12

While the two protons are in a *syn*-conformation in **3a**, in **3b** an *anti*-conformation with essentially noncoordinating anions is realized (Figure 4). Thus, the energetic difference between the *syn*- and *anti*-conformeres cannot be very high. This is also documented by the small difference in the populations revealed by dynamic NMR studies of solutions of *bis*protonated **3c** (*vide infra*).
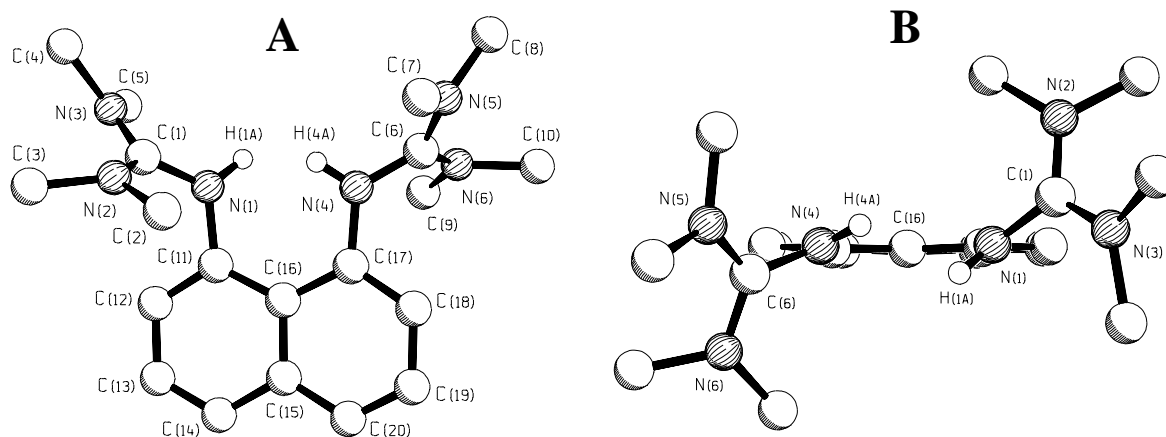

Figure 4. Molecular structure of [**1**-H$_2$][PF$_6$, BF$_4$] (**3b**), view perpendicular to mean ring plane (**A**) and front view along C(15)-C(16) (**B**) (anions omitted for clarity).[71]

Structural parameter ρ. The structural parameter ρ [25c] = 2a / (b + c) (Scheme 5) of the average C=N distances (a) and C-NR$_2$ distances (b, c), is comparatively listed for all TMGN derivatives together with representative examples in Table 2. In a free guanidine group, one double and two single bonds are present, documented by a ρ value of $\approx$ 0.92 (first section Table 2). When C=N and C-NR$_2$ bonds are of equal length as a result of protonation and perfect delocalization of positive charge, ρ assumes a value of $\approx$ 1.00 (last section Table 2). Metal complexes are placed in between ($\rho \approx 0.96$).
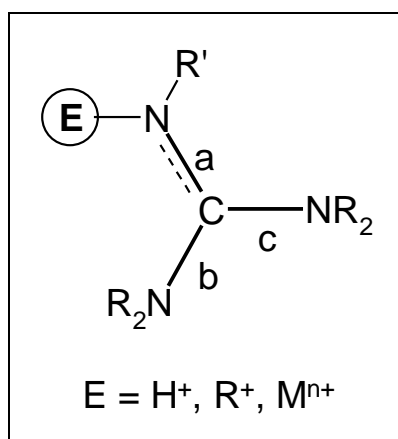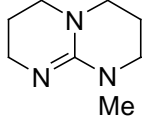

Scheme 5. C-N bonds a, b and c for the determination of quotient ρ.

NMR spectra and pK_{BH+}. The 400 MHz ^{1}H NMR spectrum of [**1**-H][PF$_6$] (**2a**) in CD$_3$CN shows a broad signal at δ_H = 14.28 ppm for the N-H proton. This relatively moderate downfield shift of the N-H proton in **2a** compared to $\delta_H \approx$ 18.6 ppm (CD$_3$CN) in DMAN and other naphthalene-based „proton sponges",[5] or even δ_H = 19.38 ppm ([D$_6$]DMSO) for QQ, is assigned to the formation of a weaker, unsymmetrical hydrogen bridge (Table 3). On the other hand the N-H resonance of the *bis*protonated analogue [**1**-H$_2$][PF$_6$, BF$_4$] (**3b**) is observed as a sharp singlet at δ_H = 7.84 ppm (CD$_3$CN) as a consequence of the lack of N-H···N hydrogen bonding. In this context, it is noted that [**1**-H$_2$][Cl, Cl$_2$H] (**3a**) gives a relatively sharp singlet at δ_H = 11.18 ppm, which is at lower field than [**1**-H$_2$][PF$_6$, BF$_4$] (**3b**) because of hydrogen bonding to the chloride anion. Furthermore, there is a broad singlet in **3a** at 4.33 ppm which is assigned to the proton of the [Cl$_2$H]$^-$ anion.[41] The resonances in the aromatic region have a typical ABX pattern.

For the determination of the pK_{BH+} value[42,43] UV/Vis spectroscopy could not be used because of the similarity of the spectra for both **1** and **2a**. Experiments to determine the basicity of **1** by ^{1}H-NMR measurements of transprotonation reactions[43,44,45] (*vide infra*) with bases of known pK_{BH+} also proved to be difficult. In contrast to typical „proton sponges" TMGN does not show the „sluggish" proton-transfer behavior reported.[16a,b,29] When we first tried to evaluate the lower and upper limits of the pK_{BH+}, mixtures of **2a** with various bases in CD$_3$CN disclosed only coalesced signals at room temperature because of the lack of hydrophobic shielding similar to QQ (Figure 5). Even at lower temperatures, a separate set of signals for each, free base and *mono*protonated form, cannot be observed, which clearly points out the rapid proton-exchange between two kinetically active bases. From the shift of the signals compared to the pure samples it could be estimated that e.g. tetramethylguanidine (TMG) was basically unable to deprotonate **2a**, whereas tris(dimethylamino)imino-phosphorane (IPNH) deprotonated **2a** to a large extent. An equimolar mixture with pentamethylguanidine (PMG) however, gave one signal for **1** / **2a** approximately at the center of the individual resonances (doublet at 6.23 and 6.49 ppm, respectively). The dynamic equilibrium could not be stopped on the NMR time scale in the temperature range of the solvent (m.p. CD$_3$CN: 229 K). When we employed the sterically more hindered guanidine base MTBD to slow down the proton exchange rates, we were able to observe a low temperature splitting of the signal in CD$_3$CN into two baseline-separated sets for all aromatic protons which could be readily integrated. In CD$_2$Cl$_2$ no split could be observed. A second

14

effect in addition to increased steric demand, is the increased basicity of MTBD (0.4 pK_{BH+} units, Table 5) compared to PMG because of better delocalization of positive charge due to enforced planarity within the guanidine moiety in contrast to the propeller-like twisting of permethylated guanidine groups. The experimental pK_{BH+} value of 25.1±0.2[46] for TMGN is in excellent agreement with the theoretically calculated value for the absolute proton affinity (APA) in MeCN: 25.4.[47] The comparison with tetramethylphenylguanidine (TMPhG, pK_{BH+} = 20.6, Table 5) states unquestionably that there is a cooperative effect which overcompensates inductive effects of the naphthalene system. This value is almost in the range of *mono*iminophosphoranes, for example IPNMe (Table 5), and even considerably higher than most ordinary guanidines,[19a,20c,48] certainly aromatic amines.[49]

Table 5. Relative basicity values.

Base	pK_{BH+} (MeCN)
Vinamidine (VA)	31.94[18]
$(Me_2N)_3P=NMe$ (IPNMe)	27.58[20c,50] / 24.49[51] (MeNO$_2$)
$(Me_2N)_3P=NH$ (IPNH)	≈ 26.15[a] / 23.12[51] (MeNO$_2$)
MTBD	25.43[19b, 20c]
TMGN (1)	25.1[b]
$(Me_2N)_2C=NMe$ (PMG)	25.00[20c]
DBU	24.32[20c]
$(Me_2N)_2C=NH$ (TMG)	23.3[20c]
$(Me_2N)_2C=NPh$ (TMPhG)	20.6[19a,21a]
DMAN	18.18[5,52]
Quinolino[7,8-h]quinoline (QQ)	12.8[14b] (DMSO)

[a] Calculated from the difference of IPNMe and IPNH in MeNO$_2$. [b] Present work.

Estimation of pK_{BH+} values by ^{1}H-NMR transprotonation studies.[43,44,45] The basicity of novel bases can be estimated by ^{1}H-NMR transprotonation studies with bases of known pK_{BH+} as a reference, which differs by not more than ± 2 pK_{BH+}-units. Equimolar amounts of the reference base and the conjugate acid of the base in question are dissolved in the same solvent as the reference indicates. In an acid-base reaction the substance reaches an equilibrium state with the reference. Integration of the separate set of signals for the base investigated and its conjugate acid provides the information necessary in order to calculate the rate constant (K). The pK_{BH+} value then can be calculated from the rate constant (equations 1 to 7).

In some cases, when the base is kinetically highly active, it is unavoidable to record low temperature NMR-spectra in order to achieve baseline-separation of the sets of signals by lower rates of proton exchange. Employment of sterically hindered bases and the use of spectrometers working at high frequencies (>400 MHz) or a combination of both may also avoid the coalescence of signals.

(1) $[AH^+] + [B] \; \underset{\leftarrow}{\overset{\rightarrow}{}} \; [A] + [BH^+]$
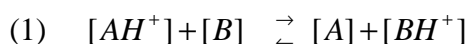
Acid-base equilibrium (A: base investigated; B: base of know pK_{BH+})

(2) $K = \dfrac{[A] \cdot [BH^+]}{[AH^+] \cdot [B]}$

Rate constant (K) of the acid-base equilibrium.

If the reference base and the conjugate acid of the investigated substance are employed in equimolar amounts, the following simplification can be made:

(3) $[AH^+] = [B] \quad und \quad [A] = [BH^+]$

Thus, it is only necessary to receive separate signals of one acid-base pair in case the other is inaccessible because of signal overlap.

For the rate constant (K) can be concluded:

$$(4) \quad K = \frac{[A]^2}{[AH^+]^2} \quad bzw. \quad K = \frac{[BH^+]^2}{[B]^2}$$

Integration of the signals corresponds directly to the molar amounts present in the equilibrium.

$$(5) \quad K = \frac{[A]^2}{[AH^+]^2} = \frac{I_A^2}{I_{AH^+}^2}$$

The unknown pK_{BH+} value is calculated from the following equations:

$$(6) \quad \log K_{(A,B)} = \Delta pK_{BH+}(A,B)$$

Whereas the algebraic sign of ΔpK_{BH+} is determined by the qualitative analyses of the experimental spectrum indicating the stronger base.

$$(7) \quad pK_{BH+}(A) = pK_{BH+}(B) + \Delta pK_{BH+}(A,B)$$

Kinetic activity. From the pK_{BH+} determination it became clear that, in contrast to the known slow proton transfer to and from classical „proton sponges"[16a,b,24,29] **1** allows rather fast rates of proton-exchange which is required for applications as auxiliary bases in base-catalyzed reactions. This tendency in kinetic activity may also be understood by the optical impression in the comparison of TMGN, DMAN, and their *mono*protonated forms along with QQ as free base in an illustration with space-filling models (Figure 5). The steric situation around the basic centers is much more congested in the environment of DMAN than for TMGN, which shows considerably less steric shielding, QQ appears to be practically unshielded.

TMGN (**1**)
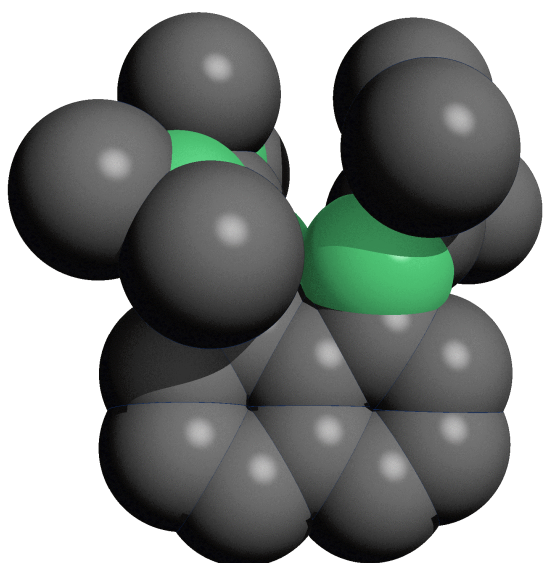
[**1**-H][PF$_6$]
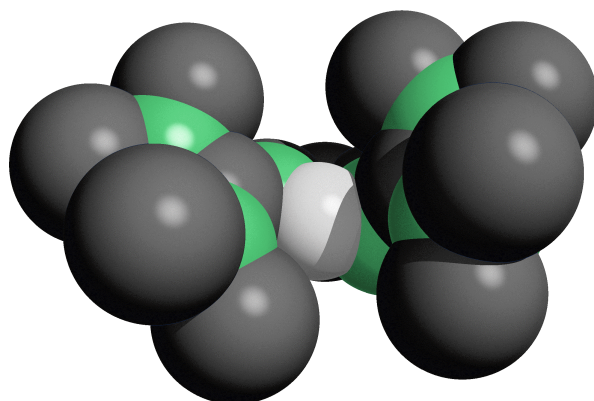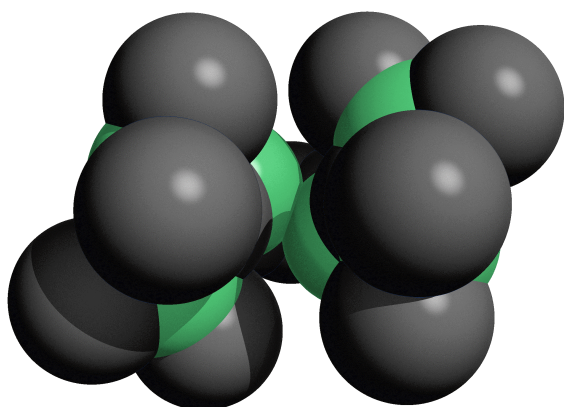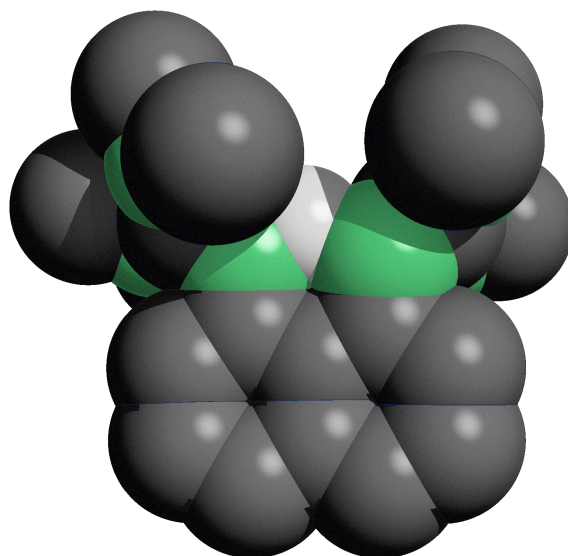
Quinolino[7,8-*h*]quinoline (QQ)
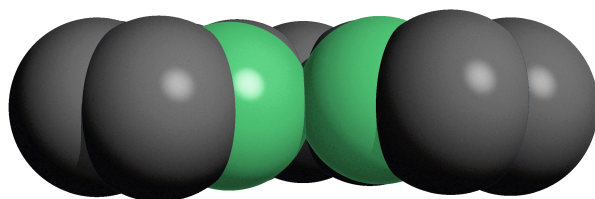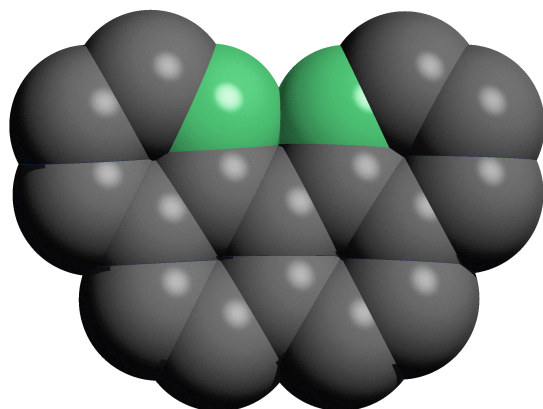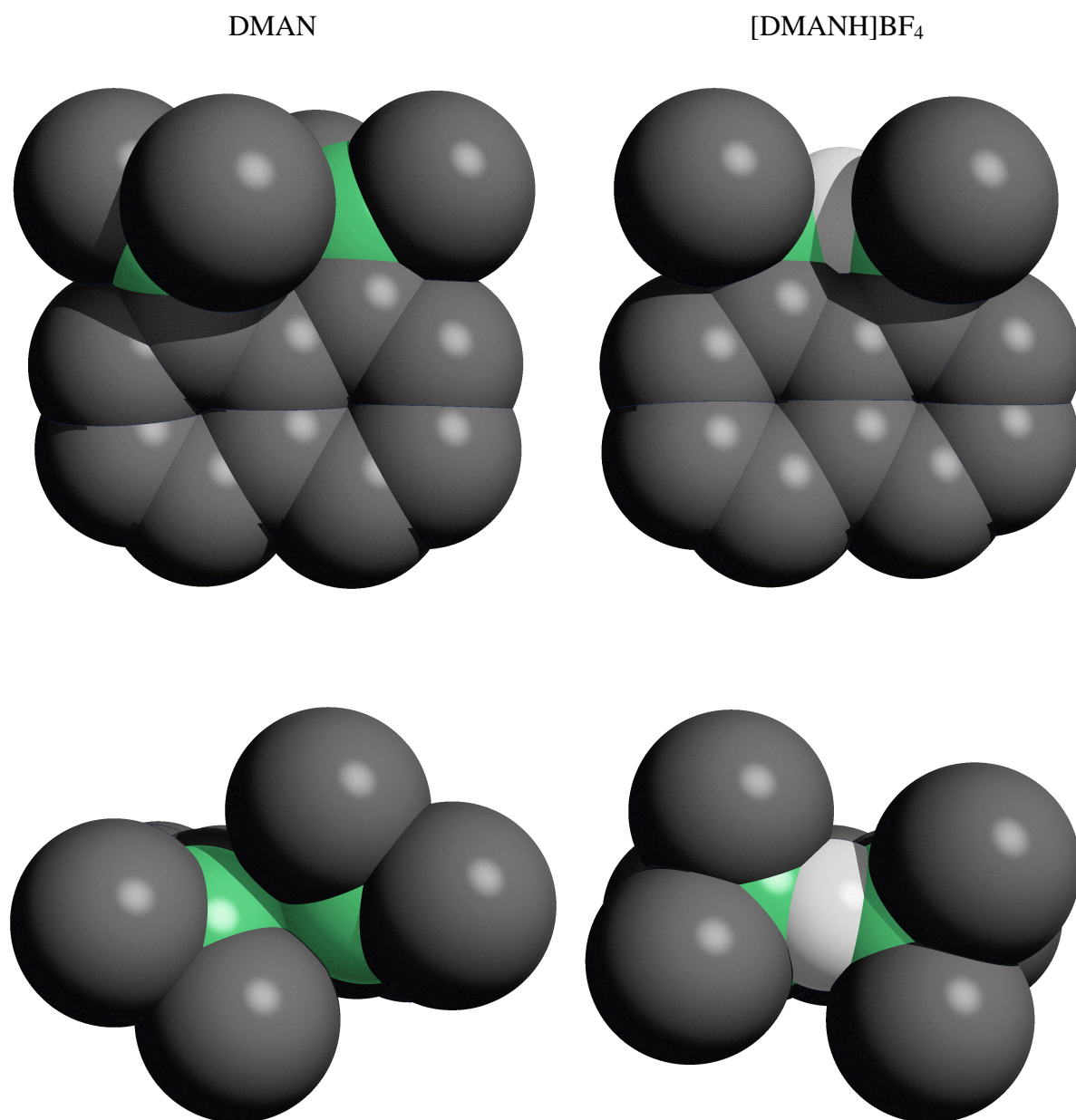
DMAN　　　　　　　　　　　　　　　　　[DMANH]BF$_4$

Figure 5. Space-filling illustration of steric shielding around the N-centers of TMGN, TMGNH$^+$, DMAN, DMANH$^+$, and QQ in two projections.[71]

The trend in kinetic activity will be demonstrated in particular by comparing the proton self-exchange rates between the free base (**1**) and the *mono*protonated form (**2a**) relative to the system DMAN / DMANH^{+}[53] as a criterion for kinetic activity. Equimolar amounts of **1** and **2a** were dissolved in CD$_3$CN and ^{1}H NMR spectra of the mixture recorded at temperatures ranging from 344 to 225 K with a coalescence signal at 300 K (500 MHz). The free energy of protonation was determined to be 59.3 kJ/mol from an Eyring plot that resulted from a line shape analysis of the variable-temperature ^{1}H NMR spectra (Figure 6).[54] However, no coalescence could be observed for DMAN / DMANH^{+}, either in CD$_3$CN or [D$_6$]DMSO up to temperatures of 336 and 371 K, respectively.[55] Therefore, it can be estimated that DMAN should exhibit a free energy of proton-exchange of > 65.5 (CD$_3$CN) or > 72.6 kJ/mol ([D$_6$]DMSO), respectively, which is in the range of the activation enthalpy estimated for the exchange of D^{+} in DMAN / DMAND^{+}.[56]
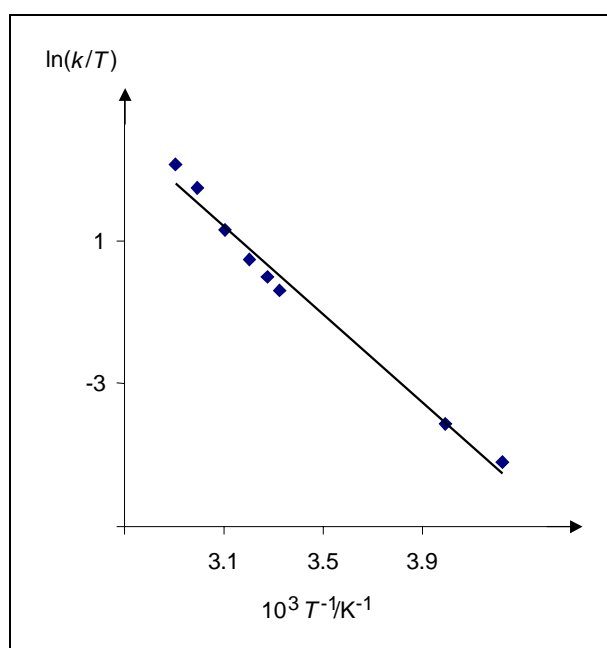

Figure 6. Eyring plot from proton self-exchange experiments of **1** / **2a**.

NMR spectra and molecular dynamics. The intrinsic dynamic behavior of the guanidine group, combined with the change in structure as a result of protonation, leads to complex intramolecular exchange processes which were investigated by dynamic ^{1}H NMR spectroscopy.

Free base 1. Compound **1** exhibits one signal for the methyl groups at room temperature. At lower temperatures, this signal splits into two signals of equal intensity (Figure 7), with a coalescence point at T_c = 253 K (400 MHz), which is attributed to hindered rotation about the C=N double bond (Scheme 6). This is caused by the typical *syn/anti*-isomerization of guanidines, which is already documented in the literature for other guanidine[25,57,58] and TMG[59] systems.
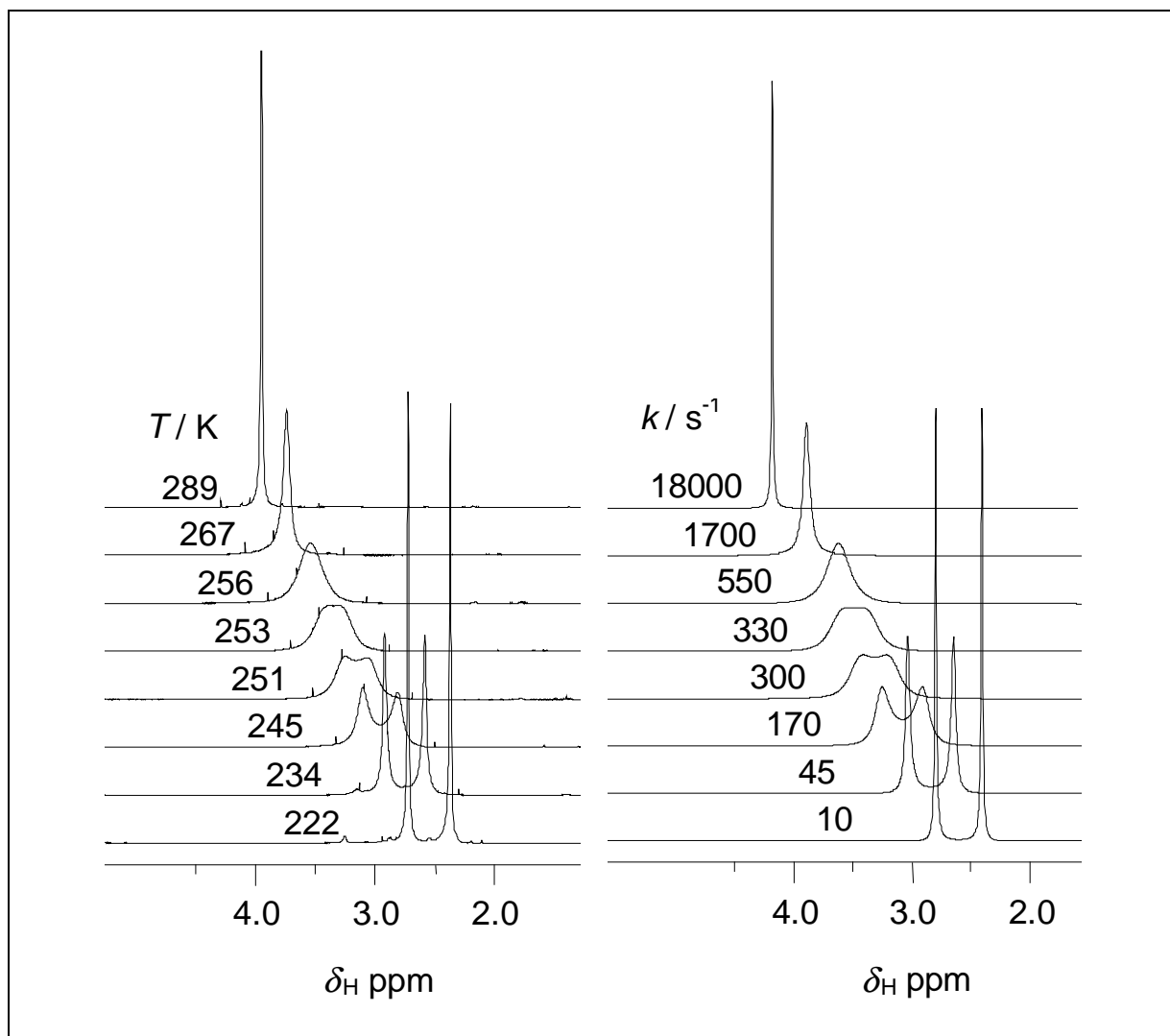

Figure 7. Temperature dependent ^{1}H NMR spectra at 400 MHz for the *N*-methyl singlet of TMGN (**1**) in CD$_2$Cl$_2$ (experimental spectra: left, simulated by iterative fitting:[54] right).

Generally, this isomerization can be caused by rotation or inversion, but in the case of **1**, only the rotation has to be considered for steric reasons and inversion is unlikely. At ambient temperature, the protons of the two *N*-dimethylamino units are equivalent. Thus, a flip mode[60] with two separate ground-state conformers as investigated by fluorescence

spectroscopy and *ab initio* calculations,[7c] such as that observed in DMAN, where free rotation is impossible because of the repulsion between the methyl groups, cannot be present. Within the guanidine base **1**, the C-NR$_2$ single bonds rotate rapidly with respect to the NMR time scale, even at low temperatures.[61]
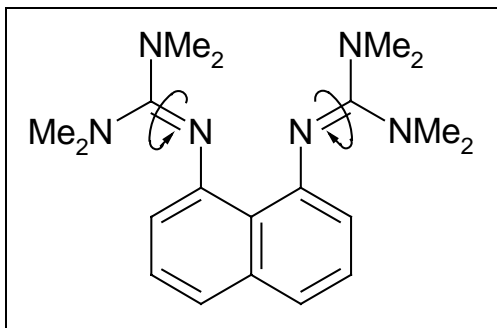
Scheme 6. Rotation about C=N bonds in TMGN (**1**).

From an Eyring plot, the free energy of activation $\Delta G^{\ddagger}$ for **1** was determined to 49.0 kJ/mol (256 K), which corresponds to be 49.3 kJ/mol at 238 K (Figure 8). This value is in agreement with the 50.7 kJ/mol (at T_c = 238 K, 60 MHz) measured with TMPhG.[59a] Of course, these values vary from alkyl substituted guanidines, which exhibit a reasonably higher barrier of activation (PMG: $\Delta G^{\ddagger}$ = 78.7 kJ/mol at T_c = 351 K, 100 MHz[58d]) because the C=N double bond is not weakened due to inductive effects of the aromatic system. In **1** however, a considerable weakening of the C=N bond order is realized by inductive effects of the naphthalene ring.
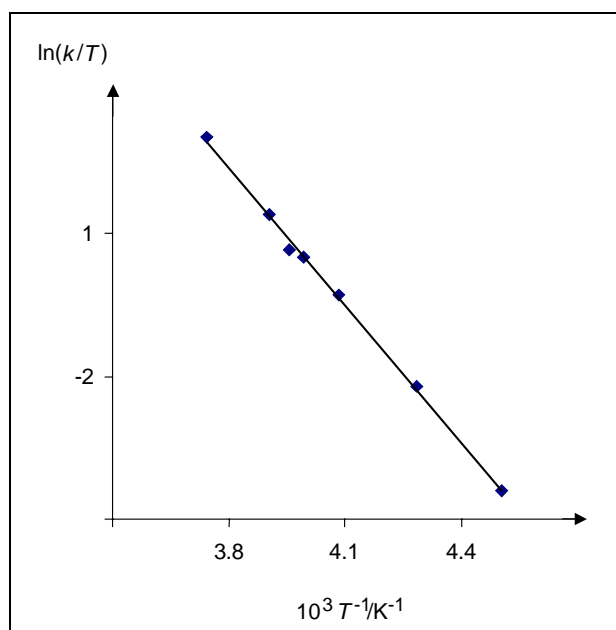

Figure 8. Eyring analysis of rates of interconversion in TMGN (**1**).

*Mono*protonated 1. The low-temperature ^{1}H NMR spectrum of **2a** reveals four separate resonances (1:1:1:1) at 190 K (Figure 9) and is markedly more complicated than that of the free base **1**. It also differs significantly from the known spectra of [HTMPhG][+] and [PMPhG][+].[57]

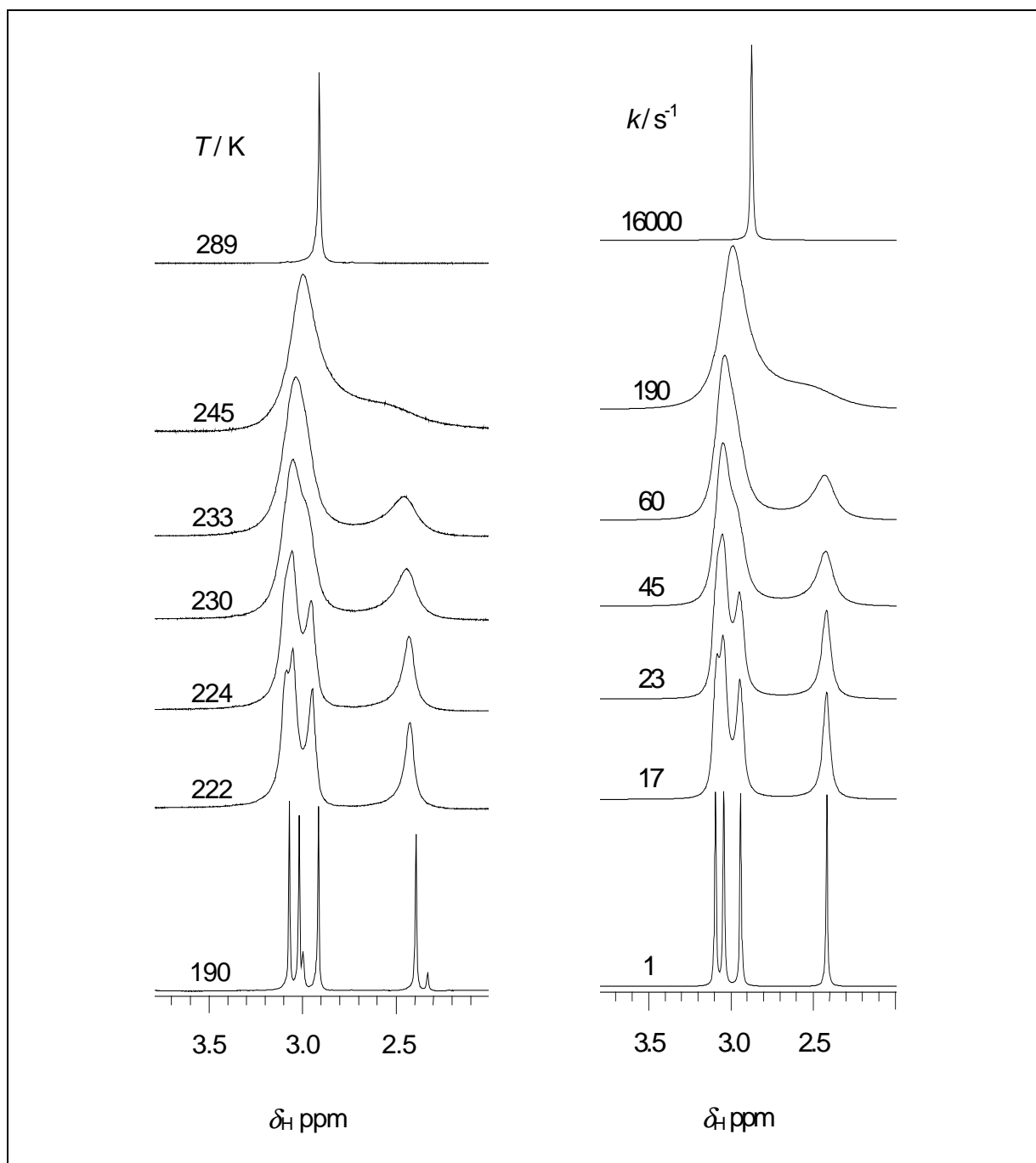**Figure 9.** Temperature dependent ^{1}H NMR spectra at 400 MHz for the *N*-methyl singlet of [**1**-H][PF$_6$] (**2a**) in CD$_2$Cl$_2$ (experimental spectra: left, simulated by iterative fitting:[54] right).

The fact that **2a** also exhibits real „proton sponge" properties in solution with a rapidly exchanging proton in an IHB (Scheme 7), is documented in the number of aromatic proton signals, along with the number of methyl signals in the range of fast exchange. Unsymmetrical protonation would result in six resonances in the aromatic region and two for the methyl signals. In **2a** only three aromatic signals and one methyl signal is observed, indicating the equivalence of both basic centers. Now two exchange phenomena are possible, leading to the four methyl resonances at in the low-temperature spectrum. A single concerted process with all four of the guanidine units exchanging at the same time. Otherwise, one rotation would be preferably restricted if the energy content of the partial double bonds would significantly differ from each other (probably as a result of conjugation of the former C=N double bond with the aromatic ring system). The latter should first cause a symmetrical split (1:1) into two singlets, followed by a second split of the two singlets at even lower temperatures into another set of singlets, which can in part be seen in [RTMPhG]$^+$ (R = H, Me).[57]
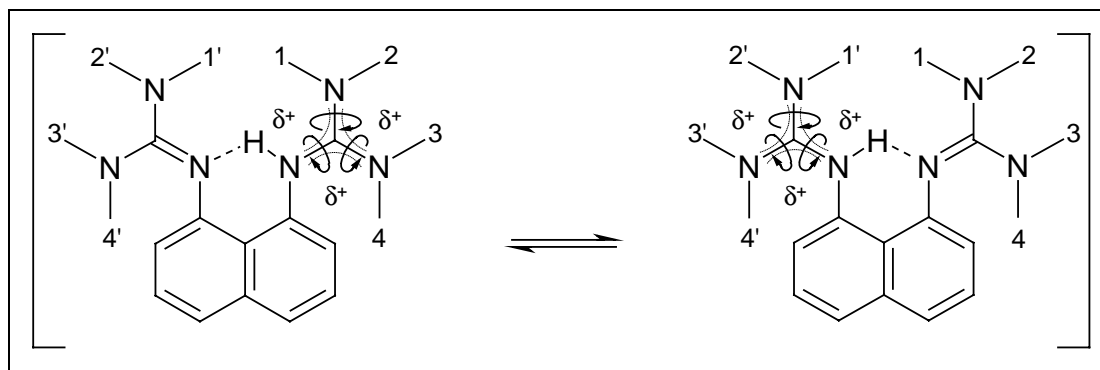
Scheme 7. Rotation about partial C=N bonds in [**1**-H][PF$_6$] (**2a**) with proton-equilibration.

There are several indications of a single concerted process in the variable-temperature spectra of **2a**. In the ^{1}H NMR spectra of **2a** recorded below 249 K (T_c^1), firstly an unsymmetrical separation of the singlet for the *N*-methyl protons with an intensity of 3:1 becomes visible; this excludes a sequential process. Thereafter, the downfield signal gradually splits into three singlets (1:1:1) that exhibit a similar chemical shift which is significantly different from the signal at higher field (for studies on mesomeric cations see ref. [62]). Moreover, the concerted process is confirmed by free energies of activation of the three observable coalescence phenomena that are obtained from an Eyring plot (Figure 10) and are very similar with $\Delta G^{\ddagger}_1$ (249 K) = 48.7, $\Delta G^{\ddagger}_2$ (231 K) = 48.6 and $\Delta G^{\ddagger}_3$ (224 K) = 48.5 kJ/mol (all recorded at 400 MHz). Furthermore, the line shape analysis on the basis of a single concerted process as the

exchange mechanism leads to an excellent agreement with the obtained experimental spectra (Figure 9). In addition, the $\Delta G^{\ddagger}$ values determined from the resulting Eyring plot are in good agreement with those received from the calculations based on the experimental coalescence points. They are in the range of the activation barriers found in [HTMPhG]$^{+[57c]}$ ($\Delta G^{\ddagger}_1$ (248 K) = 52.3, $\Delta G^{\ddagger}_2$ (248 K) = 54.0 and $\Delta G^{\ddagger}_3$ (225 K) = 46.9 kJ/mol, all recorded at 60 MHz) and quite contradictory to [PMPhG]$^{+[57a]}$ (only $\Delta G^{\ddagger}_1$ (301 K) = 64.9 and $\Delta G^{\ddagger}_2$ (227 K) = 46.5 kJ/mol were determined, 60 MHz). These findings are well in accordance with the values of benzyl-substituted guanidinium salts which show considerably higher free energies of activation ([Bz$_2$TMG]$^+$:$\Delta G^{\ddagger}$ (at T_c = 276 K, 60 MHz) = 61.1 kJ/mol$^{[58b]}$) since there is no weakening of the C=N double bond by the adjacent aromatic system resulting in lower energy barriers. In summary, the described behavior is a convincing argument that a true IHB with a rapidly equilibrating proton is formed, both guanidine groups are indiscriminate within the observed temperature region (as is reported for the NMe$_2$ units of DMANH$^{+[56]}$). Therefore, [**1**-H][PF$_6$] (**2a**) is assumed to possess a symmetrical double minimum energy profile with a low barrier of transition.[5,63]
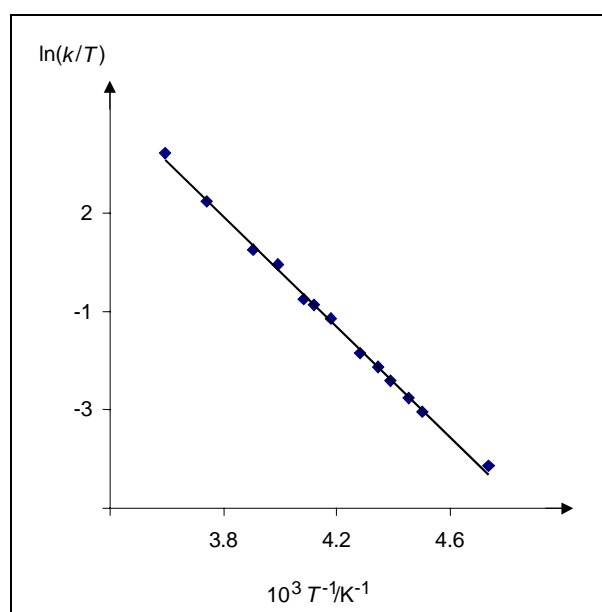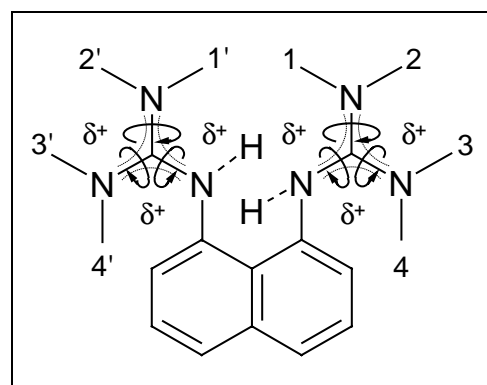

Figure 10. Eyring analysis of rates of interconversion in [**1**-H][PF$_6$].

Scheme 8. Rotation about partial C=N bonds in [TMG$_2$NH$_2$]$^{2+}$.

Bisprotonated 1. On account of the insolubility of hydrochloride **3a** in CD_2Cl_2 at low temperatures, the triflate **3c** was employed for the kinetic NMR studies. The low-temperature ^1H NMR spectra of [**1**-H_2][OTf]$_2$ (**3c**) resemble those of [**1**-H][PF$_6$] (**2a**) down to a temperature of 222 K. The split of the methyl resonances follow the same interpretation, and it becomes clear that the proton exchange in the IHB of **1**-HPF$_6$ (**2a**) does not affect the splitting of the signal, otherwise the spectra of *mono-* and *bis*protonated **1** should differ.

The free energies of activation for the first three coalescences (similar to **2a**), are calculated from the coalescence points in the experimental spectra: $\Delta G^{\ddagger}_{1/2/3}$ = 48.2 / 47.3 / 45.4 kJ/mol (T_c = 256 / 235 / 226 K). In the TMGN system and its protonated species, contrary steric and electronic effects seem to interfere. Thus, it cannot be clearly stated from the $\Delta G^{\ddagger}$ values, that as one would expect, the more the guanidine groups are protonated, the more the double bond character of the C=N bond is reduced and the barrier to rotation should decrease: Further reduction is achieved from *mono-* to *bis*protonated species, one proton has no longer to be shared between two guanidine groups and as a result the individual bond characters – single versus double – are less pronounced (Scheme 8). Therefore, the trend of the $\Delta H^{\ddagger}$ values has to be approached with great care since the value for [**1**-H_2][OTf]$_2$ (**3c**) is hampered with a rather large experimental error,[64] although in relative view this row demonstrates the expected effect (Table 6). The steric effect of the N-H protons in the *bis*protonated species obviously is of less significance – the free energy is lower than for the guanidine methyl groups despite smaller contact distance ($\Delta G^{\ddagger}_{298}$ = 47.1(**3a**) vs. 48.3 (**1**) and 49.2 (**2a**) kJ/mol, Table 6).

Table 6. Free activation energies and enthalpies of rotation, *syn/anti*-conformation and self-exchange in the *bis*(guanidine) „proton sponge" system.[a]

Compound	$\Delta G^{\ddagger}_{298}$ [kJ/mol][65]	$\Delta G^{\ddagger}_{256}$ [kJ/mol][65]	$\Delta H^{\ddagger}$ [kJ/mol][65]
TMGN (**1**)[b]	48.3±0.1	49.0±0.1	53.4±0.3
[TMGNH]PF$_6$ (**2a**)[b]	49.2±0.1	48.8±0.1	46.5±0.3
[TMGNH$_2$]OTf$_2$ (**3c**)[64]	51.9±1.0	48.2±0.1[c]	27.0±3.0
[TMGNH$_2$]OTf$_2$ (**3c**)[b]	47.1±0.1	45.6±0.1	36.1±0.3
syn/anti-N-H			
TMGN / [TMGNH]$^+$ [b]	59.3±0.1	58.2±0.1	51.6±0.3
self-exchange			

[a] Activation entropy is omitted due to large error of its determination.[66] [b] Calculated from graphical analysis of rate constants obtained from simulated spectra.[67] [c] Value obtained from coalescence points of experimental spectrum.[68]

Below 222 K further coalescence phenomena are observed, the exchange rates between the *syn*- and *anti*-conformation become detectable. Finally, at 190 K (400 MHz) no less than seven resonances are recorded for the guanidine methyl groups with two additional signals for the N-H protons (Figure 11).
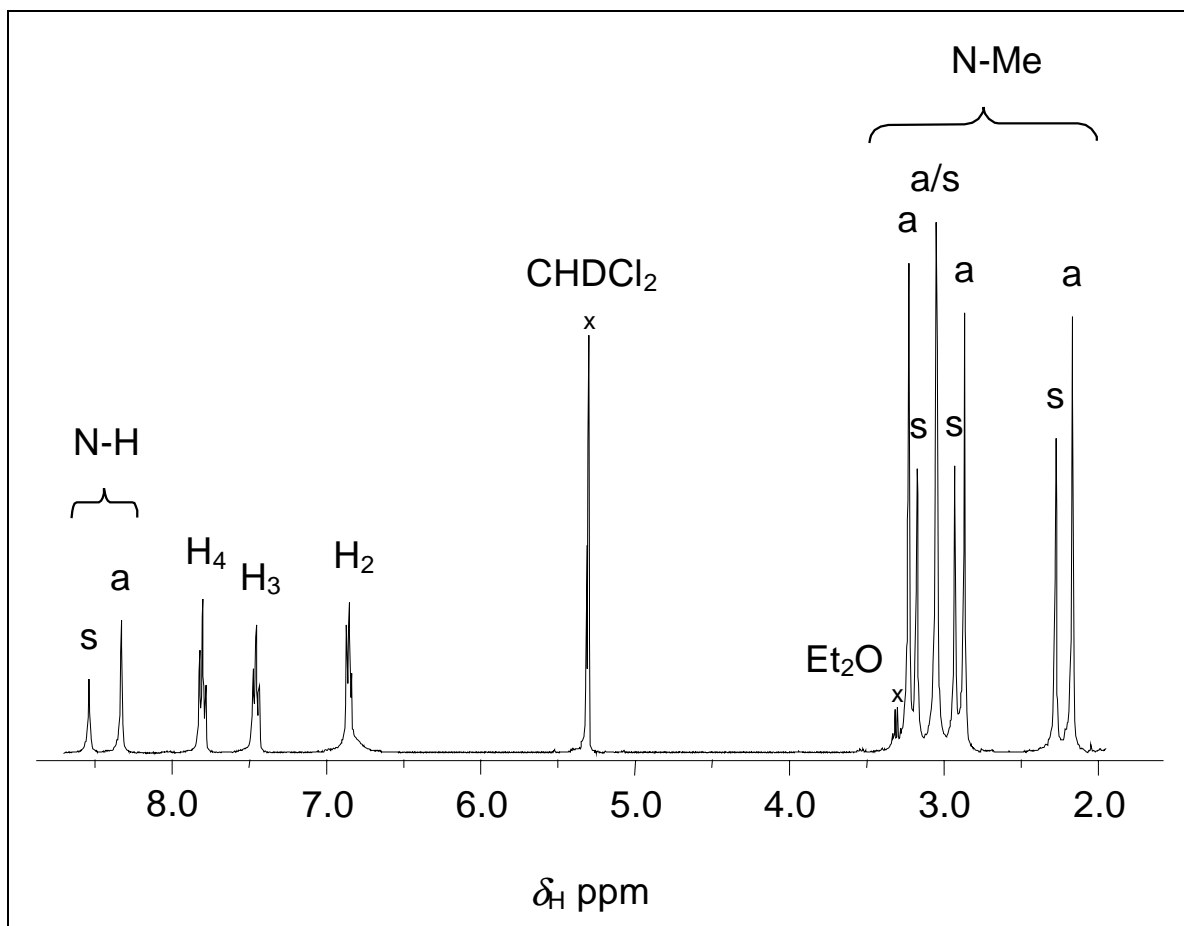

Figure 11. Low temperature (190 K) ^{1}H NMR spectrum (400 MHz) of [**1**-H$_2$][OTf]$_2$ in CD$_2$Cl$_2$.

Integration of the signals reflects a *syn*/*anti*-population ratio of 42:58. In agreement with our preliminary crystal structure determination on **3b** and theoretical calculations on the gas-phase structure of *bis*protonated **1**,[47] it is assumed that the *anti*-conformer is predominant in solution, especially if noncoordinating counteranions are employed. From the corresponding Eyring plot, the free energy of activation for the *syn*/*anti*-equilibrium is calculated to be $\Delta G^{\ddagger}_{298} = 47.1$ kJmol^{-1} (Figure 12). It is interesting to note that in the *bis*protonated **3c**, the $\Delta G^{\ddagger}_{298}$ value for the free energy of the *syn*/*anti*-process (47.1 kJmol^{-1}) is lower than the barrier to rotation (51.9 kJmol^{-1}) about the C=N bonds.
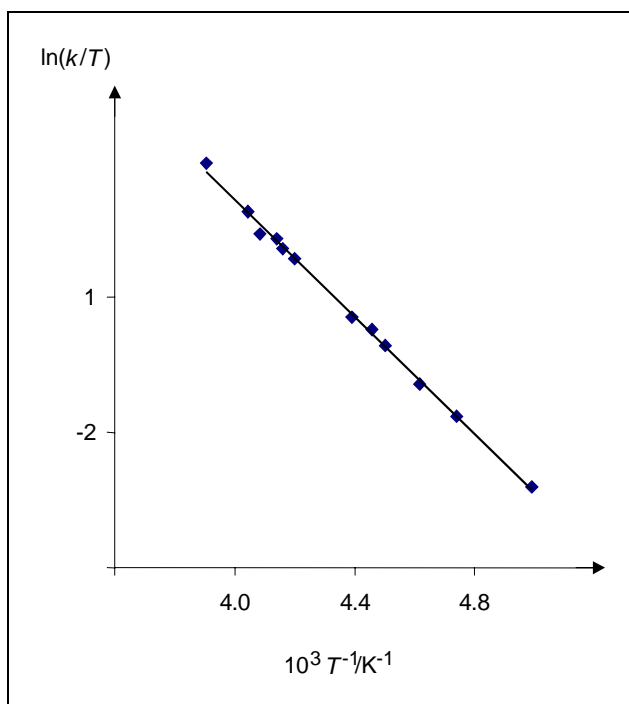
Figure 12. Graphical analysis of rate constants determined from spectra simulation for the *syn*/*anti*-conformation equilibrium of [**1**-H$_2$][OTf]$_2$ (**3c**).[69]

Unfortunately, in an attempt of a structural solution the triflate anions were found to be severely disordered, which accounts for R values of $\approx$ 9 for [**1**-H$_2$][OTf]$_2$ (**3c**), similar to a structure resolution of an amide „proton sponge" published by Lectka.[6d] It can be presumed that, based on this structural evidence, a *syn*-conformation analogous to [**1**-H$_2$][Cl, Cl$_2$H] (**3a**) is realized, and therefore *syn* should be the favored population expressed in the low-temperature NMR spectrum (Figure 11) if the interaction of the cation [**1**-H]$^+$ and an anion is taken into consideration.

Conclusion

TMGN (**1**) is a readily accessible and extremely basic guanidine derivative with the classical „proton sponge" backbone of DMAN. To date it is the most basic compound in the class of naphthalene-based „proton sponges". TMGN (**1**) has an experimentally determined pK_{BH+} value of 25.1±0.2 (MeCN) revealing a thermodynamic basicity nearly seven orders of magnitude higher than the parent DMAN. On the other hand TMGN (**1**) also has a much higher kinetic basicity than DMAN, which is demonstrated by the kinetics of its proton self-exchange ($\Delta G^{\ddagger}_{298}$ = 59.3±0.1 kJ/mol). On account of this high kinetic activity, the *mono*protonated [**1**-H]$^+$ may take up a second proton if treated with excess of strong acid.

TMGN is more stable to hydrolysis in comparison to the commercially available guanidine MTBD and less nucleophilic towards alkylating agents such as C_2H_5I. Dynamic ^{1}H NMR studies on *mono-* and *bis*protonated TMGN reveal a concerted mechanism of rotation about three close to equivalent C-N bonds. Furthermore, it is shown that there is an equilibrium between a *syn-* and an *anti*-conformation with respect to both guanidine functionalities of the *bis*protonated **3c**. The base and corresponding acids are spectroscopically and structurally characterized. It is anticipated that a high thermodynamic basicity combined with a high kinetic activity is interesting for base-catalyzed applications.

Experimental Section

Materials and methods:

All experiments were carried out in glassware assembled while hot and cooled under vacuum in an inert atmosphere of argon 4.8 dried with P_4O_{10} granulate. Solvents and triethylamine were purified according to literature procedures and also kept under inert atmosphere. 1,8-Diaminonaphthalene (Merck) was purified by distillation from zinc dust.[70] NH_4PF_6, NH_4ClO_4, trifluoromethanesulfonic acid (Aldrich), aqueous HPF_6 (60-65%, Strem Chemicals), HCl gas (MERCK), ethyl iodide (Fluka) for protonation and alkylation, respectively, were used as purchased. Substances sensitive to moisture and air were kept in nitrogen-flushed glove-box (Braun, Type MB 150 BG-I). Spectra were recorded on the following spectrometers: - NMR: Bruker DRX 500, DRX 400 and AMX 300, - IR: Bruker IFS 88 FT, - UV/Vis: Hitachi U-3410, - MS(EI, 70 eV): Varian MAT CH-7a, - MS(FD): Finnigan MAT 95 S, - MS (ESI): Hewlett Packard HP 5989 B, Elemental Analysis: Heraeus CHN-Rapid, Melting points: Büchi MP B-540 (uncorrected).

Line shape analysis:

The line shape analysis of the variable-temperature ^{1}H NMR spectra were analyzed with the dynamic NMR simulation program WIN-DYNA.[54] Errors are quoted as defined by Binsch and Kessler.[66]

Caution! Phosgene is a severe toxic agent that can cause pulmonary embolism and in case of heavy exposition may be lethal. Use only at a good ventilated fume hood.

Tetramethylchlorformamidinium chloride:[26]

Phosgene was passed through a solution of tetramethylurea (50 g) in toluene (200 mL) kept at 0 °C in a flask equipped with a reflux condenser cryostated to -30 °C for 2 h. After that time the phosgene inlet was cut off and the solution was allowed to warm to room temperature. The mixture was stirred for another 24 h, while the the reflux condensor was maintained at -30 °C. The white precipitate was filtered off, washed three times with dry ether and dried in vacuo. Yield: $\approx 95\%$.

1,8-Bis(1,1,3,3-tetramethylguanidino)naphthalene (1, TMGN):

A solution of the Vilsmeyer salt $[(Me_2N)_2C\text{-}Cl]Cl$ (10.26 g, 60.0 mmol) in acetonitrile (30 mL) was added under cooling on an ice bath to a solution of 1,8-diaminonaphthalene (4.8 g, 30.0 mmol) and triethylamine (6.1 g, 8.5 mL, 60.0 mmol) in acetonitrile (50 mL). After the exothermic reaction, the mixture was refluxed for 3 hours and a clear solution developed. Subsequently, NaOH (2.4 g, 60.0 mmol) in water (15 mL) was added under vigorous stirring in order to deprotonate the $HNEt_3Cl$. After removal of the solvent as well as excess NEt_3, the precipitate was washed three times with dry ether to remove unreacted amine, and was then dried in vacuo. TMGN (**1**) was obtained by complete deprotonation of the bis(hydrochloride) with 50% KOH (50 mL) and extraction of the aqueous phase with MeCN (3×50 mL). The combined filtrates were evaporated to dryness and taken up in warm hexane (100 mL). The solution was dried over $MgSO_4$, stirred with activated charcoal to eliminate impurities, and filtered warm through Celite. Recrystallization from hexane and drying in vacuo gave **1** as weakly beige crystals in (9.03 g, 25.5 mmol, 85%).

M.p. 123 °C; ^{1}H NMR (400.1 MHz, CD_3CN, 25 °C): δ = 7.19 (d, $^3J(H_4,H_3)$ = 8.3 Hz, 2 H; $H_{4,5}$), 7.13 (dd, $^3J(H_3,H_4) \approx {}^3J'(H_3,H_2) \approx$ 7.5 Hz, 2 H; $H_{3,6}$), 6.23 (d, $^3J(H_2,H_3)$= 6.8 Hz, 2 H; $H_{2,7}$), 2.65 (s, 24 H; CH_3) ppm; ^{1}H NMR (400.1 MHz, $[D_6]DMSO$, 25 °C): δ = 7.16-7.09 (m, 4 H; $H_{3\text{-}6}$), 6.16 (dd, $^3J(H_2,H_3)$ = 6.7 Hz, $^4J(H_2,H_4)$ = 1.6 Hz, 2 H; $H_{2,7}$), 2.62 (s, 24 H; CH_3) ppm; ^{1}H NMR (400.1 MHz, CD_2Cl_2, 28 °C): δ = 7.21 (dd, $^3J(H_4,H_3)$ = 8.3 Hz, $^4J(H_4,H_2)$ = 1.3 Hz, 2 H, $H_{4,5}$), 7.15 (dd, $^3J(H_3,H_4) \approx {}^3J'(H_3,H_2) \approx$ 7.5 Hz, 2 H; $H_{3,6}$), 6.27 (dd, $^3J(H_2,H_3)$ = 7.1 Hz, $^4J(H_2,H_4)$ = 1.5 Hz, 2 H; $H_{2,7}$), 2.66 (s, 24 H; CH_3) ppm; ^{1}H NMR (400.1 MHz, CD_2Cl_2, -73 °C): δ = 7.18 (d, $^3J(H_4,H_3)$ = 8.0 Hz, 2 H; $H_{4,5}$), 7.12 (dd, $^3J(H_3,H_4) \approx {}^3J'(H_3,H_2) \approx$ 7.5 Hz, 2 H; $H_{3,6}$), 6.29 (d, $^3J(H_2,H_3)$ = 7.2 Hz, 2 H; $H_{2,7}$), 2.71 (s, 12 H; CH_3), 2.32 (s, 12 H; CH_3) ppm; ^{13}C NMR (100.6 MHz, CD_3CN, 25 °C): δ = 155.0 (CN_3), 150.7, 137.4, 126.1,

30

119.8, 115.7 (aromat. C), 39.4 (CH$_3$) ppm; ^{13}C NMR (100.6 MHz, [D$_6$]DMSO, 25 °C): δ = 154.0 (CN$_3$), 150.1, 136.7, 125.9, 122.7, 119.6, 115.2 (aromat. C), 39.7 (CH$_3$) ppm; IR (KBr): nu(tilde) = 3440 w(br), 3002 w, 2937 m, 1630 vs, 1593 s, 1558 s, 1493 s, 1452 m, 1431 m, 1371 s, 1233 m, 1135 s, 985 m, 830 m, 760 m cm^{-1}; UV/Vis (MeCN, c = 2 × 10^{-5} molL^{-1}): λ_{max} (ϵ) = 349.0 (15600), 235.0 (46000), 213 nm (36300); MS (FD, MeCN): m/z (%) = 354 [M]$^+$; MS (EI, 70 eV): m/z (%) = 354.0 (86.5) [M]$^+$, 310.0 (7.7) [M-NMe$_2$]$^+$, 253.0 (26.1) [M-C(NMe$_2$)$_2$]$^+$, 100.0 (55.9) [C(NMe$_2$)$_2$]$^+$, 85.0 (100) [C$_4$H$_9$N$_2$]$^+$; elemental analysis calcd. (%) for C$_{20}$H$_{30}$N$_6$ (354.50): C 67.76, H 8.53, N 23.71; found C 67.55, H 8.53, N 23.53.

1,8-Bis(1,1,3,3-tetramethylguanidinium)naphthalene Hexafluorophosphate (2a, [1-H][PF$_6$]):

The *mono*protonated hexafluorophosphate salt was obtained by treatment of the free guanidine base **1** (354 mg, 1.00 mmol) with 1 eq. of NH$_4$PF$_6$ (160 mg, 0.98 mmol) dissolved in MeCN (15 mL) and stirring for 1 h at 50 °C. The solvent was evaporated the solid material was redissolved in MeCN. The solution was stirred over activated charcoal and passed through Celite. Removal of the solvent and crystallization from MeCN/Et$_2$O gave [**1**-H][PF$_6$] (**2a**) as colorless crystals in almost quantitative yield (476 mg, 0.95 mmol, 97%).

M.p. 255 °C; ^{1}H NMR (400.1 MHz, CD$_3$CN, 25 °C): δ = 14.28 (s, br, 1 H; NH), 7.40 (d, ^3J(H$_4$,H$_3$) = 8.3 Hz, 2 H; H$_{4,5}$), 7.34 (dd, ^3J(H$_3$,H$_4$) ≈ $^3J'$(H$_3$,H$_2$) ≈ 7.9 Hz, 2 H; H$_{3,6}$), 6.49 (d, ^3J(H$_2$,H$_3$) = 7.5 Hz, 2 H; H$_{2,7}$), 2.87 (s, 24 H; CH$_3$) ppm; ^{13}C NMR (100.6 MHz, CD$_3$CN, 25 °C): δ = 159.8 (CN$_3$), 142.9, 136.9, 126.7, 122.0, 114.2 (aromat. C), 39.9 (CH$_3$) ppm; IR (KBr): nu(tilde) = 3325 m, 2922 m, 1646 vs, 1547 s, 1473 m, 1431 m, 1410 m, 1371 m, 1278 vs, 1247 vs, 1171 s, 1153 s, 1068 m, 1034 vs, 848 m, 766 m, 639 s, 573 m, 517 m cm^{-1}; UV/Vis (MeCN, c = 2 × 10^{-5} molL^{-1}): λ_{max} (ϵ) = 348.0 (14300), 233.3 nm (50800); MS (FD, MeCN): m/z (%) = 355 [(**1**)H$_2$]$^+$; elemental analysis calcd. (%) for C$_{20}$H$_{31}$N$_6$PF$_6$ (500.5): C 48.00, H 6.24, N 16.79; found C 47.92, H 6.08, N 16.16.

1,8-Bis(1,1,3,3-tetramethylguanidinium)naphthalene Perchlorate (2b, [1-H][ClO$_4$]):

The *mono*protonated perchlorate salt was obtained by stirring **1** (354 mg, 1 mmol) and NH$_4$ClO$_4$ (115 mg, 0.98 mmol) in MeCN (15 mL) for 1 h at 50 °C. After Evaporation of the solvent the solid material was redissolved in dry MeCN, stirred over activated charcoal and

filtered through Celite. The volatiles were removed in vacuo and **2b** was crystallized from MeCN/Et$_2$O (428 mg, 0.94 mmol, 96%) as colorless crystals.

M.p. 229 °C (dec.); ^{1}H NMR (400.1 MHz, [D$_6$]DMSO, 25 °C): δ = 14.19 (s, br, 1 H; NH), 7.41-7.33 (m, 4 H; H$_{3-6}$), 6.50 (dd, ^3J(H$_2$,H$_3$)= 7.1 Hz, ^4J(H$_2$,H$_4$) = 1.0 Hz, 2 H; H$_{2,7}$), 2.87 (s, 24 H; CH$_3$) ppm; ^{1}H NMR (400.1 MHz, CD$_2$Cl$_2$, 28 °C): δ = 14.76 (s, br, 1H; NH), 7.40 (dd, ^3J(H$_4$,H$_3$) = 8.3 Hz, ^4J(H$_4$,H$_2$) = 1.1 Hz, 2 H; H$_{4,5}$), 7.33 (dd, ^3J(H$_3$,H$_4$) ≈ $^3J'$(H$_3$,H$_2$) ≈ 7.8 Hz, 2 H; H$_{3,6}$), 6.43 (dd, ^3J(H$_2$,H$_3$) = 7.4 Hz, ^4J(H$_2$,H$_4$) = 1.2 Hz, 2 H; H$_{2,7}$), 2.93 (s, 24 H; CH_3) ppm; ^{1}H NMR (400.1 MHz, CD$_2$Cl$_2$, -83 °C): δ = 14.63 (s, br, 1H; NH), 7.32 (dd, ^3J(H$_4$,H$_3$) = 8.2 Hz, ^4J(H$_4$,H$_2$) = 1.0 Hz, 2 H; H$_{4,5}$), 7.28 (dd, ^3J(H$_3$,H$_4$) ≈ $^3J'$(H$_3$,H$_2$) ≈ 7.6 Hz, 2 H; H$_{3,6}$), 6.30 (dd, ^3J(H$_2$,H$_3$) = 7.2 Hz, ^4J(H$_2$,H$_4$) = 1.0 Hz, 2 H; H$_{2,7}$), 3.08 (s, 6 H; CH$_3$), 3.03 (s, 6 H; CH$_3$), 2.93 (s, 6 H; CH$_3$), 2.40 (s, 6 H; CH$_3$) ppm; ^{13}C NMR (100.6 MHz, [D$_6$]DMSO, 25 °C): δ = 158.5 (CN$_3$), 142.0, 136.0, 126.1, 121.4, 117.6, 113.5 (aromat. C), 39.5 (CH$_3$) ppm; IR (KBr): nu(tilde) = 2917 m, 1617 m, 1559 s, 1467 m, 1405 s, 1371 m, 1352 m, 1235 w, 1163 m, 1088 s, 1015 w, 830 m, 769 m, 622 m cm^{-1}; UV/Vis (MeCN, c = 2 × 10^{-5} molL^{-1}): λ$_{max}$ (ε) = 348.2 (14400), 306.7 (6800), 233.3 nm (50500); MS (FD, MeCN): m/z (%) = 355 [(**1**)H$_2$]$^+$; elemental analysis calcd. (%) for C$_{20}$H$_{31}$N$_6$ClO$_4$ (455.0): C 52.80, H 6.87, N 18.47; found C 52.53, H 6.88, N 17.83.

1,8-Bis(1,1,3,3-tetramethylguanidinium)naphthalene Dichloride (3a, [1-H$_2$][Cl, Cl$_2$H]):
Gaseous HCl was bubbled into a solution of **1** (354 mg, 1 mmol) in CH$_2$Cl$_2$ (10 mL) for 5 minutes. The clear light yellow solution was stirred for 1 hour, precipitated and washed with dry ether. Crystallization from MeCN gave **3a** as colorless crystals (495 mg, 0.98 mmol, 98%). The product analyzed as an adduct of 1 molecule HCl and 1 molecule of CH$_3$CN.

M.p. 233 °C; ^{1}H NMR (400.1 MHz, CD$_3$CN, 25 °C): δ = 11.20 (s, 2 H; NH), 7.92 (d, ^3J(H$_4$,H$_3$) = 8.1 Hz, 2 H; H$_{4,5}$), 7.54 (dd, ^3J(H$_3$,H$_4$) ≈ $^3J'$(H$_3$,H$_2$) ≈ 7.9 Hz, 2 H; H$_{3,6}$), 7.02 (d, ^3J(H$_2$,H$_3$) = 7.2 Hz, 2 H; H$_{2,7}$), 4.33 (s, br, 1 H; Cl$_2$H), 2.94 (s, 24 H; CH$_3$) ppm; ^{13}C NMR (100.6 MHz, CD$_3$CN, 25 °C): δ = 161.3 (CN$_3$), 137.5, 133.8, 128.6, 127.1, 123.9, 123.1 (aromat. C), 41.0 (CH$_3$) ppm; IR (KBr): nu(tilde) = 3417 m, 3033 m, 2916 m, 1636 s, 1540 s, 1467 m, 1429 m, 1406 m, 1371 m, 1337 m, 1300 m, 1172 m, 1066 m, 1019 m, 796 m, 772 m cm^{-1}; UV/Vis (MeCN, c = 2 × 10^{-5} molL^{-1}): λ$_{max}$ (ε) = 346.7 (11800), 232.8 nm (50200); MS

(FD, MeCN): m/z (%) = 389 [[(**1**)H$_2$]Cl]$^+$, 354 [(**1**)H$_2$]$^+$; elemental analysis calcd. (%) for C$_{20}$H$_{32}$N$_6$Cl$_2$ × HCl × CH$_3$CN (427.4 × 36.5 × 41.1 (504.9)): C 52.33, H 7.19, N 19.42; found C 53.14, H 7.12, N 18.98.

1,8-Bis(1,1,3,3-tetramethylguanidinium)naphthalene Hexafluorophosphate-Tetrafluoro-borate (3b, [1-H$_2$][PF$_6$, BF$_4$]):

An impure, HBF$_4$ containing sample of aqueous hexafluorophosphoric acid (0.35 mL, 60-65%) was added dropwise to **1** (354 mg, 1 mmol) in CH$_2$Cl$_2$ (10 mL). Within seconds, a white precipitate developed which was washed with dry ether and dried in vacuo. The precipitate was recrystallized from MeOH to yield (554 mg, 0.92 mmol, 92%) **3b** as light brown crystals.

M.p. 227 °C; ^{1}H NMR (400.1 MHz, CD$_3$CN, 25 °C): δ = 7.94 (d, ^3J(H$_4$,H$_3$) = 8.3 Hz, 2 H; H$_{4,5}$), 7.84 (s, 2 H; NH), 7.58 (dd, ^3J(H$_3$,H$_4$) ≈ $^3J'$(H$_3$,H$_2$) ≈ 7.8 Hz, 2 H; H$_{3,6}$), 7.04 (d, ^3J(H$_2$,H$_3$) = 7.3 Hz, 2 H; H$_{2,7}$), 2.95 (s, 24 H; CH$_3$) ppm; ^{13}C NMR (100.6 MHz, CD$_3$CN, 25 °C): δ = 160.6 (CN$_3$), 137.2, 132.8, 128.6, 127.3, 123.1, 121.7 (aromat. C), 41.6 (CH$_3$) ppm; ^{19}F NMR (188.3 MHz, CD$_3$CN, 25 °C): δ = -70.9 (d, ^2J(F,P) = 706.6 Hz, PF$_6$), -149.6 (s, BF$_4$) ppm; ^{31}P NMR (162.0 MHz, CD$_3$CN, 25 °C): δ = -142.9 (sept, ^1J(P,F) = 706.5 Hz, PF$_6$) ppm; ^{11}B NMR (96.3 MHz, [D$_6$]DMSO, 25 °C): δ = -1.2 (s, BF$_4$) ppm; IR (KBr): nu(tilde) = 3383 m, 2950 m, 1637 s, 1544 s, 1473 m, 1434 m, 1409 m, 1344 m, 1299 m, 1281 m, 1167 m, 1065 m, 1022 m, 841 s, 762 m, 558 s cm^{-1}; MS (ESI pos, MeCN): m/z (%) = 501 [[(**1**)H$_2$]PF$_6$]$^+$, 441 [(**1**)H$_2$]BF$_4$]$^+$, 355 [(**1**)H$_2$]$^+$; MS (ESI neg, MeCN): m/z (%) = 145 [PF$_6$]$^-$, 87 [BF$_4$]$^-$; elemental analysis calcd. (%) for C$_{20}$H$_{32}$N$_6$BF$_{10}$P (588.3): C 40.83, H 5.48, N 14.29; found C 40.54, H 5.29, N 13.90.

1,8-Bis(1,1,3,3-tetramethylguanidinium)naphthalene Bistriflate (3c), [1-H$_2$][OTf]$_2$:

Compound **1** (354 mg, 1 mmol) diluted in dry Et$_2$O (30 mL) was added dropwise to triflouromethanesulfonic acid (0.9 mL, 10 mmol), which resulted in the instant precipitation of the *bis*protonated triflate salt. Subsequently, the suspension was stirred for another 2 h, and the precipitate was filtered and washed with dry Et$_2$O three times. Recrystallization from MeCN/Et$_2$O gave **3c** as colorless crystals (602 mg, 0.92 mmol, 92%).

M.p. 242 °C; ^{1}H NMR (400.1 MHz, CD$_3$CN, 25 °C): d = 8.08 (s, 2 H; NH), 7.93 (d, ^3J(H$_4$,H$_3$) = 8.3 Hz, 2 H; H$_{4,5}$), 7.57 (dd, ^3J(H$_3$,H$_4$) ≈ $^3J'$(H$_3$,H$_2$) ≈ 7.9 Hz, 2 H; H$_{3,6}$), 7.04 (d, ^3J(H$_2$,H$_3$) = 7.5 Hz, 2 H; H$_{2,7}$), 2.95 (s, 24 H; CH$_3$) ppm; ^{1}H NMR (400.1 MHz, CD$_2$Cl$_2$, 28 °C): δ = 8.51 (s, 2 H; NH), 7.86 (d, ^3J(H$_4$,H$_3$) = 7.7 Hz, 2 H; H$_{4,5}$), 7.52 (dd, ^3J(H$_3$,H$_4$) ≈ $^3J'$(H$_3$,H$_2$) ≈ 8.1 Hz, 2 H; H$_{3,6}$), 6.91 (d, ^3J(H$_2$,H$_3$) = 7.5 Hz, 2 H; H$_{2,7}$), 2.96 (s, 24 H; CH$_3$) ppm; ^{1}H NMR (400.1 MHz, CD$_2$Cl$_2$, -92 °C): δ = 8.54 (*syn*-population 42% × 2 H each NH), 8.34 (*anti*-population 58% × 2 H each NH), 7.87-7.75 (m, 2 H; H$_{4,5}$), 7.53-7.40 (m, 2 H; H$_{3,6}$), 6.93-6.75 (m, 2 H; H$_{2,7}$), 3.23 + 3.05 + 2.87 + 2.17 (*anti*-population 58% × 6 H each CH$_3$), 3.18 + 3.06 + 2.94 + 2.28 (*syn*-population 42% × 6 H each CH$_3$) ppm; ^{1}H NMR (400.1 MHz, CD$_2$Cl$_2$, 25 °C): δ = 8.51 (s, 2 H; NH), 7.86 (d, ^3J(H$_4$,H$_3$) = 7.7 Hz, 2 H; H$_{4,5}$), 7.52 (dd, ^3J(H$_3$,H$_4$) ≈ $^3J'$(H$_3$,H$_2$) ≈ 8.1 Hz, 2 H; H$_{3,6}$), 6.91 (d, ^3J(H$_2$,H$_3$) = 7.5 Hz, 2 H; H$_{2,7}$), 2.96 (s, 24 H; CH$_3$) ppm; ^{13}C NMR (100.6 MHz, CD$_3$CN, 25 °C): δ = 160.7 (CN$_3$), 137.2, 133.0, 128.6, 127.2, 123.2 (aromat. C), 40.6 (CH$_3$) ppm; IR (KBr): nu(tilde) = 3436 w(br), 2809 w, 1631 m, 1590 m, 1562 s, 1539 s, 1512 s, 1469 m, 1450 m, 1415 s, 1368 m, 1350 m, 1159 m, 1067 m, 1016 m, 837 vs, 767 m, 557 m cm^{-1}; MS (FD, MeCN): m/z (%) = 505 [[(**1**)H$_2$]OTf]$^+$, 355 [(**1**)H$_2$]$^+$; elemental analysis calcd. (%) for C$_{22}$H$_{32}$N$_6$F$_6$O$_6$S$_2$ (654.7): C 40.36, H 4.93, N 12.84; found C 39.98, H 4.89, N 12.35.

^{1}H NMR transprotonation studies:[43,44,45]

General procedure: exactly equimolar amounts (0.03 mmol) of the reference base and the corresponding acid of the base investigated are dissolved together in 0.5 mL CD_3CN. 0.1 mL of the resulting solution is diluted with another 0.5 mL CD_3CN and the ^{1}H-NMR spectra are recorded at room temperature and 230 K (500 MHz).

(AH^+): [TMGNH][PF_6](**2a**): 16.820 mg (0.0336 mmol)

(B): 7-Methyl-1,5,7-triazabicyclo[4.4.0]dec-5-ene (MTBD): 5.167 mg (0.0336 mmol)

  pK_{BH+} = 25.43[19b, 20c]
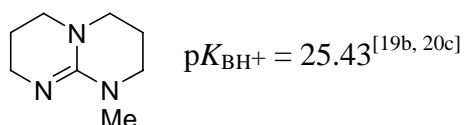
δ (ppm)	assignment	Int.	No. H	Int. / H
6.2	C-H$_{2,7}$	1	2	0.500
7.2	C-H$_{3-6}$	2.08	4	0.520
TMGN (**1**)			avg.	0.510
6.5	C-H$_{2,7}$	0.67	2	0.335
7.4	C-H$_{3-6}$	1.31	4	0.328
[TMGNH][PF$_6$](**2a**)			avg.	0.331

$$K = \frac{[A]^2}{[AH^+]^2} = \frac{I_A^2}{I_{AH^+}^2} = 2.37 \;\rightarrow\; \log K = 0.37 = \Delta pK_{BH+}$$

Qualitative analysis of the experimental spectrum indicates that MTBD is the stronger base. Therefore, the pK_{BH+} value of A (**2a**) is calculated as follows:

$$pK_{BH+}(A) = pK_{BH+}(B) + \Delta pK_{BH+}(A,B) = 25.43 + (-0.37) = 25.06$$

^{1}H NMR self-exchange experiment:

Equimolar amounts of TMGN (**1**, 1.81 mg, 5×10^{-6} mol) and [**1**-H][PF$_6$] (**2a**, 2.50 mg, 5×10^{-6} mol) were dissolved together in dry CD$_3$CN (0.5 mL), and ^{1}H NMR spectra were recorded at various temperatures ranging from 344 K to 225 K. An analogous experiment was carried out with DMAN (4.28 mg, 2×10^{-5} mol) and DMANH$^+$ (7.20 mg, 2×10^{-5} mol) in dry CD$_3$CN (0.9 mL) and dry [D$_6$]DMSO (0.8 mL), respectively.

^{1}H NMR basic hydrolysis experiment:

TMGN (**1**, 21.3 mg, 6×10^{-5} mol) and MTBD (9.0 mg, 6×10^{-5} mol) were each dissolved in dry [D$_6$]DMSO (0.5 mL). After the addition of NaOD in D$_2$O (0.1 mL, 5 M) their ^{1}H NMR spectra were recorded at various times ($t = 0\rightarrow1$ h/RT$\rightarrow1$ d/RT$\rightarrow3$ h/60 °C$\rightarrow1$ d/60 °C$\rightarrow5$ d/60 °C).

^{1}H NMR nucleophilicity experiment:

TMGN (**1**, 46.3 mg, 1.3×10^{-4} mol) and MTBD (20.0 mg, 1.3×10^{-4} mol) were each dissolved in dry CD$_2$Cl$_2$ (0.6 mL) and C$_2$H$_5$I (TMGN: 102 mg, 0.053 mL, 6.5×10^{-4} mol; MTBD: 51 mg, 0.026 mL, 3.25×10^{-4} mol) was added, 2.5 eq. of the alkylating agent per guanidine function, respectively. The ^{1}H NMR spectra were recorded at various times ($t = 0\rightarrow15$ min/RT$\rightarrow1$ h/RT$\rightarrow1$ d/RT$\rightarrow3$ d/RT).

X-ray structure analysis. Crystal data and experimental conditions are listed in Table 7 and 8. The molecular structures are illustrated as Schakal[71] plots in Figures 1-4. Selected bond lengths and angles with standard deviations in parentheses are presented in Table 1. The collected reflections were corrected for Lorentz and polarization effects. All structures were solved by direct methods and refined by full-matrix least-squares methods on F^2.[72] Hydrogen atoms were calculated and isotropically refined except H1A (**2a**) and H1 / H4 (**3a**) which were found and then isotropically refined.[73] The correctness of the absolute structure of **2a** was confirmed by the Flack parameter refined to 0.01(5).

Table 7. Crystal data and structure refinement for **1** and **2a**.

Complex	TMGN (**1**)	[**1**-H][PF$_6$] (**2a**)
Empirical formula	C$_{20}$H$_{30}$N$_6$	C$_{20}$H$_{31}$N$_6$F$_6$P
Formula weight [g mol^{-1}]	354.5	500.5
Temperature [K]	183(2)	213(2)
Crystal system	monoclinic	monoclinic
Space group	P2$_1$/n	P2$_1$
a [pm]	1313.7(1)	873.8(1)
b [pm]	1165.1(2)	1151.5(1)
c [pm]	1480.1(1)	1240.9(1)
α [°]	90	90
β [°]	113.786(6)	107.003(5)
γ [°]	90	90
Volume [Å^3]	2072.9(4)	1194.1(1)
Z	4	2
ρ [Mgm^{-3}]	1.136	1.392
μ [mm^{-1}]	0.071	1.629
F(000)	768	524
Crystal size [mm^3]	0.50 × 0.30 × 0.30	0.40 × 0.40 × 0.20
Diffractometer	Enraf Nonius CAD4	Enraf Nonius CAD4
Radiation / wavelength [pm]	MoK$_\alpha$ / 71.073	CuK$_\alpha$ / 154.178
Scan technique	ω-scan	ω-scan
θ-range for data collection [°]	2.43...24.87	3.72...59.94
Index ranges	-14 ≤ h ≤ 13,	-9 ≤ h ≤ 9,
	-13 ≤ k ≤ 0,	-12 ≤ k ≤ 0,
	0 ≤ l ≤ 17	0 ≤ l ≤ 13
Reflections collected	3725	1967
Independent refl.	3315	1875
R_{int}	0.0354	0.0156
Observed reflections [$F \geq 4\sigma(F)$]	1970	1868
Data / restraints / parameters	3315 / 0 / 243	1875 / 0 / 307
Goodness of fit on F^2	0.992	1.070
R1 [$F_0 \geq 4\sigma(F)$][a]	0.0552	0.0627
wR$_2$ (all data) [a]	0.1404	0.1681
Transmission (max./min.)	0.9791 / 0.9655	0.7365 / 0.5619
Largest diff. Peak and hole [eÅ^{-3}]	0.147 / -0.214	0.952 / -0.754

[a] $R_1 = \Sigma \left| \left| F_0 \right| - \left| F_c \right| \right| / \Sigma \left| F_0 \right|$; wR$_2 = \{\Sigma[w(F_0^2 - F_c^2)^2]/\Sigma[w(F_0^2)^2]\}^{1/2}$.

Table 8. Crystal data and structure refinement for **3a** and **3b**.

Complex	[**1**-H$_2$][Cl, Cl$_2$H] (**3a**)	[**1**-H$_2$][PF$_6$, BF$_4$] (**3b**)
Empirical formula	C$_{20}$H$_{32}$N$_6$Cl$_2$ × HCl, CH$_3$CN	C$_{20}$H$_{32}$N$_6$BF$_{10}$P
Formula weight [g mol^{-1}]	504.9	588.3
Temperature [K]	213(2)	213(2)
Crystal system	monoclinic	orthorhombic
Space group	P2$_1$/c	Pca2$_1$
a [pm]	1083.0(1)	1465.4(1)
b [pm]	3374.5(1)	1289.9(1)
c [pm]	743.5(1)	1432.6(1)
α [°]	90	90
β [°]	101.311(4)	90
γ [°]	90	90
Volume [Å^3]	2664.3(2)	2707.9(3)
Z	4	4
ρ [Mgm^{-3}]	1.259	1.478
μ [mm^{-1}]	3.292	2.247
F(000)	1072	1248
Crystal size [mm^3]	0.45 × 0.27 × 0.12	0.50 × 0.45 × 0.18
Diffractometer	Enraf Nonius CAD4	Enraf Nonius CAD4
Radiation / wavelength [pm]	CuK$_\alpha$ / 154.178	CuK$_\alpha$ / 154.178
Scan technique	ω-scan	ω-scan
θ-range for data collection [°]	2.62...59.90	3.43...59.88
Index ranges	0 ≤ h ≤ 12,	0 ≤ h ≤ 16,
	0 ≤ k ≤ 37,	0 ≤ k ≤ 14,
	-8 ≤ l ≤ 8	0 ≤ l ≤ 16
Reflections collected	4166	2097
Independent refl.	3942	2097
R_{int}	0.0478	0.0000
Observed reflections [$F ≥ 4\sigma(F)$]	3468	2059
Data / restraints / parameters	3942 / 0 / 310	2097 / 1 / 353
Goodness of fit on F^2	1.054	1.052
R1 [$F_0 ≥ 4\sigma(F)$][a]	0.0573	0.1712
wR$_2$ (all data) [a]	0.1575	0.4824
Transmission (max./min.)	0.6934 / 0.3189	0.6879 / 3996
Largest diff. Peak and hole [eÅ^{-3}]	0.676 / -0.400	0.957 / -0.828

[a] $R_1 = \Sigma\left|\left|F_0\right| - \left|F_c\right|\right|/\Sigma\left|F_0\right|$; wR$_2 = \{\Sigma[w(F_0^2 - F_c^2)^2]/\Sigma[w(F_0^2)^2]\}^{1/2}$.

References

[1]   R. W. Alder, P. S. Bowman, W. R. S. Steele, D. R. Winterman, *J. Chem. Soc. Chem. Comm.* **1968**, 723-724.

[2]   R. W. Alder, *Chem. Rev.* **1989**, *89*, 1215-1223.

[3]   H. A. Staab, T. Saupe, *Angew. Chem.* **1988**, *100*, 895-909; *Angew. Chem. Int. Ed. Engl.* **1988**, *27*, 865-879.

[4]   A. L. Llamas-Saiz, C. Foces-Foces, J. Elguero, *J. Mol. Struct.* **1994**, *328*, 297-323.

[5]   A. F. Pozharskii, *Russ. Chem. Rev.* **1998**, *67*, 1-24.

[6]   a) M. Pietrzak, J. Wehling, H.-H. Limbach, N. S. Golubev, C. López, R. M. Claramunt, J. Elguero, *J. Am. Chem. Soc.* **2001**, *123*, 4338-4339; b) H. A. Staab, A. Kirsch, T. Barth, C. Krieger, F. A. Neugebauer, *Eur. J. Org. Chem.* **2000**, 1617-1622; c) H. A. Staab, K. Elbl-Weiser, C. Krieger, *Eur. J. Org. Chem.* **2000**, 327-333; d) P. Hodgson, G. C. Lloyd-Jones, M. Murray, T. M. Peakman, R. L. Woodward, *Chem. Eur. J.* **2000**, *6*, 4451-4460; e) C. Cox, H. Wack, T. Lectka, *Angew. Chem.* **1999**, *111*, 864-867; *Angew. Chem. Int. Ed. Engl.* **1999**, *38*, 798-800; f) J. P. H. Charmant, G. C. Lloyd-Jones, T. M. Peakman, R. L. Woodward, *Eur. J. Org. Chem.* **1999**, 2501-2510; g) J. P. H. Charmant, G. C. Lloyd-Jones, T. M. Peakman, R. L. Woodward, *Tetrahedron Lett.* **1998**, *39*, 4733-4736; h) H. A. Staab, C. Krieger, G. Hieber, K. Oberdorf, *Angew. Chem.* **1997**, *109*, 1946-1949; *Angew. Chem. Int. Ed. Engl.* **1997**, *36*, 1884-1886.

[7]   a) S. T. Howard, *J. Am. Chem. Soc.* **2000**, *122*, 8238-8244; b) V. A. Ozeryanskii, A. F. Pozharskii, G. R. Milgizina, S. T. Howard, *J. Org. Chem.* **2000**, *65*, 7707-7709; c) P. R. Mallinson, K. Wozniak, C. C. Wilson, K. L. McCormack, D. S. Yufit, *J. Am. Chem. Soc.* **1999**, *121*, 4640-4646; d) S. T. Howard, J. A. Platts, *J. Org. Chem.* **1998**, *63*, 3568-3571; e) A. Szemik-Hojniak, J. M. Zwier, W. J. Buma, R. Bursi, J. H. van der Waals, *J. Am. Chem. Soc.* **1998**, *120*, 4840-4844; f) P. R. Mallinson, K. Wozniak, G. T. Smith, K. L. McCormack, *J. Am. Chem. Soc.* **1997**, *119*, 11502-11509; g) M. Peräkylä, J. Org. Chem. 1996, 61, 7420-7425; h) J. A. Platts, S. T. Howard, J. Org. Chem. 1996, 61, 4480-4482; i) A. L. Llamas-Saiz, C. Foces-Foces, A. Martínez, J. Elguero, *J. Chem. Soc. Perkin Trans. 2* **1995**, 923-927.

[8]   H. A. Staab, T. Saupe, C. Krieger, *Angew. Chem.* **1983**, *95*, 748-749; *Angew. Chem. Int. Ed. Engl.* **1983**, *22*, 731-732.

[9]   H. A. Staab, M. Höne, C. Krieger, *Tetrahedron Lett.* **1988**, *29*, 1905-1908.

[10]   T. Saupe, C. Krieger, H. A. Staab, *Angew. Chem.* **1986**, *98*, 460-461; *Angew. Chem. Int. Ed. Engl.* **1986**, *25*, 451-452.

[11]   H. A. Staab, M. Höne, C. Krieger, *Tetrahedron Lett.* **1988**, *29*, 5629-5632.

[12]   R. W. Alder, M. R. Bryce, N. C. Goode, N. Miller, J. Owen, *J. Chem. Soc. Perkin Trans. 1* **1981**, 2840-2847.

[13]   a) W. Wong-Ng, S. C. Nyburg, A. Awwal, R. Jankie, A. J. Kresge, *Acta Cryst.* **1982**, *B38*, 559-564; b) Y. Nagawa, M. Goto, K. Honda, H. Nakanishi, *Acta Cryst.* **1986**, *C42*, 478-480; c) G. Rimmler, C. Krieger, F. A. Neugebauer, *Chem. Ber.* **1992**, *125*, 723-728.

[14]   a) C. Krieger, I. Newsom, M. A. Zirnstein, H. A. Staab, *Angew. Chem.* **1989**, *101*, 72-73; *Angew. Chem. Int. Ed. Engl.* **1989**, *28*, 84-86; b) M. A. Zirnstein, H. A. Staab, *Angew. Chem.* **1987**, *99*, 460-461; *Angew. Chem. Int. Ed. Engl.* **1987**, *26*, 460-461; c) P. G. Jones, *Z. Kristallogr.* **1993**, *208*, 341-343.

[15]   a) A. L. Llamas-Saiz, C. Foces-Foces, P. Molina, M. Alajarin, A. Vidal, R. M. Claramunt, J. Elguero, *J. Chem. Soc. Perkin Trans. 2* **1991**, 1025-1031; b) A. L. Llamas-Saiz, C. Foces-Foces, J. Elguero, P. Molina, M. Alajarin, A. Vidal, *J. Chem. Soc. Perkin Trans. 2* **1991**, 1667-1677; c) A. L. Llamas-Saiz, C. Foces-Foces, J. Elguero, P. Molina, M. Alajarin, A. Vidal, *J. Chem. Soc. Perkin Trans. 2* **1991**, 2033-2041; d) J. Laynez, M. Menéndez, J. L. S. Velasco, A. L. Llamas-Saiz, C. Foces-Foces, J. Elguero, P. Molina, M. Alajarin, A. Vidal, *J. Chem. Soc. Perkin Trans. 2* **1993**, 709-713; e) A. L. Llamas-Saiz, C. Foces-Foces, J. Elguero, F. Aguilar-Parrilla, H.-H. Limbach, P. Molina, M. Alajarin, A. Vidal, R. M. Claramunt, C. López, *J. Chem. Soc. Perkin Trans. 2* **1994**, 209-212.

[16]   a) R. W. Alder, N. C. Goode, N. Miller, F. Hibbert, K. P. P. Hunte, H. J. Robbins, *J. Chem. Soc. Chem. Comm.* **1978**, 89-90; b) F. Hibbert, K. P. P. Hunte, *J. Chem. Soc. Perkin Trans. 2* **1983**, 1895-1899; c) F. Hibbert, G. R. Simpson, *J. Chem. Soc. Perkin Trans. 2* **1987**, 243-246.

[17]   a) H. A. Staab, M. Diehm, C. Krieger, *Tetrahedron Lett.* **1994**, *35*, 8357-8360; b) H. A. Staab, M. A. Zirnstein, C. Krieger, *Angew. Chem.* **1989**, *101*, 73-75; *Angew. Chem. Int. Ed. Engl.* **1989**, *28*, 86-88.

[18] R. Schwesinger, M. Mißfeld, K. Peters, H. G. von Schnering, *Angew. Chem.* **1987**, *99*, 1210-1212; *Angew. Chem. Int. Ed. Engl.* **1987**, *26*, 1165-1167.

[19] a) I. Kaljurand, T. Rodima, I. Leito, I. A. Koppel, R. Schwesinger, *J. Org. Chem.* **2000**, *65*, 6202-6208; b) R. Schwesinger, *Chimia* **1985**, *39*, 269-272; c) G. Wieland, G. Simchen, *Liebigs Ann. Chem.* **1985**, 2178-2193; d) D. H. R. Barton, J. D. Elliot, S. D. Géro, *J. Chem. Soc., Perkin Trans. I* **1982**, 2085-2090; e) D. H. R. Barton, J. K. Kervagoret, S. Z. Zard, *Tetrahedron* **1990**, *46*, 7587-7598.

[20] a) P. A. S. Smith in *The Chemistry of Open-Chain Organic Nitrogen Compounds, Vol. 1*, W. A. Benjamin Inc., New York, **1965**, pp. 277-290; b) Y. Yamamoto, S. Kojima in *The Chemistry of Amidines and Imidates, Vol. 2*, J. Wiley & Sons, Chichester, **1991**, pp. 485-526; c) R. Schwesinger, *Nachr. Chem. Tech. Lab.* **1990**, *38*, 1214-1226.

[21] a) K. T. Leffek, P. Pruszynski, K. Thanapaalasingham, *Can. J. Chem.* **1989**, *67*, 590-595; b) P. Pruszynski, *Can. J. Chem.* **1987**, *65*, 626-629.

[22] P. Pruszynski, K. T. Leffek, B. Borecka, T. S. Cameron, *Acta Cryst.* **1992**, *C48*, 1638-1641.

[23] a) W. Galezowski, M. Stanczyk, I. Grzeskowiak, A. Jarczewski, *J. Chem. Soc. Perkin Trans. 2* **1996**, 2647-2651; b) P. Pruszynski, K. T. Leffek, *Can. J. Chem.* **1991**, *69*, 205-210; c)

[24] a) F. Hibbert, *Acc. Chem. Res.* **1984**, *17*, 115-120; b) F. Hibbert, *J. Chem. Soc. Perkin Trans. 2* **1974**, 1862-1866.

[25] a) H. Wittmann, A. Schorm, J. Sundermeyer, *Z. Anorg. Allg. Chem.* **2000**, *626*, 1583-1590; b) H. Wittmann, V. Raab, A. Schorm, J. Plackmeyer, J. Sundermeyer, *Eur. J. Inorg. Chem.* **2001**, 1937-1948; c) V. Raab, J. Kipke, O. Burghaus, J. Sundermeyer *Inorg. Chem.* **2001**, *40*, 6964-6971; d) V. Raab, J. Kipke, A. Schorm, J. Sundermeyer *J. Chem. Soc. Dalton Trans.* **2002**, submitted.

[26] I. A. Cliffe in *Comprehensive Organic Functional Group Transformations, Vol. 6*, Elsevier Science Ltd., Oxford, **1987**, pp. 639-675.

[27] T. Barth, C. Krieger, F. A. Neugebauer, H. A. Staab, *Angew. Chem.* **1991**, *103*, 1006-1008; *Angew. Chem. Int. Ed. Engl.* **1991**, *30*, 1028-1030.

[28] a) B. Brzezinski, G. Schroeder, E. Grech, Z. Malarski, L. Sobczyk, *J. Mol. Struct.* **1992**, *274*, 75-82; b) J. Klimkiewicz, L. Stefaniak, B. Brzezinski, E. Grech, S. Kuroki, I.

Ando, G. A. Webb, *J. Mol. Struct.* **1994**, *323*, 193-195.

[29] R. W. Alder, M. R. Bryce, N. C. Goode, *J. Chem. Soc. Perkin Trans. 2* **1982**, 477-483.

[30] A. Gobbi, G. Frenking, *J. Am. Chem. Soc.* **1993**, *115*, 2362-2372.

[31] R. Boese, D. Bläser, W. Petz, *Z. Naturforsch.* **1988**, *43(B)*, 945-948.

[32] The ρ value of 0.994 in the $[C(NMe_2)_3]^+$ cation is due to crystal packing effects and assumes the ideal value of 1.00 in other complexes; W. Petz,[31] personal communication.

[33] H. Einspahr, J. B. Robert, R. E. Marsh, J. D. Roberts, *Acta Cryst.* **1973**, *B29*, 1611-1617.

[34] a) M. R. Truter, B. L. Vickery, *J. Chem. Soc. Dalton Trans.* **1972**, 395-402; b) K. Wozniak, T. M. Krygowski, B. Kariuki, W. Jones, E. Grech, *J. Mol. Struct.* **1990**, 240, 111-118; c) J. A. Kanters, A. Schouten, J. Kroon, E. Grech, *Acta Cryst.* **1991**, *C47*, 807-810.

[35] K. Wozniak, C. C. Wilson, K. S. Knight, W. Jones, E. Grech, *Acta Cryst.* **1996**, *B52*, 691-696.

[36] E. Haselbach, A. Henriksson, F. Jachimowicz, J. Wirz, *Helv. Chim. Acta* **1972**, *55*, 1757-1759.

[37] J. L. Atwood, S. G. Bott, C. M. Means, A. W. Coleman, H. Zhang, M. T. May, *Inorg. Chem.* **1990**, *29*, 467-470.

[38] U. Müller, H.-D. Dörner, *Z. Naturforsch. (B)* **1982**, *37*, 198-200.

[39] A. Deeg, T. Dahlems, D. Mootz, *Z. Kristallogr. - New Cryst. Struct.* **1997**, *212*, 401-402.

[40] G. Y. S. Chan, M. G. B. Drew, M. J. Hudson, N. S. Isaacs, P. Byers, C. Madic, *Polyhedron* **1996**, *15*, 3385-3398.

[41] According to a search of the CCDC database (May 2001), no NMR spectroscopic data are available in the original publications of structurally characterized compounds with the $[Cl_2H]^-$ anion.

[42] a) A. Albert, E. P. Serjeant in *The Determination of Ionization Constants*, Chapman & Hall, London, **1984**; b) C. H. Rochester in *Acidity Functions*, Org. Chem. *17*, Academic Press, London & New York, **1970**, Ch. 1.

[43] R. F. Cookson, *Chem. Rev.* **1974**, *74*, 5-28.

[44] a) F. Hibbert, *J. Chem. Soc. Chem. Comm.* **1973**, 463.; b) A. Awwal, F. Hibbert, *J. Chem. Soc. Perkin Trans. 2* **1977**, 1589-1592; c) R. W. Alder, N. C. Goode, N. Miller, F. Hibbert, K. P. P. Hunte, H. J. Robbins, *J. Chem. Soc. Chem. Comm.* **1978**, 89-90; d) F. Hibbert, H. J. Robbins, *J. Am. Chem. Soc.* **1978**, *100*, 8239-8244; e) W. M. Latimer, W. H. Rodebush, *J. Am. Chem. Soc.* **1920**, *42*, 1419-1433.

[45] T. Saupe, *Dissertation* **1985**, University of Heidelberg.

[46] Experimental error estimated from Integration of ^{1}H NMR resonances (± 2%) and weight content of **1** and MTBD in sample (± 0.01 mg).

[47] In collaboration with Z. B. Maksic, B. Kovacevic, Quantum Organic Chemistry Group, Rudjer Boskovic Institute, P.O. Box 1016, 10000 Zagreb (Croatia). Fax: (+385)1-4561118; E-mail: zmaksic@spider.irb.hr. For recent publications on the APA of polyguanidines and other highly basic organic molecules, see: a) Z. B. Maksic, B. Kovacevic, *J. Org. Chem.* **2000**, *65*, 3303-3309; b) Z. B. Maksic, B. Kovacevic, *J. Phys. Chem. A* **1999**, *103*, 6678-6684; c) Z. B. Maksic, B. Kovacevic, *J. Phys. Chem. A* **1998**, *102*, 7324-7328.

[48] E. D. Raczynska, P.-C. Maria, J.-F. Gal, M. Decouzon, *J. Phys. Org. Chem.* **1994**, *7*, 725-733.

[49] E. Fujiwara, K. Omoto, H. Fujimoto, *J. Org. Chem.* **1997**, *62*, 7234-7238.

[50] R. Schwesinger, H. Schlemper, *Angew. Chem.* **1987**, 99, 1212-1214; *Angew. Chem. Int. Ed. Engl.* **1987**, *26*, 1167-1169.

[51] Y. P. Egorov, A. A. Kudryavtsev, *J. Gen. Chem. USSR* **1983**, *53*, 2003-2008.

[52] pK_{BH+} (MeCN, 22 °C): 18.50 according to A. F. Pozharskii, N. L. Chikina, N. V. Vistorobskii, V. A. Ozeryanskii, *Russ. J. Org. Chem.* **1997**, *33*, 1810-1813.

[53] Synthesized analogous to [**1**-H][PF$_6$] (**2a**).

[54] T. Lenzen, G. Hägele and Bruker Analytik GmbH, *WIN-DYNA 32*, *Program for the Simulation and Iteration of Dynamic NMR*, **1994-98**, Heinrich-Heine University, Düsseldorf (Germany).

[55] Maximum recording temperature, higher temperatures resulted in inhomogeneous field (bp. CD$_3$CN: 81 °C; [D$_6$]DMSO: 189 °C).

[56] R. L. de Groot, D. J. Sikkema, *J. R. Neth. Chem. Soc.* **1976**, *95*, 10-14.

[57] a) H. Kessler, D. Leibfritz, *Chem. Ber.* **1971**, *104*, 2158-2169; b) H. Kessler, *Angew.*

Chem. **1970**, *82*, 237-253; *Angew. Chem. Int. Ed. Engl.* **1970**, *9*, 219-235; c) H. Kessler, D. Leibfritz, *Tetrahedron* **1969**, *25*, 5127-5145.

[58] a) K. Kanamori, J. D. Roberts, *J. Am. Chem. Soc.* **1983**, *105*, 4698-4701; b) A. V. Santoro, G. Mickevicius, *J. Org. Chem.* **1979**, *44*, 117-120; c) H. Kessler, D. Leibfritz, *Tetrahedron Lett.* **1969**, *6*, 427-430; d) V. J. Bauer, W. Fulmor, G. O. Morton, S. R. Safir, *J. Am. Chem. Soc.* **1968**, *90*, 6846-6847.

[59] a) H. Kessler, D. Leibfritz, *Tetrahedron* **1970**, *26*, 1805-1820; b) H. Kessler, D. Leibfritz, *Liebigs Ann. Chem.* **1970**, *737*, 53-60.

[60] R. W. Alder, J. E. Anderson, *J. Chem. Soc. Perkin Trans. 2* **1973**, 2086-2088.

[61] Minimum ^{1}H NMR recording temperature in CD_2Cl_2: 181 K.

[62] a) H. O. Kalinowski, H. Kessler, *Org. Magn. Res.* **1975**, *7*, 128-135; b) H. O. Kalinowski, H. Kessler, *Org. Magn. Res.* **1974**, *6*, 305-312.

[63] a) L. J. Altman, D. Laungani, G. Gunnarsson, H. Wennerström, S. Forsén, *J. Am. Chem. Soc.* **1978**, *100*, 8264-8266; b) G. Gunnarsson, H. Wennerström, W. Egan, S. Forsén, *Chem. Phys. Lett.* **1976**, *38*, 96-99.

[64] $\Delta H^{\ddagger}$ and $\Delta G^{\ddagger}_{298}$ of [**1**-H$_2$][OTf]$_2$ (**3c**) were obtained by extrapolation on the basis of the three experimentally determined individual $\Delta G^{\ddagger}_{1/2/3}$ values (T_c = 256 / 235 / 226 K).

[65] Experimental errors $\Delta \nu = \pm 2$ Hz, $\Delta T = \pm 2$ K and $\Delta k = \pm 2$ % result in an error of $\Delta G^{\ddagger}$ / $\Delta H^{\ddagger} = \pm 0.1 / 0.3$ kJ/mol.

[66] G. Binsch, H. Kessler, *Angew. Chem.* **1980**, *92*, 445-463; *Angew. Chem. Int. Ed. Engl.* **1980**, *19*, 411-429.

[67] Calculated with: $\ln(k/T) = 23.76 - (\Delta H^{\ddagger}/R) \times 1/T + (\Delta S^{\ddagger}/R)$, $\Delta G^{\ddagger} = \Delta H^{\ddagger} - T\Delta S^{\ddagger}$; H. Günther in *NMR-Spektroskopie, 3. Aufl.*, Thieme Verlag, Stuttgart, New York, **1992**.

[68] Calculated by: $\Delta G^{\ddagger} = 19.1 \times 10^{-3} \times T_c$ (9.97 + logT_c - log|ν_A - ν_B|); M. Hesse, H. Meier, B. Zeeh in *Spektoskopische Methoden in der organischen Chemie, 4. Aufl.*, Thieme Verlag, Stuttgart, New York, **1991**.

[69] Rate constants corresponding to $T > 256$ K and $T < 200$ K have been omitted because the experimental error of the simulation for the high temperature values are large in the area of very rapid exchange while in the other case temperature effects (viscosity of solvent e.g.) account for large inaccuracy of its determination.[66]

[70] H. O. House, D. G. Koepsell, W. J. Campbell, *J. Org. Chem.* **1972**, *37*, 1003-1011.

[71] E. Keller, *Schakal-97, Program for the Graphic Representation of Molecule and Crystallographic Models*, **1997**, University of Freiburg, Germany.

[72] a) G. M. Sheldrick, *SHELXS-97, Program for Crystal Structure Solution* and *SHELXL-97, Program for Crystal Structure Refinement*, **1997**, University of Göttingen, Germany; b) Siemens Analytical X-ray Instruments Inc., *SHELXTL 5.06*, **1995**, Madison, WI, USA.

[73] Crystallographic data (excluding structure factors) for the structures reported in this paper have been deposited with the Cambridge Crystallographic Data Centre as supplementary publication no. CCDC-170726 (**1**), CCDC-170727 (**2a**), and CCDC-170728 (**3a**). Copies of the data can be obtained free of charge on application to CCDC, 12 Union Road, Cambridge CB2 1EZ, UK (fax: (+ 44) 1223 336-033; email: deposit@ccdc.cam.ac.uk).

— Chapter 5.2 —

1,8-Bis(hexamethylphosphoraneimino)naphthalene (HMPIN):

The Next Generation of Superbasic Proton Sponges

Results and Discussion

In analogy to the guanidine route (see parent Ch. 5.1) we set out to synthesize a „proton sponge" derivative based on iminophosphorane (IP) N-donor groups. IP´s even surpass guanidines in basicity by approximately 2 to 3 orders of magnitude.[1,2b] Well known and commercially available examples of the so called phosphazene bases with extreme steric demand and pK_{BH+}´s of 27.5 up to 45-46 were developed by Schwesinger et al.[2] The synthesis of IP-substituted (N=PPh$_3$) „proton sponges" has been reported by Llamas-Saiz et al. but the free base could not be isolated, only the *mono*protonated salts were presented along with their crystal structure. Determination of pK_{BH+} values proved to be difficult due to decomposition of the „sponge".[3]
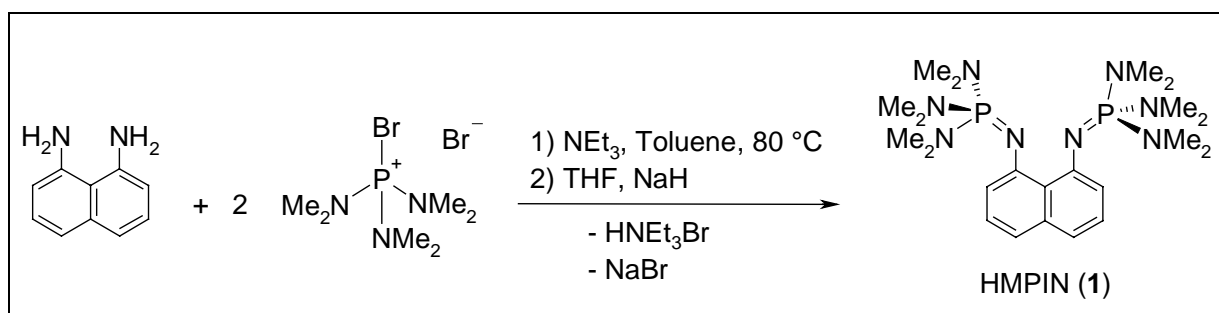
Scheme 1. Synthesis of HMPIN (**1**).

Endeavours to prepare the tris(dimethylamino)iminophosphorane analogon to our tetramethylguanidino proton sponge by the reaction of 1,8-diaminonaphthalene with the salt [Cl-P(NMe$_2$)$_3$]Cl in the presence of NEt$_3$ failed, regardless of the solvent and reaction conditions applied. Also the lithiation of the amine prior to the reaction in order to increase nucleophilicity did not show any success as the reaction becomes very unselective according to ^{31}P NMR studies. However, when the more reactive salt [Br-P(NMe$_2$)$_3$]Br, prepared by an analogous method previously described for the synthesis of Ph$_3$PBr$_2$,[4] and toluene as solvent were employed, a first sample of HMPIN could be isolated as beige colored crystalline material. Formation of the target molecule was also spectroscopically observed (NMR, MS)

working in THF or MeCN. The latter giving considerable amounts of byproducts and in both cases the conversion was too low for the isolation of more product and large amounts of starting material is detected. The FD mass spectra of HMPIN reveals the parent molecule and the elemental analysis is correct. The ^{1}H NMR spectrum shows the typical ABX pattern in the aromatic region along with a dublet at 2.69 ppm (CD$_3$CN, 25 °C) for the methyl protons and accurate integration which indicates that the disubstituted species is formed. In the ^{31}P NMR spectrum only one resonance is observed at 17.1 ppm for the IP group, obviously no byproduct, e.g. the monosubstituted derivative is detected. However, the yield of this synthesis is still unsatisfactory (12 %) and is hampered by low conversion and formation of the hydrolysis product of the IP group: HMPT, which in turn is probably inhibiting further reaction due to hydrogen bonding to the amino groups of the substrate. Moreover, the properties of HMPIN are not yet clarified, for example the substance seems to be adsorbed by activated charcoal and Celite. It is soluble in warm pentane, hexane and MeCN and in cold toluene and Et$_2$O. Attempts to prepare the title compound with commercially available [Br-P(NMe$_2$)$_3$]PF$_6$ as electrophile gave even poorer yields.

The pK_{BH+} of HMPIN can be estimated to be > 27.58, based on the comparison of pentamethylguanidine (PMG) with its „proton sponge" analogue TMGN and the corresponding iminophosphorane derivative (Me$_2$N)$_3$P=NMe (IPNMe), pK_{BH+} = 27.58 (see Table 4, parent Ch. 5.1).[2a,b]

Experimental

Materials and methods: (see parent chapter 5.1)

Caution! During the synthesis of HMPIN the formation of highly toxic HMPT was observed.

Tris(dimethylamino)bromophosphoniumbromide ([Br-P(NMe$_2$)$_3$]Br):
Tris(dimethylamino)phosphine (16.3 g, 100 mmol) in dry benzene (50 mL) was slowly added to a stirred solution of bromine (15.9 g, 5.1 mL, 100 mmol) in the same solvent (100 mL) at 0 °C under argon. A light orange precipitate was collected after the mixture was stirred for 1 h at RT. The precipitate was washed with dry ether and dried in vacuo to give 95 % (30.8 g, 95 mmol) of a yellow powder.

^{1}H NMR (200.1 MHz, CD$_3$CN, 25 °C): δ = 2.79 (d, $^3J_{HP}$ = 13.5 Hz, 18 H, CH_3) ppm; ^{31}P NMR (81.0 MHz, CD$_3$CN, 25 °C): δ = 53.5 ppm.

1,8-Bis[tris-(dimethylamino)phosphoranylideneamino]naphthalene (HMPIN, 1):

Tris(dimethylamino)bromophosphoniumbromide ([Br-P(NMe$_2$)$_3$]Br) (1280 mg, 3.96 mmol) and 1,8-diaminonaphthalene (317 mg, 2.00 mmol) are placed together in a schlenk tube and suspended in dry toluene (20 mL). After addition of triethylamine ($\approx$ 0.8 g, 1.10 mL, 8 mmol) a clear orange supernatant solution and a brown sticky residue developed. The reaction mixture was stirred for 5 d at 80 °C and occasionally treated with ultrasonic waves. The reaction mixture was evaporated to dryness, washed with dry ether and dried in vacuo. The residue was suspended in 30 mL of dry THF and 1.2 g (25 eq., 50 mmol) sodiumhydride was added portionwise for deprotonation, followed by 3 hours stirring at 50 °C. After filtration through Celite (5 mm layer), the lightly red colored solution was evaporated to dryness, taken up in hexane, stirred at 50 °C over activated charcoal (500 mg) and passed again through Celite. Evaporation of the volatiles yielded 120 mg (0.25 mmol, 12 %) of a beige solid.

M.p. 156 °C; ^{1}H NMR (400.1 MHz, CD$_3$CN, 25 °C): δ = 6.90 (dd, $^3J \approx {}^3J´ \approx$ 6.7 Hz, 2 H, $H_{4,5}$), 6.77 (d, $^3J_{HH}$ = 6.5 Hz, 2 H, $H_{3,6}$), 6.34 (d, $^3J_{HH}$ = 5.8 Hz, 2 H, $H_{2,7}$), 2.69 (d, $^3J_{HP}$ = 9.2 Hz, 36 H, CH_3) ppm; ^{13}C NMR (100.6 MHz, CD$_3$CN, 25 °C): δ = 126.1, 118.2, 115.9 (C_{aromat}), 37.9 (d, $^3J_{CP}$ = 3.6 Hz, CH$_3$) ppm; ^{31}P NMR (162.0 MHz, CD$_3$CN, 25 °C): δ = 17.1 ppm; ^{1}H NMR (400.1 MHz, [D$_8$]-toluene, 25 °C): δ = 7.25-7.17 (m, 4 H, $H_{4,5}$ + $H_{3,6}$), 6.57-6.51 (m, 2 H, $H_{2,7}$), 2.51 (d, $^3J_{HP}$ = 9.4 Hz, 36 H CH_3) ppm; ^{31}P NMR (162.0 MHz, [D$_8$]-toluene, 25 °C): δ = 15.2 ppm; IR (KBr): $\tilde{\nu}$ = 2879 m, 2837 m, 2792 m, 1549 s, 1451 s, 1435 s, 1392 s, 1366 m, 1352 m, 1293 s, 1196 s, 1133 m, 1060 m, 981 vs, 816 m, 753 m cm^{-1}; HR-MS (EI): C$_{22}$H$_{42}$N$_8$P$_2$ requires m/z 480.3008, found 480.3001; MS (EI, 70 eV): m/z (%) = 480.7 (89) [M]$^+$, 393.6 (93) [M-2 NMe$_2$]$^+$, 348.5 (32) [M-3 NMe$_2$]$^+$, 319.4 (9) [M-P(NMe$_2$)$_3$]$^+$, 186.2 (13) [M-3 NMe$_2$, P(NMe$_2$)$_3$]$^+$, 119.2 (100) [P(NMe$_2$)$_2$]$^+$; MS (FD, MeCN): m/z = 481 [M]$^+$, 319 [M-P(NMe$_2$)$_3$]$^+$; elemental analysis calcd (%) for C$_{22}$H$_{42}$N$_8$P$_2$ (480.58): C 54.98, H 8.81, N 23.32; found C 55.23, H 8.97, N 22.36.

References

[1]   I. Kaljurand, T. Rodima, I. Leito, I. A. Koppel, R. Schwesinger, *J. Org. Chem.* **2000**, *65*, 6202-6208.

[2]   a) R. Schwesinger, H. Schlemper, *Angew. Chem.* **1987**, *99*, 1212-1214; *Angew. Chem. Int. Ed. Engl.* **1987**, *26*, 1167-1169; b) R. Schwesinger, *Nachr. Chem. Tech. Lab.* **1990**, *38*, 1214-1226; c) R. Schwesinger, C. Hasenfratz, H. Schlemper, L. Walz, E.-M. Peters, K. Peters, H. G. von Schnering, *Angew. Chem.* **1993**, *105*, 1420-1422; *Angew. Chem. Int. Ed. Engl.* **1993**, *32*, 1361-1363; d) R. Schwesinger, J. Willaredt, H. Schlemper, M. Keller, D. Schmitt, H. Fritz, *Chem. Ber.* **1994**, *127*, 2435-2454; e) R. Schwesinger, H. Schlemper, C. Hasenfratz, J. Willaredt, T. Dambacher, T. Breuer, C. Ottaway, M. Fletschinger, J. Boele, H. Fritz, D. Putzas, H. W. Rotter, F. G. Bordwell, A. V. Satish, G.-Z. Ji, E.-M. Peters, K. Peters, H. G. von Schnering, L. Walz, *Liebigs Ann.* **1996**, 1055-1081.

[3]   a) A. L. Llamas-Saiz, C. Foces-Foces, P. Molina, M. Alajarin, A. Vidal, R. M. Claramunt, J. Elguero, *J. Chem. Soc. Perkin Trans. 2* **1991**, 1025-1031; b) A. L. Llamas-Saiz, C. Foces-Foces, J. Elguero, P. Molina, M. Alajarin, A. Vidal, *J. Chem. Soc. Perkin Trans. 2* **1991**, 1667-1677; c) A. L. Llamas-Saiz, C. Foces-Foces, J. Elguero, P. Molina, M. Alajarin, A. Vidal, *J. Chem. Soc. Perkin Trans. 2* **1991**, 2033-2041; d) J. Laynez, M. Menéndez, J. L. S. Velasco, A. L. Llamas-Saiz, C. Foces-Foces, J. Elguero, P. Molina, M. Alajarin, A. Vidal, *J. Chem. Soc. Perkin Trans. 2* **1993**, 709-713; e) A. L. Llamas-Saiz, C. Foces-Foces, J. Elguero, F. Aguilar-Parrilla, H.-H. Limbach, P. Molina, M. Alajarin, A. Vidal, R. M. Claramunt, C. López, *J. Chem. Soc. Perkin Trans. 2* **1994**, 209-212.

[4]   K.-W. Lee, L. A. Singer, *J. Org. Chem.* **1974**, *39*, 3780-3781.

4

SUMMARY

The present work discloses new perspectives in peralkyl guanidine chemistry. Several multidentate chiral or tripodal oligoguanidines have been synthesized, their copper(I/II) complexes prepared, and their potential in the oxidative nitrene and OR-radical transfer has been investigated.

Chapter 1. In the asymmetric aziridination of styrene good yields of up to 98% were achieved while unfortunately, the enantiomeric excess remained at a dissatisfactory level of $\leq 8\%$ ee for the best catalyst system [TMG$_2$BN $\times$ Cu(I)ClO$_4$] (Scheme 1).
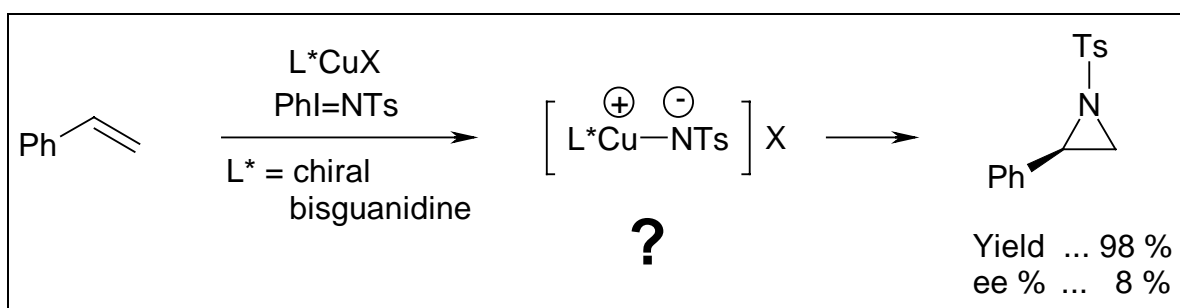
Scheme 1. Copper catalyzed asymmetric aziridination of styrene.

The high activity, accompanied with poor enantioselectivity, is attributed to the fact that Cu(I) prefers the linear and not tetrahedral coordination geometry, so that our C_2 symmetric, chiral guanidines do not form chelate complexes with copper(I) (Figure 1). According to a crystal structure determination this does apply for Cu(II) (Figure 2).
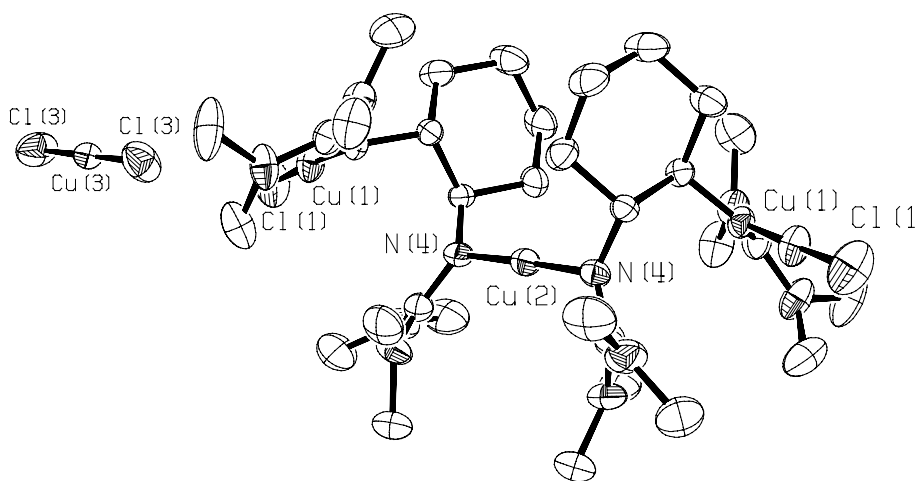
**Figure 1.** Molecular structure of [Cu^I{(μ^2-L)Cu^{I}Cl}$_2$][Cu^{I}Cl$_2$].
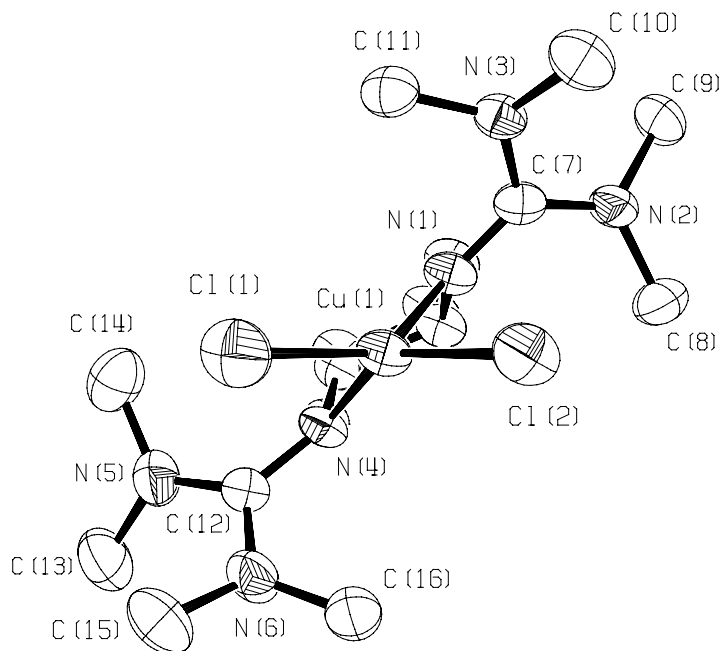
Figure 2. Molecular structure of [(L)Cu^{II}Cl$_2$].

Chapter 2. Peralkyl guanidine copper complexes also revealed their ability in the catalytic activation of molecular oxygen as found in the catalytic oxidative carbonylation of methanol to dimethyl carbonate (DMC) (Scheme 2). In comparison with a blank sample of copper(II) chloride as catalyst, a system used in many patents, the tripodal guanidine complex [(TMG$_3$tren)CuCl]Cl gave twice as much conversion (15 vs. 29%) and an enhanced selectivity (46 vs. 55%). However, the best catalytic performance in activity (55% conversion) and selectivity (95%) is achieved with another CuL$_4$Cl$_2$ complex containing *N*-methyl imidazole as ligand. That result was further improved to a conversion of 87% at a lower selectivity of 75% by employing 3Å molecular sieves as water trapping agent. Optimization of many parameters of this homogeneous oxidation catalysis led to the highest activity and selectivity ever reported in this DMC synthesis.
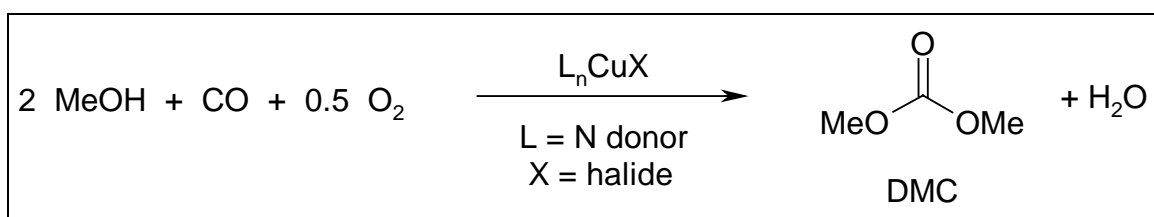
Scheme 2. Copper catalyzed oxidative carbonylation of MeOH to DMC.

Chapter 3 and 4. Our interest in the development of a coordination chemistry with biomimetic 3d transition metals such as copper, manganese, iron and zinc which could serve as precursors in the activation of small molecules, e.g. dioxygen, stimulated us to synthesize and structurally characterize a series of complexes with the TMG$_3$tren ligand (Figure 3, Scheme 3). In particular the trigonal monopyramidal Cu(I) complexes are promising since they contain a remarkable structural feature - a free coordination site within the TMG$_3$tren molecular pocket.
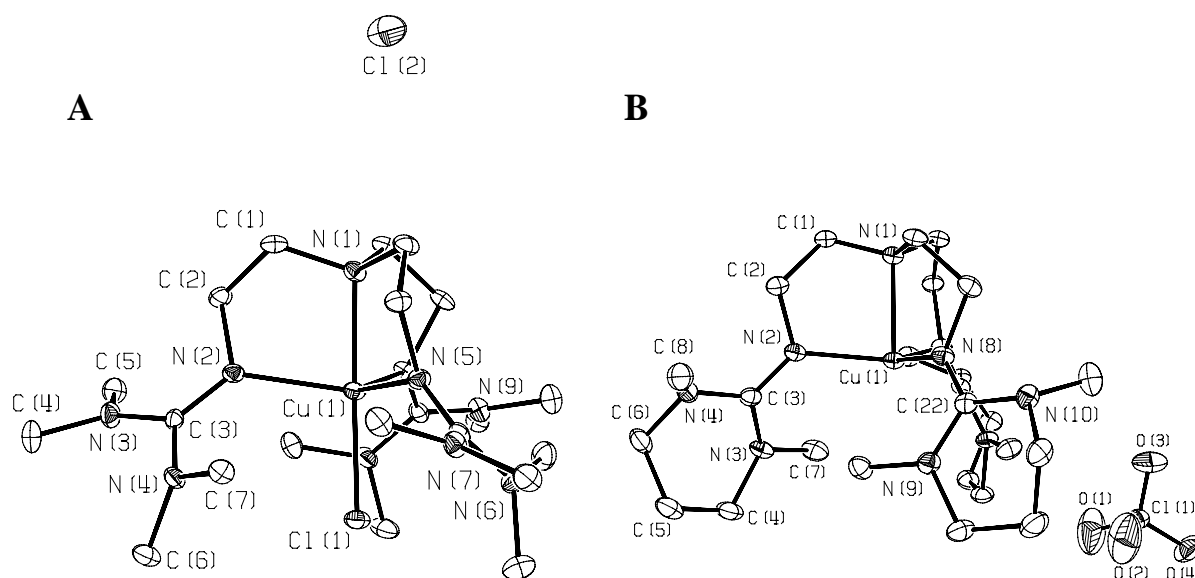
Figure 3. Molecular structures of [(TMG$_3$tren)Cu^{II}Cl]Cl (**A**) and [(DMPG$_3$tren)Cu^{I}]ClO$_4$ (**B**).
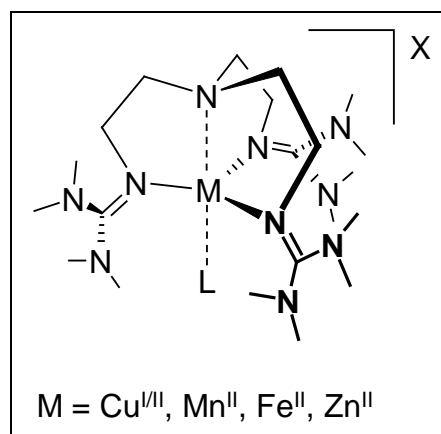
Scheme 3. Transition metal complexes with the trisguanidine TMG$_3$tren.

First results in their investigation towards dioxygen activation were obtained by UV/Vis and resonance raman spectroscopy which revealed the reversible formation of a monomeric end-on superoxo complex (Scheme 4). Further studies and attempts to receive single crystals for an X-ray structure analysis are ongoing.
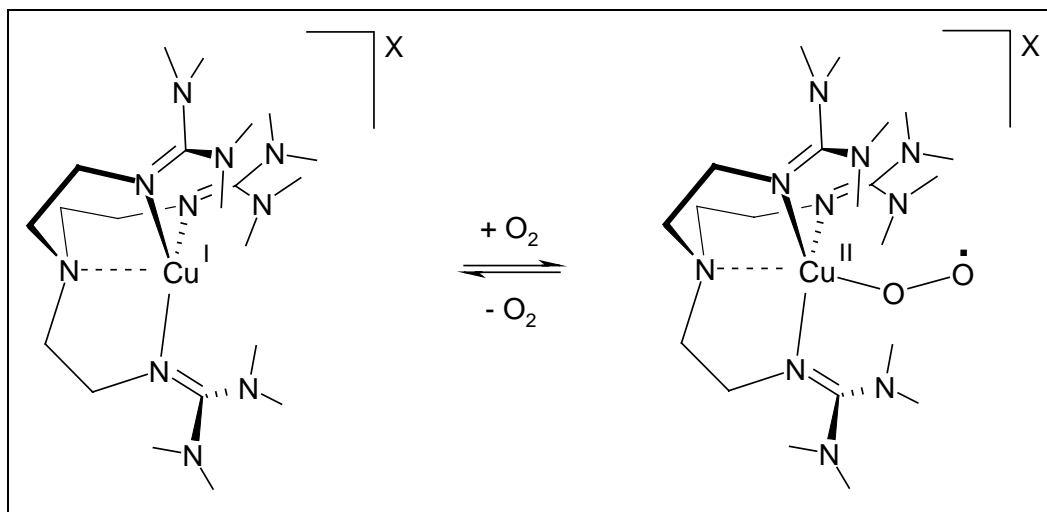
Scheme 4. Reversible reaction of [(TMG$_3$tren)Cu]X with dioxygen to a mononuclear end-on superoxo complex.

Chapter 5.1. Finally, the general idea of creating multifunctional receptors for metal cations and protons was emphasized by the development of a novel „proton sponge" with chelating superbasic tetramethylguanidine functionalities. This „proton sponge", TMGN, is based on the 1,8-diamino naphthalene skeleton (Figure 4). It does not only show a high pK_{BH+} value of 25.1 (MeCN) - in addition to its high thermodynamic basicity it reveals also an unusually high kinetic basicity which makes this superbase highly attractive for base catalyzed applications. The protonated species of TMGN show fascinating coalescence phenomena in their low temperature limiting ^{1}H NMR spectra allowing insight into their bonding situation as well as on kinetics of the proton self exchange (Scheme 5).
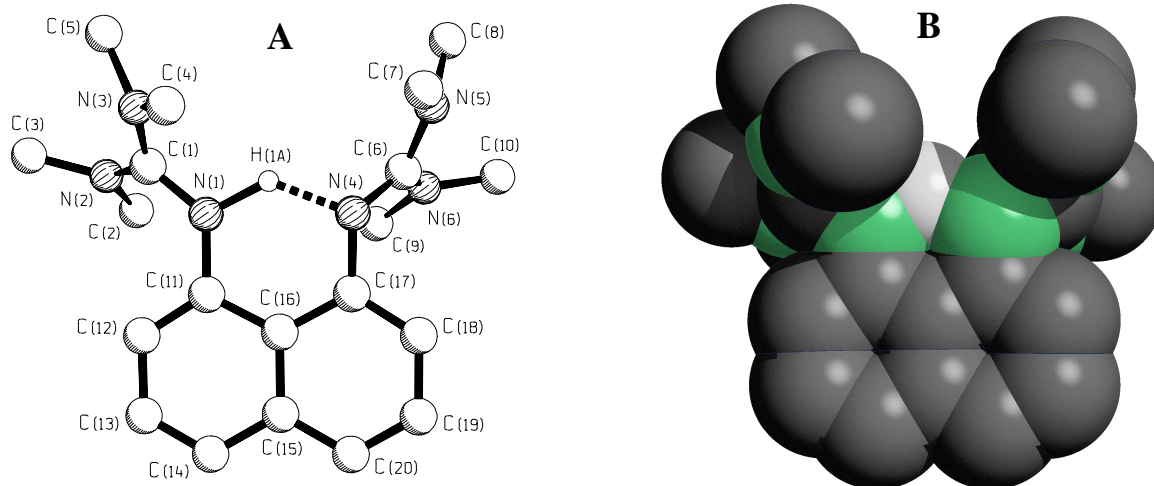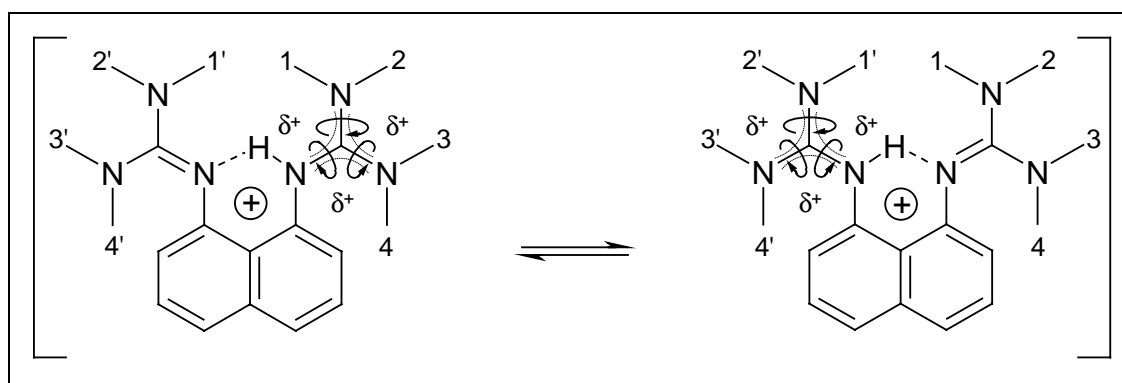
Figure 4. Molecular structure (**A**) and space filling model (**B**) of [TMGNH]$^+$.


Scheme 5. Dynamic behavior of monoprotonated TMGN.

Throughout these studies of peralkyl guanidines a structural parameter $\rho = 2a / (b + c)$ (quotient of average C=N vs. C-NR$_2$ bond distance) derived, which allows the estimation of charge delocalization within the guanidine moiety depending on the coordinated electrophile (E) (Scheme 6).
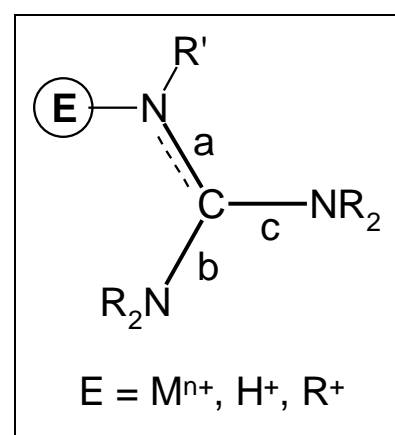
Scheme 6. C-N bonds a,b and c for the determination of quotient ρ.

5

Chapter 5.2. Last but not least the ultimative goal to synthesize a phosphazene „proton sponge" with two iminophosphoranes as chelating proton acceptors has been realized (Scheme 7). Its chemistry is still under investigation but it is anticipated that HMPIN has a pK_{BH+} value 2-3 orders of magnitude higher than the guanidine based derivative.
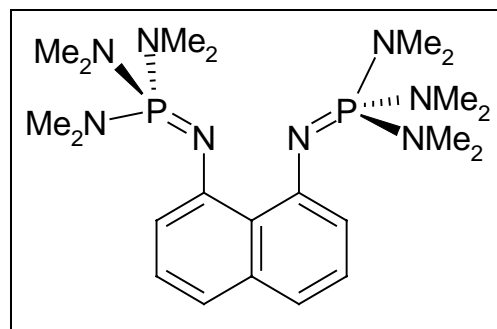
Scheme 7. Superbasic iminophosphorane „proton sponge".

OUTLOOK

Future perspectives for the further development of guanidine chemistry are outlined as follows:

Fine tuning of the tren ligand in terms of steric and electronic aspects still has to be investigated. A motive commonly used in tripod coordination chemistry, the substitution of only one or two arms of the tren ligand with a peralkyl guanidino group, could significantly affect the reactivity due to variable steric demand and donor capacity. The steric demand could also be influenced by variation of the alkyl rest of the guanidine group itself from Me to *n*-Bu, *i*-Pr or *t*-Bu which goes along with solubility properties. The idea of enhancing the basicity of the peralkyl guanidine group and crystallization properties could be further improved by introduction of five-membered rings in the guanidine moiety instead of six-membered ones. 5-rings should force the *N*-alkyl groups of the guanidine into an even more planar conformation and should therefore be more suitable for charge delocalization due to better p-orbital overlap. Furthermore, five-membered rings could improve the tendency of the complexes to crystallize since the degree of freedom for rotation is minimized.

The chiral ligands, among which especially the C_2 symmetric binaphthyl derivative (TMG$_2$BN) in combination with preferably copper(II), have not yet unfolded their potential in asymmetric syntheses, e.g. cyclopropanation or epoxidation of olefins. Furthermore, the bidentate systems could offer an entirely different reactivity, e.g., the activation of dioxygen according to an example of T. D. P. Stack (see Ch. 1, structural discussion of Cu(I) complex) because of their enhanced flexibility in comparison with the rigid tren ligand system.

Probably the above mentioned fine tuning of the tren ligand offers the long desired mechanistic insight to reactions such as nitrene transfer via a postulated copper nitrene intermediate or copper methoxy and methoxycarbonyl species in the catalysis of dimethyl carbonate by stabilizing these in a custom made ligand regime.

In the DMC catalysis, the exclusion of water remains the fundamental problem as is indicated by an experiment with molecular sieves as water withdrawing agent. The solution might be to establish the conditions of a two-phase system to avoid the re-reaction of DMC with water to MeOH and CO_2.

As for the „proton sponge" (TMGN), it would be interesting to synthesize derivatives with changes in the guanidine groups, e.g., 5-ring *N*-alkyl substituents should enhance the basicity. Still, the preparative route to its iminophosphorane analogon has to be improved. Again, the question has to be elucidated whether 5-ring *N*-alkyl substituents at the phosphorous atoms provide an increase of basicity. Moreover, a five-membered ring is less sterically hindered compared to an NMe_2 group which could facilitate the synthesis.
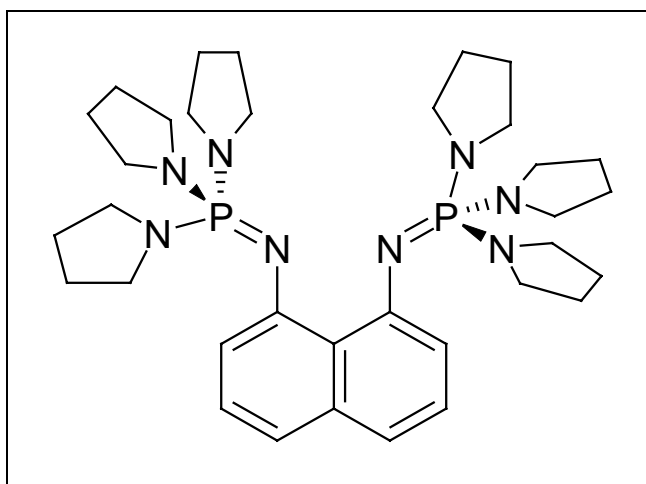
Scheme 1. Superbasic iminophosphorane „proton sponge".